

INFORMATION TO USERS

This manuscript has been reproduced from the microfilm master. UMI films the text directly from the original or copy submitted. Thus, some thesis and dissertation copies are in typewriter face, while others may be from any type of computer printer.

The quality of this reproduction is dependent upon the quality of the copy submitted. Broken or indistinct print, colored or poor quality illustrations and photographs, print bleedthrough, substandard margins, and improper alignment can adversely affect reproduction.

In the unlikely event that the author did not send UMI a complete manuscript and there are missing pages, these will be noted. Also, if unauthorized copyright material had to be removed, a note will indicate the deletion.

Oversize materials (e.g., maps, drawings, charts) are reproduced by sectioning the original, beginning at the upper left-hand corner and continuing from left to right in equal sections with small overlaps.

Photographs included in the original manuscript have been reproduced xerographically in this copy. Higher quality 6" x 9" black and white photographic prints are available for any photographs or illustrations appearing in this copy for an additional charge. Contact UMI directly to order.

**Bell & Howell Information and Learning
300 North Zeeb Road, Ann Arbor, MI 48106-1346 USA
800-521-0600**

UMI[®]

**EFFECT OF AMNIOTIC FLUID AND MECONIUM
IN THE LUNG OF NEONATAL FISCHER 344 RATS**

A Thesis

Submitted to the Graduate Faculty

in Partial Fulfilment of the Requirements

for the Degree of

Doctor of Philosophy

in the Department of Pathology and Microbiology

Faculty of Veterinary Medicine

University of Prince Edward Island

Julio Martinez-Burnes

Charlottetown, P.E.I.

April, 2000

© 2000. J. Martinez-Burnes



National Library
of Canada

Acquisitions and
Bibliographic Services
395 Wellington Street
Ottawa ON K1A 0N4
Canada

Bibliothèque nationale
du Canada

Acquisitions et
services bibliographiques
395, rue Wellington
Ottawa ON K1A 0N4
Canada

Your file Votre référence

Our file Notre référence

The author has granted a non-exclusive licence allowing the National Library of Canada to reproduce, loan, distribute or sell copies of this thesis in microform, paper or electronic formats.

The author retains ownership of the copyright in this thesis. Neither the thesis nor substantial extracts from it may be printed or otherwise reproduced without the author's permission.

L'auteur a accordé une licence non exclusive permettant à la Bibliothèque nationale du Canada de reproduire, prêter, distribuer ou vendre des copies de cette thèse sous la forme de microfiche/film, de reproduction sur papier ou sur format électronique.

L'auteur conserve la propriété du droit d'auteur qui protège cette thèse. Ni la thèse ni des extraits substantiels de celle-ci ne doivent être imprimés ou autrement reproduits sans son autorisation.

0-612-48805-5

Canada

CONDITIONS OF USE

The author has agreed that the Library, University of Prince Edward Island, may make this thesis freely available for inspection. Moreover, the author has agreed that permission for extensive copying of this thesis for scholarly purposes may be granted by the professor or professors who supervised the thesis work recorded herein or, in their absence, by the Chairman of the Department or the Dean of the Faculty in which the thesis work was done. It is understood that due recognition will be given to the author of this thesis and to the University of Prince Edward Island in any use of the material in this thesis. Copying or publication or any other use of the thesis for financial gain without approval by the University of Prince Edward Island and the author's written permission is prohibited.

Requests for permission to copy or to make any other use of material in this thesis in whole or in part should be addressed to:

Chairman of the Department of Pathology and Microbiology

Faculty of Veterinary Medicine

University of Prince Edward Island

Charlottetown, P.E.I.

Canada C1A 4P3

SIGNATURE PAGES

iii-iv

REMOVED

ABSTRACT

Meconium aspiration syndrome (MAS) is a major contributor to neonatal respiratory distress and an important cause of morbidity and mortality in infants. This syndrome has been recognized in foals, calves and puppies and pulmonary lesions in these animals are similar to those described in babies with MAS. There are few reliable animal models to evaluate the lesions and inflammatory response associated with MAS under laboratory conditions. The objectives of this investigation were: 1.- to standardize a murine model of MAS using intratracheal inoculation (ITI) in 7-day-old Fisher-344 rats. 2.- to quantify the cytological and biochemical changes in the bronchoalveolar lavage (BAL) after ITI of amniotic fluid and meconium. 3.- to evaluate and quantify the microscopic and ultrastructural changes in the lungs after ITI of meconium.

Results of this investigation showed that pulmonary alveolar macrophages (PAM) are present in the fetal lung and the numbers increase significantly ($p<0.05$) during the first 3 days of life. After 3 days, the cell counts are comparable to young or adult rats. During the postnatal period, there is a transient ($p<0.05$) influx of neutrophils (PMN) into the bronchoalveolar space. The lungs of normal rat neonates have high activities of alkaline phosphatase (ALP) and lactate dehydrogenase, and gamma-glutamyltransferase (GGT) and protein increase transiently during the first few days of life.

Saline did not cause changes in the composition of BAL nor induce any morphologic changes in the lung. Therefore, saline solution is an innocuous vehicle for ITI inoculation in neonatal rats. Amniotic fluid did not change the composition of BAL following inoculation but elicited a mild and transient histiocytic response.

In contrast, 20% unfiltered homologous meconium induced a sharp increase in PMN ($p<0.01$) shortly after inoculation. Meconium also induced a significant influx of PAM, vascular sequestration of PMN and aggregation of platelets in capillaries. Meconium caused a transient injury to the cells of the respiratory membrane characterized by a significant increase ($p<0.01$) of enzymatic activity. Ultrastructurally, cell injury was moderate and transient and did not lead to extensive necrosis of epithelial cells. Protein leakage suggesting an alteration of vascular permeability was also detected in the neonates inoculated with meconium. Other meconium-associated changes included atelectasis and hyperinflation and a significant ($p<0.01$) thickening of alveolar septa. Ultrastructurally, alveolar thickening coincided with interstitial edema and sequestration of PMN. The early neutrophilic response progressed into a persistent multifocal histiocytic and granulomatous reaction and some granulomatous foci eventually calcified or became lined by cuboidal cells. There were moderate hypertrophy and hyperplasia of type II pneumocytes, mild interstitial proliferation of mesenchymal cells and focal intraalveolar fibrosis. Topographically, the centriacinar region and neighboring alveoli were the main sites affected by meconium.

It was concluded that ITI of meconium in 7-day-old F-344 neonatal rats provides a reliable animal model for human MAS. To our knowledge, this is the first description of intratracheal (transoral) inoculation in neonatal rats. This murine model offers a method to study the pathogenesis of pulmonary lesions and test therapeutic interventions in MAS.

ACKNOWLEDGEMENTS

I gratefully acknowledge the financial support from the Canadian International Development Agency (CIDA) and the AVC Internal Research Fund, 1998. Thanks also to the Consejo Nacional de Ciencia y Tecnología (CONACYT) and the Universidad Autónoma de Tamaulipas, México.

I also extend my appreciation to the members of my supervisory committee, Drs. Barbara Horney, Glenda Wright, William Ireland and Fred Markham for their input into this research. Thanks also to the members of my examiner committee, Drs. Donald Dungworth, William Ireland, Pierre Daoust and David Speare.

I particularly thank my supervisor, Dr. Alfonso Lopez, for his guidance, support and friendship.

I wish to thank to Dr. Michael Brimacombe, for his advice in statistics, Dr. Kip Lemke for his anesthesia expertise and Dr. David Sims for the imaging support.

I appreciate and thank the technical efforts, skills and friendship of Allan MacKenzie, Greg Dobbin, Dorota Wadowska, Evelyn Daley, Chris McQuaid and Matthew Zawadzki. The professionalism and help of Shelley Ebbet and Tom MacDonald. The always excellent disposition of Monica Britain is highly appreciated.

I would like to extend my gratitude to Dr. Fernando Arizpe Garcia for his support and friendship.

My sincere appreciation to all members of the Department of Pathology and Microbiology in AVC.

I thank all my friends that made possible my stay in Prince Edward Island.

I especially thank my wife Catalina, and our kids Caty, Julio Adrian and Lucia Isabel. None of this would have been possible without their love and support.

TABLE OF CONTENTS

| | |
|---|----|
| 1. GENERAL INTRODUCTION | |
| 1.1. Meconium aspiration syndrome (MAS) in human medicine | 1 |
| 1.1.1. Definition | 1 |
| 1.1.2. Epidemiology | 1 |
| 1.1.3. Clinical presentation | 1 |
| 1.1.3.1. Radiographic features | 3 |
| 1.1.4. Pathophysiology | 4 |
| 1.1.5. Autopsy findings | 9 |
| 1.1.6. Diagnosis | 9 |
| 1.1.7. Prevention and treatment | 10 |
| 1.1.7.1. Intrapartum management | 10 |
| 1.1.7.2. Postpartum management | 11 |
| 1.1.7.3. Neonatal management | 12 |
| 1.2. Meconium aspiration syndrome in Veterinary Medicine | 15 |
| 1.2.1. Epidemiology and clinical presentation | 15 |
| 1.2.2. Animal models of MAS | 18 |
| 1.3. Objectives | 18 |
| 1.4. References | 20 |
| 2. EXPERIMENTAL MODEL OF MECONIUM ASPIRATION SYNDROME | |
| 2.1. Introduction | 29 |
| 2.2. Material and methods | 33 |
| 2.2.1. Animals and breeding programs | 33 |
| 2.2.2. Preconditioning programs | 34 |
| 2.2.3. Tattooing | 35 |
| 2.2.4. Anesthesia | 35 |
| 2.2.5. Collection of amniotic fluid | 36 |
| 2.2.6. Collection of meconium | 37 |
| 2.2.7. Dose range-finding study | 38 |
| 2.2.7.1. Maximum tolerated dose (MTD) for saline solution .. | 38 |
| 2.2.7.2. Maximum tolerated dose for amniotic fluid | 38 |
| 2.2.7.3. Maximum tolerated dose for meconium | 39 |
| 2.2.8. Intratracheal inoculation | 40 |
| 2.2.9. Euthanasia | 43 |
| 2.3. Results | 43 |
| 2.3.1. Breeding programs | 43 |
| 2.3.2. Preconditioning programs | 43 |
| 2.3.3. Anesthesia | 44 |
| 2.3.4. Collection of amniotic fluid | 45 |
| 2.3.5. Collection of meconium | 45 |
| 2.3.6. Dose range-finding study | 45 |

| | |
|---|----|
| 2.3.7. Intratracheal inoculation (ITI) in neonatal rat pups | 47 |
| 2.4. Discussion | 51 |
| 2.5. References | 58 |
| 3. CYTOLOGICAL AND BIOCHEMICAL CHANGES IN THE LUNG OF NEONATAL RATS INOCULATED WITH AMNIOTIC FLUID AND MECONIUM | |
| 3.1. Introduction | 64 |
| 3.2. Material and Methods | 69 |
| 3.2.1. Animals | 69 |
| 3.2.2. Anesthesia | 70 |
| 3.2.3. Inoculum | 70 |
| 3.2.4. Intratracheal inoculation (ITI) | 71 |
| 3.2.5. Euthanasia | 72 |
| 3.2.6. Experimental design | 72 |
| 3.2.6.1. Leukocyte kinetics and biochemistry of BAL from fetuses and neonates | 72 |
| 3.2.6.2. Effect of saline on the cytological and biochemical composition of BAL | 73 |
| 3.2.6.3. Cytological and biochemical changes after inoculation of amniotic fluid | 74 |
| 3.2.6.4. Cytological and biochemical changes after inoculation of meconium | 75 |
| 3.2.7. Bronchoalveolar lavage (BAL) | 76 |
| 3.2.8. Bronchoalveolar cell counts | 77 |
| 3.2.9. Differential count of alveolar macrophages and neutrophils .. | 77 |
| 3.2.10. Absolute number of alveolar macrophages and neutrophils .. | 78 |
| 3.2.11. Biochemistry of BAL fluid | 78 |
| 3.2.12. Statistical analysis | 79 |
| 3.3. Results | 80 |
| 3.3.1. Leukocyte kinetics and biochemistry of BAL from neonatal fetuses and neonates | 80 |
| 3.3.1.1. Cytology | 80 |
| 3.3.1.2. Biochemistry | 84 |
| 3.3.2. Effect of saline solution on the biochemical and cytological composition of the BAL | 86 |
| 3.3.2.1. Cytology | 86 |
| 3.3.2.2. Biochemistry | 86 |
| 3.3.3. Effect of amniotic fluid on the cytological and biochemical composition of the BAL | 89 |
| 3.3.3.1. First study of amniotic fluid (PID 1,3 and 7) | 89 |
| 3.3.3.1.1. Cytology | 89 |
| 3.3.3.1.2. Biochemistry | 89 |

| | |
|---|-----|
| 3.3.3.2. Second study of amniotic fluid (PID 3,7 and 14) | 92 |
| 3.3.3.2.1. Cytology | 92 |
| 3.3.3.2.2. Biochemistry | 92 |
| 3.3.4. Effect of meconium on the cytological and biochemical composition of the lung | 95 |
| 3.3.4.1. Cytology | 95 |
| 3.3.4.2. Biochemistry | 100 |
| 3.4. Discussion | 102 |
| 3.4.1. Leukocyte kinetics and biochemistry of BAL from normal fetuses and neonates | 102 |
| 3.4.2. Effect of saline solution on the cytological and biochemical composition of BAL | 106 |
| 3.4.3. Effect of amniotic fluid on the cytological and biochemical composition of BAL | 107 |
| 3.4.4. Effect of meconium on the cytological and biochemical composition of BAL | 109 |
| 3.5. References | 112 |
| 4. MICROSCOPIC CHANGES INDUCED BY THE INTRATRACHEAL INOCULATION OF AMNIOTIC FLUID AND MECONIUM IN THE LUNG OF NEONATAL RATS | |
| 4.1. Introduction | 122 |
| 4.2. Material and methods | 129 |
| 4.2.1. Animals | 129 |
| 4.2.2. Anesthesia | 130 |
| 4.2.3. Inoculum | 130 |
| 4.2.4. Intratracheal inoculation (ITI) | 131 |
| 4.2.5. Euthanasia | 131 |
| 4.2.6. Lung fixation | 132 |
| 4.2.7. Light microscopy | 133 |
| 4.2.8. Experimental design | 134 |
| 4.2.9. Statistical analysis | 136 |
| 4.3. Results | 136 |
| 4.3.1. Body weight | 136 |
| 4.3.2. Acute study | 140 |
| 4.3.2.1. Gross lesions | 140 |
| 4.3.2.2. Microscopic lesions | 140 |
| 4.3.3. Chronic study | 158 |
| 4.4. Discussion | 162 |
| 4.5. References | 176 |

5. MORPHOMETRIC CHANGES INDUCED BY THE INTRATRACHEAL INOCULATION OF MECONIUM IN THE LUNG OF NEONATAL RATS

| | |
|---|-----|
| 5.1. Introduction | 187 |
| 5.2. Material and methods | 195 |
| 5.2.1. Animals | 195 |
| 5.2.2. Anesthesia | 195 |
| 5.2.3. Inoculum | 195 |
| 5.2.4. Intratracheal inoculation of meconium | 196 |
| 5.2.5. Euthanasia | 196 |
| 5.2.6. Experimental design | 196 |
| 5.2.7. Lung sampling | 197 |
| 5.2.8. Lung processing | 197 |
| 5.2.8.1. <i>In situ</i> perfusion of lung for light microscopy | 197 |
| 5.2.8.2. Lung volume | 197 |
| 5.2.8.3. Light microscopy | 199 |
| 5.2.9. Morphometry | 201 |
| 5.2.9.1. Pilot study | 201 |
| 5.2.9.1.1. Morphometrical procedures | 201 |
| 5.2.9.1.1.1. Alveolar fraction | 201 |
| 5.2.9.1.1.2. Random selection of fields | 201 |
| 5.2.9.1.1.3. Volume fraction | 202 |
| 5.2.9.1.1.4. Absolute volume | 203 |
| 5.2.9.1.1.5. Volume density, surface density and arithmetic mean thickness | 203 |
| 5.2.9.1.1.5.1. Volume density | 203 |
| 5.2.9.1.1.5.2. Surface density | 205 |
| 5.2.9.1.1.5.3. AMT | 206 |
| 5.2.9.1.2. Statistical Analysis | 206 |
| 5.3. Results | 207 |
| 5.3.1. General condition of the animals | 207 |
| 5.3.2. Body weights | 208 |
| 5.3.3. Pilot study | 208 |
| 5.3.3.1. Volume fractions of compartments | 208 |
| 5.3.3.2. Absolute volumes of compartments | 211 |
| 5.3.3.3. Volume density of alveolar septa | 212 |
| 5.3.3.4. Surface density of alveolar septa | 212 |
| 5.3.3.5. Arithmetic mean thickness of alveolar septa | 213 |
| 5.3.4. Main Study | 217 |
| 5.3.4.1. Fixed lung volume | 217 |
| 5.3.4.2. Volume fractions of compartments | 217 |
| 5.3.4.3. Absolute volumes of compartments | 220 |
| 5.3.4.4. Volume density of alveolar septa | 221 |
| 5.3.4.5. Surface density of alveolar septa | 224 |
| 5.3.4.6. Arithmetic mean thickness of alveolar septa | 224 |

| | |
|--|-----|
| 5.4. Discussion | 226 |
| 5.4.1. Clinical observations and mortality | 226 |
| 5.4.2. Body weight | 226 |
| 5.4.3. Lung volume and weight | 227 |
| 5.4.4. Volume fractions of compartments | 228 |
| 5.4.5. Absolute volumes of compartments | 231 |
| 5.4.6. Volume density of alveolar septa | 232 |
| 5.4.7. Surface density of alveolar septa | 233 |
| 5.4.8. Arithmetic mean thickness of alveolar septa | 233 |
| 5.5. References | 237 |
| 6. ULTRASTRUCTURAL EVALUATION OF THE BRONCHIOLAR AND ALVEOLAR REGION IN NEONATAL RATS INTRATRACHEALLY INOCULATED WITH MECONIUM | |
| 6.1. Introduction | 242 |
| 6.2. Material and methods | 247 |
| 6.2.1. Animals | 247 |
| 6.2.2. Anesthesia | 247 |
| 6.2.3. Inoculum | 247 |
| 6.2.4. Intratracheal inoculation of meconium | 248 |
| 6.2.5. Euthanasia | 248 |
| 6.2.6. Experimental design | 248 |
| 6.2.7. Intratracheal lung perfusion of fixative | 249 |
| 6.2.8. Sampling | 250 |
| 6.2.9. Isolation of alveolar region | 250 |
| 6.2.10. Tissue processing | 251 |
| 6.2.11. Thick sections and light microscopy | 252 |
| 6.2.12. Thin sections and transmission electron microscopy | 252 |
| 6.3. Results | 253 |
| 6.3.1. Intratracheal lung perfusion | 253 |
| 6.3.2. Gross lesions | 253 |
| 6.3.3. Morphological changes | 254 |
| 6.3.3.1. Meconium | 254 |
| 6.3.3.2. Bronchiolar response to meconium | 259 |
| 6.3.3.3. Alveolar response to meconium | 259 |
| 6.4. Discussion | 285 |
| 6.4.1. Meconium | 286 |
| 6.4.2. Bronchiolar response to meconium | 287 |
| 6.4.3. Alveolar response to meconium | 288 |
| 6.4.4. Site of injury | 292 |
| 6.4.5. Conclusions | 293 |
| 6.5. References | 294 |
| 7. GENERAL DISCUSSION AND CONCLUSIONS | 301 |

LIST OF FIGURES

| | | |
|------------|---|----|
| Figure 1. | Schematic representation of the pathogenesis of Meconium Aspiration Syndrome | 6 |
| Figure 2. | Otoscope/throat illuminator system components | 42 |
| Figure 3. | Intratracheal inoculation | 42 |
| Figure 4. | Total cell counts in BAL fluid of normal fetuses and neonatal rats at different ages | 81 |
| Figure 5. | Differential of leukocyte counts in BAL from fetuses and neonatal rats at different ages | 81 |
| Figure 6. | Absolute number of leukocytes in BAL fluid from fetuses and neonatal rats | 83 |
| Figure 7. | Comparison between total cell count and PAM in BAL from fetuses and neonatal rats | 83 |
| Figure 8. | Enzymatic activity and total protein content in BAL fluid of normal rats | 85 |
| Figure 9. | Total cell count, and absolute number of PAM and PMN in BAL fluid, after inoculation of 7-day-old neonates with saline | 87 |
| Figure 10. | Enzymatic activity and total protein content in BAL fluid, after inoculation of 7-day-old neonates with saline | 88 |
| Figure 11. | Total cell count, and absolute number of PAM and PMN in BAL fluid, after inoculation of 7-day-old neonates with amniotic fluid (PID 1,3, and 7) | 90 |
| Figure 12. | Enzymatic activity and total protein content in BAL fluid, after inoculation of 7-day-old neonates with amniotic fluid (PID 1,3 and 7) | 91 |
| Figure 13. | Total cell count, and number of PAM and PMN in BAL fluid, after inoculation with amniotic fluid (PID 3,7, and 14) | 93 |
| Figure 14. | Enzymatic activity and total protein content in BAL fluid, after inoculation with amniotic fluid (PID 3,7 and 14) | 94 |

| | | |
|-------------|---|-----|
| Figure 15. | Total cell count in BAL fluid after the inoculation with meconium | 96 |
| Figure 16. | Differential of leukocytes in BAL after the inoculation of 7-day-old neonates with meconium | 97 |
| Figure 17. | Photomicrographs of recovered cells from BAL at PID1, isolated with the Cystospin centrifuge and stained with Wright-Giemsa | 98 |
| Figure 18. | Absolute number of leukocytes in BAL fluid after the inoculation with meconium | 99 |
| Figure 19. | Enzymatic activity and total protein content in BAL fluid, after the inoculation with meconium | 101 |
| Figure 20. | Body weight of the neonates in the acute study | 138 |
| Figure 21. | Body weight of the neonates in the chronic study | 139 |
| Figure 22. | Neonatal rat lung; saline control PID 1. Alveoli are well distended with no evidence of inflammation | 141 |
| Figure 23. | Neonatal rat lung; amniotic fluid PID 1. Foreign body response in proximal alveolar region. | 141 |
| Figure 24. | Lungs from neonatal rats inoculated with meconium. Meconium is present in bronchioles and exhibits different stainabilities | 143 |
| Figure 25. | Neonatal rat lung; meconium PID 3. Meconium fills the bronchiole. | 145 |
| Figure 26. | Neonatal rat lung; meconium PID 1. Meconium fills an alveolus. | 145 |
| Figure 27. | Neonatal rat lung; meconium PID 1. Meconium present in bronchiole is surrounded by neutrophils and macrophages. | 147 |
| Figure 28. | Neonatal rat lung; meconium PID 1. Meconium within alveoli in the peripheral subpleural region. | 147 |
| Figure 29A. | Neonatal rat lung; meconium PID 1. Collapsed alveoli are evident close to bronchiole filled with meconium. | 149 |
| Figure 29B. | Neonatal rat lung; control PID 1. Bronchiole and alveoli are clean and normally distended. | 149 |

| | | |
|-------------|--|-----|
| Figure 30. | Rat lung; meconium PID 1. Atelectatic alveoli alternating with hyperinflation close to meconium in bronchiole | 151 |
| Figure 31A. | Neonatal rat lung; meconium PID 1. Exudative inflammation with neutrophils and macrophages within alveoli | 153 |
| Figure 31B. | Neonatal rat lung; saline control PID 1. Alveoli with clean airspaces and non distended alveolar septa | 153 |
| Figure 32. | Neonatal rat lung; meconium PID 1. Meconium is present in a terminal bronchiole along with meconium-laden macrophages | 156 |
| Figure 33. | Neonatal rat lung; meconium PID 7. Transition from neutrophilic to histiocytic inflammation composed of macrophages in alveoli | 156 |
| Figure 34. | Neonatal lung; meconium PID 14. Granulomatous response characterized by macrophages and multinucleated giant cells in an alveolus | 157 |
| Figure 35. | Neonatal lung; meconium PID 28. Granuloma formation in alveoli by macrophages and thickening of alveolar septa | 157 |
| Figure 36. | Neonatal lung; meconium group PID 28. Meconium in an alveolus surrounded by fibroblastic cells and a region of columnar epithelial cells | 160 |
| Figure 37. | Rat lung; meconium group PID 56. Meconium sequestered in the lung and covered by fibroblastic cells, multinucleated cells and a single layer of cuboidal cells | 160 |
| Figure 38. | Rat lung; meconium group PID 56. Meconium remained trapped in alveoli and encapsulated by fibroblastic cells | 161 |
| Figure 39. | Rat lung; meconium group PID 112. Persistent multifocal granulomatous inflammation in alveoli | 161 |
| Figure 40. | Flow diagram of the tiered or multiple stage sampling procedure for morphometric analysis of lung tissue. | 198 |
| Figure 41. | Gravimetric method used for determination of the fixed lung volume by the weight of displaced fluid | 200 |
| Figure 42. | Computer screen containing a test grid with 84 lines and 168 | |

| | |
|--|-----|
| test points used to determine the volume fractions of the compartments of the lung by point counting | 204 |
| Figure 43. Computer monitor containing a test grid to determine the volume density and surface density of the alveolar septa using point counting and line intersections | 204 |
| Figure 44. Body weight of the neonatal rats at different postinoculation times .. | 209 |
| Figure 45. Percentage of daily body weight gained per group at different postinoculation times | 210 |
| Figure 46. Main Study. Volume density of the alveolar septa in the apical lobe at different postinoculation times. | 223 |
| Figure 47. Main Study. Arithmetic mean thickness of the alveolar septa in the apical lobe at different postinoculation times. | 225 |
| Figure 48. Meconium in bronchiole of a neonatal rat, meconium group, PID 3 .. | 256 |
| Figure 49. Meconium plug in bronchiole at PID 3 | 258 |
| Figure 50. Alveolar region from a rat inoculated with meconium;PID 1, showing an enlarged PAM containing numerous phagolysosomes, vacuoles and pseudopods closely apposed to a type I pneumocyte | 258 |
| Figure 51. Bronchiole from a rat inoculated with meconium, PID 3 | 261 |
| Figures 52. Alveoli; rat inoculated with meconium, PID 1. A typical type II pneumocyte showing lamellar bodies and microvilli | 264 |
| Figures 53. Alveoli; rat inoculated with meconium, PID 1. Characteristic attenuated cytoplasmic extension of an intact type I pneumocyte | 264 |
| Figure 54. Alveoli; rat inoculated with meconium, PID 1. | 266 |
| Figure 55. Alveolar septum from meconium group, PID 1. A blood vessel shows aggregation of platelets | 268 |
| Figure 56. Alveolar septum from meconium group, PID 1. Sequestration of neutrophils in capillary associated with interstitial edema | 268 |
| Figure 57. Alveolar septum, PID 1. A. Control rat. B. Rat meconium group. | 271 |

| | | |
|------------|--|-----|
| Figure 58. | Light micrograph of thick resin section; alveolar space, PID 7 | 273 |
| Figure 59. | Alveolar space, meconium group, PID 7 | 273 |
| Figure 60. | Light micrograph of thick resin section; alveolar space, meconium group, PID 7 | 275 |
| Figure 61. | Alveolus; meconium group, PID 7 | 275 |
| Figure 62. | Type II pneumocyte; meconium group, PID 7 | 275 |
| Figure 63. | Type II pneumocyte; control group, PID 7 | 278 |
| Figure 64. | Type II pneumocyte; meconium group, PID 7 | 278 |
| Figure 65. | Type II pneumocyte; meconium group, PID 7 | 278 |
| Figure 66. | Light micrograph of thick resin section; alveolar septum, meconium group at PID 7 | 280 |
| Figure 67. | Alveolar septum; meconium group, PID 7 | 280 |
| Figure 68. | Alveolar septum; meconium group, PID 7 | 280 |
| Figure 69. | Alveolar interstitium; meconium group, PID 7 | 282 |
| Figure 70. | Alveolar interstitium; meconium group, PID 7 | 282 |
| Figure 71. | Light micrograph of thick resin section from meconium group showing a large proliferative mass at the region of transition between terminal bronchiole and alveoli and protruding from the interstitium to the alveolar space | 284 |
| Figure 72. | Transition from bronchiolar nonciliated cell to alveolus, meconium group, PID 7 | 284 |
| Figure 73. | Light micrograph of boxed area in figure 71; meconium group, PID 7 | 284 |
| Figure 74. | Proliferative mass; meconium group, PID 7, showing myofibroblasts rich in lipid droplets | 284 |

LIST OF TABLES

| | | |
|-------------|---|-----|
| Table I. | Design for dose range-finding study for intratracheal inoculation of saline solution, amniotic fluid and meconium | 40 |
| Table II. | Number of Fischer 344 neonates, body weight and induction and recovery times in the two different protocols of anesthesia | 44 |
| Table III. | Complications and mortality in the dose range-finding study for intratracheal inoculation of saline, AF and meconium in 7-day-old rat pups | 46 |
| Table IV. | Neonatal rats with microscopic evidence of meconium in conducting airways and the interlobar distribution after the intratracheal inoculation | 49 |
| Table V. | Neonatal rats with microscopic evidence of meconium in alveoli and the interlobar distribution after the intratracheal inoculation | 49 |
| Table VI. | Acute study. Number of animals, body weight at the inoculation time, and survival rate | 50 |
| Table VII. | Number of rats used in the leukocyte kinetics and biochemistry of BAL fluid | 72 |
| Table VIII. | Number of neonates used to study the effect of saline solution on leukocyte kinetics and biochemistry of BALs | 73 |
| Table IX. | Number of neonates used to evaluate cytological and biochemical changes in BAL after the inoculation with amniotic fluid (1,3,7) | 74 |
| Table X. | Number of neonates used to determine cytological and biochemical changes in BAL after the inoculation with amniotic fluid (3,7,14) | 74 |
| Table XI. | Cytological and biochemical changes in BAL after inoculation of meconium in neonatal rats | 75 |
| Table XII. | Acute microscopic changes in the lung of 7-day-old neonatal rats intratracheally inoculated with amniotic fluid and meconium | 135 |
| Table XIII. | Chronic microscopic changes in the lung of 7-day-old neonatal rats intratracheally inoculated with amniotic fluid and meconium | 135 |

| | | |
|---------------|--|-----|
| Table XIV. | Histologic scoring for the evaluation of the frequency and severity of changes induced after ITI of meconium in the lung of neonatal rats . | 146 |
| Table XV. | Acute study. Neonatal lungs with evidence of atelectasis after the intratracheal inoculation of meconium and its interlobar distribution .. | 150 |
| Table XVI. | Acute study. Neonatal lungs with exudative inflammation after the intratracheal inoculation of meconium and its interlobar distribution .. | 150 |
| Table XVII. | Acute study. Neonatal rat lungs with presence of thickening of alveolar septa after intratracheal inoculation of meconium and their interlobar distribution .. | 155 |
| Table XVIII. | Formulas used in the morphometric study .. | 191 |
| Table XIX. | Experimental design. Number of neonatal rats per treatment and days postinoculation .. | 196 |
| Table XX. | Number of rats, body weight at inoculation time, and survival rate .. | 208 |
| Table XXI. | Pilot Study. Number of rats, lobes, fields, points counted and volume fractions of the compartments of the lung at PID 1 .. | 214 |
| Table XXII. | Pilot Study. Number of rats, body weight, fixed lung volume and volumes of the compartments of the lung at PID 1 .. | 215 |
| Table XXIII. | Pilot Study. Number of rats, lobes, fields, points counted, volume density, surface density and AMT of the alveolar septa at PID 1 .. | 216 |
| Table XXIV. | Pilot Study. Volume density, surface density and AMT of the alveolar septa in different lobes at PID 1. .. | 216 |
| Table XXV. | Main Study. Number of rats, body weight, fixed lung volume and volumes of the compartments of apical lobe at PID 1, 3 and 7 .. | 218 |
| Table XXVI. | Main Study. Number of rats, lobes, fields, points counted, and volume fractions of the compartments of the apical lobe at different PIDs. . | 219 |
| Table XXVII. | Main Study. Volume density, surface density and AMT of the alveolar septa in the apical lobe at different PIDs. . | 222 |
| Table XXVIII. | Ultrastructural study. Number of neonatal rats per treatment and days postinoculation .. | 249 |

ABBREVIATIONS

| Abbreviation | Term |
|---------------------------------|---|
| Abs, Airbr | Absolute volume of compartments Air from bronchi and bronchioles |
| Alair | Air from alveoli |
| ALP | Alkaline phosphatase |
| Alv | Alveoli |
| ANOVA | Analysis of variance |
| AF | Amniotic fluid |
| AMT | Arithmetic mean thickness |
| ARDS | Acute respiratory distress syndrome |
| AVC | Atlantic Veterinary College |
| BAL | Bronchoalveolar lavage |
| Br | Bronchiole |
| BTS | British Toxicological Society |
| Bv | Blood vessel |
| °C | Degree celsius |
| Cc | Ciliated epithelial cell |
| C | Capillary |
| cm | Centimeter |
| cm ³ | Cubic centimeter |
| CO ₂ | Carbon dioxide |
| CV | Coefficient of variation |
| ECMO | Extracorporeal membrane oxygenation |
| EEC | European Economic Community |
| EP I | Type I pneumocyte |
| EP II | Type II pneumocyte |
| F | Fibrillar network of meconium |
| Fc | Fibroblastic-cells |
| F-344 | Fischer 344 rats |
| g | Gram |
| x g | Gravities |
| GGT | Gamma-glutamyltransferase |
| GLM | Generalized linear models |
| h | Hour (s) |
| HE | Hematoxylin and eosin |
| I | Interstitial |
| I _a , I _o | Number of line intersections with the alveolar surface |
| I _L | Number of intersections per test line length |
| IL-1 β | Interleukin 1beta |
| IL-8 | Interleukin-8 |

| | |
|-------------------|---|
| ITI | Intratracheal inoculation |
| IU | International unit |
| kV | Kilovolts |
| L | Lipid droplet |
| LB | Lamellar body |
| LD ₅₀ | Lethal dose 50% |
| LDH | Lactate dehydrogenase |
| Lo | Total length of the lines falling on alveolar septa |
| Log 10 | Logarithm (to base 10) |
| LPS | Lipopolysaccharides |
| M | Meconium |
| Mf | Myofibroblast |
| MAS | Meconium aspiration syndrome |
| min | Minute |
| ml | Milliliter |
| mosmol | Milliosmol |
| mg | Milligram |
| mm | Millimeter |
| mm ₃ | Cubic millimeter |
| MSAF | Meconium stained amniotic fluid |
| MTD | Maximum tolerated dose |
| n | Number of observations |
| NaCl | Sodium chloride |
| NAD | Nicotinamide adenine dinucleotide |
| NC | Non ciliated epithelial cell |
| NI | Normal distribution |
| NIH | National Institute of Health |
| nm | Nanometer |
| NO | Nitric oxide |
| NO ₂ | Nitrogen dioxide |
| O ₂ | Oxygen |
| p | Probability |
| P | Proliferative mass |
| PaO ₂ | Arterial oxygen pressure |
| PaCO ₂ | Arterial carbon dioxide pressure |
| PAM | Pulmonary alveolar macrophages |
| PAR | Proximal alveolar region |
| PAS | Periodic acid Schiff stain |
| PEEP | Positive-end expiratory pressure |
| pH | Hydrogen ion activity |
| PFC | Perfluorocarbon |
| PID | Postinoculation day (s) |
| PL | Phagolysosomes |

| | |
|---------------|--|
| PO | Propylene oxide |
| P_t | Number of points on tissue being studied |
| P_t | Total points |
| PMN | Polymorphonuclear neutrophils |
| PPHN | Persistent pulmonary hypertension of the neonate |
| r | Coefficient of correlation |
| R | Right |
| SD | Standard deviation |
| SEM | Standard error of the mean |
| SIRS | Systemic inflammatory response syndrome |
| SS | Saline solution |
| σ_e | (Variance) Square sigma of error |
| Svs | Specific surface density |
| TEM | Transmission electron microscopy |
| TIFF | Tagged image format files |
| TNF- α | Tumor necrosis factor-alfa |
| τ_t | Arithmetic mean thickness |
| U | Units |
| Uc | Undifferentiated cell |
| μg | Micrograms |
| μl | Microliters |
| μm | Micrometer |
| V | Volts |
| Vo | Volume of object (alveolar septa) |
| Vref | Volume of reference space (lung) |
| Vv | Volume fraction of compartments |
| Vvalv | Volume density of alveolar septa |
| Vvap | Volume density of alveolar septa to parenchyma |
| Vvn | Volume density of nonparenchyma |
| Vvp | Volume density of parenchyma |
| Z | Length of test line |

1. GENERAL INTRODUCTION

1.1. Meconium aspiration syndrome (MAS) in human medicine

1.1.1. *Definition*

Meconium aspiration syndrome (MAS) has been defined as respiratory distress in an infant born with meconium stained amniotic fluid (MSAF) who has compatible roentgenographic findings and whose symptoms cannot be otherwise explained (1). MAS represents one of the most common causes of neonatal respiratory distress (2).

1.1.2. *Epidemiology*

MAS is a common problem faced by pediatricians and obstetricians. According to a review of more than 30 reports in the literature, until 1990 the overall frequency of live births complicated by meconium stained amniotic fluid in United States was approximately 12.5% of all deliveries, with a wide range from 7 to 22% (1-3). Of those born with MSAF, approximately 5% developed MAS, of whom more than 4% died. Mortality rates ranged from 4.2 to 46% (3,4). Since 1990 the frequency of MSAF has ranged from 5.6% to 24.6%. MAS has occurred in 1.7% to 35.8% of infants born with MSAF (1,4), approximately 4% of all live births. Mortality occurred in 4.9% to 37% of infants with MAS (1). Unfortunately, it seems from the epidemiological information published that MAS remains as an important cause of neonatal respiratory distress in spite of advances in the understanding of its pathophysiology and the introduction of new therapies.

1.1.3. *Clinical Presentation*

From the clinical point of view, MAS is most strictly defined as the presence of any meconium below the vocal cords, however, most clinical definitions include a triad of: (1)

the presence of MSAF; (2) aspiration of meconium from below the vocal cords and (3) a chest radiograph consistent with MAS.

The characteristic clinical picture may be a mild and transient respiratory distress or a severe respiratory failure with hypoxemia, acidosis, and pulmonary hypertension (5,6). Classically, the infant with MAS is term or post term (postmature) and shows signs of weight loss and yellow-stained nails, skin, and umbilical cord (6,7). Signs of respiratory distress may not develop until the neonate is 2-4 hours old and the severity of the illness is dependent on the amount and consistency of aspirated meconium (6,8).

The human infant with minimal meconium aspiration will develop a mild disease shortly after birth, usually associated with tachypnea, mild cyanosis and a possible marked overdistension of the chest (5-7). This form of the illness is considered self-limiting, resolving between 48 to 72 hours, with the arterial carbon dioxide pressure ($PaCO_2$) either normal or low and a normal pH (7). In contrast, severe disease results from massive aspiration, and is characterized by severe asphyxia at birth, peripheral circulatory failure, intense pallor, and difficult resuscitation. Respirations are irregular and gasping, and the chest is hyperinflated with crepitation on auscultation. Respiratory distress is severe and hypoxemia, CO_2 retention and severe metabolic acidosis may be present at birth or develop during the first 24 hours. The aforementioned produce a persistent fetal circulation with intense pulmonary vasospasm leading to right to left shunt, often through a patent ductus arteriosus or foramen ovale (5). As many as 66% of all cases of persistent pulmonary hypertension of the neonate (PPHN) are related to MAS (4,9). Pneumothorax is also a common complication in these babies (7).

Neurologic sequelae have been linked to MSAF and MAS. The finding of meconium staining alone does not prove that a term infant experienced a degree of asphyxia sufficient to account for later neurological abnormalities. However, the rate of severe mental handicap and cerebral palsy is significantly higher among infants born with MSAF (9). Neonatal seizures and chronic seizures are more likely to occur with a history of MSAF (10,11). Survivors of severe MAS are at relatively high risk for both cerebral palsy and neonatal seizures (12).

Long term abnormal pulmonary function effects or respiratory symptoms among children who had MAS as neonates have been documented. The pulmonary function testing was done in children from 6 to 11 years after birth and revealed large components of obstructive airway disease with wheezing and exercise-induced bronchospasm (13,14). A study documented a much higher prevalence of asthmatic symptoms and abnormal bronchial reactivity among survivors of MAS than in the general child population (13). Another study documented lower airway obstruction in infants recovering from severe MAS who needed extracorporeal membrane oxygenation treatment (15). Moreover, infants with MAS account for the largest number of full-term babies with respiratory disorders who subsequently developed chronic lung disease (9). In summary, aspiration of meconium may have long term consequences for the developing respiratory tract and is associated with abnormal respiratory function in later childhood.

1.1.3.1. Radiographic features

The classical radiographic features of MAS were initially described by Peterson and Pendleton (16) as patchy infiltrates, radiating from the hilus into the peripheral lung fields.

However, the diverse mechanisms involved in MAS lead to a variety of radiographic findings, including infiltrates, consolidation, atelectasis, pleural effusions, and air leaks (e.g. pneumothorax, pneumomediastinum), hyperinflation, a wet-lung picture, hypovascularity, or a relatively normal appearance (1,3,6,8,17). In some studies, consolidation and atelectasis, most commonly associated with thick meconium aspiration, appeared to be the most significant determinant of poor outcome. Infants with consolidation or atelectasis were sicker, and required longer duration of oxygen intake (17). Sequential radiologic studies using labeled meconium have shown migration of meconium into the lung parenchyma over the first 4 hours after birth (8,18,19). Areas of diminished aeration clear within 24 hours and 80% of all X-rays films are clear within 48 hours (3). In spite of the fact that 40 to 73% of infants born with MSAF have positive chest X-ray findings, fewer than a half of them show respiratory distress. Paradoxically, the severity of roentgenographic findings may not always correlate with the clinical disease. Some infants may experience severe disease with minimal X-ray findings, while other neonates have remarkable X-ray findings without clinical disease (1,3,20).

1.1.4. Pathophysiology

The term *meconium* is derived from the Greek *meconium-arion*, meaning “opium-like”, and was coined by Aristotle because he believed it induced fetal sleep (9). Meconium is a viscous green sterile material composed of a mixture of gastrointestinal secretions, bile, bile acids, mucus, pancreatic juice, cellular debris, swallowed amniotic fluid and vernix caseosa, lanugo and blood (4,21). Mucopolysaccharides comprise approximately 80% of meconium’s dry weight (22). Meconium may first be found in the fetal gastrointestinal tract

between the 10th and 16th week of gestation, and from 60 to 200g may be passed by a full-term neonate at birth (23). *In utero* passage of meconium is uncommon in normal conditions due to relative lack of peristalsis, good anal sphincter tone, and a plug of viscous meconium in the rectum (9).

For most infants, passage of meconium represents a maturational event, being rare before 37 weeks of gestation, but may occur in 35% or more pregnancies lasting longer than 42 weeks. The most widely accepted hypothesis regarding the passage of meconium into amniotic fluid is related to fetal hypoxia. According to this hypothesis, *in utero* hypoxia causes redistribution of blood in the fetus with consequent increased intestinal peristalsis and relaxed anal sphincter tone, leading to meconium passage (4,9,24). Additionally, compression of umbilical cord or fetal head, may cause vagal stimulation and meconium passage (24). Numerous investigators have concluded that the presence of meconium in amniotic fluid is an indicator of fetal hypoxia or acidosis (25-28), while others concluded that meconium passage does not independently correlate with fetal distress (3).

After aspiration of meconium, a cascade of complex events occurs leading to the development of MAS. A schematic diagram of the pathophysiology of MAS is presented in Fig.1.

Aspiration of meconium produces many mechanical and physiological changes in the neonate that are related to the amount and viscosity of meconium (29). Aspiration of a large quantity of thick meconium may produce complete obstruction of the proximal airways, resulting in severe hypoxia, respiratory failure and death unless recognized and treated.

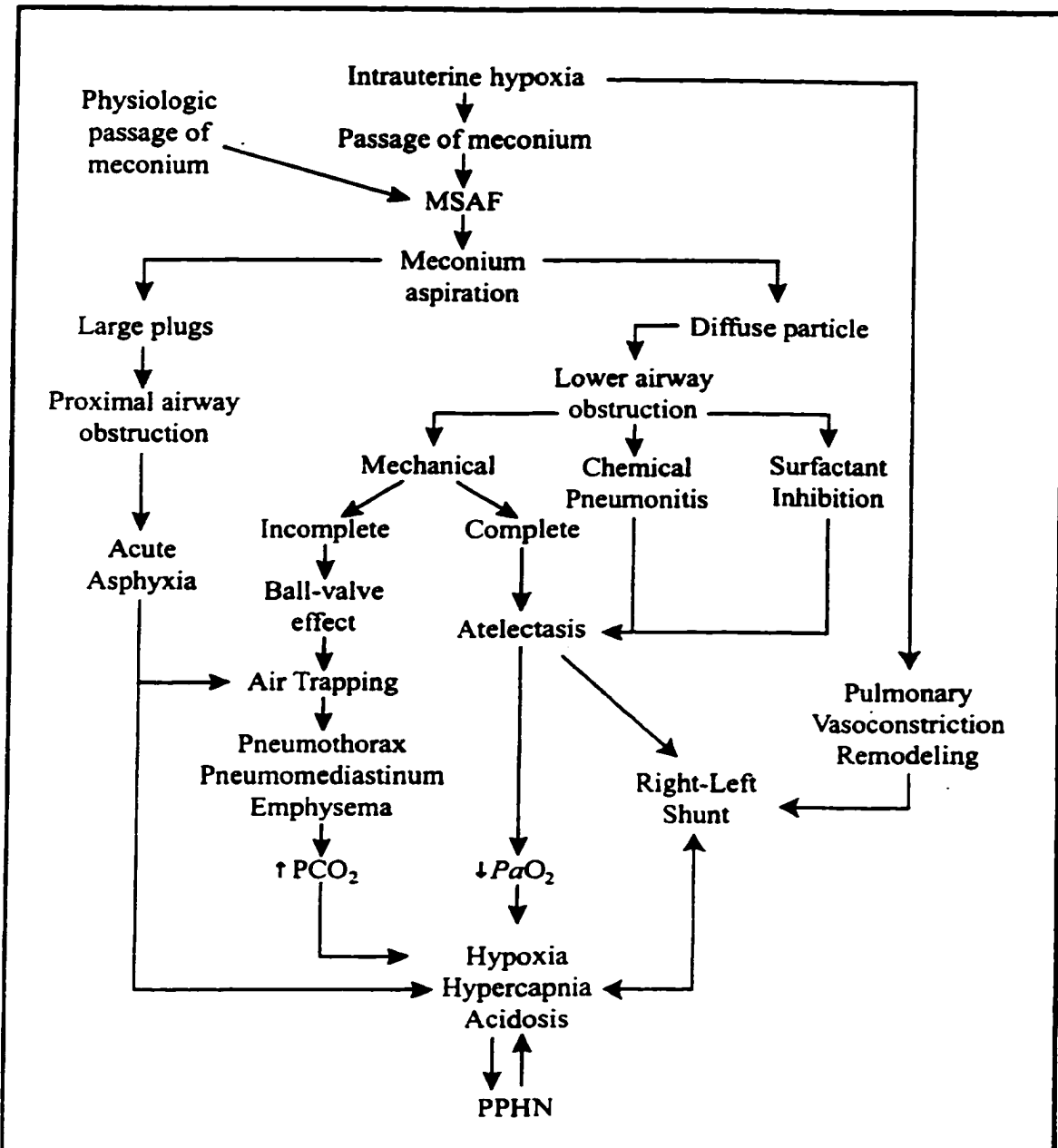


Figure 1. Schematic representation of the pathogenesis of Meconium Aspiration Syndrome. Modified from Wiswell, T.E.: Meconium staining and the meconium aspiration syndrome. Unresolved issues. *Pediatr Clin North Am* 40:957, 1993. MSAF: Meconium stained amniotic fluid. PPHN: persistent pulmonary hypertension of the neonate.

More commonly, however, smaller amounts of particulate meconium may reach the periphery of the lung, inducing obstruction of the lower or distal airways with two different outcomes. If meconium produces complete obstruction of the smaller bronchioles, it causes atelectasis and ventilation perfusion mismatch. Incomplete lower respiratory tract obstruction results in a ball-valve type effect, creating air trapping and air leaks and leading to pneumothorax, pneumomediastinum, or interstitial emphysema (4). The obstructive properties of meconium result in the characteristic roentgenographic and histologic findings of MAS: atelectasis and consolidation, admixed with overdistended hyperexpanded areas (30,31).

Meconium and its components like bile salts may also act as an irritant to the lung and produce the so called “chemical pneumonitis”, characterized by an intense and diffuse inflammatory response with edema, necrosis and recruitment of polymorphonuclear leukocytes and alveolar macrophages (30,31). One study has shown how meconium affects neutrophil function by inhibiting oxidative bursts and phagocytosis (32). Another study has demonstrated that meconium induces lung injury by activating alveolar macrophages and generating an increased production of superoxide anion (33). According to some studies, recruitment of inflammatory cells and edema is primarily mediated by pro-inflammatory cytokines such as tumor necrosis factor (TNF α), interleukin-1 β and 8 (IL-1 β and IL-8) released by macrophages in response to the pulmonary injury caused by meconium (34-36). In addition, a recent report confirmed that IL-8, a powerful chemoattractant for neutrophils, is present in meconium and could be a major mediator of inflammation in MAS (37). These substances may in turn directly injure lung parenchyma and lead to vascular leakage,

resulting in an injury pattern similar to the acute respiratory distress syndrome (ARDS)(38). Cytokines and vasoactive mediators also play an important role in the pathogenesis of vasoconstriction and the pulmonary arterial hypertension of the neonate (PPHN) which is so frequently associated with MAS (39-41).

More recent studies have suggested an additive pathogenic mechanism in which meconium induces displacement (42) or inactivation (43) of the surfactant, which is a critical element in preventing alveolar collapse. The ability of meconium to inactivate surfactant has been shown in both *in vivo* and *in vitro* studies (43,44). A direct effect of meconium on type II pneumocyte function has also been recently demonstrated (45). Another study has indicated that some chemical components of meconium, like bile salts, free fatty acids and bilirubin, may modify the biological properties of surfactant thereby predisposing to alveolar collapse (46). In addition, *in vitro* studies have demonstrated that the inflammatory response with neutrophils and plasma proteins in the alveolar milieu is a potential inhibitor of surfactant (47). In conclusion, unequivocally, the dysfunction of surfactant, due to the direct effect of meconium or the inhibitory effect of inflammatory components, plays an important role in the alveolar collapse characteristic of MAS.

All the aforementioned mechanisms may lead to hypoxemia, acidosis, and hypercapnia. These factors in the end can produce pulmonary vasoconstriction, resulting in persistent pulmonary hypertension of the neonate (PPHN)(48,49). Additionally, it has been demonstrated that infants may respond to ongoing fetal hypoxia by remodeling their pulmonary vasculature, resulting in abnormally thick muscularization that extends distally

along intra-acinar vessels (49,50). Finally, the vicious cycle of shunting, hypoxemia, and acidosis can further lead to pulmonary hypertension with poor prognosis.

1.1.5. Autopsy findings

Autopsy reports of babies who died of acute MAS describe multifocal “patchy” atelectasis and consolidation of the lung as the most relevant gross findings. The classical histopathologic findings of MAS are described as patchy infiltrates or consolidation and multifocal atelectasis (5). Meconium in the lungs of babies with MAS is characterized as a yellow-brown pigment, appearing either as glossy globules or granular debris within airways and alveoli, and by the frequent presence of squamous epithelial cells and keratin (51,52). The complex pathophysiological events resulting from meconium aspiration include the exudation of polymorphonuclear leukocytes (PMN) and pulmonary alveolar macrophages, necrosis, atelectasis, air trapping, emphysema, haemorrhages and intra-alveolar leakage of serum proteins and fibrin, and hyaline membrane formation (53,54). In addition, pulmonary vasoconstriction, haemorrhages, microthrombi, and increased muscularization and medial thickness of the distal arterioles within the lungs have been described (40,52,55,56). It has been suggested that some of these vascular changes have been induced by hypoxia *in utero* or perinatal asphyxia in natural cases of MAS (3,57).

1.1.6. Diagnosis

MAS should be suspected in any neonate with a history of meconium stained amniotic fluid (MSAF) and evidence of respiratory distress. However the diagnosis requires not only MSAF, but also the presence of meconium in the upper airway at birth, followed by radiological confirmation in the presence of respiratory distress (5,7). The presence of

a thin umbilical cord, meconium staining of the nails and cord and distress are frequent accompanying signs (5). Infants are more likely to be symptomatic if the delivery is by cesarean section or following vacuum extraction, if the Apgar score (58) is less than 6, or in cases where there is intra-uterine bradycardia, or when there are large amounts of meconium in the trachea or the mouth (7). A model of risk factors has been developed to predict which babies will develop MAS. These include labor induction with nonreassuring fetal heart tracings, need for suctioning of the baby's trachea, one-minute Apgar score of 4 or less, and caesarean-section delivery. In this model, infants without any of these risk factors will not develop MAS and thus can be safely allowed to room with their mothers (59). The clinical hallmarks to be considered include infants with varying degrees of respiratory distress, with severe cases showing evidence of hypoxemia, acidosis, and evidence of right to left shunt. Echocardiographic evaluation should be done in all cases of MAS to rule out congenital heart disease and also to calculate the pulmonary arterial pressure (4). Chest X-ray typically shows hyperinflation of lung fields, flattened diaphragm, and coarse irregular patchy infiltrates with increased lung fluid, and pneumothorax or pneumomediastinum may be present (4,7).

1.1.7. Prevention and treatment

In spite of the numerous research efforts focused on prevention and new therapies for MAS, there is still controversy concerning the best treatment option. Since it is difficult to get consensus on the right protocol to be followed, only the summarized concepts will be covered.

1.1.7.1. Intrapartum management

The most important step in MAS management is the early detection of MSAF and fetal distress by careful monitoring of high-risk pregnancies. Perhaps the most promising intrapartum intervention in the management of MSAF cases is amnioinfusion. This involves infusing normal saline into the amniotic space. This dilutes meconium and decompresses the umbilical cord or the head (4). A decrease in umbilical cord compression will result in less fetal gasping and, by a dilution of meconium, *in utero* gasping and deep breathing will result in less inhaled meconium (3). Some initial reports from the late 1980s and early 1990s revealed lower incidences of meconium below the vocal cords, fewer cesarean sections, higher Apgar scores and a decrease in the occurrence of MAS among patients receiving amnioinfusion (9,60). However, more recent reports questioned the benefit of amnioinfusion and the decrease in incidence of MAS. Moreover, amnioinfusion has been associated with more fetal heart rate abnormalities, increased rates of cesarean section and instrumented-assisted deliveries (forceps, vacuum extraction), and increased rates of neonatal sepsis (59,61).

As a summary, amnioinfusion may alleviate respiratory distress, acidosis, and the incidence of MAS, but also may increase the incidence of fetal heart rate abnormalities and of cesarean and instrumented-assisted deliveries.

1.1.7.2. Postpartum management

Carson *et al.* (62) were the first to document the beneficial effects of suctioning the oropharynx prior to the delivery of the infant's shoulder. Routine oropharyngeal suctioning while the head is still at the perineum using the De Lee catheter or bulb syringe has played

an important role in preventing MAS (20,62). However, there are several studies questioning the efficacy of obstetric hypopharyngeal suctioning as well as neonatal intratracheal suctioning in preventing or alleviating the severity of MAS. These studies also highlight the risks and complications associated with these procedures (3,63). Ongoing debate continues concerning universal versus selective intratracheal suctioning. Some groups of researchers have been critical of the selective intubation approach and support the current guidelines of the American Academy of Pediatrics and American Heart Association. This committee recommended intubation of all infants born with moderately- thick or thick-consistency MSAF. Infants born through thin-consistency meconium may not require intubation if there is no evidence of fetal distress, or if adequate oropharyngeal suctioning is performed, and the infant is vigorous and does not need positive-pressure ventilation (29). Finally, a recent multicenter trial comparing selective versus universal intubation in the management of apparently vigorous meconium-stained infants concluded that intubation of such infants does not result in a decreased incidence of respiratory distress (64). As a summary, to date, tracheal suctioning has been shown to decrease the incidence of MAS, however deciding which patients should be managed with tracheal suctioning still remains controversial.

1.1.7.3. Neonatal management

As a routine procedure, all infants with MAS should be admitted to the neonatal intensive care unit, receive supplemental oxygen, have their vital signs monitored continuously and the severity of the respiratory distress assessed. If the infant is in respiratory failure, intubation and mechanical ventilation are required (4). One third of all

infants with MAS require mechanical ventilation (64). Different mechanical ventilation strategies have been used in the management of MAS. Some studies found endotracheally applied continuous positive-end expiratory pressure (PEEP) to improve oxygenation in babies with MAS (65,66). However, others have found that air trapping may be exacerbated by PEEP and they support low inspiratory pressure, short inspiratory times and rapid ventilatory rates (67). One of the common treatments of PPHN has been hyperventilation, with the aim of attaining respiratory alkalosis and achieving pulmonary vasodilation (1). Other researchers support a “gentle” ventilation strategy and suggest their approach is as good or better than hyperventilation (68).

Using high-frequency ventilation in treating MAS has the advantages as documented by several authors of less barotrauma, increased mobilization of airway secretions, ease of attaining respiratory alkalosis and fewer histopathological changes (30,69,70).

Extracorporeal membrane oxygenation (ECMO) is a technique which oxygenates blood outside the body, obviating the need for gas exchange in the lungs, and, if necessary, providing cardiovascular support. ECMO has been widely used to manage severe neonatal respiratory failure since the early 1980s, reporting the best results in infants with MAS (4). Comparative studies in infants with severe respiratory failure treated with ECMO or continued intensive conventional management in United Kingdom collaborative trials showed clear advantage with ECMO, including lower mortality rates (71). However, it is expensive and some reports describe complications and sequelae (72,73).

Liquid ventilation with perfluorocarbon (PFC) has demonstrated efficacy in the management of MAS in animal models. The rationale of this method is related to removal

of meconium from the airways and alveolar surface, lung volume recruitment, reduction of surface forces, and improvement in ventilation/perfusion mismatch. The effect of PFC ventilation in a newborn lamb model of MAS demonstrated a significant increase in arterial oxygenation and pulmonary compliance (74).

Nitric oxide (NO) alone or combined with surfactant in the management of MAS has been evaluated in animal models demonstrating significant improvement in oxygenation (75,76). A study in human neonates with PPHN and MAS concluded that combined high frequency ventilation plus NO proved to be more effective than using each of the methods separately (77). However, multicenter trials in neonates with respiratory failure using NO did not find differences between mortality and duration of mechanical ventilation, frequency of air leaks, or length of hospitalization (78).

There is substantial evidence to support the theory that meconium displaces or inhibits intrinsic surfactant in neonates. Considerable research is therefore currently focused on the effect of replacement with bovine, porcine or synthetic surfactant in the management of MAS in animal models and human infants. Studies in rat and rabbit models of MAS showed that exogenous surfactant administration significantly reduced mortality and the severity of morphological changes and improved lung compliance and oxygenation (44,79-81). However, one study in a piglet model failed to find significant differences in oxygenation or microscopic changes with administration of surfactant (82). Clinical trials conducted in human neonates with MAS and treated with surfactant have shown improvements in oxygenation, reduction in duration of mechanical ventilation, and oxygen

requirements, as well as a decrease in air leaks and number of infants requiring ECMO (83-85).

Other studies have evaluated the effect of bronchoalveolar lavage (BAL) using surfactant with the aim of recovering the aspirated meconium. One study in a rabbit model of MAS recovered significantly more meconium than the saline control (86). In another similar study in a piglet model of MAS the researchers demonstrated significant improvement in oxygenation using the surfactant lavage (87).

The use of antibiotics in patients with MAS has three rationales: meconium produces segmental atelectasis which may mimic bacterial pneumonia, fetal bacterial infection may have been the initial factor that caused meconium passage and aspiration, and there has been evidence of *in vitro* enhancement of bacterial growth by meconium (7,29). However, its beneficial effect in all cases is still controversial (5,88).

In summary, despite significant advances in its management and new therapies, MAS remains one of the principal causes of neonatal respiratory failure.

1.2. Meconium aspiration syndrome in veterinary medicine

1.2.1. Epidemiology and clinical presentation.

In contrast to the information available in human neonatology, the prevalence and significance of aspirated meconium in animals are relatively unknown in veterinary medicine. Little information has been published in natural cases associated with aspiration of amniotic fluid and meconium in animals. Nevertheless, it is generally accepted that aspiration of amniotic fluid and meconium by fetuses is a terminal event associated with severe and prolonged intrauterine hypoxia (89,90). Also, intrauterine aspiration of

meconium is one of the most common events preceding abortion in bovine fetuses (91,92). The presence of mixed inflammatory cell exudates containing meconium and epithelial squames has been described in airways of aborted bovine fetuses (93).

Lopez *et al.* (94) reported that 54% of bovine Holstein fetuses submitted for necropsy had microscopic evidence of inflammation and aspiration of amniotic fluid with or without meconium. Lesions were characterized by diffuse influx of neutrophils into bronchi, bronchioles and alveolar ducts as well as acute necrosis and exfoliation of bronchiolar epithelial cells. As many as 36% of the fetuses contained meconium and/or squamous epithelial cells in their lungs. However, it was concluded that aspirated meconium, squamous epithelial cells, or amniotic fluid appeared not to induce notable necrosis and/or inflammatory response in contrast to the presence of bacteria (94). In a previous report, the same authors had described the unexpected presence of meconium in the airways of bovine aborted fetuses negative for the isolation of *Brucella abortus* (91).

Studies conducted in calves which died of infectious and noninfectious diseases in the first 2 weeks of life and were submitted for postmortem examination, revealed that 42.5% had evidence of meconium, squamous cells, or keratin in their lungs (95). Lesions consisted of a mild but diffuse alveolitis characterized by exudation of neutrophils, macrophages and multinucleated giant cells. It was concluded that the microscopic findings in the lungs of calves were similar to those described in human babies with MAS (95). The high frequency of meconium and squames in the lungs raised the possibility that amniotic aspiration could be a normal incidental finding in newborn calves and not associated with hypoxia. To answer this question, a second study was designed to investigate if aspiration of meconium

and pulmonary inflammation were associated to neonatal acidosis (96). Results of this study showed that keratin and meconium often were accompanied by mild exudative alveolitis and focal atelectasis. However, aspiration of these materials was not necessarily accompanied by neonatal hypoxemia, acidosis, or failure of passive transfer of colostral immunoglobulins (96).

MAS has also been recognized as one of the factors associated with perinatal asphyxia in foals which has several repercussions including respiratory distress (97,98). The presence of meconium, squamous epithelial cells and atelectasis has also been described in foals that died on or before 5 days of age. Interestingly, a condition morphologically indistinguishable from hyaline membrane disease in infants with atelectasis has also been described in foals (99).

MAS has been sporadically reported but not well documented in small animal medicine. A single case study reported the death of a puppy from a litter of healthy dogs 48 hours after birth. The lungs of this puppy had microscopic evidence of meconium, keratin and epidermal cells in association with moderate alveolar inflammation in bronchioles and alveoli (100). Microscopic lesions in the lungs of this puppy were consistent with MAS. It was also suggested that this condition is not well documented in puppies, perhaps because of the low number of canine neonates submitted for postmortem examination or because microscopic changes are subtle and overlooked.

Although few reports have been published in veterinary medicine in contrast with human medicine, the evidence that is available strongly supports the natural occurrence of MAS in domestic animals, such as calves, foals and dogs.

1.2.2. Animal models of MAS

Most of the published morphological information associated with the aspiration of amniotic fluid and meconium in lungs has been from descriptions of natural cases in humans and in experimental animal models. As in many other human diseases, attempts have been made to reproduce MAS experimentally in laboratory animals and under controlled conditions to study the nature and progression of lung lesions. Different animal species have been used as animal models of MAS, including rabbits (31,44,81,101-103), guinea pigs (57), rats (54,79,80,104), dogs (18), cats (105), pigs (30,38,41,82,106), lambs (74,107) and baboons (108). These animal models have been utilized to investigate, under experimental conditions, the effect of meconium and its natural vehicle in MAS, the amniotic fluid. The same pathogenesis and lesions of MAS as in humans have been successfully demonstrated in animal models.

Experimental animal models of MAS have mainly focused on evaluating the management and therapy of the illness with different methods of ventilation, corticosteroids, nitric oxide and replacement of surfactant. It is important to note that most of the experimental animal models have been developed using adult animals in spite of the fact that MAS is a disease of the newborn. It is also axiomatic the structural differences between the developing and the adult lung, in addition to the different inflammatory response and defense mechanisms in neonates. The aforementioned, question the validity of using adult animals to reproduce a neonatal syndrome. Hence, there is a need for neonatal models to evaluate the injury and inflammatory response and to better understand the pathogenesis in order to eventually prevent MAS.

1.3. Objectives

General objective

The general objective of this study was to evaluate the effect of amniotic fluid and meconium in the lungs of neonatal rats.

Specific objectives

1. To standardize a neonatal rat model of MAS in Fischer-344 rats
2. To determine the normal cellular and biochemical composition of the BAL fluid in neonatal rats.
3. To quantify the cytological and biochemical changes in the BAL as indicators of the magnitude of pulmonary injury and inflammatory response in neonatal rats intratracheally inoculated with homologous amniotic fluid and meconium.
4. To evaluate the acute and chronic microscopic changes in the lungs of neonatal rats intratracheally inoculated with amniotic fluid and meconium.
5. To investigate the effect of meconium on the morphometry and ultrastructure of the lungs in neonatal rats.

1.4. REFERENCES

1. CLEARY GM, WISWELL TE. Meconium-stained amniotic fluid and the meconium aspiration syndrome. An update. *Pediatr Clin North Am* 1998; 45: 511-529.
2. WISWELL TE, TUGGLE JM, TURNER BS. Meconium aspiration syndrome: have we made a difference? *Pediatrics* 1990; 85: 715-721.
3. KATZ VL, BOWES WAJ. Meconium aspiration syndrome: reflections on a murky subject. *Am J Obstet Gynecol* 1992; 166: 171-183.
4. SRINIVASAN HB, VIDYASAGAR D. Meconium aspiration syndrome: current concepts and management. *Compr Ther* 1999; 25: 82-89.
5. BRADY JP, GOLDMAN SL. Management of Meconium Aspiration Syndrome. In: Thibeault D W, Gregory GA, eds. *Neonatal Pulmonary Care*. Connecticut: Appleton-Century-Crofts, 1986: 483-498.
6. BACSIK RD. Meconium aspiration syndrome. *Pediatr Clin North Am* 1977; 24: 463-479.
7. VYAS H, MILNER AD. Other respiratory diseases in the neonate. In: Robertson N R Ceds. *Textbook of Neonatology*. New York: Churchill Livingstone, 1986: 317-318.
8. GOODING CA, GREGORY GA. Roentgenographic analysis of meconium aspiration of the newborn. *Radiology* 1971; 100: 131-140.
9. WISWELL TE, BENT RC. Meconium staining and the meconium aspiration syndrome. Unresolved issues. *Pediatr Clin North Am* 1993; 40: 955-981.
10. BERKUS MD, LANGER O, SAMUELOFF A, XENAKIS EM, FIELD NT, RIDGWAY LE. Meconium-stained amniotic fluid: increased risk for adverse neonatal outcome. *Obstet Gynecol* 1994; 84: 115-120.
11. LIEN JM, TOWERS CV, QUILLIGAN EJ, DE VECIANA M, TOOHEY JS, MORGAN MA. Term early-onset neonatal seizures: obstetric characteristics, etiologic classifications, and perinatal care. *Obstet Gynecol* 1995; 85: 163-169.
12. MAZOR M, FURMAN B, WIZNITZER A, SHOHAM-VARDI I, COHEN J, GHEZZI F. Maternal and perinatal outcome of patients with preterm labor and meconium-stained amniotic fluid. *Obstet Gynecol* 1995; 86: 830-833.
13. MACFARLANE PI, HEAF DP. Pulmonary function in children after neonatal meconium aspiration syndrome. *Arch Dis Child* 1988; 63: 368-372.

14. SWAMINATHAN S, QUINN J, STABILE MW, BADER D, PLATZKER AC, KEENS TG. Long-term pulmonary sequelae of meconium aspiration syndrome. *J Pediatr* 1989; 114: 356-361.
15. KOUMBOURLIS AC, MUTICH RL, MOTOYAMA EK. Contribution of airway hyperresponsiveness to lower airway obstruction after extracorporeal membrane oxygenation for meconium aspiration syndrome. *Crit Care Med* 1995; 23: 749-754.
16. PETERSON HG, PENDLETON ME. Contrasting roentgenographic pulmonary patterns of the hyaline membrane and fetal aspiration syndromes. *Am J Roentgenol* 1955; 74: 800-813.
17. YEH TF, HARRIS V, SRINIVASAN G, LILIEN L, PYATI S, PILDES RS. Roentgenographic findings in infants with meconium aspiration syndrome. *JAMA* 1979; 242: 60-63.
18. GOODING CA, GREGORY GA, TABER P, WRIGHT RR. An experimental model for the study of meconium aspiration of the newborn. *Radiology* 1971; 100: 137-140.
19. TRAN N, LOWE C, SIVIERI EM, SHAFFER TH. Sequential effects of acute meconium obstruction on pulmonary function. *Pediatr Res* 1980; 14: 34-38.
20. GREGORY GA, GOODING CA, PHIBBS RH, TOOLEY WH. Meconium aspiration in infants--a prospective study. *J Pediatr* 1974; 85: 848-852.
21. RAPOPORT S, BUCHANAN DJ. The composition of meconium: Isolation of blood-group-specific polysaccharides. Abnormal composition of meconium in meconium ileus. *Science* 1950; 112: 150-153.
22. HOUNSELL EF, LAWSON AM, STOLL MS, KANE DP, CASHMORE GC, CARRUTHERS RA, FEENEY J, FEIZI T. Characterisation by mass spectrometry and 500-MHz proton nuclear magnetic resonance spectroscopy of penta- and hexasaccharide chains of human foetal gastrointestinal mucins (meconium glycoproteins). *Eur J Biochem* 1989; 186: 597-610.
23. ANTONOWICZ I, SHWACHMAN H. Meconium in health and in disease. *Adv Pediatr* 1979; 26: 275-310.
24. CO E, VIDYASAGAR D. Meconium aspiration syndrome. *Compr Ther* 1990; 16: 34-39.
25. MEIS PJ, HALL M, MARSHALL JR, HOBEL CJ. Meconium passage: a new classification for risk assessment during labor. *Am J Obstet Gynecol* 1978; 131: 509-513.

26. STARK RI, DANIEL SS, HUSAIN MK, SANOCKA UM, ZUBROW AB, JAMES LS. Vasopressin concentration in amniotic fluid as an index of fetal hypoxia: mechanism of release in sheep. *Pediatr Res* 1984; 18: 552-558.
27. MITCHELL J, SCHULMAN H, FLEISCHER A, FARMAKIDES G, NADEAU D. Meconium aspiration and fetal acidosis. *Obstet Gynecol* 1985; 65: 352-355.
28. STARKS GC. Correlation of meconium-stained amniotic fluid, early intrapartum fetal pH, and Apgar scores as predictors of perinatal outcome. *Obstet Gynecol* 1980; 56: 604-609.
29. WISWELL TE, HENLEY MA. Intratracheal suctioning, systemic infection, and the meconium aspiration syndrome. *Pediatrics* 1992; 89: 203-206.
30. WISWELL TE, FOSTER NH, SLAYTER MV, HACHEY WE. Management of a piglet model of the meconium aspiration syndrome with high-frequency or conventional ventilation. *Am J Dis Child* 1992; 146: 1287-1293.
31. TYLER DC, MURPHY J, CHENEY FW. Mechanical and chemical damage to lung tissue caused by meconium aspiration. *Pediatrics* 1978; 62: 454-459.
32. CLARK P, DUFF P. Inhibition of neutrophil oxidative burst and phagocytosis by meconium. *Am J Obstet Gynecol* 1995; 173: 1301-1305.
33. KOJIMA T, HATTORI K, FUJIWARA T, SASAI TM, KOBAYASHI Y. Meconium-induced lung injury mediated by activation of alveolar macrophages. *Life Sci* 1994; 54: 1559-1562.
34. JONES CA, CAYABYAB RG, HAMDAN H. Early production of proinflammatory cytokines in the pathogenesis of neonatal adult respiratory distress syndrome (ARDS) associated with meconium aspiration. *Pediatr Res* 1994; 35: 339A-
35. JONES CA, CAYABYAB RG, KWONG KY, STOTTS C, WONG B, HAMDAN H, MINOO P, DELEMOS RA. Undetectable interleukin (IL)-10 and persistent IL-8 expression early in hyaline membrane disease: a possible developmental basis for the predisposition to chronic lung inflammation in preterm newborns. *Pediatr Res* 1996; 39: 966-975.
36. SHABAREK FM, XUE H, LALLY KP. Human meconium stimulates murine alveolar macrophage procoagulant activity. *Pediatr Res* 1997; 41: 267A-
37. DE BEAUFORT AJ, PELIKAN DM, ELFERINK JG, BERGER HM. Effect of interleukin 8 in meconium on in-vitro neutrophil chemotaxis. *Lancet* 1998; 352: 102-105.

38. SOUKKA H, RAUTANEN M, HALKOLA L, KERO P, KÄÄPÄ P. Meconium aspiration induces ARDS-like pulmonary response in lungs of ten-week-old pigs. *Pediatr Pulmonol* 1997; 23: 205-211.
39. WU JM, YEH TF, WANG JY, WANG JN, LIN YJ, HSIEH WS, LIN CH. The role of pulmonary inflammation in the development of pulmonary hypertension in newborn with meconium aspiration syndrome (MAS). *Pediatr Pulmonol Suppl* 1999; 18: 205-208.
40. SOUKKA H, JALONEN J, KERO P, KÄÄPÄ P. Endothelin-1, atrial natriuretic peptide and pathophysiology of pulmonary hypertension in porcine meconium aspiration. *Acta Paediatr* 1998; 87: 424-428.
41. SOUKKA H, VIINIKKA L, KÄÄPÄ P. Involvement of thromboxane A2 and prostacyclin in the early pulmonary hypertension after porcine meconium aspiration. *Pediatr Res* 1998; 44: 838-842.
42. CLARK DA, NIEMAN GF, THOMPSON JE, PASKANIK AM, ROKHAR JE, BREDENBERG CE. Surfactant displacement by meconium free fatty acids: an alternative explanation for atelectasis in meconium aspiration syndrome. *J Pediatr* 1987; 110: 765-770.
43. MOSES D, HOLM BA, SPITALE P, LIU MY, ENHORNING G. Inhibition of pulmonary surfactant function by meconium. *Am J Obstet Gynecol* 1991; 164: 477-481.
44. SUN B, CURSTEDT T, ROBERTSON B. Surfactant inhibition in experimental meconium aspiration. *Acta Paediatr* 1993; 82: 182-189.
45. HIGGINS ST, WU AM, SEN N, SPITZER AR, CHANDER A. Meconium increases surfactant secretion in isolated rat alveolar type II cells. *Pediatr Res* 1996; 39: 443-447.
46. BAE CW, TAKAHASHI A, CHIDA S, SASAKI M. Morphology and function of pulmonary surfactant inhibited by meconium. *Pediatr Res* 1998; 44: 187-191.
47. DAVEY AM, BECKER JD, DAVIS JM. Meconium aspiration syndrome: physiological and inflammatory changes in a newborn piglet model. *Pediatr Pulmonol* 1993; 16: 101-108.
48. HÖRNCHEN H, MERZ U, WICHER W, MÜHLER E. [Persistent pulmonary hypertension of newborn. The PFC syndrome]. *Z Kinderchir* 1990; 45: 336-341.
49. MURPHY JD, RABINOVITCH M, GOLDSTEIN JD, REID LM. The structural basis of persistent pulmonary hypertension of the newborn infant. *J Pediatr* 1981; 98: 962-967.

50. MURPHY JD, VAWTER GF, REID LM. Pulmonary vascular disease in fatal meconium aspiration. *J Pediatr* 1984; 104: 758-762.
51. DAVIS RO, PHILIPS JB, HARRIS BAJ, WILSON ER, HUDDLESTON JF. Fatal meconium aspiration syndrome occurring despite airway management considered appropriate. *Am J Obstet Gynecol* 1985; 151: 731-736.
52. SERGI C, STEIN KM, BEEDGEN B, ZILOW E, LINDERKAMP O, OTTO HF. Meconium aspiration syndrome complicated by massive intravascular thrombosis. *Am J Perinatol* 1998; 15: 375-379.
53. BROWN BL, GLEICHER N. Intrauterine meconium aspiration. *Obstet Gynecol* 1981; 57: 26-29.
54. CLEARY GM, ANTUNES MJ, CIESIELKA DA, HIGGINS ST, SPITZER AR, CHANDER A. Exudative lung injury is associated with decreased levels of surfactant proteins in a rat model of meconium aspiration. *Pediatrics* 1997; 100: 998-1003.
55. PERLMAN EJ, MOORE GW, HUTCHINS GM. The pulmonary vasculature in meconium aspiration. *Hum Pathol* 1989; 20: 701-706.
56. LEVIN DL, WEINBERG AG, PERKIN RM. Pulmonary microthrombi syndrome in newborn infants with unresponsive persistent pulmonary hypertension. *J Pediatr* 1983; 102: 299-303.
57. JOVANOVIC R, NGUYEN HT. Experimental meconium aspiration in guinea pigs. *Obstet Gynecol* 1989; 73: 652-656.
58. SCHOFIELD D, COTRAN RS. Diseases of infancy and childhood. In: Cotran R S, Kumar V, Collins T, eds. *Robbins pathologic basis of disease*. Philadelphia: W.B. Saunders, Co., 1999: 459-491.
59. USTA IM, MERCER BM, SIBAI BM. Risk factors for meconium aspiration syndrome. *Obstet Gynecol* 1995; 86: 230-234.
60. DYE T, AUBRY R, GROSS S, ARTAL R. Amnioinfusion and the intrauterine prevention of meconium aspiration. *Am J Obstet Gynecol* 1994; 171: 1601-1605.
61. SPONG CY, OGUNDIPE OA, ROSS MG. Prophylactic amnioinfusion for meconium-stained amniotic fluid. *Am J Obstet Gynecol* 1994; 171: 931-935.
62. CARSON BS, LOSEY RW, BOWES WAJ, SIMMONS MA. Combined obstetric and pediatric approach to prevent meconium aspiration syndrome. *Am J Obstet Gynecol* 1976; 126: 712-715.

63. FALCIGLIA HS, HENDERSCHOTT C, POTTER P, HELMCHEN R. Does DeLee suction at the perineum prevent meconium aspiration syndrome?. *Am J Obstet Gynecol* 1992; 167: 1243-1249.
64. WISWELL TE, GANNON CM, JACOB J, GOLDSMITH L, SZYLD E, WEISS K, SCHUTZMAN D, CLEARY GM, FILIPOV P, KURLAT I, CABALLERO CL, ABASSI S, SPRAGUE D, OLTORF C, PADULA M. Delivery room management of the apparently vigorous meconium-stained neonate: results of the multicenter, international collaborative trial. *Pediatrics* 2000; 105: 1-7.
65. FOX WW, BERMAN LS, DOWNES JJ, PECKHAM GJ. The therapeutic application of end-expiratory pressure in the meconium aspiration syndrome. *Pediatrics* 1975; 56: 214-217.
66. TRUOG WE, LYRENE RK, STANDAERT TA, MURPHY J, WOODRUM DE. Effects of PEEP and tolazoline infusion on respiratory and inert gas exchange in experimental meconium aspiration. *J Pediatr* 1982; 100: 284-290.
67. YEH TF, LILIEN LD, BARATHI A, PILDES RS. Lung volume, dynamic lung compliance, and blood gases during the first 3 days of postnatal life in infants with meconium aspiration syndrome. *Crit Care Med* 1982; 10: 588-592.
68. WUNG JT, JAMES LS, KILCHEVSKY E, JAMES E. Management of infants with severe respiratory failure and persistence of the fetal circulation, without hyperventilation. *Pediatrics* 1985; 76: 488-494.
69. CARTER JM, GERSTMANN DR, CLARK RH, SNYDER G, CORNISH JD, NULL DMJ, DELEMOS RA. High-frequency oscillatory ventilation and extracorporeal membrane oxygenation for the treatment of acute neonatal respiratory failure. *Pediatrics* 1990; 85: 159-164.
70. CLARK RH, YODER BA, SELL MS. Prospective, randomized comparison of high-frequency oscillation and conventional ventilation in candidates for extracorporeal membrane oxygenation. *J Pediatr* 1994; 124: 447-454.
71. UK collaborative randomised trial of neonatal extracorporeal membrane oxygenation. UK Collaborative ECMO Trail Group. *Lancet* 1996; 348: 75-82.
72. BERNBAUM J, SCHWARTZ IP, GERDES M, DAGOSTINO JA, COBURN CE, POLIN RA. Survivors of extracorporeal membrane oxygenation at 1 year of age: the relationship of primary diagnosis with health and neurodevelopmental sequelae. *Pediatrics* 1995; 96: 907-913.

73. CHOUP, BLEI ED, SHEN SS, GONZALEZ CF, REYNOLDS M. Pulmonary changes following extracorporeal membrane oxygenation: autopsy study of 23 cases. *Hum Pathol* 1993; 24: 405-412.
74. FOUST R, TRAN NN, COX C, MILLER TFJ, GREENSPAN JS, WOLFSON MR, SHAFFER TH. Liquid assisted ventilation: an alternative ventilatory strategy for acute meconium aspiration injury. *Pediatr Pulmonol* 1996; 21: 316-322.
75. BARRINGTON KJ, FINER NN, PELIOWSKI A, ETCHES PC, GRAHAM AJ, CHAN WK. Inhaled nitric oxide improves oxygenation in piglets with meconium aspiration. *Pediatr Pulmonol* 1995; 20: 27-33.
76. RAIS-BAHRAMI K, RIVERA O, SEALE WR, SHORT BL. Effect of nitric oxide in meconium aspiration syndrome after treatment with surfactant. *Crit Care Med* 1997; 25: 1744-1747.
77. KINSELLA JP, TRUOG WE, WALSH WF, GOLDBERG RN, BANCALARI E, MAYOCK DE, REDDING GJ, DELEMOS RA, SARDESAI S, MCCURNIN DC, MORELAND SG, CUTTER GR, ABMAN SH. Randomized, multicenter trial of inhaled nitric oxide and high-frequency oscillatory ventilation in severe, persistent pulmonary hypertension of the newborn. *J Pediatr* 1997; 131: 55-62.
78. Inhaled nitric oxide in full-term and nearly full-term infants with hypoxic respiratory failure. The Neonatal Inhaled Nitric Oxide Study Group [published erratum appears in *N Engl J Med* 1997 Aug 7;337(6):434]. *N Engl J Med* 1997; 336: 597-604.
79. SUN B, HERTING E, CURSTEDT T, ROBERTSON B. Exogenous surfactant improves lung compliance and oxygenation in adult rats with meconium aspiration. *J Appl Physiol* 1994; 77: 1961-1971.
80. SUN B, CURSTEDT T, ROBERTSON B. Exogenous surfactant improves ventilation efficiency and alveolar expansion in rats with meconium aspiration. *Am J Respir Crit Care Med* 1996; 154: 764-770.
81. SUN B, CURSTEDT T, SONG GW, ROBERTSON B. Surfactant improves lung function and morphology in newborn rabbits with meconium aspiration. *Biol Neonate* 1993; 63: 96-104.
82. WISWELL TE, PEABODY SS, DAVIS JM, SLAYTER MV, BENT RC, MERRITT TA. Surfactant therapy and high-frequency jet ventilation in the management of a piglet model of the meconium aspiration syndrome. *Pediatr Res* 1994; 36: 494-500.
83. FINDLAY RD, TAEUSCH HW, WALTHER FJ. Surfactant replacement therapy for meconium aspiration syndrome. *Pediatrics* 1996; 97: 48-52.

84. HALLIDAY HL, SPEER CP, ROBERTSON B. Treatment of severe meconium aspiration syndrome with porcine surfactant. Collaborative Surfactant Study Group. *Eur J Pediatr* 1996; 155: 1047-1051.
85. SUN B. Use of surfactant in pulmonary disorders in full-term infants. *Curr Opin Pediatr* 1996; 8: 113-117.
86. OHAMA Y, ITAKURA Y, KOYAMA N, EGUCHI H, OGAWA Y. Effect of surfactant lavage in a rabbit model of meconium aspiration syndrome. *Acta Paediatr Jpn* 1994; 36: 236-238.
87. PARANKA MS, WALSH WF, STANCOMBE BB. Surfactant lavage in a piglet model of meconium aspiration syndrome. *Pediatr Res* 1992; 31: 625-628.
88. KRISHNAN L, NASRUDDIN, PRABHAKAR P, BHASKARANAND N. Routine antibiotic cover for newborns intubated for aspirating meconium: is it necessary? *Indian Pediatr* 1995; 32: 529-531.
89. KOTERBA AM. Disorders of the Neonatal Foal. In: Beech Jeds. *Equine Respiratory Disorders*. Philadelphia: Lea & Febiger, 1991: 403-429.
90. SMITH BP. *Large Animal Internal Medicine*. Toronto: The CV Mosby Company, 1990.
91. LÓPEZ A, HITOS F, PÉREZ A, NAVARRO FR. Lung lesions in bovine fetuses aborted by *Brucella abortus*. *Can J Comp Med* 1984; 48: 275-277.
92. MILLER RB. A summary of some of the pathogenetic mechanisms involved in bovine abortion. *Can Vet J* 1977; 18: 87-95.
93. MILLER RB, QUINN PJ. Observations on abortions in cattle: a comparison of pathological, microbiological and immunological findings in aborted foetuses and foetuses collected at abattoirs. *Can J Comp Med* 1975; 39: 270-290.
94. LOPEZ A, PEREZ A, ANGULO G. Distribution of lesions in the lungs of aborted bovine fetuses. *Can Vet J* 1989; 30: 519-521.
95. LOPEZ A, BILDFELL R. Pulmonary inflammation associated with aspirated meconium and epithelial cells in calves. *Vet Pathol* 1992; 29: 104-111.
96. LOPEZ A, LÖFSTEDT J, BILDFELL R, HORNEY B, BURTON S. Pulmonary histopathologic findings, acid-base status, and absorption of colostral immunoglobulins in newborn calves. *Am J Vet Res* 1994; 55: 1303-1307.

97. FURR M. Perinatal asphyxia in foals. *Compend Contin Educ Pract Vet* 1996; 18: 1342-1351.
98. KOTERBA A, HAIBEL G. Respiratory distress in a premature foal secondary to hydrops allantois and placentitis. *Compend Contin Educ Pract Vet* 1983; 5: 121-125.
99. DUBIELZIG RR. Pulmonary lesions of neonatal foals. *Equine Med Surg* 1977; 1: 419-425.
100. FUENTEALBA C, LOPEZ A. Intrauterine aspiration pneumonia. Diseases of the respiratory system. Western Conference of Veterinary Diagnostic Pathologists; Saskatoon, Saskatchewan: 1998.
101. CRUICKSHANK AH. The effects of the introduction of amniotic fluid into the rabbits' lungs. *J Pathol Bact* 1949; 61: 527-531.
102. FRANTZ ID, WANG NS, THACH BT. Experimental meconium aspiration: Effects of glucocorticoid treatment. *J Pediatr* 1975; 86: 438-441.
103. AL MATEEN KB, DAILEY K, GRIMES MM, GUTCHER GR. Improved oxygenation with exogenous surfactant administration in experimental meconium aspiration syndrome. *Pediatr Pulmonol* 1994; 17: 75-80.
104. CALKOVSKA A, SUN B, CURSTEDT T, RENHEIM G, ROBERTSON B. Combined effects of high-frequency ventilation and surfactant treatment in experimental meconium aspiration syndrome. *Acta Anaesthesiol Scand* 1999; 43: 135-145.
105. MAMMEL MC, GORDON MJ, CONNETT JE, BOROS SJ. Comparison of high-frequency jet ventilation and conventional mechanical ventilation in a meconium aspiration model. *J Pediatr* 1983; 103: 630-634.
106. SOUKKA H, HALKOLA L, AHO H, RAUTANEN M, KERO P, KÄÄPÄ P. Methylprednisolone attenuates the pulmonary hypertensive response in porcine meconium aspiration. *Pediatr Res* 1997; 42: 145-150.
107. SHELDON G, BRAZY J, TUGGLE B, CRENSHAW CJ, BRUMLEY G. Fetal lamb lung lavage and its effect on lung phosphatidylcholine. *Pediatr Res* 1979; 13: 599-602.
108. BLOCK MF, KALLENBERGER DA, KERN JD, NEPVEUX RD. In utero meconium aspiration by the baboon fetus. *Obstet Gynecol* 1981; 57: 37-40.

2. EXPERIMENTAL MODEL OF MECONIUM ASPIRATION SYNDROME

2.1. Introduction

Meconium aspiration syndrome (MAS) remains a major contributor to neonatal respiratory distress and an important cause of morbidity and mortality in term and post-term infants. The pathophysiology of the pulmonary injury in MAS is still unclear, but includes airway obstruction, pulmonary inflammation, surfactant dysfunction and pulmonary hypertension (1-3). In Veterinary Medicine, MAS has been recognized as one of the main factors involved in perinatal asphyxia and respiratory distress in foals (4-6) and has been reported in calves (7,8) and in dogs (9). The microscopic changes in the lungs of animals with aspiration of amniotic fluid and meconium are similar to those described in human babies with MAS.

To advance the understanding of the pathophysiology of MAS, experimental models have been put forth by various researchers using baboons (10), lambs (11,12), pigs (13-16), dogs (16,17), cats (18), rabbits (3,18,19), guinea pigs (20) and rats (21-24). These models are based on the experimental inoculation of meconium and amniotic fluid into the lungs. More recently, animal models have been used to evaluate therapies in MAS, but little has been reported about the injury and inflammatory response in the lungs of experimental animals (13,23,25).

A major criticism of many of these experimental models of MAS, and particularly those with laboratory rodents, could be the use of adult animals when in fact this is a neonatal syndrome and the inflammatory response and defense mechanisms are known to be different in neonates (26-29). Several factors may explain why researchers have avoided

using neonatal rodents in experimental MAS (3,35). First, the small size of the neonatal rodent makes intratracheal inoculation a very difficult task, since it requires direct visualization of the laryngeal lumen under general anesthesia (30-32). The metal laryngoscope routinely used for intratracheal inoculation of adult rodents is unsuitable for rat pups, not only because of the small size of the oral cavity, but also because of the extreme fragility of neonatal mucosal tissues (31). These have limited attempts to utilize neonatal rats for models of MAS.

There are additional biological factors that hinder experimental work with neonatal rodents. Rat pups are notably susceptible to hypothermia and hypoglycemia which may reduce survival rates following anesthesia and intratracheal inoculation (33,34). Maternal rejection and cannibalism, which constitutes other perplexing phenomena in periparturient rodents, creates additional problems following anesthesia and manipulation (34,35). Fortunately, these maternal problems can be avoided by means of preconditioning programs, some of which include exposing the dam to the odors of experimental substances and materials prior to parturition (34,36,37).

Rats are one of the preferred animal species for experimental lung research because they are reasonably priced, easy to raise in disease-free environments, available from commercial sources, and genetically homogeneous, and have lungs of suitable size for morphological studies (38,39). The Fischer 344 rat has important advantages in experimental lung research over the other strains primarily because of its relative resistance to pulmonary infections, small body size, and uniform growth of the lungs (38). As a result of the widespread use of this strain of rat, there is abundant information on methods for lung

fixation, normal pulmonary morphology, lung pathology, ultrastructure and lung morphometry (40,41). For all these reasons, F-344 rats could provide a good animal model for experimental study of the pulmonary changes in MAS.

A second criticism of experimental models of MAS in laboratory animals could be the use of heterologous meconium collected from newborn babies (42,43). One reason why human meconium is commonly used in animal studies is perhaps due to the difficulty in collecting meconium from small neonatal rodents, particularly rats. For instance, one newborn human baby may provide from 60 to 200g of meconium while many neonatal rats are needed to obtain sufficient meconium for inoculum preparation (44). Human meconium is generally used as inoculum in the form of fresh slurry diluted with saline (3,19). In other instances, human meconium is frozen or lyophilized (42), filtered (43), or filtered and lyophilized (49) prior to inoculation (45).

The viscosity of the meconium is another important factor that needs to be considered in experimental models of MAS. Frequently, meconium is filtered or diluted in saline solution to prevent airway obstruction, asphyxia and death during inoculation (45). Different concentrations of human meconium have been used in the experimental models of MAS in adult animals (10,43,46), puppies (16), piglets (1,13), neonatal rabbits (45) and guinea pigs (20). Some of these studies reported complications and unexpected mortalities in experimental animals following meconium inoculation (3,16,24).

Amniotic fluid (AF) is also an inherent component of aspirated material in MAS, yet the effect of this fluid in the neonatal lung following perinatal aspiration has been poorly investigated (18,20). In one experimental model, amniotic fluid was collected directly from

the uterus in euthanized rabbits or by hysterectomy and inoculated in adult rabbits (18). Results of this study showed pulmonary inflammatory response consistent with MAS.

Similar to experimental models of MAS, laboratory investigations have been conducted inoculating heterologous amniotic fluid collected by amniocentesis from pregnant women (18,20) or from cows (47). However, little has been done to standardize the collection of amniotic fluid from term-pregnant rats that could be used as homologous inoculum in a rat model of MAS.

In order to standardize a reliable animal model of MAS, it is also necessary to find an intratracheal dose of meconium and AF, that when inoculated, could consistently reproduce morphologic changes in the lungs. This dose should be non-lethal yet able to cause significant airway obstruction, inflammation and atelectasis, the main pulmonary changes observed in MAS (48). The LD₅₀ for meconium and amniotic fluid in intratracheal inoculations is unknown and, according to current animal care guidelines, determination of this value is no longer acceptable (49,50). An alternate and acceptable approach to the LD₅₀ is the so-called "BTS Fixed Dose Method"(51). This novel approach, suggested by the British Toxicological Society for use in acute toxicity testing, was validated in 1991 and has been adopted by countries of the European Economic Community (EEC)(49,52,53).

Finally, to standardize an animal model for MAS, it would be necessary to find a good method of inoculation that would permit delivery of meconium and amniotic fluid into the neonatal lung. Because of its physical properties, including viscosity and particle size, it is not practical to deliver meconium by conventional aerosol system (32,54). Instead, it is better, as reported by others, to deliver meconium and amniotic fluid directly into the

lungs by means of intratracheal inoculation (22,47). The advantages of intratracheal inoculation include a fairly simple and rapid procedure, a wide range of treatment-doses that can be administered to experimental animals, and the fact that the inoculum can be placed directly in the lungs, thus bypassing the upper respiratory tract (31,32). Intratracheal administration also simulates aspiration of oropharyngeal material into the lower airways, mimicking the route of exposure in natural cases of MAS (55).

Laboratory methods for introducing meconium and amniotic fluid into the distal airways of adult rats have also been described in the literature. In one method, the lungs are cannulated by means of a tracheotomy (22,24,25), while in the other, intratracheal inoculation is done by endotracheal or transoral intubation (22,47). In models using neonatal rats, the only method of inoculation that has been described is the use of microspheres inoculated using surgical incision and transtracheal intubation (30). To our knowledge, intratracheal (transoral) inoculation has not been validated in neonatal rats.

The general objective of this study was to standardize a neonatal rat model of MAS in Fischer 344 rats. The specific objectives included the standardization of: 1- a method for intratracheal (transoral) inoculation in rat pups; 2- a method for the collection of meconium and amniotic fluid in rats; 3- an intratracheal dose of homologous meconium and amniotic fluid in rats that would closely mimic natural cases of MAS.

2.2. Material and methods

2.2.1. Animals and breeding programs

Fischer 344 pregnant rats were obtained from commercial sources (Charles River, Quebec) 14-16 days before parturition as original breeding stock at the AVC. Once pups

were born, female and some male neonates were selected to be part of a timed pregnancy program following standard reproductive protocols described by others (56,57). Rats were housed individually, provided with commercial food (Rodent laboratory Chow 5001, Purina) and water *ad libitum*, and maintained on a 12/12-hour light/dark cycle at 22°C and 50% relative humidity.

Groups of 5 female rats were housed in a cage with 2 male rats for 6 days. Cell patterns during the estrous cycle and mating were determined using daily vaginal cytology (56,57). The presence of sperm in vaginal samples indicated that mating had taken place and was recorded as day zero. All births were carefully monitored and the age and sex of rat pups recorded. To avoid confounding effects due to sex (58) only male pups were utilized for inoculation studies. Female pups were euthanised and frozen immediately after birth and subsequently used for collection of meconium. Male pups were kept with their dams in groups of 5 to 6 and were only removed from the cage for inoculation.

2.2.2. *Preconditioning programs*

To reduce infant rejection and cannibalism of the offspring, pregnant rats were preconditioned 7-10 days before parturition following the protocol described by Park *et al.* (34). During this period, dams were exposed in their cages to the smell of materials to be used with neonatal rats. Perforated stainless steel oval containers were attached to the cage's wire lid and suspended free into the cage. A piece of cotton was introduced in the container and several drops (0.39ml) of anesthetic, ethanol, saline solution and tattoo ink along with small pieces (2 x 2 cm) of latex gloves were placed daily inside of the oval container. Twelve litters with an average of 8 pups per litter were used, 6 of them were exposed to the

preconditioning program and the remaining 6 as controls without the procedure. To assess rejection and cannibalism, pups were manipulated after delivery and weighed every day during the first week and also tattooed and exposed to anesthesia and to the inoculation procedure.

2.2.3. Tattooing

For identification purposes, animal tattoo ink (Ketchum Manufacturing Inc., Ottawa) was injected subcutaneously using a 0.5 ml disposable plastic syringe with 28-gauge needle (Becton Dickinson, Franklin Lakes, NJ). Five different anatomical sites were selected for ink injection: flanks, abdomen, the base of the tail, the dorsal middle aspect of the tail, and the dorsal posterior aspect of the tail. Tattoo integrity and visibility were evaluated daily for 30 days.

2.2.4. Anesthesia

To choose and standardize the best type of anesthesia for intratracheal inoculation in neonatal rats, two different anesthetic protocols were tested. In the first protocol, neonates were anesthetized with halothane via a gas anesthetic machine with a modified delivery system adapted for small neonates (34). Pups were removed from the cage one at a time and placed in ventral recumbency on a heating pad maintained at 38°C. Each pup's nose was gently inserted into a small nose chamber connected with plastic tubing to the anesthetic circuit. The dose of anesthetic was 3% halothane (Fluotane®, MTC Pharmaceutical, Mississauga, Ontario, Canada) in 100% oxygen administered at 100-200 ml/minute. All the experimental procedures involving halothane anesthesia were performed in a fume hood.

The second protocol included a neuroleptoanalgesic combination (34,59). For induction of anesthesia Fentanyl, an opioid ($0.05\mu\text{g/g}$; Janssen-Ortho Inc, Toronto) and Midazolam, a benzodiazepine ($2.5\mu\text{g/g}$; Hoffmann- La Roche Ltd, Mississauga, ON) were subcutaneously injected in the dorsal region. To reverse the effect, Naloxone, an opioid antagonist ($0.1\mu\text{g/g}$; Dupont Pharma, Mississauga, ON), and Flumazenil, a benzodiazepine antagonist ($0.1\mu\text{g/g}$; Hoffmann-La Roche Ltd, Mississauga, ON), were also administered subcutaneously (59).

Two pilot studies were conducted in 15 pups (1-day-old) and in 15 pups (5-days-old). Each study was further divided into three subgroups according to the following protocol: 5 pups received halothane anesthesia, 5 pups received the neuroleptoanalgesic combination, and the remaining 5 animals were kept as controls. Control pups received oxygen for 15 min. A third study was conducted in 42 7-day-old neonates receiving just halothane anesthesia. Pups were selected at random and removed from the dam one at a time. The loss of pedal reflex was used as an indicator of the depth of anesthesia level required for intratracheal inoculation (59). Neonates were carefully observed and the induction and recovery times were recorded.

2.2.5. Collection of amniotic fluid

Full-term pregnant rats (21 days) were individually anesthetized with halothane in a plexiglass chamber following standard procedures (47,59). After induction (~ 3 min), each rat was transferred to a board held at 45° and kept under halothane using a nose chamber. Under deep anesthesia, an incision was made in the abdominal midline and the uterus was removed *en toto*. After extraction, the uterus was placed in a sterile petri dish and the rat was

euthanised with an overdose of halothane anesthesia. Under sterile conditions, the uterus was suspended with forceps in a support stand with clamps and the uterus and placenta were punctured with a 25-gauge (0.50mm x 16mm) needle (Becton Dickinson, Franklin Lakes, NJ). The amniotic fluid was aseptically collected using sterile capillary tubes and simultaneously transferred to sterile plastic vials and stored at 4-6°C. Samples contaminated with blood were discarded. Samples of amniotic fluid were submitted for routine cytology and bacteriological cultures. The final volume and concentration of amniotic fluid was adjusted for the inoculation of neonatal rats according to the results of the dose-range finding study reported in section 2.2.7.

2.2.6. Collection of meconium

Female rat pups were killed at the time of birth before intake of colostrum with an anesthetic overdose of halothane, and kept frozen at -20°C until processing. Frozen neonates were immersed in 10% Povidone-iodine (Purdue Frederick, Inc, ON), transferred to a board held at 45° and secured with adhesive tape. An abdominal incision was made, and the large intestine was carefully removed and placed in sterile petri dishes. Meconium was collected by gently squeezing the intestine under aseptic conditions. Once removed from the intestine, meconium was put in cryovials (Nalge Company, NY) and kept frozen at -80°C until preparation of the inoculum. When required, meconium was thawed and suspended in saline solution and homogenized using a Vortex mixer (Fisher Scientific, N.Y.). Samples of meconium were also submitted for routine bacteriological cultures to ensure sterility. The final concentration of unfiltered meconium was adjusted for the inoculation of rat neonates according to the results of the dose-range finding study reported in the next section.

2.2.7. Dose range-finding study

The dose of meconium, amniotic fluid and saline solution for intratracheal inoculation in 7-day-old Fischer 344 rats was determined according to the method suggested by the British Toxicology Society (51). These maximum tolerated doses were calculated as follows:

2.2.7.1 Maximum tolerated dose (MTD) for saline solution

Based on preliminary observations and information obtained from other laboratories (Dr. Pinkerton, personal communication) regarding the total lung capacity of Fischer 344 neonates, four different doses of saline solution (0.05, 0.10, 0.15 and 0.20 ml) were used. This study was considered an acute toxicity study, therefore, clinical signs, respiratory collapse and death were evaluated during a period of 15 days after inoculation. The number of neonates and the different doses of intratracheal inocula are summarized in Table I.

The initial dose selected for intratracheal inoculation was 0.1 ml and the following assumptions were followed: if the first dose produced no signs of respiratory collapse, a second higher dose (0.15 ml) was used. If the second dose produced no signs, then, the inoculation was conducted using 0.20 ml. If 0.1ml induced respiratory collapse and death, however, a lower dose (0.05ml) was selected for inoculation. The overall purpose of the test was to identify the MTD with less respiratory collapse and no mortality. The maximum tolerated dose was used as the volume of vehicle for control groups.

2.2.7.2. Maximum tolerated dose for amniotic fluid

The initial dose of amniotic fluid selected was 0.1 ml. If the dose produced no signs of respiratory collapse, the second higher dose (0.15 ml) was used. If the second dose

produced no signs, then the experiment was conducted with the higher dose. However, if 0.1 ml induced respiratory collapse and death, the lowest dose (0.05ml) was used (Table I). The objective of the test was to identify the MTD of 100% amniotic fluid without inducing respiratory collapse or death. The MTD was used as the high dose for inoculations. The lowest dose was 0.5 of the concentration of the MTD (50% amniotic fluid diluted in saline).

2.2.7.3. Maximum tolerated dose for meconium

Once the MTD dose of saline (vehicle) solution was determined, the last step was to carry out a dose range-finding study for the concentration of meconium diluted in saline solution to be used as inoculum. Theoretically, meconium is highly diluted into the amniotic fluid before it is aspirated *in utero* by the human neonate in MAS. With the aim of mimicking the natural conditions of MAS in this rat model, and based on some models of ITI of meconium in dogs (16,17), adult rabbits (3,18), and adult rats (21-23) four levels of meconium concentration (10%,15%, 20% and 25 %) were tested (Table I).

The initial concentration of meconium selected was 20%, because this is similar to the concentration of meconium in AF in natural cases in humans (60). If respiratory collapse or death did not occur, the experiment was repeated at 25%. If the initial dose produced no signs or deaths, then the inoculation was conducted with a higher dose. If 20% induced respiratory collapse and death, however, the lowest concentration (10%) was used. The objective of this test was to identify the maximal tolerated dose of meconium without inducing respiratory collapse or death. The maximum tolerated dose was used for ITI.

Table I. Design for dose range-finding study for intratracheal inoculation of saline solution, amniotic fluid and meconium in 7-day-old rat pups.

| Saline Solution | Neonates | Amniotic Fluid | Neonates | Meconium in Saline (0.05ml) | Neonates |
|-------------------------|----------|------------------|----------|-----------------------------|----------|
| Dose 1 (0.05 ml) | 5 | (0.05ml) | 5 | (10%) | 5 |
| <u>Dose 2 (0.10 ml)</u> | 5 | <u>(0.10 ml)</u> | 5 | <u>(20%)</u> | 5 |
| Dose 3 (0.15 ml) | 5 | (0.15 ml) | 5 | (30%) | 5 |
| Dose 4 (0.20 ml) | 5 | (0.20 ml) | 5 | (40%) | 5 |
| Total | 20 | | 20 | | 20 |

*Underlined numbers indicate the initial dose selected

2.2.8. *Intratracheal inoculation (ITI).*

In pilot studies, several methods of intratracheal inoculation (ITI) were tested in dead neonatal rats. These included percutaneous-transtracheal inoculation, with and without cervical transillumination, and with a murine laryngoscope (31). To ensure successful delivery of inoculum into the neonatal lung, ITI techniques were first tested in dead animals using a liquid marker (Methylene Blue) and a 25-gauge needle. Once standardized, ITI's were performed in anesthetized pups with saline solution at different ages, starting with 15-day-old neonates and reducing the age until 7-day-old rats were successfully inoculated.

Under deep halothane anesthesia (loss of pedal reflex), the neonate was lifted and placed in a supine position in the left hand of the operator. The mouth of the neonate was opened and the tongue was gently pulled to one side. The oral cavity was moved towards

the tip of an operating otoscope (Welch Allyn, Skaneateles Falls, NY) attached to a support stand with clamps. The larynx was visualized using a small sterile speculum and otoscope/throat illuminator system (power source handle model 70500, 2.5 V and an illuminator model 21600 Welch Allyn, Skaneateles Falls, NY). Details of the otoscope are illustrated in (Fig. 2). A sterile spinal needle 25-gauge, 8.8 cm length (Becton Dickinson, Franklin Lakes, NJ) with the edge rounded, was connected to a 1-ml syringe and inserted into the proximal trachea. Once in place, the inoculum was instilled into the trachea and lungs (Fig. 3). Following inoculation, pups were maintained in direct observation on a heating pad (38°C) until respiratory movements were regular and pups had recovered from anesthesia. The pups were then placed in a recovery nest with heating pad and were closely monitored for at least 30 minutes. Pups completely recovered were reunited with the dam. Neonates from the control group were inoculated with 0.05 ml of sterile saline solution. Two levels of doses of amniotic fluid were used in the neonatal rat pups. The high dose consisted of 0.05 ml of non-diluted (100%) amniotic fluid and the low dose consisted of 0.05 ml of amniotic fluid diluted in saline (50%). The final concentration of meconium was 20% in 0.05 ml saline solution. Any animal showing severe respiratory distress (dyspnea, stertor or cyanosis) was humanely euthanised with an overdose of halothane.

Twenty four hours after the inoculation, animals were euthanised and the gross distribution of the inoculum was recorded. Lungs of inoculated neonates were fixed in formalin and samples of the different lobes were processed, embedded in paraffin, sectioned at a thickness of 3 μ m and stained with hematoxylin and eosin following routine procedures

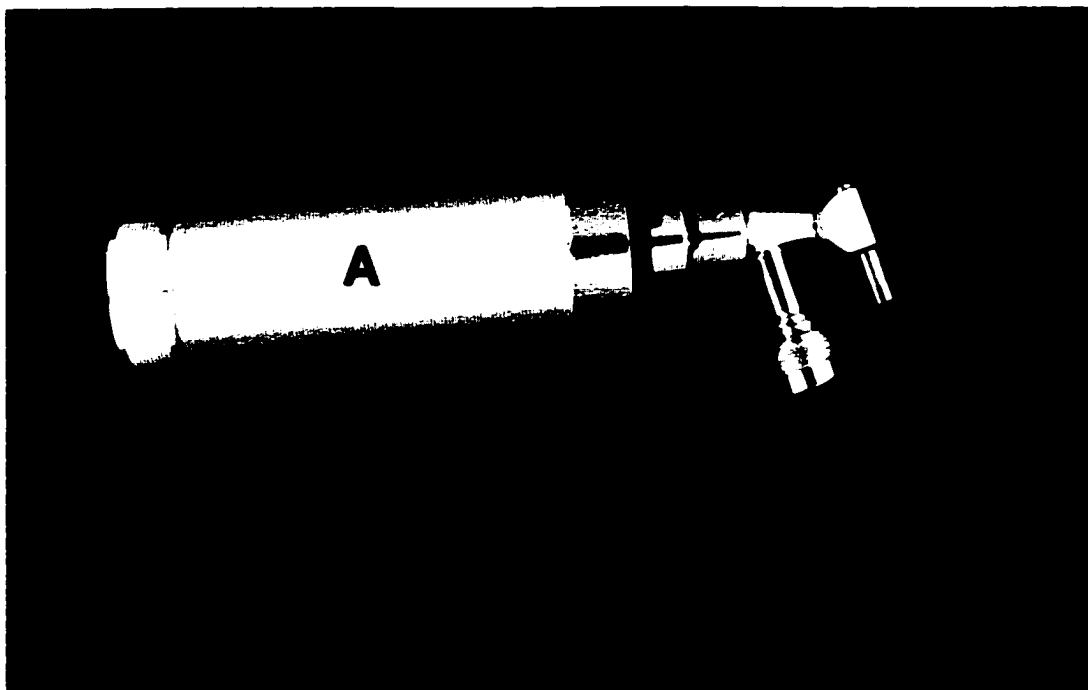


Figure. 2. Otoscope/throat illuminator system components. A. Power source 2.5V; B. Transilluminator; C. Magnifying lens; D. Speculum; E. Spinal needle 25-gauge, 8.8 cm length with the edge rounded and slightly bend.



Figure. 3. Intratracheal inoculation. The otoscope/throat illuminator system (A) is attached to a support stand (B) to achieve the proper height to the operator's view.

described in detail in section 4.2.7. Microscopic distribution of the inoculum and associated morphological changes were evaluated in all groups.

2.2.9. *Euthanasia*

The procedure of euthanasia for neonates was developed by modifying methods used in studies with adult rats (47). Neonates were euthanised with an overdose of halothane (halothane 5% in 1000 ml oxygen; 5-6 min)(Fluothane®, MTC Pharmaceutical, Missisauga, Ontario, Canada), in a plexiglass chamber connected to the anesthesia machine, and exsanguinated by severing the renal arteries.

The anesthetic protocol used for terminal cesarean section for collection of amniotic fluid was performed using halothane 5% in 1000 ml oxygen, for 12 min in a plexiglass chamber. After extraction of uterus, the dam was euthanised by sectioning of the renal arteries. Experiments were conducted following the guidelines of the Canadian Council on Animal Care (61).

2. 3. Results:

2.3.1. Breeding programs

Using vaginal cytology evaluated daily, it was possible to recognize cellular patterns of the different phases of the estrous cycle (diestrus, pro-estrus, estrus and meta-estrus). Mating occurred in late estrus and, after detection of sperm by cytology, was counted as day 0. From the sperm positive females, 90% delivered pups in 21.8 ± 0.47 days of gestation.

2.3.2. Preconditioning programs

Handling rat neonates after birth was achieved without the development of an aggressive behavior in the dams. Infant rejection or cannibalism was not detected after

weighing, tattooing, anesthesia or inoculation. Interestingly, rejection or cannibalism was also not detected in the 6 litters of rats that were not preconditioned.

2.3.3. Anesthesia:

The number of neonates, body weight, induction and recovery times are summarized in Table II. Neonates anesthetised with halothane had faster induction and recovery times. The neuroleptoanalgesic combination induced some tenderness and discomfort at the site of subcutaneous inoculation. In addition, some pups developed cyanosis and the induction times were longer than the limit of 20 min originally established for this study. Mortality was not observed in any experimental group. Based on these results, halothane was selected as the anesthetic used to facilitate the intratracheal inoculation of neonatal rats.

Table II. Number of Fischer 344 neonates, body weight and induction and recovery times in the two different protocols of anesthesia. (Weights and times are given as means \pm SD).

| Age & body weight | Halothane ¹ | | Neuroleptanalgesic ² | | Control ³ | |
|----------------------------------|------------------------|---------------------|---------------------------------|---------------------|----------------------|---------------------|
| | Induction Time (min) | Recovery Time (min) | Induction Time (min) | Recovery Time (min) | Induction Time (min) | Recovery Time (min) |
| 1 day (n=15) 4.95 \pm 0.16g | 10.95 \pm 1.45 | 1.95 \pm 1.10 | > 20 | ND | 5 | 5 |
| 5 days(n=15) 7.85 \pm 0.53g | 10.65 \pm 1.45 | 0.95 \pm 0.23 | >20 | ND | 5 | 5 |
| 7 days(n=42) 13.9 \pm 1.81g | 7.81 \pm 0.69 | 0.88 \pm 0.32 | | | | |

¹. Induction: Halothane 3% and oxygen 200 ml/min. Maintenance: Halothane 2%, oxygen 200ml/min.

². Neuroleptanalgesic combination:

Induction: Fentanyl (0.05 μ g/g) & Midazolam (2.5 μ g/g).

Reverse: Naloxone (0.1 μ g/g) & Flumazenil (0.1 μ g/g).

³. Controls: Induction: oxygen 200 ml/min, maintenance: oxygen 200 ml/min.

2.3.4. Collection of amniotic fluid

Suspension of the pregnant uterus facilitated the collection of the amniotic fluid by gravity. The volume of amniotic fluid collected varied slightly (2-2.5 ml/uterus). Further, the volume of amniotic fluid recovered from a uterus in late gestation (21-22 days) yielded smaller volumes of fluid than that at 18-20 days. Bacteriological cultures from different collections of amniotic fluid were consistently negative.

2.3.5. Collection of meconium

Dissection of the abdominal cavity, isolation of the distal large intestine and collection of meconium were easier in frozen neonates. Proper dissection and collection were not easily achieved in fresh neonates. The amount of meconium collected from each neonate was minimal and pooling the contents of several animals was necessary to obtain sufficient inoculum. Bacteriological cultures from samples of meconium were negative.

2.3.6. Dose range-finding study

The results of the dose range-finding study for saline solution, amniotic fluid and meconium are summarized in Table III. Considering that the initial selected dose of 0.1 ml of saline solution induced respiratory collapse in 60% and 20% mortality, the dose was lowered to 0.05ml. No mortality was observed in pups given the lower dose.

The initial dose of amniotic fluid was set at 0.1 ml of 100% amniotic fluid, however, this dose induced respiratory collapse in 100% of inoculated pups and 40% of them died immediately following inoculation. The second dose was 0.05 ml and induced only transient respiratory collapse in all inoculated pups and 20% mortality. Based on this low mortality, and being the minimal volume feasible to be handled, the 0.05ml of 100% amniotic fluid was

Table III. Complications and mortality in the dose range-finding study for intratracheal inoculation of saline solution, AF and meconium in 7-day-old rat pups. (Weights are given as means \pm SD).

| Inoculum | Dose | N | Weight (g) | Respiratory collapse | Survivability | Mortality |
|----------|----------|---|------------------|----------------------|---------------|-----------|
| Saline | 0.1 ml | 5 | 11.24 \pm 0.66 | 3/5 | 4/5 | 1/5 |
| | 0.05 ml* | 5 | 11.78 \pm 0.66 | 0/5 | 5/5 | 0/5 |
| AF | 0.1 ml | 5 | 10.6 \pm 0.21 | 5/5 | 3/5 | 2/5 |
| | 0.05 ml* | 5 | 10.37 \pm 0.41 | 5/5 | 4/5 | 1/5 |
| Meconium | 20%* | 5 | 15.1 | 0/5 | 5/5 | 0/5 |
| | 0.05 ml | | \pm 0.35 | | | |
| | 30% | 5 | 15.1 | 1/5 | 5/5 | 0/5 |
| | 0.05 ml | | \pm 0.54 | | | |
| | 40% | 5 | 15.4 | 4/5 | 1/5 | 4/5 |
| | 0.05 ml | | \pm 0.24 | | | |

* Selected dose for the inoculation studies

established as the high dose while 50% amniotic fluid diluted in saline was selected as the lowest dose for the inoculation studies.

The initial dose of meconium diluted in saline solution was 0.05 ml of a 20% solution and did not induce respiratory collapse nor mortality. Administration of a 30% meconium solution induced respiratory collapse in 20% of neonates but not mortality. Administration of a 40% of meconium solution induced respiratory collapse in 80% of the pups and 80% mortality. At the latter dose, the surviving neonates had to be humanely euthanized three days postinoculation because of severe respiratory distress. Based on these results, 0.05 ml of a 20% meconium solution was selected as the maximum tolerated dose that could be inoculated without causing complications or mortality.

2.3.7. Intratracheal inoculation (ITI) in neonatal rat pups

ITI was easily achieved using the otoscope instead of the laryngoscope routinely recommended for mature rats. ITI was well tolerated by pups and the inoculation time was less than 1 minute. The minimum age at which the ITI could be consistently and safely achieved was 7 days. The small magnifying lens in the transilluminator allowed direct observation of the larynx and left enough free space to introduce the spinal needle in the speculum. This magnifying lens also made the placing of the needle into the tracheal lumen much easier. Bending of the last portion of the spinal needle at a 30° angle facilitated the introduction of the needle through the cone shape of the speculum and placement of the inoculum into the larynx. After intratracheal injections of inocula, a brief apnea was observed in many neonates but all regained normal respiratory movements within 2 minutes.

In the pilot studies, ITI of methylene blue stain showed multifocal distribution of inoculum involving all pulmonary lobes. Inoculation of saline solution or amniotic fluid did not cause noticeable gross changes in the lungs. However, the lungs of neonates inoculated with meconium consistently showed multifocal areas of consolidation and a green discolouration of the pulmonary parenchyma. In addition, the lungs from pups inoculated with meconium did not appear well-distended following *in situ* perfusion of fixative. In contrast, the lungs of neonates inoculated with saline or amniotic fluid distended well following intratracheal fixation.

Light microscopy showed that the lungs of neonates inoculated with saline solution and killed at different postinoculation times were well aerated and did not reveal any visible morphologic changes. The lungs of neonates inoculated with amniotic fluid were also uniformly distended but revealed occasional squamous epithelial cells and keratin. These materials were diffusely but unevenly distributed in all pulmonary lobes. Sporadic histiocytic responses associated with keratin or squames were most frequently observed at 1 and 3 days postinoculation (PID). In the meconium inoculated pups, this material was present in the lungs of 100% of pups at PID 1. The distribution of meconium was widespread in all areas of the lung as shown by the percentage of pulmonary lobes containing this material. The distribution of meconium in conducting airways and alveoli at PID 1 to 14 is shown in Tables IV and V. At PID 1, meconium in conducting airways was present in 100% of pups and involved 95% of the pulmonary lobes. Meconium was microscopically seen in conducting airways of all pulmonary lobes of all pups except for the right caudal (diaphragmatic) lobe where it was only detected in 3 out of 4 of the total caudal

Table IV. Neonatal rats with microscopic evidence of meconium in conducting airways and the interlobar distribution after intratracheal inoculation.

| PID | N | Microscopic evidence of meconium | | | | | | |
|-----|---|----------------------------------|-------|------|-----------|----------|----------|-----------|
| | | Lungs | Lobes | Left | R.Cranial | R.Middle | R.Median | R. Caudal |
| 1 | 4 | 4/4 | 19/20 | 4/4 | 4/4 | 4/4 | 4/4 | 3/4 |
| 3 | 4 | 4/4 | 20/20 | 4/4 | 4/4 | 4/4 | 4/4 | 4/4 |
| 7 | 4 | 4/4 | 7/20 | 2/4 | 1/4 | 2/4 | 2/4 | 0/4 |
| 14 | 5 | 3/5 | 5/25 | 2/5 | 1/5 | 1/5 | 0/5 | 1/5 |

Table V. Neonatal rats with microscopic evidence of meconium in alveoli and the interlobar distribution after the intratracheal inoculation.

| PID | N | Microscopic evidence of meconium | | | | | | |
|-----|---|----------------------------------|-------|------|-----------|----------|----------|----------|
| | | Lungs | Lobes | Left | R.Cranial | R.Middle | R.Median | R.Caudal |
| 1 | 4 | 4/4 | 20/20 | 4/4 | 4/4 | 4/4 | 4/4 | 4/4 |
| 3 | 4 | 4/4 | 20/20 | 4/4 | 4/4 | 4/4 | 4/4 | 4/4 |
| 7 | 4 | 4/4 | 18/20 | 4/4 | 3/4 | 4/4 | 3/4 | 4/4 |
| 14 | 5 | 5/5 | 22/25 | 5/5 | 4/5 | 3/5 | 4/5 | 5/5 |

lobes studied. Meconium was present in alveoli from 100% of animals and in 100% of lobes.

The number of neonates used in the acute morphological study, their body weights at inoculation time and survival rates are shown in Table VI. Sixty three neonates were included in the inoculation and fifty six survived the whole experiment. The overall mortality rate during inoculation was 11.1%. During inoculation, one neonate in the saline group, two in the amniotic fluid group, and four in the meconium group died from respiratory collapse (5%, 9.5% and 18.2% respectively). No mortality was observed in any experimental group after the initial inoculation.

Table VI. Acute Study. Number of animals, body weight at the inoculation time, and survival rate (Body weight are given as means \pm SD).

| Group | n | Body weight (g) | Survival Rate | |
|----------------------------------|----|--------------------|---------------|------|
| | | | n | % |
| Saline (Control) | 20 | 13.41 \pm 0.13 | 19 | 95 |
| Amniotic Fluid (100%, 0.05ml) | 21 | 13.75 \pm 1.57 | 19 | 90.5 |
| Meconium (20%, 0.05ml) | 22 | 14.6 \pm 1.21 | 18 | 81.8 |
| Total | 63 | 13.94 \pm 1.59 | 56 | 88.9 |

Intratracheal inoculation of unfiltered 20% meconium induced multifocal areas of atelectasis and exudative inflammation, characterized by recruitment of neutrophils and alveolar macrophages. Edema and thickening of the alveolar septa were also seen in the lungs of all pups inoculated with meconium.

2.4. Discussion

It is well known that the conception rate in laboratory rats after mating is high (57). Results of this study showed that the probability of pregnancy in young Fischer-344 rats with a sperm-positive vaginal test was 90%. Pilot studies also confirmed what has been reported by others, that fertility and litter size progressively drops with age (33). Female rats older than one year should be withdrawn from breeding stock when the litter size begins to decline, when the inter-birth interval exceeds six weeks or when four consecutive estrous cycles occur without conception (33). The timed pregnancy-program played a pivotal role in obtaining neonates of the same age and body size as experimental animal units in our neonatal rat model of MAS.

Under the experimental conditions of this study, no difference in maternal rejection or cannibalism was observed between the preconditioned and non-preconditioned litters of Fischer-344. This was in agreement with observations by other researchers who have indicated that cannibalism in rats is restricted to stillborn pups, dead pups or those weakened by experimental procedures (35). Nonetheless, preconditioning should be used to prevent unnecessary risks in experimental work involving neonatal surgery (34,36,37). Preconditioning may also reduce risks of maternal rejection associated with animal randomization when pups of different litters and cages are mixed to obtain uniform experimental groups. This system, called crossfostering, is a technique whereby whole litters or parts of litters are reciprocally transferred from one mother to another, allowing the creation of single sex or identically sized litters (33,56).

After testing different stains (33) and anatomic sites for tattooing of neonatal pups, it was concluded that the dorsal aspect of the tail is the site of choice for dye injection. The abdominal region should be avoided in neonates as pilot studies demonstrated the tattoos in this site rapidly disappear. Three different tail sites are sufficient to properly identify pups for as long as one month after application.

Halothane dispensed by a modified delivery system proved to be an effective anesthetic technique for intratracheal inoculation in neonatal rats. The modified apparatus can be easily constructed and provides a quick solution to the scarcity of commercial devices for anesthesia in rat neonates (34). As well as being a good anesthetic for intratracheal inoculation studies in 7-day-old pups, halothane was also effective for euthanasia of neonates and adult rats. Compared to fentanyl-midazolam, halothane had faster induction and recovery times and abolished the laryngeal reflex thus allowing smooth access to the tracheal lumen (59). Another advantage of halothane in experimental lung research is the fact that, unlike other anesthetics such as barbiturates, it induces few confounding effects on biochemical parameters of BAL (62). It has been demonstrated that halothane used to euthanise adult rats induced less effect on vascular permeability, as evidenced by lower protein and sialic acids, and less erythrocytes in BAL fluid compared with other anesthetics (62). Although this lack of effect on BAL has only been reported to occur in mature or adult rats (62), it is likely that neonates anesthetized with halothane would be the same. Future studies should test the effect of halothane and other anesthetic agents on the biochemical parameters of BAL collected from newborn rats. This information would be particularly relevant in studies in which there are reduced numbers of pups in control groups.

Some authors have suggested methoxyfluorane or isofluorane as anesthetic agents for neonatal animals (59,63,64). However, the physiologic effects of these anesthetics on experimental lung research with neonates have not been well investigated (34,34). Additionally, isofluorane is more pungent than halothane and causes direct irritation of the airways which may lead to coughing, laryngospasm, and bronchospasm (65). Although hypothermic anesthesia has been recommended for neonatal rodents (66), its use is controversial (34) and therefore was not tested as an alternative in the intratracheal inoculations of this study.

The lack of anesthetic and analgesic effect of fentanyl and midazolam in the Fischer-344 neonates was an unexpected finding since good results had been reported in 1-day-old Long Evans rats (34). However, a deep plane of anesthesia is required to suppress the laryngeal reflex which is difficult to achieve with opioid-benzodiazepine combinations. Additional work is necessary to investigate the response of Fischer 344 to fentanyl and midazolam.

Another interesting finding was halothane's long induction time in rat pups compared to what has been reported in mature or adult rats. According to some reports (34,59), anesthesia in adult rats is achieved within three minutes. In contrast, 7-day-old F-344 neonates required an average of 7.8 min of halothane anesthesia. This age-related difference has been observed by others and it is likely due to physiologic variations between newborn and adult animals (34).

Bacterial contamination in fluids experimentally injected into the lung has a confounding and synergistic effect in the pathogenesis of infections and pneumonia (67).

Therefore, it is very important in experimental lung research to collect amniotic fluid under strictly sterile conditions. Bacteriologic cultures of the amniotic fluid from pregnant Fischer-344 rats were negative, indicating that sterile fluid can be collected and safely introduced intratracheally into the lungs. An important observation derived from this study was the relationship between gestation age and volume of amniotic fluid. At the end of pregnancy (day 21-22) there is less collectable amniotic fluid than in rats at 18 to 20 days of gestation. This is perhaps related to fetal size since term fetuses occupy most of the placental space causing a reduction in the volume of amniotic fluid (68). For future studies, 18-20 day pregnant rats are recommended for collection of amniotic fluid.

Standardizing the method for collection of meconium was difficult because of the small size of the newborn rats. It was necessary to pool meconium from 4-5 neonates to prepare inoculum for one inoculation, and a diligent aseptic technique was required to keep meconium free of bacterial contamination. Immersing the pups in disinfectant and dissecting the abdominal cavity under a hood were used to obtain uncontaminated samples. This difficulty in obtaining homologous meconium for intratracheal inoculation may explain in part why researchers may prefer heterologous human meconium for animal models of MAS (3,22,24). Further studies are necessary to validate if sterile human meconium can be used as inoculum in neonatal rat models of experimental MAS.

Although the technique for intratracheal (transoral) inoculation in neonatal rats required a meticulous approach, it provided consistent results and allowed for inoculation of a large number of neonates in a short time. Once standardized, this technique for neonatal inoculation is as effective and as rapid as the techniques recommended for mature and adult

rats (22,32,57). The apnea observed in some pups immediately after inoculation was only transient and rarely required resuscitation. These findings were similar to those that have been reported in studies with adult rats (31).

The modified otoscope illuminator system used in this study was essential to perform the laryngeal intubation. The routine laryngoscopic method for adult rats reported by others is not appropriate for neonatal inoculation (31). Attaching the illuminator to a fixed metal support proved to be a useful approach as it frees one hand of the operator for intubation and injection of the inoculum. Most other techniques generally require two operators, one to administer the anesthetic, and hold the rat and illuminator, and another to inject the inoculum (32).

One important attribute of intratracheal inoculation is that relatively larger quantities of inoculum may be rapidly administered and thus lead to the distribution of particles in the different lobes of the lung (30,54). Results of this study showed an excellent distribution of inoculum in the lung as illustrated by the presence of meconium in 100% of inoculated lungs. The distribution within individual lobes (lobar distribution) was also widespread as shown by the high percentage of pulmonary lobes with meconium in conducting airways and alveoli. Meconium was observed in 100% of the left, right cranial, right middle and right median lobes. The only exception was the right caudal (diaphragmatic) lobe, in which meconium remained in 100% of the alveoli, but was only in 3 out of 4 of the conductive airways. The reason for differences in distribution to the right caudal lobe is unclear but may be not biologically significant, related with the effect of the supine position during

inoculation or to the anatomical branching of bronchi as suggested by researchers investigating particle deposition in inhalation studies (54,69).

The tendency of meconium to lodge in terminal bronchioles and proximal alveoli, and to a much lesser extent in larger bronchi, has been previously described. In a study in hamsters it was found that particle deposition following intratracheal inoculation was higher in bronchioles and proximal alveoli (69). However, it is important to note that distribution of meconium in the present study was not part of a quantitative study but merely a histologic assessment of the distribution of meconium in the lobes and compartments of the lung. The tendency of meconium to disperse primarily in the proximal alveolar regions was consistent with other findings in pups inoculated with this material. This tendency is presumably the result of "peripheral" migration of meconium and has been previously documented in rabbits (19,70) and piglets (1). Migration of aspirated meconium within the lung compartments presumably starts just hours after the inoculation.

Complications and mortality rates in rat pups inoculated with amniotic fluid were minimal and comparable to values reported in newborn guinea pigs inoculated with clear amniotic fluid (20). In comparison, inoculation of bovine amniotic fluid in adult rats or homologous amniotic fluid in adult rabbits produced no mortalities (18,47). Overall, these investigations show that sterile amniotic fluid is well tolerated and that complications occur only if there is severe mechanical obstruction in major airways immediately following inoculation.

The mortality rates and complications after meconium inoculation in several species of laboratory animals appear to be more pronounced than for amniotic fluid alone (18,20).

In one study, 6.93% of adult Sprague-Dawley rats developed acidosis and died following intratracheal inoculation of 4 to 6 ml/kg body weight (25 mg[dry weight]/ml) of human meconium suspended in saline solution (23). In contrast, the same authors in another study described that 6 of 12 rats (50%) died of severe respiratory failure, hypoxemia and acidosis after inoculation of the same volume and concentration of human meconium (24). In a recent study, also conducted in adult Sprague-Dawley rats, intratracheal instillation of 0.1 ml (4.3 mg of dry weight) of 20% human meconium did not induce mortality (22).

Complications and mortality rates were low in this study with the Fischer-344 neonatal rats, particularly if the age of these animals and the dose of meconium are taken into consideration. In spite of abundant meconium particles present in the conducting airways and alveoli, the loss of experimental animals was only 18.2 % in 7-day-old pups inoculated with 0.05 ml. However, there is no detailed description of the distribution of meconium in the lungs in most experimental studies, therefore comparisons on survival rates are rather difficult to make.

It was concluded from the results of this investigation that using a modified illuminator (otoscope) simplifies intratracheal inoculation in neonatal rats. Also, intratracheal inoculation of 0.05 ml of 20% unfiltered homologous meconium in neonatal rats is well tolerated and induces microscopic changes typical of MAS. Neonatal rats are tolerant of the intratracheal inoculation of amniotic fluid and saline solution which are used as control vehicles to experimentally deliver meconium into the lung. This neonatal rat model offers a very reliable alternative method to study the pathogenesis of MAS and could be used to test therapeutic interventions for this neonatal syndrome.

2.5. REFERENCES

1. DAVEY AM, BECKER JD, DAVIS JM. Meconium aspiration syndrome: physiological and inflammatory changes in a newborn piglet model. *Pediatr Pulmonol* 1993; 16: 101-108.
2. WISWELL TE, PEABODY SS, DAVIS JM, SLAYTER MV, BENT RC, MERRITT TA. Surfactant therapy and high-frequency jet ventilation in the management of a piglet model of the meconium aspiration syndrome. *Pediatr Res* 1994; 36: 494-500.
3. TYLER DC, MURPHY J, CHENEY FW. Mechanical and chemical damage to lung tissue caused by meconium aspiration. *Pediatrics* 1978; 62: 454-459.
4. FURR M. Perinatal asphyxia in foals. *Compend Contin Educ Pract Vet* 1996; 18: 1342-1351.
5. KOTERBA A, HAIBEL G. Respiratory distress in a premature foal secondary to hydrops allantois and placentitis. *Compend Contin Educ Pract Vet* 1983; 5: 121-125.
6. DUBIELZIG RR. Pulmonary lesions of neonatal foals. *EquineMed Surg* 1977; 1: 419-425.
7. LOPEZ A, BILDFELL R. Pulmonary inflammation associated with aspirated meconium and epithelial cells in calves. *Vet Pathol* 1992; 29: 104-111.
8. LOPEZ A, LÖFSTEDT J, BILDFELL R, HORNEY B, BURTON S. Pulmonary histopathologic findings, acid-base status, and absorption of colostral immunoglobulins in newborn calves. *Am J Vet Res* 1994; 55: 1303-1307.
9. FUENTEALBA C, LOPEZ A. Intrauterine aspiration pneumonia. Diseases of the respiratory system. Western Conference of Veterinary Diagnostic Pathologists ; Saskatoon, Saskatchewan: 1998;
10. BLOCK MF, KALLENBERGER DA, KERN JD, NEPVEUX RD. In utero meconium aspiration by the baboon fetus. *Obstet Gynecol* 1981; 57: 37-40.
11. FOUST R, TRAN NN, COX C, MILLER TFJ, GREENSPAN JS, WOLFSON MR, SHAFFER TH. Liquid assisted ventilation: an alternative ventilatory strategy for acute meconium aspiration injury. *Pediatr Pulmonol* 1996; 21: 316-322.
12. SHELDON G, BRAZY J, TUGGLE B, CRENSHAW CJ, BRUMLEY G. Fetal lamb lung lavage and its effect on lung phosphatidylcholine. *Pediatr Res* 1979; 13: 599-602.

13. WISWELL TE, FOSTER NH, SLAYTER MV, HACHEY WE. Management of a piglet model of the meconium aspiration syndrome with high-frequency or conventional ventilation. *Am J Dis Child* 1992; 146: 1287-1293.
14. SOUKKA H, RAUTANEN M, HALKOLA L, KERO P, KÄÄPÄ P. Meconium aspiration induces ARDS-like pulmonary response in lungs of ten-week-old pigs. *Pediatr Pulmonol* 1997; 23: 205-211.
15. SOUKKA H, HALKOLA L, AHO H, RAUTANEN M, KERO P, KÄÄPÄ P. Methylprednisolone attenuates the pulmonary hypertensive response in porcine meconium aspiration. *Pediatr Res* 1997; 42: 145-150.
16. GOODING CA, GREGORY GA, TABER P, WRIGHT RR. An experimental model for the study of meconium aspiration of the newborn. *Radiol* 1971; 100: 137-140.
17. CHEN CT, TOUNG TJ, ROGERS MC. Effect of intra-alveolar meconium on pulmonary surface tension properties. *Crit Care Med* 1985; 13: 233-236.
18. CRUICKSHANK AH. The effects of the introduction of amniotic fluid into the rabbits' lungs. *J Pathol Bact* 1949; 61: 527-531.
19. FRANTZ ID, WANG NS, THACH BT. Experimental meconium aspiration: Effects of glucocorticoid treatment. *J Pediatr* 1975; 86: 438-441.
20. JOVANOVIC R, NGUYEN HT. Experimental meconium aspiration in guinea pigs. *Obstet Gynecol* 1989; 73: 652-656.
21. CALKOVSKA A, SUN B, CURSTEDT T, RENHEIM G, ROBERTSON B. Combined effects of high-frequency ventilation and surfactant treatment in experimental meconium aspiration syndrome. *Acta Anaesthesiol Scand* 1999; 43: 135-145.
22. CLEARY GM, ANTUNES MJ, CIESIELKA DA, HIGGINS ST, SPITZER AR, CHANDER A. Exudative lung injury is associated with decreased levels of surfactant proteins in a rat model of meconium aspiration. *Pediatrics* 1997; 100: 998-1003.
23. SUN B, HERTING E, CURSTEDT T, ROBERTSON B. Exogenous surfactant improves lung compliance and oxygenation in adult rats with meconium aspiration. *J Appl Physiol* 1994; 77: 1961-1971.
24. SUN B, CURSTEDT T, ROBERTSON B. Exogenous surfactant improves ventilation efficiency and alveolar expansion in rats with meconium aspiration. *Am J Respir Crit Care Med* 1996; 154: 764-770.

25. BARRINGTON KJ, FINER NN, PELIOWSKI A, ETCHE'S PC, GRAHAM AJ, CHAN WK. Inhaled nitric oxide improves oxygenation in piglets with meconium aspiration. *Pediatr Pulmonol* 1995; 20: 27-33.
26. SUGIMOTO M, ANDO M, SENBA H, TOKUOMI H. Lung defenses in neonates: effects of bronchial lavage fluids from adult and neonatal rabbits on superoxide production by their alveolar macrophages. *J Reticuloendothel Soc* 1980; 27: 595-606.
27. SIEGER L. Pulmonary alveolar macrophages in pre- and post-natal rabbits. *J Reticuloendothel Soc* 1978; 23: 389-395.
28. SHERMAN M, GOLDSTEIN E, LIPPERT W, WENNBERG R. Neonatal lung defense mechanisms: a study of the alveolar macrophage system in neonatal rabbits. *Am Rev Respir Dis* 1977; 116: 433-440.
29. COIGNOUL FL, BERTRAM TA, ROTH JA, CHEVILLE NF. Functional and ultrastructural evaluation of neutrophils from foals and lactating and nonlactating mares. *Am J Vet Res* 1984; 45: 898-902.
30. RUZINSKI JT, SKERRETT SJ, CHI EY, MARTIN TR. Deposition of particles in the lungs of infant and adult rats after direct intratracheal administration. *Lab Anim Sci* 1995; 45: 205-210.
31. NICHOLSON JW, KINKEAD ER. A simple device for intratracheal injections in rats. *Lab Anim Sci* 1982; 32: 509-510.
32. HENRY CJ, KOURIE E. Specialized Test Article Administration: Nose-Only Exposure and Intratracheal Inoculation. In: Salem Heds. New York: Marcel Dekker, 1987: 121-134.
33. WEIHE WH. The Laboratory Rat. In: Poole T Beds. The UFAW Handbook on the Care and Management of Laboratory Animals. England: Longman Scientific & Technical, 1987: 309-330.
34. PARK CM, CLEGG KE, HARVEY CC, HOLLENBERG MJ. Improved techniques for successful neonatal rat surgery. *Lab Anim Sci* 1992; 42: 508-513.
35. REYNOLDS RD. Preventing maternal cannibalism in rats [letter]. *Science* 1981; 213: 1146-
36. LIBBIN RM, PERSON P. Neonatal rat surgery: avoiding maternal cannibalism. *Science* 1979; 206: 66.-
37. HAYEK A, KUEHN C. A method for preventing maternal cannibalism after neonatal rat surgery. *Lab Anim Sci* 1982; 32: 171-172.

38. PINKERTON KE, CRAPO JD. Morphometry of the alveolar region of the lung. In: Witschi M D, Brain JD, eds. *Toxicology of inhaled materials*. New York: Springer-Verlag, 1985: 259-285.
39. CUMMINGS EC. Physiological measurements following inhalation exposures. In: Salem, H. *Inhalation toxicology: Research methods, applications, and evaluation*. New York: Marcel Dekker. 1987; p.153-184.
40. PINKERTON KE, BARRY BE, ONEIL JJ, RAUB JA, PRATT PC, CRAPO JD. Morphologic changes in the lung during the lifespan of Fischer 344 rats. *Am J Anat* 1982; 164: 155-174.
41. BOORMAN GA, EUSTIS SL. Lung. In: Boorman G A, Eustis SL, Elwell MR, Montgomery CA, MacKenzie WF, eds. *Pathology of the Fischer rat: reference and atlas*. California: Academic Press, 1990: 339-367.
42. OHAMA Y, ITAKURA Y, KOYAMA N, EGUCHI H, OGAWA Y. Effect of surfactant lavage in a rabbit model of meconium aspiration syndrome. *Acta Paediatr Jpn* 1994; 36: 236-238.
43. AL MATEEN KB, DAILEY K, GRIMES MM, GUTCHER GR. Improved oxygenation with exogenous surfactant administration in experimental meconium aspiration syndrome. *Pediatr Pulmonol* 1994; 17: 75-80.
44. ANTONOWICZ I, SHWACHMAN H. Meconium in health and in disease. *Adv Pediatr* 1979; 26: 275-310.
45. SUN B, CURSTEDT T, SONG GW, ROBERTSON B. Surfactant improves lung function and morphology in newborn rabbits with meconium aspiration. *Biol Neonate* 1993; 63: 96-104.
46. MARRARO G, BONATI M, FERRARI A, BARZAGHI MM, PAGANI C, BORTOLOTTI A, GALBIATI A, LUCHETTI M, CROCE A. Perfluorocarbon broncho-alveolar lavage and liquid ventilation versus saline broncho-alveolar lavage in adult guinea pig experimental model of meconium inhalation. *Intensive Care Med* 1998; 24: 501-508.
47. CARVAJAL-DE LA FUENTE V, LOPEZ-MAYAGOITIA A, MARTINEZ-BURNES J, BARRON-VARGAS C, LOREDO-OSTI JC. Efecto antiinflamatorio del líquido amniótico en el pulmón de ratas inoculadas intratraquealmente con sílice. *Vet Mex* 1998; 29: 147-153.
48. BRADY JP, GOLDMAN SL. Management of Meconium Aspiration Syndrome. In: Thibeault D W, Gregory GA, eds. *Neonatal pulmonary care*. Connecticut: Appleton-Century-Crofts, 1986: 483-498.

49. CLARK DG, FIELDER R, JOSEPH C, GARDNER J, SMITH M. The future for acute oral toxicity testing. In: Balls M, Bridges J, Southee J, eds. *Animals and alternatives in toxicology*. Cambridge: MacMillan Academic and Professional Ltd, 1991: 1-21.
50. MEYER O. Implications of animal welfare on toxicity testing. *Hum Exp Toxicol* 1993; 12: 516-521.
51. BRITISH TOXICOLOGICAL SOCIETY. A new approach to the classification of substances and preparations on the basis of their acute toxicity. A report by the British Toxicology Society working party on toxicity. *Hum Toxicol* 1984; 3: 85-92.
52. VAN DEN HEUVEL MJ, DAYAN AD, SHILLAKER RO. Evaluation of the BTS approach to the testing of substances and preparations for their acute toxicity. *Hum Toxicol* 1987; 6: 279-291.
53. VANDEN HEUVEL MJ, CLARK DG, FIELDER RJ, KOUNDAKJIAN PP, OLIVER GJ, PELLING D, TOMLINSON NJ, WALKER AP. The international validation of a fixed-dose procedure as an alternative to the classical LD₅₀ test. *Food Chem Toxicol* 1990; 28: 469-482.
54. PRITCHARD JN, HOLMES A, EVANS JC, EVANS N, EVANS RJ, MORGAN A. The distribution of dust in the rat lung following administration by inhalation and by single intratracheal instillation. *Environ Res* 1985; 36: 268-297.
55. CLEARY GM, WISWELL TE. Meconium-stained amniotic fluid and the meconium aspiration syndrome. An update. *Pediatr Clin North Am* 1998; 45: 511-529.
56. BAKER DEJ. Reproduction and Breeding. In: Baker H J, Lindsey JR, Weisbroth SH, eds. *The Laboratory Rat*. Orlando: Academic Press, 1979: 154-166.
57. WAYNFORTH HB. Experimental and surgical technique in the rat. New York: Academic Press, 1980.
58. LOPEZ A, YONG S, SHARMA A, MORWOOD CM, LILLIE LE, ALBASSAM M. Effect of sex and age on the activities of lactate dehydrogenase and alkaline phosphatase in the lungs of rats. *Can J Vet Res* 1986; 50: 397-401.
59. FLECKNELL P. *Laboratory Animal Anaesthesia*. San Diego, CA: Academic Press, 1996.
60. HOLOPAINEN R, SOUKKA H, HALKOLA L, KÄÄPÄ P. Meconium aspiration induces a concentration-dependent pulmonary hypertensive response in newborn piglets. *Pediatr Pulmonol* 1998; 25: 107-113.

61. CANADIAN COUNCIL ON ANIMAL CARE. Guide to the Care and Use of Experimental Animals. Ottawa, Ont.: CCAC, 1993.
62. HENDERSON RF, LOWREY JS. Effect of anesthetic agents on lavage fluid parameters used as indicators of pulmonary injury. *Lab Anim Sci* 1983; 33: 60-62.
63. HARKNESS JE, WAGNER JE. The Biology and Medicine of Rabbits and Rodents. Philadelphia: Williams & Wilkins, 1995.
64. GREEN CJ. Anaesthetic gases and health risks to laboratory personnel: a review. *Lab Anim* 1981; 15: 397-403.
65. EGER EI. Isoflurane: a review. *Anesthesiology* 1981; 55: 559-576.
66. PHIFER CB, TERRY LM. Use of hypothermia for general anesthesia in preweanling rodents. *Physiol Behav* 1986; 38: 887-890.
67. BERENDT RF. Relationship of method of administration to respiratory virulence of *Klebsiella pneumoniae* for mice and squirrel monkeys. *Infect Immun* 1978; 20: 581-583.
68. ABRAMOVICH DR. The volume of amniotic fluid and its regulating factors. In: Fairweather D V I, Eskes TKAB, eds. *Amniotic Fluid. Research and clinical application*. Amsterdam: Elsevier/North-Holland Biomedicla Press, 1978: 31-49.
69. BRAIN JD, KNUDSON DE, SOROKIN SP, DAVIS MA. Pulmonary distribution of particles given by intratracheal instillation or by aerosol inhalation. *Environ Res* 1976; 11: 13-33.
70. TRAN N, LOWE C, SIVIERI EM, SHAFFER TH. Sequential effects of acute meconium obstruction on pulmonary function. *Pediatr Res* 1980; 14: 34-38.

3. CYTOLOGICAL AND BIOCHEMICAL CHANGES IN THE LUNG OF NEONATAL RATS INOCULATED WITH AMNIOTIC FLUID AND MECONIUM

3.1. Introduction

Meconium aspiration syndrome (MAS) in human beings is one of the most important causes of neonatal respiratory distress, frequently leading to respiratory failure and even death (1,2). Aspiration of meconium into the distal region of the lungs occurs when severe intrauterine hypoxia induces fetal respiration or when meconium previously lodged in the hypopharynx is aspirated into the lungs when the first breaths of air are taken by the neonate (1,3).

There are many pulmonary changes associated with the aspiration of meconium, including airway obstruction, inflammation, release of vasoactive substances, surfactant displacement, surfactant dysfunction and pulmonary hypertension (4-6). Once in the lungs, meconium produces chemical pneumonia during the first few hours of life characterized by a rapid recruitment of polymorphonuclear leukocytes (PMN) and alveolar macrophages (PAM) into the bronchoalveolar spaces (2,4,7,8). Recruitment of inflammatory cells in MAS is largely caused by the local release of pro-inflammatory cytokines such as tumor necrosis factor- α (TNF- α), interleukin 1 β (IL-1 β), and interleukin-8 (IL-8)(9-11). In addition, a recent study demonstrated that normal meconium contains significant amounts of IL-8, a powerful chemoattractant for PMN (12).

Desquamated keratin and squamous epithelial cells normally floating in the amniotic fluid also contribute to an inflammatory response in the lungs of babies and animals with MAS (13-15). A recent study suggested that the magnitude of cellular exudation is related

to the volume of amniotic fluid aspirated into the lung (16). Although amniotic fluid and meconium are known to cause inflammation, it is still unclear if these two materials cause significant injury to the fetal or neonatal respiratory membrane.

In the last few years it has been suggested that the pathogenesis of pulmonary lesions in MAS shares some similarities with the acute respiratory distress syndrome (ARDS) (8,17). This working hypothesis seems to have been substantiated since experimental inoculation of meconium in laboratory animals produces alterations in the air-blood barrier that lead to alveolar edema, exudation of protein-rich fluid, alveolitis and formation of hyaline membranes, all of which are known to occur in natural cases of ARDS (2,6,18,19). In spite of this possible association between MAS and ARDS, there is little information about the relationship between pulmonary injury and leakage of protein in the lungs of animals experimentally inoculated with meconium.

For many years, bronchoalveolar lavage (BAL) has been used in clinical medicine as a valuable diagnostic tool for degenerative, infectious and neoplastic diseases of the lungs (20-24). According to Hunninghake *et al.* (21) BAL is “an invaluable means of accurately evaluating the inflammatory and immune processes of the lung”. There are major advantages of BAL over other diagnostic techniques like lung biopsies: BAL is easy to perform, only moderately invasive, and provides a generous sample of the cells and secretions present at all levels of the respiratory tree (23,24).

In veterinary medicine, the use of BAL as a tool for diagnosis and research has notably increased in the last few years and the procedure has yielded valuable information about pulmonary diseases, particularly in cattle (25-28), horses (22,29,30), sheep (31,32),

dogs (33-36), pigs (4,37) and cats (38,39). Some of these studies have increased our understanding of the pathogenesis of lung diseases in domestic animals (40-42).

In the last few decades, BAL in rodents has been used extensively in inhalation toxicology to evaluate the magnitude of pulmonary damage caused by toxic gases and particulates (43-45). This procedure has been properly validated and it is considered by many as the “golden standard” in screening and evaluating pulmonary damage in toxicological studies (43,46-48). The methods for bronchoalveolar lavage have been described in detail in rabbits (49,50), guinea pigs (51,52), hamsters (53,54), rats (45,55-60) and mice (61-63).

The basic principle of BAL in experimental studies is to obtain a sufficiently large and representative sample of cells and biochemical components of the distal lung by injecting and retrieving known volumes of sampling fluid. For laboratory rodents, BAL is generally a terminal technique performed after euthanasia which allows sequential infusion of fluid with volumes close to the lung capacity (43,47). These large volumes of lavage fluid cannot, for obvious reasons, be used in the live animal. Many studies have demonstrated that cellular and biochemical changes in BAL fluid in laboratory rodents accurately reflect the degree of injury and inflammation caused by pneumotoxins (43,64). It is also widely accepted the high sensitivity of BAL analysis in detecting pulmonary injury and inflammation (43,47,58). Further, since values obtained from BAL analyses are expressed as continuous variables, it is possible to apply rigorous statistical methods to discriminate and compare differences between treated and control animals (47,58,59).

In inhalation studies, BAL is typically analyzed for changes in the cellular and biochemical composition of the lavage fluid. Based on data collected from numerous studies, it has been shown that changes in the numbers and types of leukocytes in the BAL fluid accurately reflect the type and severity of the acute inflammatory response in the lung. For instance, in an acute inflammatory response there is a sharp increase in the absolute number of neutrophils which dramatically changes the PAM:PMN ratio in the BAL fluid. As this process becomes chronic, the number of PAMs progressively increases remaining high as long as the source of inflammation persists in the lung, as is the case with toxic particulates such as asbestos, silica, etc.(43,45,59). The sensitivity of BAL analysis in toxicological studies is so high that exposure of the rodent lung to low levels of irritants like small volumes of saline solution is sufficient to cause noticeable changes in the cellular composition of BAL (64). The pulmonary inflammation caused by saline inoculation or lower concentrations of pneumotoxicants generally goes undetected in microscopic examination of lungs (33,64).

The baseline cell counts in BAL fluid have been well documented for the young and adult healthy rat but are lacking for the fetal and neonatal rat. According to the literature, 21 days-old is the earliest age at which BAL cell counts have been determined for young rats (65). Results of this study showed that the number of free cells (macrophages) declined with increasing age, but differential leukocyte counts were not documented.

The biochemical composition of BAL fluid has also been widely used in laboratory animals as a sensitive indicator of alterations in vascular permeability and pulmonary cell injury (47,66). Under experimental conditions, the levels of protein in BAL fluid increase

when damage to the air-blood barrier results in an increase in vascular permeability. For instance, hydrogen sulfide, ozone, lipopolysaccharides (LPS) and acid aspiration cause notable increases in protein contents of BAL due to the disruption of the air-blood barrier (58,67,68). It is presumed that alveolar leakage of plasma fluid and protein occurs when the integrity of endothelial cells or pneumocytes has been altered by the toxic insult (58).

Enzymatic changes in the BAL fluid are used as a biochemical marker for respiratory injury (43,43,69,70). Data collected from many inhalation studies have shown that the magnitude of cell injury in the respiratory membrane is paralleled by a concomitant increase in the activity of some cytosolic or membrane-bound enzymes in the BAL fluid. Although various enzymes have been used as indicators of lung injury, lactate dehydrogenase (LDH), alkaline phosphatase (ALP) and gamma-glutamyltransferase (GGT) are the most common in experimental lung research (43,44,47,56,58,64,71-73). The fundamentals of enzymatic analyses in BAL reside in the fact that cytosolic and membrane-bound enzymes are promptly released into the bronchoalveolar milieu following cell injury. For instance, ALP, which is present in considerable quantities in basal cells, Clara cells and to a lesser extent in ciliated cells from bronchioles and type II pneumocytes, is released into the air spaces following acute cellular injury (74-76). Changes in enzymatic activity in BAL fluid are considerably more sensitive than histopathology for the detection of early lesions in the lungs (43,58).

The combined approach of using cytological and biochemical analyses of the BAL fluid has proven valuable for the discrimination between pulmonary cell damage (*in vivo* cytotoxicity) and host inflammatory response (43,64). For instance, some toxic gases are known to induce notable increases in enzymatic activities but only minimal changes in

neutrophil counts suggesting a severe pulmonary damage with a mild inflammatory response (43).

There are only a few reports in the literature dealing with the effect of meconium or amniotic fluid on the cytological and biochemical composition of the BAL fluid. One study showed that intratracheal inoculation of amniotic fluid in rats caused increased numbers of macrophages and neutrophils in the BAL (16). However, since no biochemical analyses were done in that study, it remained inconclusive whether amniotic fluid causes substantial injury to the respiratory membrane. There are some other reports in which BAL was done following inoculation of meconium, but the primary focus of these investigations was to test surfactant activity and ventilation and not pulmonary injury (2,18,77). Finally, there is a report in which tracheal aspirate composition was determined in pigs inoculated with meconium. This showed that neutrophils and protein increased significantly in the first 12 hours and remained high until 48 hours postinoculation (4).

The objectives of this study are twofold: 1- To determine the normal cellular and biochemical composition of the BAL fluid collected using a uniform protocol in neonatal rats. 2- To quantify the magnitude of pulmonary injury and inflammatory response as reflected in BAL alterations in neonatal rats intratracheally inoculated with homologous amniotic fluid and meconium.

3.2. Material and Methods

3.2.1. Animals

Neonatal rats born at AVC from "time pregnant" Fischer-344 females which were originally obtained from commercial sources (Charles River, Quebec) were used in this

study. The timed pregnancy program was based on vaginal cytology, following the reproductive protocols published elsewhere (78,79), and described in detail in Section 2.2.1. Pregnant rats were housed individually, provided with commercial rat food and water *ad libitum*, and maintained on a 12/12-hour light/dark cycle at 22 °C and 50% relative humidity. To reduce infant rejection and cannibalism, dams were preconditioned 7 days before parturition, following the protocol outlined by Park *et al.* (80) and described in Section 2.2.2. Male pups used in the inoculation studies were 7-day-old at the inoculation time.

For the kinetic studies, rat fetuses were obtained through cesarean section from pregnant Fischer-344 rats under halothane anesthesia following standard procedures (81). Fetuses were closely monitored at the extraction time to corroborate absence of respiratory movements and to assure no aspiration of amniotic fluid.

3.2.2. Anesthesia

Neonates used for inoculation procedures were removed one at a time from their cages and placed in sternal recumbency on a heating pad at 37 °C. Pups were anesthetized with 3% halothane in 100% oxygen at a flow rate of 100-200 ml/minute (Fluothane®, MTC Pharmaceutical, Mississauga, Ontario, Canada) using a protocol (82,83) modified at AVC. The anesthesia protocol is described in section 2.2.4.

Anesthesia for the cesarean section was performed using 3% halothane in 100% oxygen at a flow rate of 500 ml/min. in a plexiglass chamber connected to the anesthesia machine. After 3 minutes of induction, the dam was transferred to a slanting board and anesthesia continued by using a small anesthesia mask.

3.2.3. Inoculum

Amniotic fluid was aseptically collected following the procedure described in section 2.2.5. Briefly, the uterus from a full-term pregnant rat was exposed through cesarean section under deep halothane anesthesia. Under sterile conditions, the uterus and placenta were punctured and the amniotic fluid collected using sterile capillary tubes. Amniotic fluid was transferred to sterile plastic vials and stored at 4-6°C. A high dose (100%) of a non diluted amniotic fluid or a low dose (50%) diluted in saline were used as inocula.

Meconium was aseptically collected from the intestines of female rat pups killed at the time of birth with an anesthetic overdose of halothane and before the intake of colostrum. Once removed from the intestine, the meconium was maintained frozen at -80°C until preparation of the inoculum. Samples of the amniotic fluid and meconium were submitted for routine bacteriological cultures to ensure sterility of the inocula. Meconium was suspended in saline solution and homogenized using a Vortex mixer (Fisher Scientific, N.Y.). Based on the results of the dose-range finding study (Section 2.2.7.), the final concentration of unfiltered meconium was adjusted to 200 mg/ml (wet weight).

3.2.4. Intratracheal inoculation (ITI)

The method of ITI for 7-day-old rat neonates was standardized using techniques described elsewhere (82,83) and adapted to the size of neonatal rats. A detailed description on this protocol is included in section 2.2.8. Briefly, neonates were anesthetized with halothane and the larynx was visualized using an otoscope with a sterile speculum (Welch Allyn, Skaneateles Falls, NY). A sterile spinal needle 25-gauge, 8.89 cm length (Becton Dickinson, Franklin Lakes, NJ) with the edge rounded was passed through the laryngeal

opening into the trachea. A 1.0 ml disposable syringe (Becton Dickinson, Rutherford, NJ) was connected to the needle and the inoculum injected into the lungs.

The total volume of amniotic fluid and the meconium suspension inoculated into the lungs was 0.05 ml per rat. Control rats were inoculated with 0.05 ml of sterile saline solution or 0.05 ml of air. To prevent hypothermia, pups were maintained in direct observation on a heating pad (37°C) until recovery from the anesthesia and then moved into their cages.

3.2.5. *Euthanasia*

Rats were euthanised with an overdose of halothane and exsanguinated by excising the renal arteries as described in section 2.2.9. Experiments were conducted following the guidelines of the Canadian Council on Animal Care (84).

3.2.6. *Experimental design*

3.2.6.1. *Leukocyte kinetics and biochemistry of BAL from normal fetuses and neonates*

To evaluate the normal cellular and biochemical composition of the BAL fluid in neonatal rats, a total of 13 male fetuses and 61 normal male neonatal rats were used (Table VII). Control neonates were exposed to the experimental procedure of anesthesia and all neonates older than 7-day-old to the inoculation of air. The cell counts in BAL fluid were determined in non-inoculated normal fetuses. Cell and biochemical determinations were conducted in the neonates from ages 1 until 120 days.

Table VII. Number of rats used in the leukocyte kinetics and biochemistry of BAL fluid.

| Group | Fetus | Birth | Postpartum Age (Days) | | | | | | | | Total | |
|-------------|-------|-------|-----------------------|---|---|----|----|----|----|----|-------|----|
| | -3 -1 | 0 | 1 | 3 | 7 | 11 | 15 | 22 | 36 | 64 | 120 | |
| Control N = | 6 | 7 | 6 | 6 | 5 | 7 | 5 | 7 | 6 | 5 | 7 | 74 |

The following hypothesis was tested:

- 1) The cytological and biochemical composition of the BAL do not change by time from fetuses up to 120-day-old rats.

3.2.6.2 Effect of saline on the cytological and biochemical composition of BAL.

To evaluate the effect of saline as vehicle on the cytology and biochemistry of BALs, 83 male 7-day-old neonatal rats with an average weight of 13.2 ± 1.73 g were randomly assigned to two different experimental groups (Control and Saline Solution). The saline group received 0.05 ml of sterile saline solution, and control rats were subjected to the same experimental procedures of anesthesia and inoculation, but just 0.05 ml of air was inoculated into the trachea. Neonates were euthanised at postinoculation day (PID) 1, 3, 7, 14, 28, 56 and 112 (Table VIII). Cytological and biochemical analyses of BAL were performed.

Table VIII. Number of 7-day-old neonates used to study the effect of saline solution on leukocyte kinetics and biochemistry of BALs.

| Treatment | Postinoculation (Days) | | | | | | 56 | 112 | Total |
|-------------|------------------------|----|----|----|----|--|----|-----|-------|
| | 1 | 3 | 7 | 14 | 28 | | | | |
| Control | 6 | 5 | 7 | 6 | 5 | | 7 | 8 | 44 |
| Saline Sol. | 5 | 5 | 6 | 6 | 6 | | 6 | 5 | 39 |
| Total | 11 | 10 | 13 | 12 | 11 | | 13 | 13 | 83 |

The hypotheses tested in this study were:

- 1). The inoculation of saline solution does not change the cytological and biochemical composition of the BAL (saline solution = control).
- 2). The cytological and biochemical composition of the BAL do not change by time after the inoculation of saline and in controls.

3.2.6.3. Cytological and biochemical changes after inoculation of amniotic fluid.

A total of 90 male 7-day-old neonatal rats with an average weight of 13.8 ± 1.8 g were randomly assigned to three experimental groups (amniotic fluid low dose, amniotic fluid high dose, and control). Two independent studies using the same design but different postinoculation times were conducted for amniotic fluid. Neonates from the low dose group received 0.05ml of amniotic fluid diluted in 50% saline solution. The high dose group received 0.05ml of non diluted amniotic fluid (100%). Control animals were inoculated with 0.05 ml of saline solution. Neonates were euthanised under deep halothane anaesthesia at 1, 3, 7 and 14 days postinoculation (PID 1, 3, 7 and 14)(Tables IX and X). Cytological and biochemical analyses of BAL were conducted.

Table IX. Neonates used to evaluate cytological and biochemical changes in BAL after inoculation with amniotic fluid (PID 1,3,7).

| Treatment | Post-inoculation (Days) | | | Total Neonates |
|----------------------------|-------------------------|-----------|-----------|----------------|
| | 1 | 3 | 7 | |
| Control (Saline solution) | 4 | 4 | 5 | 13 |
| Low Dose(50% AF, 0.05ml) | 4 | 4 | 5 | 13 |
| High Dose(100% AF, 0.05ml) | 4 | 5 | 5 | 14 |
| Total | 12 | 13 | 15 | 40 |

AF: Amniotic fluid

Table X. Number of pups used to determine cytological and biochemical changes in BAL after inoculation of amniotic fluid (PID 3,7,14).

| Treatment | Post-inoculation (Days) | | | Total Neonates |
|----------------------------|-------------------------|-----------|-----------|----------------|
| | 3 | 7 | 14 | |
| Control (Saline solution) | 6 | 6 | 8 | 20 |
| Low Dose(50% AF, 0.05ml) | 5 | 5 | 5 | 15 |
| High Dose(100% AF, 0.05ml) | 5 | 5 | 5 | 15 |
| Total | 16 | 16 | 18 | 50 |

The following hypotheses were tested:

| Main effect | Null Hypotheses | Alternative Hypotheses |
|-------------|--------------------------------|---------------------------|
| Treatment | AF Low dose=High dose= Control | At least one is different |
| Time | PID 1 = PID 3 = PID 7 = PID14 | At least one is different |

3.2.6.4. Cytological and biochemical changes after inoculation of meconium.

A total of 63 male 7-day-old neonates rats weighing an average of 13.8 ± 0.95 g were randomly assigned to two experimental groups (Control and Meconium 20%). Neonates from the meconium group were inoculated with 0.05ml of a suspension of 20% meconium. Control animals received 0.05 ml of saline solution. Neonates were euthanised under halothane anesthesia at PID 1, 3, 7 and 14 (Table XI). Cytological and biochemical analyses of BAL were performed.

Table XI. Cytological and biochemical changes in BAL after inoculation of meconium in neonatal rats.

| Treatment | Post- inoculation (Days) | | | | Total |
|---------------------------|--------------------------|----|----|----|-------|
| | 1 | 3 | 7 | 14 | |
| Control (Saline solution) | 8 | 8 | 8 | 11 | 35 |
| Meconium (20%) | 7 | 7 | 7 | 7 | 28 |
| Total | 15 | 15 | 15 | 18 | 63 |

The following hypotheses were tested:

| Main effect | Null Hypotheses | Alternative Hypotheses |
|-------------|--------------------------------|---------------------------|
| Treatment | Meconium = Control | At least one is different |
| Time | PID 1 = PID 3 = PID 7 = PID 14 | At least one is different |

3.2.7. *Bronchoalveolar lavage (BAL).*

Neonates were euthanised with an overdose of halothane and placed in a supine position on a board held at 45° and restrained using a rubber band under the upper incisors and adhesive tape across the forelimbs and hindlimbs. The abdomen was opened, animals were exsanguinated by section of the renal arteries, and bilateral pneumothorax was induced by diaphragmatic puncture. The thorax was opened through a bilateral costotomy and the trachea was exposed by removing the cervical muscles. Plastic catheters with different diameters depending upon age (24-gauge, 19 mm for fetuses -3, -1 and at birth; 22-gauge, 25mm for day 1 and 3 age, Angiocath, Becton & Dickinson, Utah) (20-gauge, 32 mm length for neonates at day 1, 3 and 7 PI; 18-gauge; 32mm length for day 14 PI; 16-gauge; 57 mm for day 28 PI; and 14-gauge, 57mm for 56 to 112 days PI, Cathlon IV, Critikon Canada Inc, Markham, Ontario) were inserted through a transverse slit made in the wall of the trachea between the first and second tracheal rings. Catheters were connected to disposable syringes containing saline solution with heparin (15 IU/ml; Leo Laboratories, Ontario) at volumes adjusted to the different ages of fetuses and neonates (0.05 ml for fetuses; 0.06ml for neonates at birth; 0.08 ml at day 1; 0.12ml for day 3; 0.30 ml for day 7 and PID 1, 3 , 7 and 14; 0.40ml for PID 28; 0.50ml for PID 56 and 5ml for PID 112). The catheter was saline-filled to prevent injection of air into the lungs. The solution was slowly introduced to the trachea and after a gentle massage of the lungs to facilitate the detachment of bronchoalveolar cells, the lavage fluid was recovered. Three consecutive lavages with the same volume of additional fluid were performed and the recovered volume was recorded. Recovered fluids were pooled into a single plastic vial and were kept on ice. From the pooled lavage 0.10 µl were used for the cell counts using a haemocytometer. The remaining

pooled bronchoalveolar lavage fluid from each neonate was centrifugated at 500 x g for 20 min. at 5°C. The supernatant was removed and retained, and the cell pellet was resuspended in 0.5 ml of saline solution. The resuspended cell pack was used for the differentiation of leukocytes. From the supernatant, 100 µl were used for biochemistry.

3.2.8. Bronchoalveolar cell counts

The number of bronchoalveolar cells in the pooled BAL fluid of each neonate was determined using a hemocytometer (Boeckel, Co. Scient. Equip. B. Hamburg, Germany) and standard procedures previously described (16,61). Each sample was counted in both hemocytometer chambers and the mean count recorded. The values were expressed as the total number of nucleated cells/ml of BAL fluid, using the following formula:

$$\text{Nucleated cells} = (\text{count} / 4) \times 10,000$$

where:

Nucleated cells = Number of nucleated cells per ml of BAL

Count = Number of cells in 4 squares of haemocytometer

4 = Number of squares counted (1 square = 1 mm² x depth 0.1 mm)

10,000 = Conversion factor to obtain cells per ml (1 square = 0.1 mm³ = 0.0001 ml)

3.2.9. Differential count of alveolar macrophages and neutrophils

The cell pellet (200 µl) was resuspended and centrifugated at 72.4 x g for 10 min. (Cytospin, Shandon Inc. Pittsburgh, PA). Cytospin slides were stained with Wright-Giemsa stain (VWR, CanLab, Mississauga, ON) and were labeled using random numbers cross referenced to the actual specimen identity. Readings of slides were performed without knowledge of the identity of the specimens. Differential counts of 200 nucleated cells (non epithelial) were performed under a light microscope (Nikon Labophot, 104, Japan) and values were expressed as percentage of each leukocyte type.

3.2.10. Absolute number of alveolar macrophages and neutrophils

The absolute number of alveolar macrophages (PAM) and neutrophils (PMN) were obtained using the methodology previously described (61) and based on the total cell counts and the differential of each leukocyte using the following formula:

$$\frac{\text{Absolute count of PAM and PMN}}{100} = \frac{\text{Total number of nucleated cells}}{\text{Total number of nucleated cells}} \times \frac{\% \text{ of PMN or PAM}}{100}$$

Absolute values of PAM and PMN were expressed as cells/ml of lavage fluid.

3.2.11. Biochemistry of BAL fluid

The supernatant BAL fluid was analyzed using an automated biochemical analyzer (Hitachi 911, BMC, Indianapolis, IN) to determine the protein and enzymatic activity. Determinations of enzyme activity were carried out using a kinetic method. For quality assurance, the tests were run simultaneously with normal and elevated human control sera (Precitol®-N and Precitol™-A, BMC, Indianapolis, IL). Lactate dehydrogenase (LDH) determination was performed using lactic acid as a substrate, and NAD (nicotinamide adenine dinucleotide) as cofactor (85). The reaction was read bichromatically at 340-376 nm with a linearity of ≤ 1000 U/L (LDH, BMC, Indianapolis, IL). Alkaline phosphatase (ALP) was determined using p-nitrophenyl phosphate as a substrate to form p-nitrophenol at pH 10.5 (86). The reading of the reaction was performed using a bichromatic analysis at 415-700 nm with reaction linearity ≤ 1200 U/L (ALP, BMC, Indianapolis, IL). Gamma-glutamyl transferase (GGT) was determined using L- γ -glutamyl-3-carboxy-4-nitroanilide as substrate to form 5-amino-2-nitrobenzoate (87). The reaction was read using bichromatic analysis at 415-700 nm with a system linearity of ≤ 1200 U/L (GGT, BMC, Indianapolis, IL). Total

protein was determined using the Randox total protein reagent for urine and cerebrospinal fluid (Randox Laboratories, Ltd, Crumlin, CO) with human serum albumin as protein standard, and based on the principle described by Watanabe *et al.*(88). A human-based control (RANDOX) was run at the same time as the samples for quality control. The reaction was read at 600 nm with a linearity of ≤ 2.5 g/L. Enzymatic activity and protein concentrations were expressed as units (U) per liter and grams per liter, respectively.

3.2.12. Statistical analysis

Values for each group were expressed as means and standard deviations (SD). Logarithmic transformations (Log 10) were also used in cell counts. The effect of treatment and interactions were statistically evaluated by Analysis of Variance (GLM-ANOVA) according to the following model:

$$Y_{ij} = \mu + T_i + D_j + TD_{ij} + E_{ij}$$

where:

Y_{ij} = individual observation on the j day of the i -th treatment.

μ = general population mean.

T_i = Effect of the i -th treatment;

($i = 1$ for kinetic and 2 for saline studies)

($i = 2$ for meconium and 3 for amniotic studies)

D_j = Effect of the j -th day

($j = 1, 2, 3, 4, 5, 6, 7, 8, 9, 10, 11, 12$ for kinetic studies)

($j = 1, 2, 3, 4, 5, 6, 7$ for saline studies)

($j = 1, 2, 3, 4$ for amniotic and meconium studies)

TD_{ij} = interaction

E_{ij} = Random error associated with each observation $\sim NI(0, \sigma^2 e)$.

Differences between groups of treatments and days postinoculation were examined with One-Way Analysis of Variance (ANOVA) followed by the non-parametric Kruskal-Wallis test and Tukey's (89). The associations between each biochemical determinant and the number of bronchoalveolar lavage cells was determined by Correlation Analysis. A p-value below 0.05 was considered statistically significant.

3.3. Results

3.3.1. Leukocyte kinetics and biochemistry of BAL from normal fetuses and neonates

3.3.1.1. Cytology

The percentage of fluid recovered after the three lung lavages in fetuses ranged from 65 to 88.8% of instilled volume with an average of $76.9\% \pm 16.8\%$. From the time of birth and until 120 days of age the average recovered volume of BAL fluid was $84.1\% \pm 6.3\%$.

The total cell counts from the BAL fluid in fetuses at -3 days before birth did not reveal the presence of leukocytes, but these cells were demonstrated at -1 day and at birth. After day 0 (at birth), day 1 and 3, a significant increase in the number of recovered cells ($p < 0.05$) was observed. By 3 days after birth, and until 120 days, the number of cells remained constant ($p > 0.05$) (Fig. 4). A decreasing trend after 36 days was observed, but not enough to achieve statistical differences. An overall time effect ($p \leq 0.01$) was demonstrated.

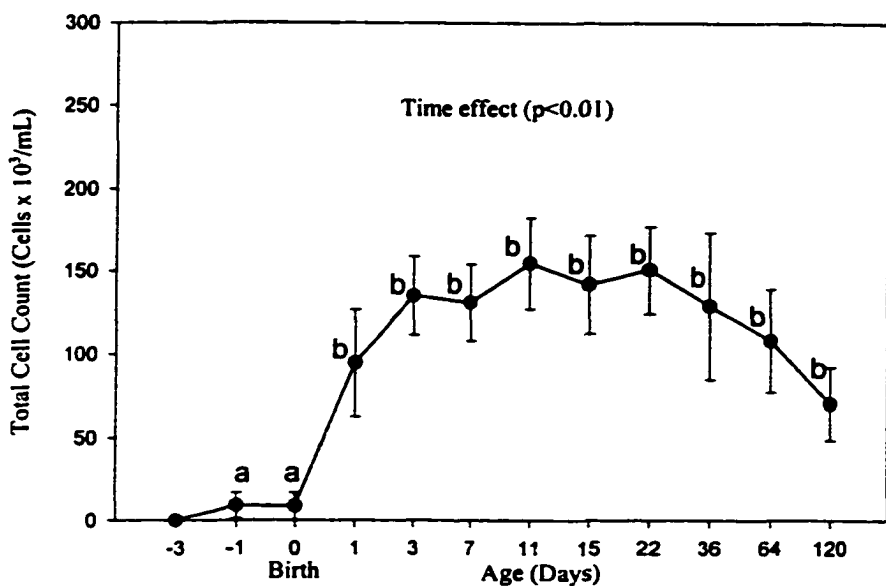


Fig. 4. Total cell counts in BAL fluid of normal fetuses and neonatal rats at different ages. Symbols and bars represent mean and SD ($n = 5$ to 8 animals each group). Means with different letter are significantly different ($p < 0.05$) as determined by Tukey's comparison test.

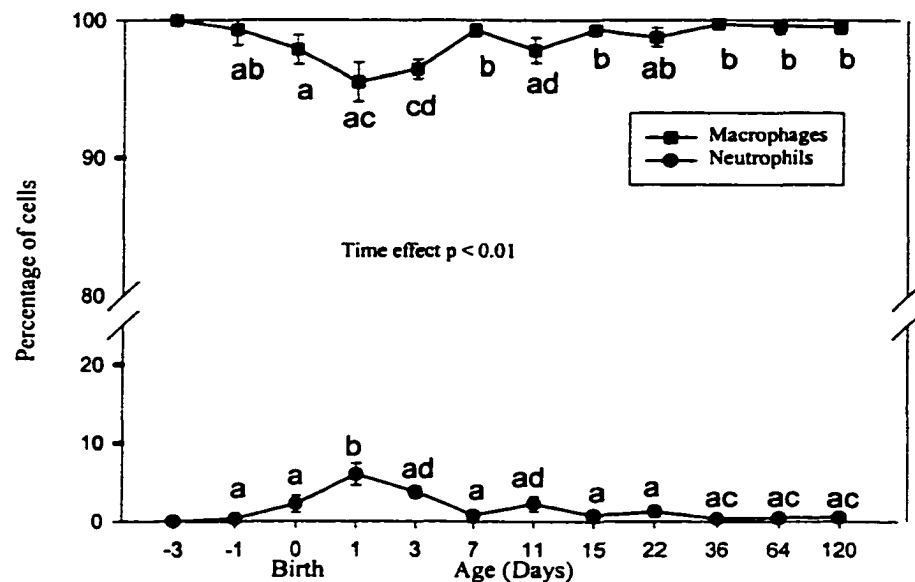


Fig. 5. Differential of leukocyte counts in BAL from fetuses and neonatal rats at different ages. Symbols and bars represent mean and SD ($n = 5$ to 8 animals each group). Means with different letter are significantly different ($p < 0.05$) as determined by Tukey's comparison test.

In the differential cell counts, alveolar macrophages (PAM) were present in low number in 2 out of 6 fetuses at day -3 and in 4 out of 7 at -1 day. When PAM were present, they accounted for more than 99.0% of recovered cells at these times (Fig. 5). After birth, the percentage of PAM decreased significantly ($p<0.05$) at day 1 and 3, however, after day 3, PAM remained unchanged ($p>0.05$). PAM accounted for more than 95.5% of recovered cells from normal fetuses and neonates. An overall time effect ($p<0.01$) in the percentage of macrophages was found in these animals.

Polymorphonuclear leukocytes (PMN) were first detected in the BAL fluid at day -1, accounting for less than 1% of the total cells at the time. A significant increase ($p<0.05$) in the percentage of PMN at birth, day 1 and 3 was observed compared with the fetuses. This increase in percentage of PMN paralleled the decrease in percentage of PAM (Fig. 5). After day 3 and until 120 days the percentage of neutrophils in the BAL fluid of rats remained unchanged ($p>0.05$). Neutrophils ranged from 0 to 9% throughout the study. An overall significant time effect ($p<0.01$) in the percentage of PMN was also detected.

The absolute number of PAM increased significantly after birth and until day 3 of age ($p<0.05$). From day 3 and until day 120 no significant differences ($p>0.05$) were observed (Fig. 6). A significant increase in the absolute number of PMN after birth at day 1 and 3 was found ($p<0.05$). After day 3 no differences in the absolute number of PMN were observed ($p>0.05$). An overall significant day effect in the absolute number of PAM and PMN was detected ($p<0.01$), however differences were observed prior to the third day after birth. A high correlation ($r = 0.91$) between the total cell count and the number of macrophages

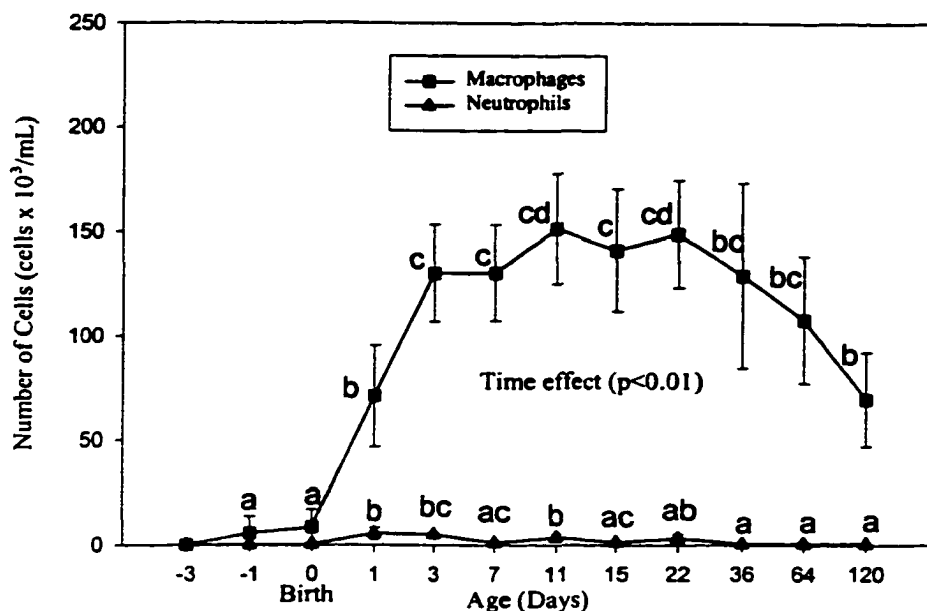


Fig. 6. Absolute number of leukocytes in BAL fluid from fetuses and neonatal rats. Symbols and bars represent mean and SD ($n=5$ to 8 animals each group). Means with different letter are significantly different ($p<0.05$) as determined by Tukey's comparison test.

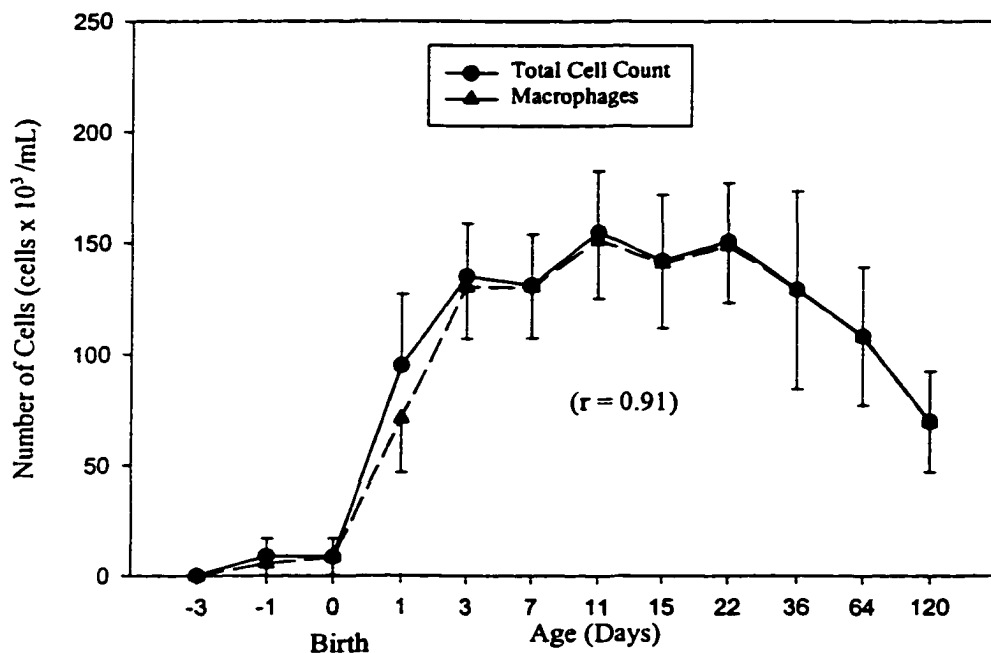


Fig. 7. Comparison between total cell count and PAM in BAL from fetuses and neonatal rats. Symbols and bars represent mean and SD ($n=5$ to 8 animals each group). r = Coefficient of correlation.

was found (Fig. 7). No relevant correlations were detected between the number of leukocytes and enzymes or proteins in the BAL fluid.

3.3.1.2. Biochemistry

An initial high activity of alkaline phosphatase (ALP) at day 1 and 3 but not enough to achieve statistical significance was detected (Fig. 8) in the BAL fluid from normal neonates. From day 7 and until day 36 no significant differences were found. However, a significant decrease ($p<0.05$) in ALP activity was observed at days 64 and 120 (Fig. 8). There was an overall significant time effect ($p<0.01$) in ALP activity.

Activity of lactate dehydrogenase (LDH) was also high during the first week of life (Fig. 8) and significant differences in activity were detected on day 1 and 3 ($p<0.05$) compared with other ages. There was a general tendency of this enzyme to decrease with time (Fig. 8) with an overall time effect ($p<0.01$).

There was a tendency of gamma glutamyl transferase (GGT) to increase at day 3 but not significantly ($p>0.05$). A second trend to increase from day 11 to 36 was observed and there were significant differences ($p<0.05$) at day 36 and 64. A significant overall time effect ($P<0.01$) was found, however, differences did not follow a defined pattern (Fig. 8).

Total protein in the lavage fluid collected from normal neonatal rats was significantly higher ($p<0.05$) at day 3 (Fig. 8). An overall significant day effect ($p<0.01$) was found, however, with the exception of day 3, total protein remained unchanged throughout the study.

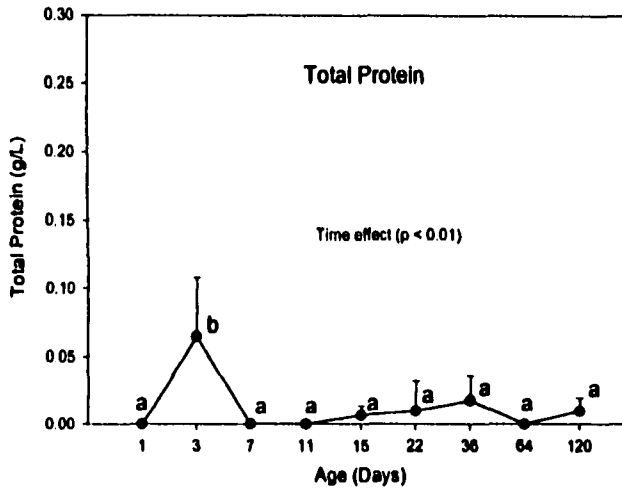
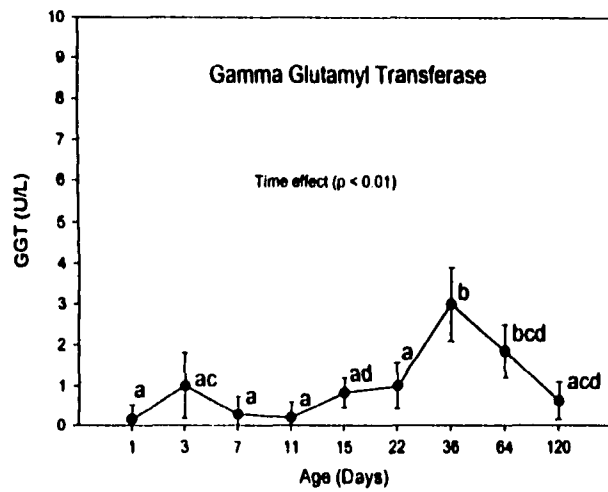
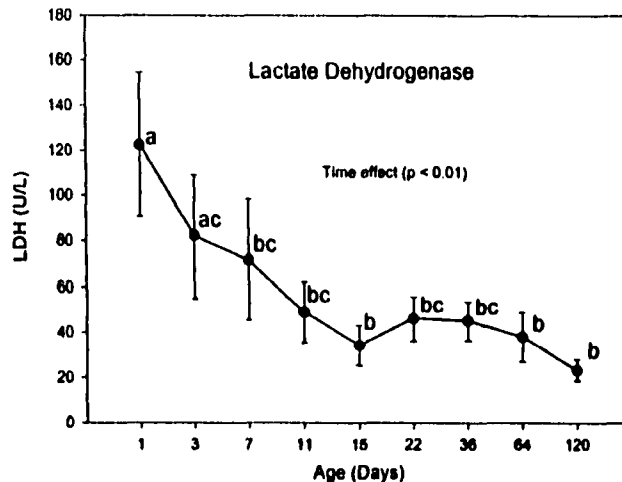
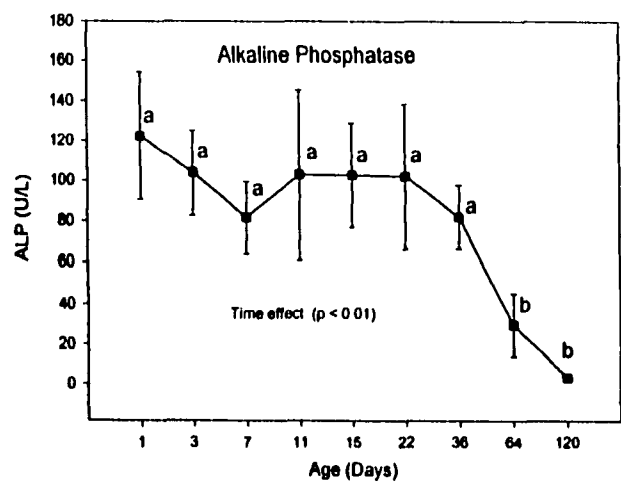


Fig. 8. Enzymatic activity and total protein content in BAL fluid of normal rats. Symbols and bars represent mean and SD ($n= 5$ to 8 pups each group). Means with different letters are significantly different ($p \leq 0.05$) as determined by Tukey's comparison test.

3.3.2. Effect of saline solution on the biochemical and cytological composition of the BAL.

3.3.2.1 Cytology

The overall volume of fluid recovered from the volume instilled was similar in the control and saline groups with an average of $84\% \pm 1.7\%$. Inoculation of saline solution did not induce significant changes in the number of cells in the bronchoalveolar spaces as assessed by BAL compared with the controls ($p \geq 0.05$). However, there was a slight tendency of cells in the saline group to be increased at PID 1 and 7. A significant time effect ($p \leq 0.05$) with a progressive reduction by time after PID 7 in the two experimental groups was observed (Fig. 9). However, no significant interactions between treatment with saline and time were detected.

Intratracheal inoculation of saline did not have any effect on the number of PAM and PMN ($p \geq 0.05$) when compared with the controls (Fig. 9). A tendency of PAM to increase from PID 1 to 7, but non-significantly, was observed. A significant time effect ($p \leq 0.01$) with a progressive reduction in PAM and PMN after PID 7 was detected in both groups. No interactions between treatment and time were detected.

3.3.2.2 Biochemistry

Intratracheal inoculation of saline solution did not induce any significant change ($p \geq 0.05$) in the enzymatic activity or protein in the BAL fluid (Fig. 10). A significant time effect ($p \leq 0.01$) with the tendency to decrease by time in ALP and LDH, and to increase in GGT were observed in both saline and control groups.

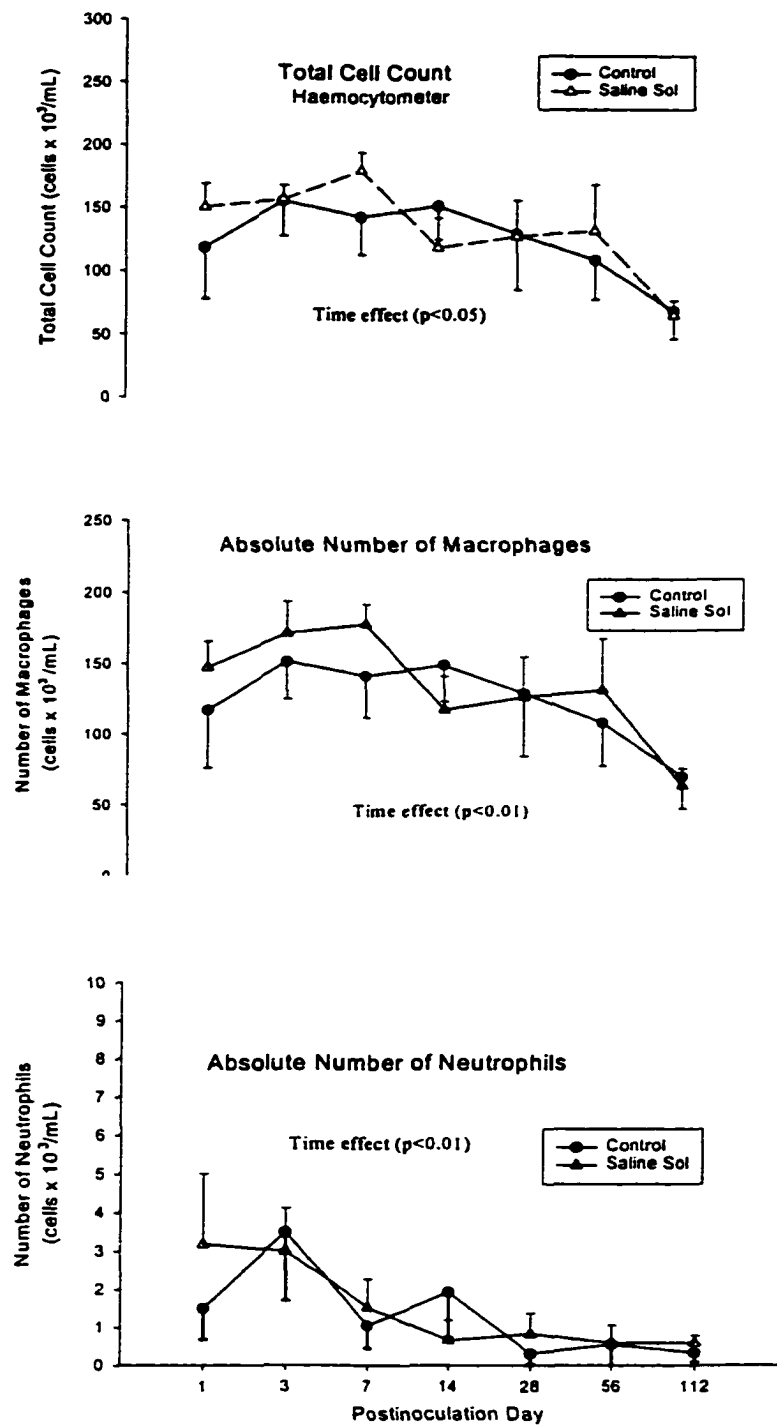


Fig. 9. Total cell count, and absolute number of PAM and PMN in BAL fluid, after inoculation of 7-day-old neonates with saline. Symbols and bars represent mean and SD ($n = 5$ to 8 neonates per group).

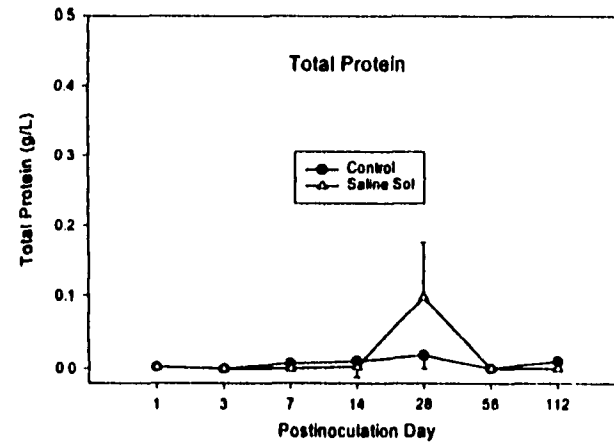
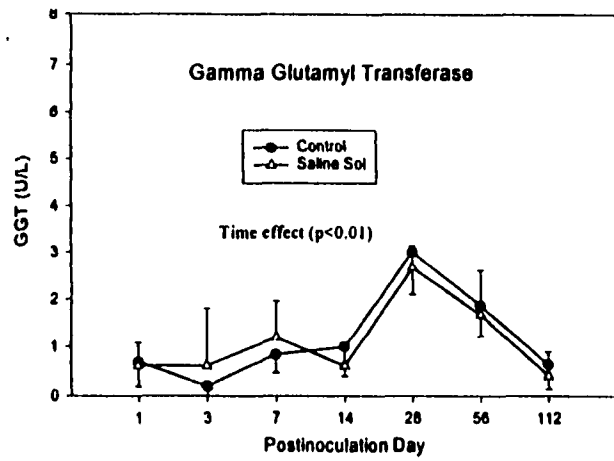
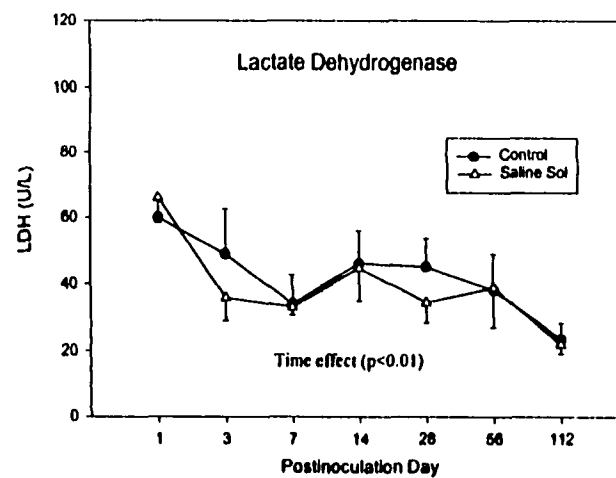
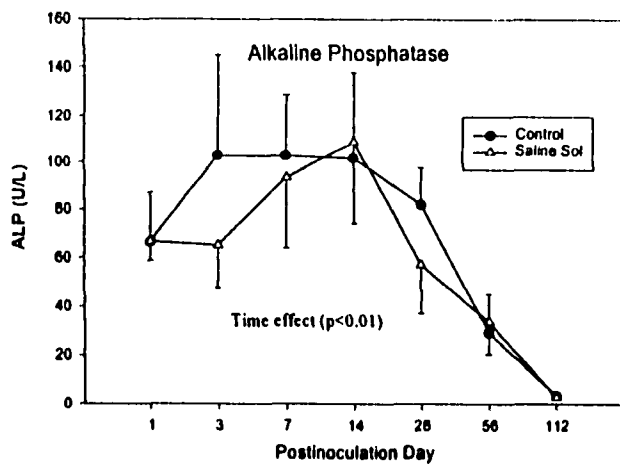


Fig. 10. Enzymatic activity and total protein level in BAL fluid, after the inoculation of 7-day-old neonates with saline. Symbols and bars represent mean and SD ($n = 5$ to 8 animals per group).

3.3.3. Effect of amniotic fluid on the cytological and biochemical composition of the lung.

3.3.3.1. First study of amniotic fluid (1, 3 and 7 postinoculation days).

3.3.3.1.1. Cytology

The overall recovered volume of the lavage fluid in the amniotic and control groups at different postinoculation times was $79.3\% \pm 4.3\%$.

Intratracheal inoculation with low (50%) or high doses (100%) of amniotic fluid did not induce significant changes ($p>0.05$) in the number of cells recovered by BAL at PID 1, 3, and 7 compared with the control rats inoculated with saline solution (Fig. 11). A significant increase was observed in number of cells with time ($p<0.01$) in the amniotic and control groups.

No significant differences in the percentage and absolute numbers of macrophages and neutrophils ($p>0.05$) were detected in rats following the inoculation of low or high doses of amniotic fluid (Fig. 11). However, the absolute number of macrophages increased by time in all groups with a significant day effect ($p<0.01$) (Fig. 11). An overall interaction in the number of macrophages between treatment and time was detected ($p<0.01$). Non-significant differences or interactions in neutrophils were observed ($p>0.05$).

3.3.3.1.2. Biochemistry

Intratracheal inoculation of amniotic fluid did not cause any significant change ($p>0.05$) in the enzymatic activity or protein content in the BAL fluid during the 7 days of this study (Fig. 12).

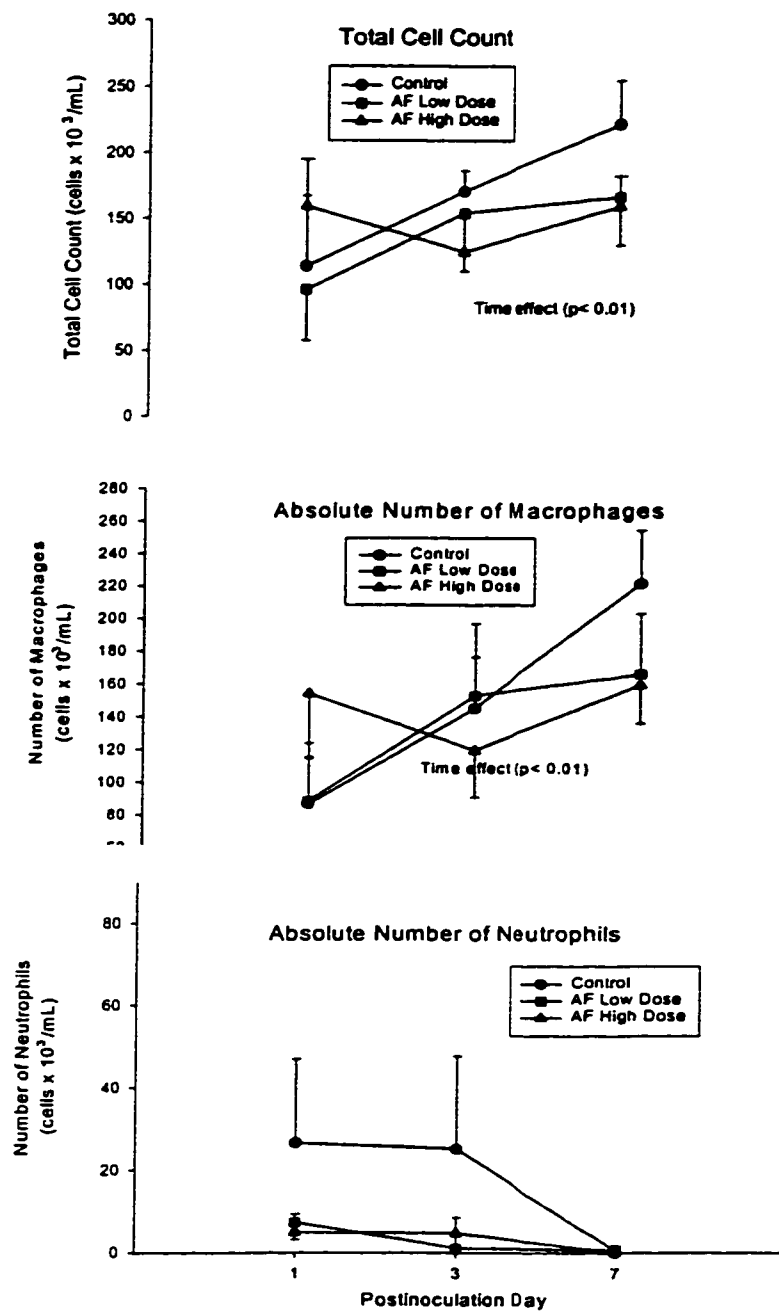


Fig. 11. Total cell count, and absolute number of PAM and PMN in BAL fluid, after inoculation of 7-day-old neonates with amniotic fluid. Symbols and bars represent mean and SD ($n = 4$ or 5 neonates per group).

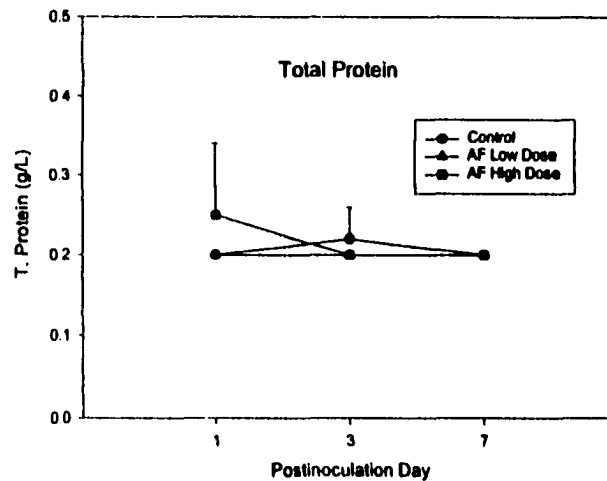
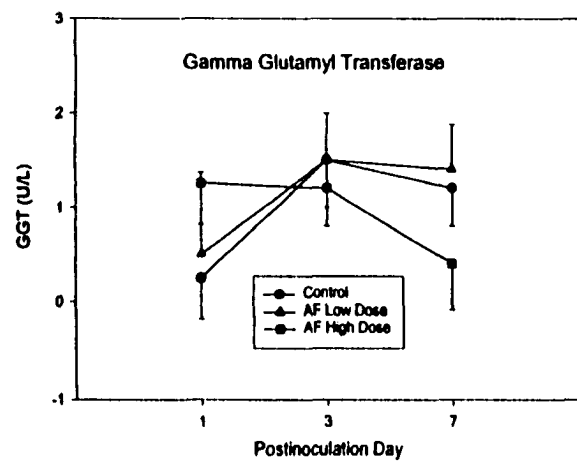
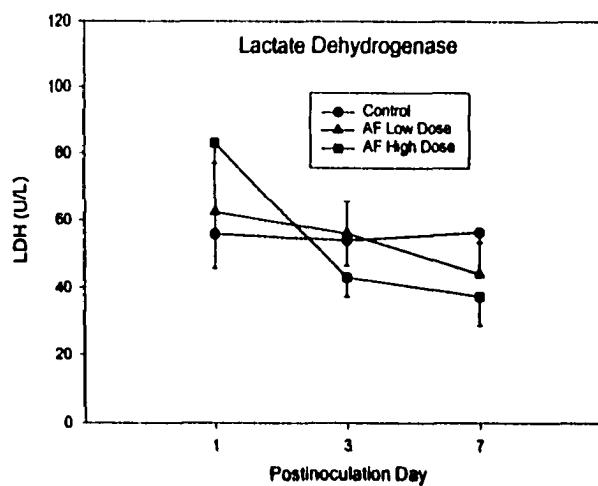
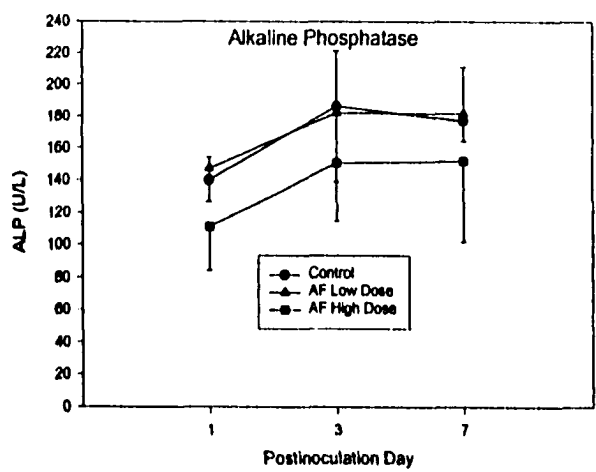


Fig. 12. Enzymatic activity and total protein content in BAL after inoculation of 7-day-old neonates with amniotic fluid. Symbols and bars represent mean and SD ($n = 4$ or 5 neonates per group).

3.3.3.2. Second study of amniotic fluid (3, 7 and 14 postinoculation days).

3.3.3.2.1. Cytology

The overall volume of lavage fluid recovered was $81.8\% \pm 8.3\%$ in the three groups at PID 3, 7 and 14. Inoculation of low (50%) or high doses (100%) of amniotic fluid caused no significant differences ($p>0.05$) in the number of cells recovered compared with the control (Fig. 13). No significant interactions between treatment and time were detected ($p>0.05$).

Amniotic fluid did not induce changes in the percentage and number of PAM and PMN ($p>0.05$) compared with the controls (Fig. 13). A tendency of PMN numbers to significantly increase with time ($p<0.05$) in the amniotic groups was observed. However, no interactions between treatment and time were detected in these rats ($p>0.05$).

A high coefficient of correlation ($r = 1$) was detected between the total cell count and absolute number of macrophages.

3.3.3.2.2. Biochemistry

Inoculation of amniotic fluid induced an overall significant treatment effect ($p<0.05$) on ALP activity in the bronchoalveolar space (Fig. 14). However, the difference was characterized by lower levels of ALP in the group inoculated with low dose (50%) of amniotic fluid compared with the control and only at PID 3. A significant decrease in enzyme levels with time in amniotic and control groups was detected in ALP ($p<0.05$) and LDH ($p<0.01$). Total protein and GGT in the BAL fluid did not change either after the inoculation with amniotic fluid or with time (Fig. 14). No relevant correlations between leukocytes and enzymes or protein were found in the BAL fluid of these rats.

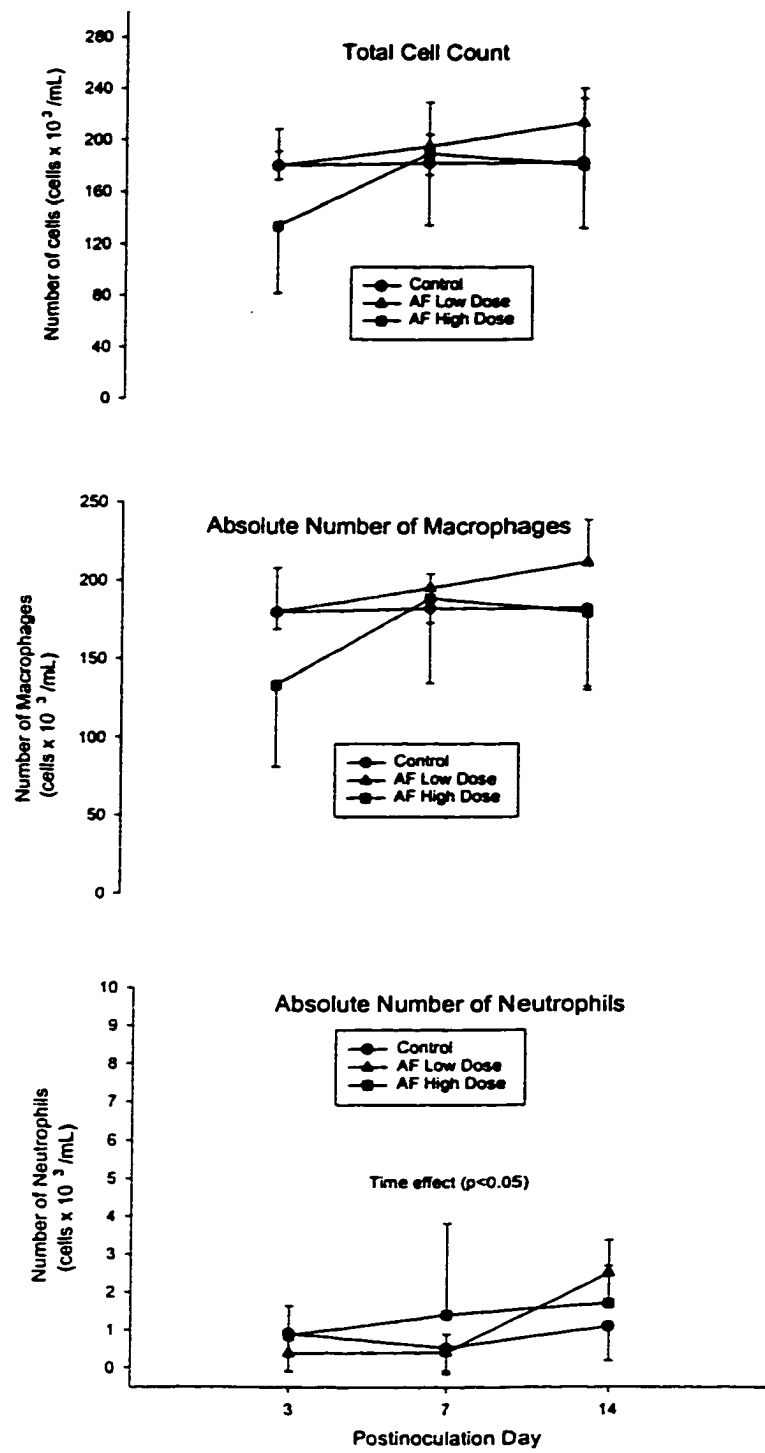


Fig. 13. Total cell count, and number of PAM and PMN in BAL fluid after amniotic inoculation. Symbols and bars represent mean and SD ($n = 5$ or 6 neonates per group).

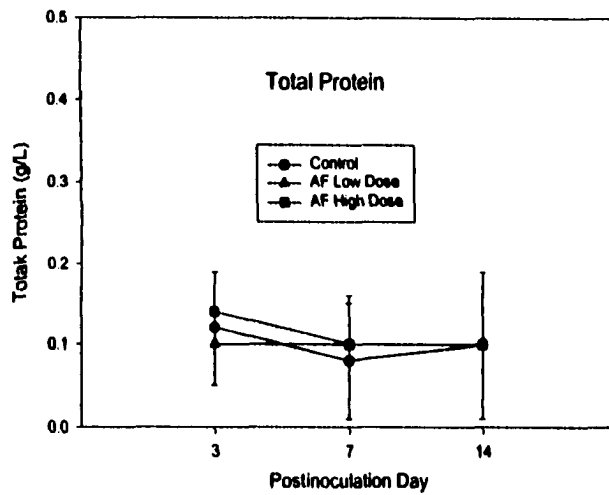
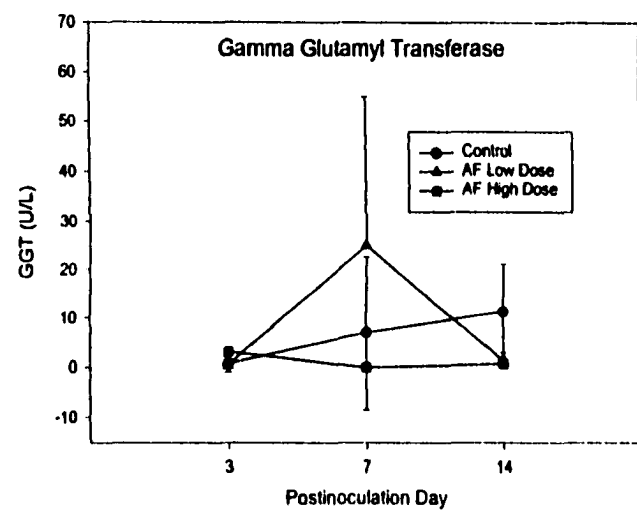
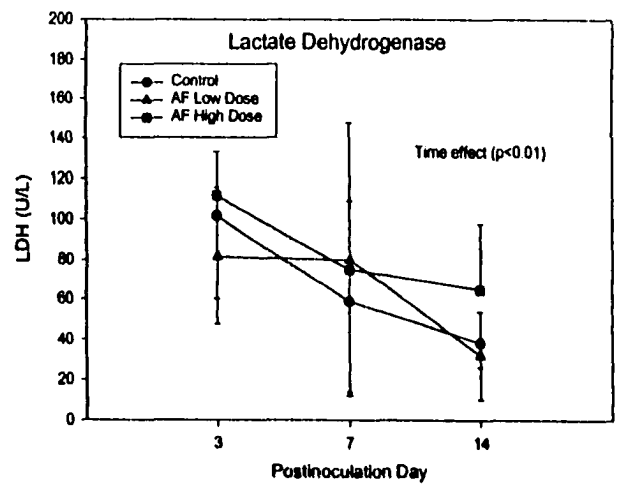
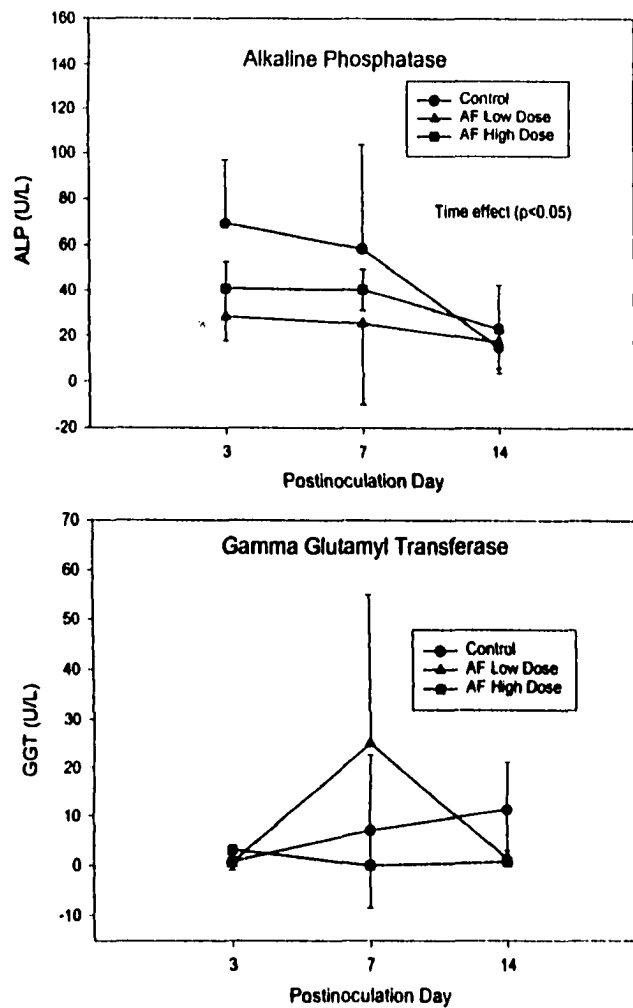


Fig. 14. Enzymatic activity and total protein in BAL fluid, after the inoculation of amniotic fluid. Symbols and bars represent mean and SD ($n= 5$ or 6 neonates per group). * Significantly different from the control ($p<0.05$) at the same time.

3.3.4. Effect of meconium on the cytological and biochemical composition of the lung.

3.3.4.1. Cytology

The volume of BAL fluid recovered in the meconium and control groups was 76.5% \pm 7.64% of the instilled volume.

Intratracheal inoculation of meconium induced a significant increase in the number of leukocytes ($p<0.01$) in the bronchoalveolar space starting at PID 1 with a peak at PID 3. The high number of leukocytes returned to baseline levels by PID 7 and 14 (Fig. 15). The number of leukocytes remained unchanged in the controls inoculated with saline. A significant time effect and interaction between treatment and time were also found ($p<0.01$).

Inoculation with meconium induced significant changes in the percentage of macrophages and neutrophils ($p<0.01$). There was a remarkable shift in the macrophage (PAM)-to-neutrophil (PMN) ratio at PID 1 and 3. The ratio of PAM:PMN in the control was 93:7, compared with 27:73 in the meconium group at PID 1, and 98:2 in control group compared with 28:72 in meconium group at PID 3 (Fig. 16). This rapid shift in the population of leukocytes associated with the meconium inoculation was easily detected in the cytopsin smears (Fig. 17).

Inoculation of meconium did not induce a significant change in the number of macrophages at PID 1. A tendency of macrophages to increase at PID 3, but not significantly ($p>0.05$) compared with the control, was observed (Fig. 18). Macrophage numbers had an initial tendency to increase by time in both groups with a significant time effect ($p<0.01$).

Meconium induced a significant influx of neutrophils ($p<0.01$) to the bronchoalveolar space at PID 1 and 3, returning to the baseline levels at PID 7. A significant time effect

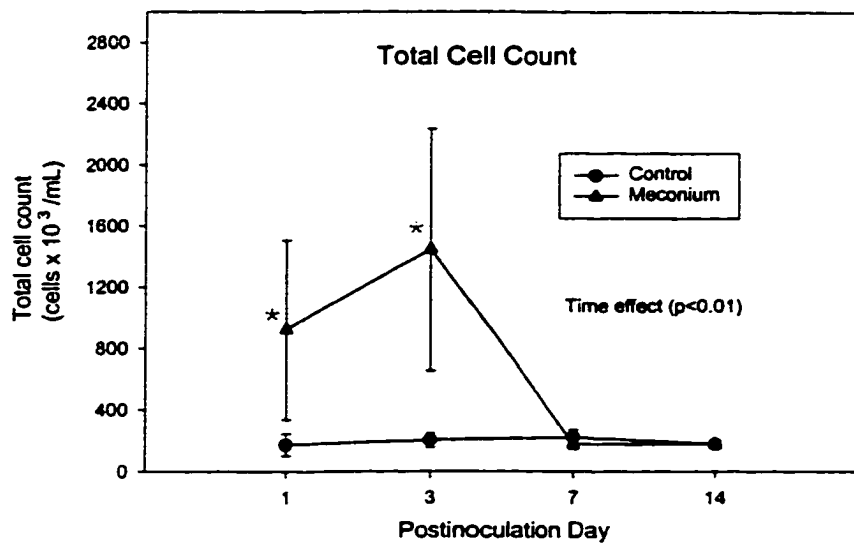


Fig. 15. Total cell count in BAL fluid after the inoculation of 7-day-old rats with meconium. Symbols and bars represent mean and SD ($n = 7$ or 8 animals per group). * Significantly different ($p < 0.01$) compared with control.

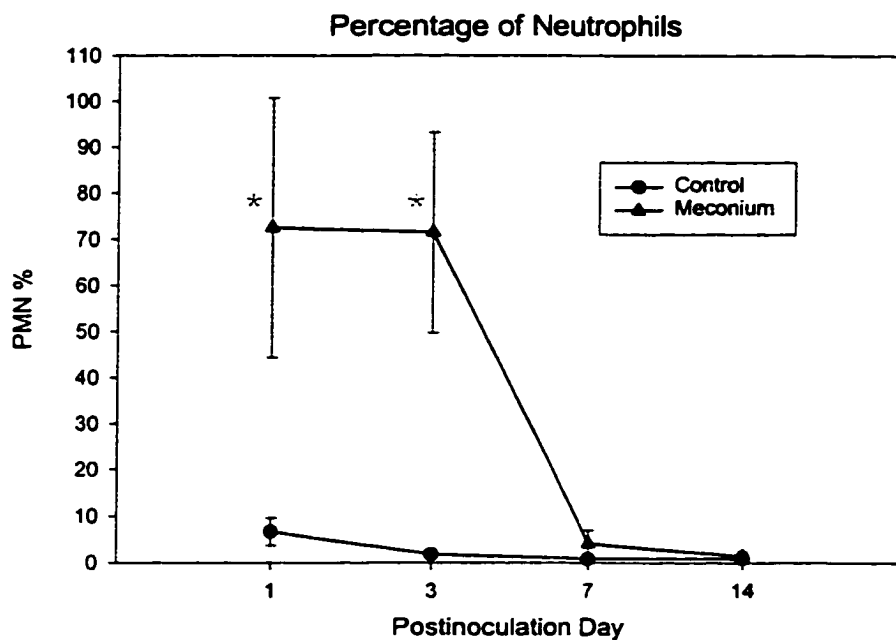
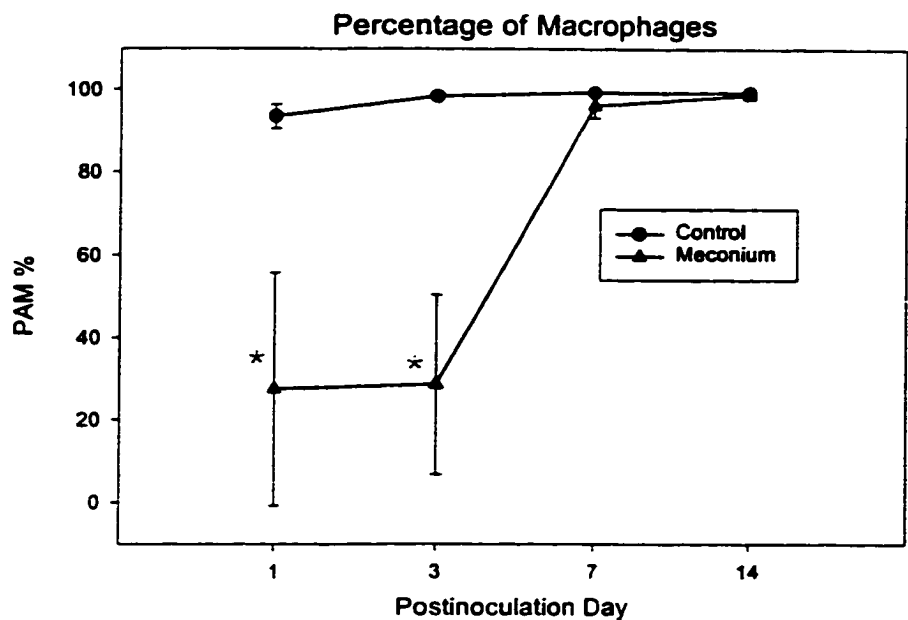


Fig. 16. Differential of leukocytes in BAL after the inoculation of 7-day-old rats with meconium. Symbols and bars represent mean and SD ($n= 7$ or 8 animals each group). * Significantly different ($p<0.01$) compared with control.

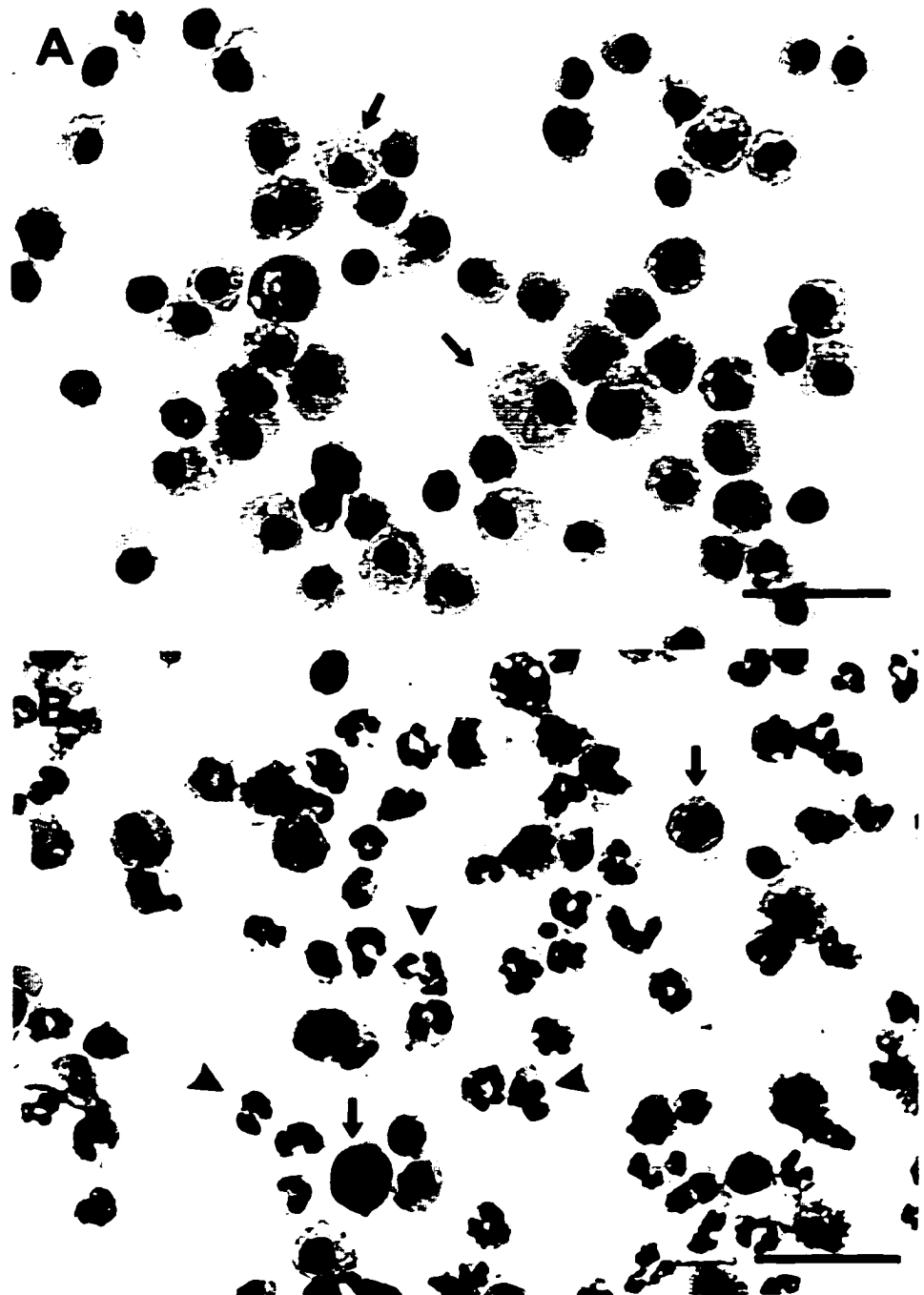


Fig. 17. Photomicrographs of recovered cells from BAL at PID 1, isolated with the Cytospin centrifuge and stained with Wright-Giemsa. A. Normal population of leukocytes in control inoculated with saline. B. Shift in macrophage-to-neutrophil ratio in neonate inoculated with meconium. Note the predominance of neutrophils (arrowheads). Macrophages (arrows). Bar = 40 μ m.

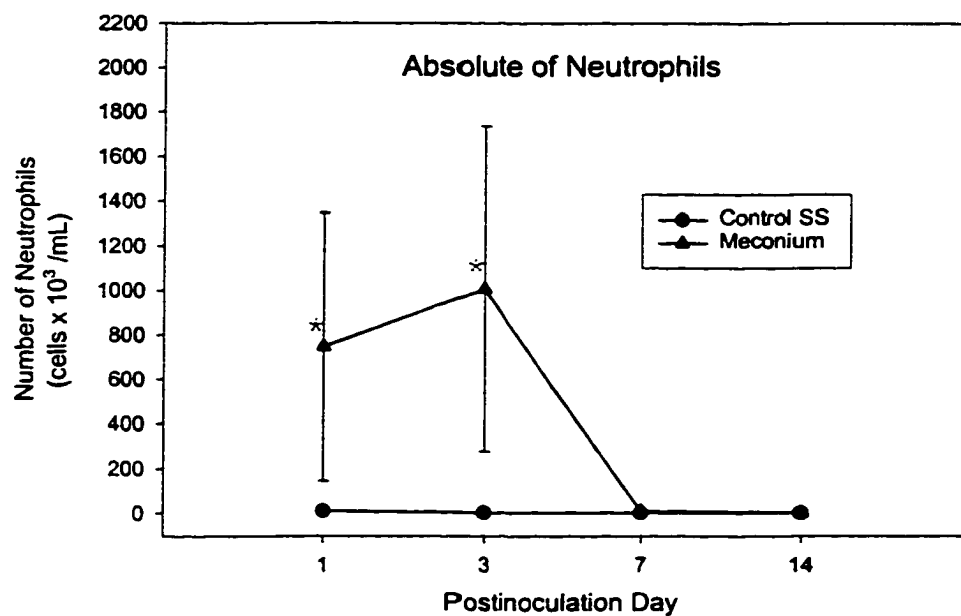
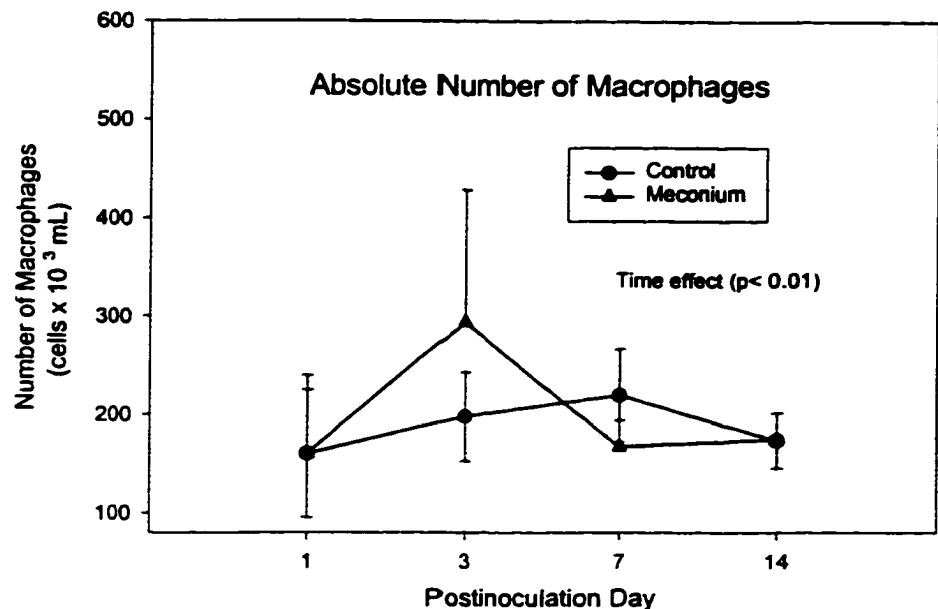


Fig. 18. Absolute number of leukocytes in BAL fluid after the inoculation of meconium. Symbols and bars represent mean and SD ($n = 7$ or 8 animals per group). * Significantly different compared with the control ($p < 0.01$).

and interaction between treatment and time ($p<0.01$) were also found (Fig. 18).

A high correlation ($r = 0.97$) between the number of cells recovered in the BAL fluid and the absolute number of neutrophils in the meconium group was demonstrated.

3.3.4.1. Biochemistry

After the inoculation of meconium, a significant increase ($p<0.01$) in the ALP, LDH and GGT activities in the BAL fluid was detected at PID 3 compared with the control. ALP activity decreased significantly ($p<0.01$) at PID 7 and 14. Values of ALP, LDH, and GGT in meconium inoculated rats decreased progressively at PID 7 and 14 with a significant time effect ($p<0.01$) (Fig. 19). Interaction between treatment and time were significant ($p<0.01$) in the three studied enzymes.

Total protein was increased significantly ($p<0.01$) in the meconium group at PID 1, compared with the control inoculated with saline (Fig. 19). Total protein decreased in a progressive pattern from PID 3 to 14 with a significant time effect and interaction treatment and time ($p<0.01$).

LDH activity was moderately correlated with the number of cells recovered in the BAL fluid ($r = 0.75$) and with the number of neutrophils ($r = 0.72$). No other relevant correlations between cells and enzymes were detected.

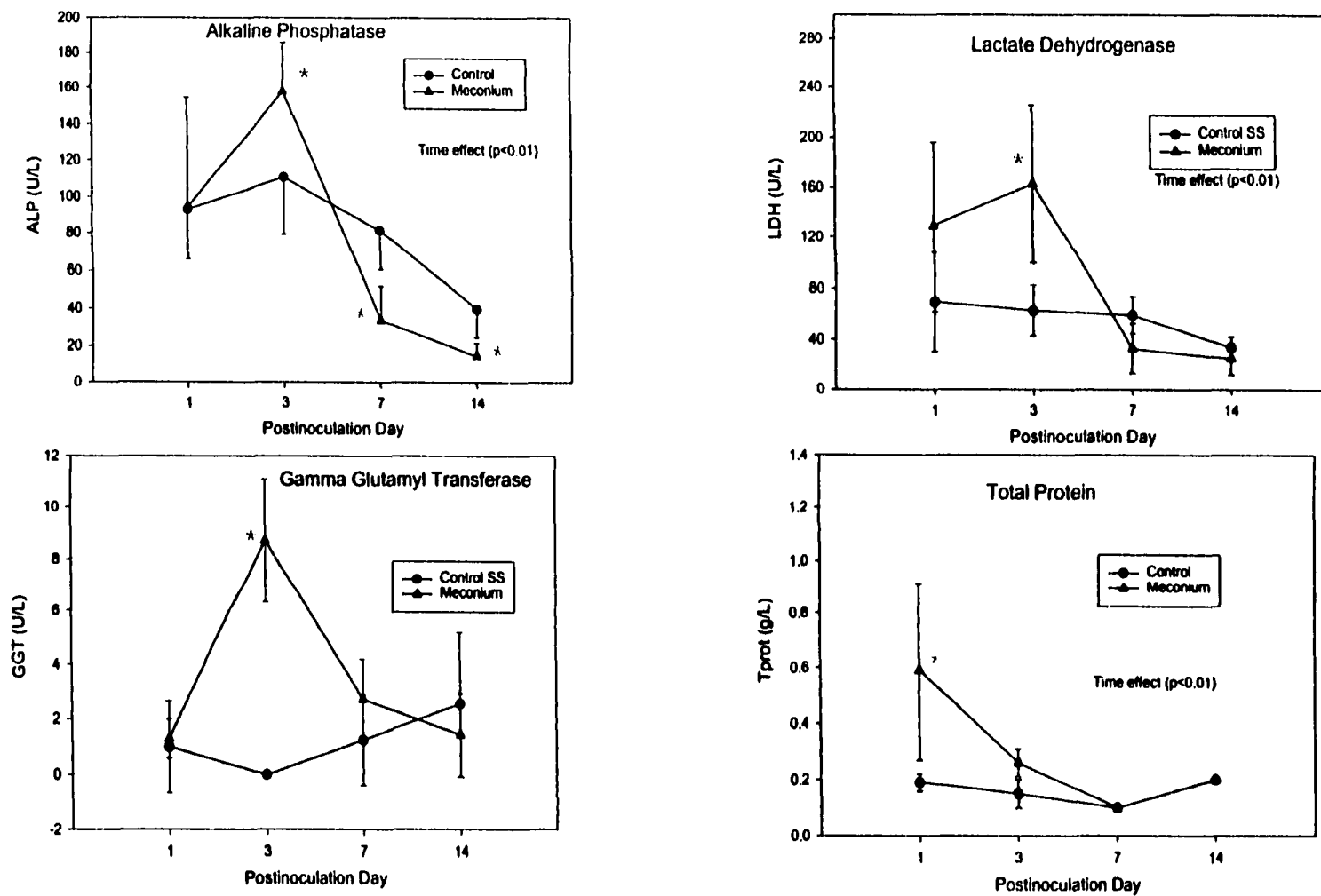


Fig. 19. Enzymatic activity and total protein in BAL fluid, after inoculation of 7-day-old rats with meconium. Symbols and bars represent mean and SD ($n = 7$ or 8 neonates per group). * Significant different from control ($p < 0.01$).

3.4. Discussion

3.4.1. Leukocyte kinetics and biochemistry of BAL from normal fetuses and neonates

Cytological analyses of BAL fluid collected from normal Fischer 344 fetuses indicated that normal fetal rats have a very low cellularity in the bronchoalveolar space and that alveolar macrophages (PAMs) account for 99% of the cell population. Immediately after birth, there was a substantial increase in the number of bronchoalveolar cells, and by 3 days of age, the cell population became stable until 36 days of age when there was a slight decline. Increased cellularity during the perinatal period was largely attributed to macrophage recruitment into the bronchoalveolar space. A similar trend in BAL cytology has been well documented in human and rabbit fetuses. For instance, rabbit fetuses delivered 10 days prematurely had low BAL cellularity but soon after birth the cell counts increased and PAMs represented around 90% of the recovered cells (90,91). Similarly, BAL analysis in human fetuses and newborn premature infants showed a progressive increase in the number of PAMs with increasing lung maturity (91). This sharp increase in PAMs during the first few days of postnatal life suggests a normal adaptative pulmonary response (90,92).

The high percentage of PAMs recovered from the BAL in the neonatal rats after birth to 120 days of age was similar to the 90-97% of PAM reported in prenatal and postnatal rabbits (90,91,93). The overall percentage of PMN remained less than 5% in the neonatal rats which indicates that, as in adults rats, PMN counts remain low under normal conditions (2,45,59). Although there is scant information about the total cell counts in BAL of rats during the prenatal or early postnatal periods, there are some reports referring to a reduction

in cell numbers in adult rats. A study in Sprague-Dawley rats showed a significant decline in the cell numbers similar to what was found in the Fischer-344 after 36 days of age (65). In another study, conducted in Long Evans rats, comparison of the number of cells recovered by BAL between 8 and 10 weeks old showed no significant difference (57). However, the differential evaluation of leukocyte types was not done in this last study. A decrease in the percentage of PAMs, but not in the total number of cells recovered by BAL, has also been documented in young animals. For instance, in calves the total cell count remained unchanged despite a reduction in the number of PAMs which was explained by a concomitant increase in the numbers of epithelial cells and neutrophils recovered in the BAL (27). Neonatal foals normally have low numbers of PAMs, but numbers increase sharply during the first two weeks of life and remain relatively constant thereafter (94). Approximately 86% of cells recovered in the lungs of foals up to 3 weeks of age were PAMs, but unlike rodents, during the first 2 months of life PAMs decreased to 71% whereas the percentage of lymphocytes increased from 5 to 20% (94).

There are some possible explanations regarding the increase in PAM counts in newborn babies and neonatal animals. It has been suggested that the prenatal influx of PAM is a physiological response to prepare the alveoli for the early postnatal life, and thyroid and estrogen hormones have been implicated in this phenomenon (95,96). Another possible mechanism is leukotaxis induced by lipids and lipoproteins of the pulmonary surfactant present in the neonatal alveoli (97). It has been suggested that surfactant-related phospholipids released into the alveoli at birth and during the first days after being born may play a role as chemotactic agents (92). This view is further supported by the fact that

abundant surfactant-related phospholipids have been observed in the phagolysosomes of PAMs in newborn rabbits (92). In addition, it is possible that lung exposure to gases and particles at birth send signals to recruit additional PAMs into the bronchoalveolar space (43,45,98). The transient increase in the percentage and absolute numbers of PMN found in the neonatal rats could have several possible explanations. First, it is feasible that the air distending the lung at birth is sufficient to attract PMNs into the bronchoalveolar space since it is reported that high concentrations of inspired O₂ cause neutrophil migration into the neonatal lung (99). Second, PMNs could be recruited in response to chemokines released by PAMs which are actively involved in the clearance of surfactant and debris during the first few hours of life (92). This concept is based on the premise that activated macrophages regulate the influx of PMNs thorough the release of specific chemokines (100,101). Finally, since PMNs also contribute to the clearance of surfactant, it is also possible that these cells may be physiologically attracted to the alveolar lining material during the perinatal period (102).

To our knowledge, this is the first description of the leukocyte kinetics in the bronchoalveolar space of normal fetal and neonatal Fischer 344 rats. Results clearly showed that during the perinatal period, there is noticeable influx of PAMs and PMNs into the bronchoalveolar space starting 1 day before parturition and lasting for 3 days after birth. Thereafter, the cell counts of PAM and PMN remain relatively constant with values comparable with those of adult rats.

The biochemical analysis of BAL fluid showed that rat pups are born with high activities of alkaline phosphatase (ALP) and lactate dehydrogenase (LDH), and that gamma

glutamyl transferase (GGT) and protein concentration increase temporarily during the first few days of life. With time, there was a trend towards decreased enzymatic activity in the neonatal lung. It is not clear why rats are born with high ALP and LDH enzymatic activities but these may be related to the surfactant, pulmonary fluids and cellular debris in the bronchoalveolar space during the perinatal life. Interestingly, other researchers also found high activities of LDH and protein in the lungs of newborn rabbits. According to these authors, high enzyme values and protein in the bronchoalveolar spaces are presumably connected with the availability of substrates, phagocytic loads of surfactant and abundant cellular debris in the lungs at birth (92,103). Since PMNs account for less than 10% of the total cell population in a normal lung and only accounted for 5% in the neonatal rats of this study, it is unlikely that the high activities of LDH and ALP were related to PMNs at days 1 and 3. A more reasonable explanation for the high ALP, LDH and GGT activities in the first days of life is that these enzymes are derived from secretion of surfactant from type II pneumocytes (73,75).

The lack of statistical correlation between enzymatic activity and leukocyte counts in the BAL of the neonatal rats supports the notion that enzymatic activity in the lung does not originate from phagocytic cells in the airways (56). The concentration of these enzymes in PAMs and PMNs appears to be insufficient to explain the high values obtained in BAL collected from animals exposed to pneumotoxins (44,58,104,105). Further, iso-enzyme analysis in BAL fluid has also demonstrated that the increase in enzymatic activity following acute lung injury originates from damaged epithelial cells and not from phagocytic cells or leaked plasma (69,106).

It was concluded from the results of this study that protein and enzymatic activities are high during the first three days of life, and as the lung matures, the values decrease. Higher activities during the perinatal period are presumably the result of increased availability of substrates, cellular debris and increased release of surfactant during birth and the first few days of life.

3.4.2. Effect of saline solution on the cytological and biochemical composition of the BAL.

Cytological analysis of BAL fluid showed no significant changes in the total and differential cell counts after the inoculation of saline, compared with the control rats with sham inoculation with air. This was an interesting finding since it has been reported that saline solution alone induces a transient influx of leukocytes into the bronchoalveolar space (33,59,64). One possible explanation for this discrepancy is that the 0.05ml inoculated to the neonatal rats was an insufficient volume of inoculum to cause detectable changes in the composition of the BAL. Supporting this view, is the known dose-effect relationship between the volume of saline and physiologic events in the bronchoalveolar space (59,107). It has been demonstrated that the volume of vehicle (saline) significantly enhances the pulmonary injury and the inflammatory response in rats (59) and also has a synergistic effect on the development of bacterial pneumonia in mice and squirrel monkeys (107). Further studies should compare the effect of volume of inoculum and lung maturity in the inflammatory response induced by intratracheal inoculation of saline solution. Another possible but unsubstantiated explanation is that the immature lung cannot mount the tangible inflammatory response that occurs in adult animals inoculated with saline solution (33,59,64). In summary, it was concluded that low volumes of saline inoculated into the

lungs of neonatal rats do not cause detectable changes in the cellular composition of the alveolar space as determined by BAL.

Inoculation of saline solution in neonatal rats did not have any effect on the enzymatic activities and protein content in BAL fluid indicating that this fluid caused no ostensible damage to the respiratory membrane. This finding is consistent with other experimental work where intratracheal inoculation of saline solution (0.5ml) did not alter the LDH, ALP and protein values in the BAL fluid in rats (64). According to some investigators, only high volumes of saline can cause damage to the respiratory mucosa and increase the activities of LDH and ALP in the BAL fluid (59).

In brief, intratracheal inoculation of 0.05ml of sterile saline solution in 7-day-old neonatal rats does not cause significant injury in the respiratory membrane measured by BAL analysis. Therefore, a small volume of sterile saline solution is an innocuous and reliable vehicle to deliver substances into the distal lung of neonatal rats.

3.4.3. Effect of amniotic fluid on the cytological and biochemical composition of the BAL.

The intratracheal inoculation of low doses (50%) or high doses (100%) of amniotic fluid did not elicit significant changes in the number of cells and leukocytes recovered by BAL compared with the controls inoculated with saline solution. Since no differences were noted between control and inoculated rats, the transient increase in PAM counts from PID1 to 7 in both groups of inoculated rats was interpreted as a normal and nonspecific change related to lung maturation as described in normal neonates, corresponding to ages 8, 11 and 15 days (Section 3.3.1.). This lack of response to amniotic fluid was certainly surprising since amniotic fluid contains keratin and squamous epithelial cells which are

known to induce a “foreign body” histiocytic response (13,108). Moreover, previous studies have shown that intratracheal inoculation of bovine amniotic fluid to adult rats caused an increase in numbers of PAMs and PMNs, and that the magnitude of pulmonary inflammation was dose-dependent (16). Similarly, inoculation of amniotic fluid did not induce any detectable change in the enzymatic activity and total protein indicating that this vehicular fluid, used in experimental lung research, does not cause meaningful injury to the respiratory membrane or air-blood barrier. These findings were consistent with the histologic study in which inoculation of amniotic fluid did not produce significant microscopic lesions in the lung (Section 4.3.2.2).

There are several possible explanations for the lack of changes in the cellular or enzymatic composition of BAL fluid following inoculation of amniotic fluid in rat neonates. First, it is possible that the dose of amniotic fluid inoculated to neonatal rats was too low or insufficient to induce detectable changes in the respiratory mucosa (16). However, this is unlikely since keratin and epidermal cells were noticed microscopically in the lungs (Section 4.3.2.2.). Further, the volume of inoculum administered to the neonatal rats was close to the maximum tolerated dose previously established in a pilot study. Another possible explanation is that the numbers of cells recovered are influenced by “stickiness” of the cells at the sites of accumulation. It should also be kept in mind that the immature lung does not necessarily react in the same way as the mature lung (93). Finally, as alluded to by others (16,109), amniotic fluid itself may down-regulate the inflammatory response in the lung which may explain why some animals with intrauterine asphyxia are born with large numbers of epidermal squames and keratin in the lung but show only minimal pulmonary

inflammation. Future studies should be designed to test all these hypotheses and investigate if there are any chemical messengers in amniotic fluid that reduce the intensity of the inflammatory reaction in the lung.

3.4.4. Effect of meconium on the cytological and biochemical composition of the BAL.

The dramatic increase in the number of cells recovered by BAL after intratracheal inoculation of meconium is qualitatively similar to that produced by other pneumotoxicants such as silica (59), NO₂ (66), LPS (64) and inhaled bacteria (61,61,64,110). This sharp increase in neutrophils caused by homologous meconium in neonatal rats was in agreement with results obtained in adult rats intratracheally inoculated with heterologous human meconium (2). It has been already confirmed that low concentrations of human meconium cause a reversible, time-dependent pulmonary inflammation in adult rats (2,77). Similar conclusions were obtained in a newborn piglet model of MAS using 20% human meconium as the inoculum (4).

In contrast to amniotic fluid, meconium induced an acute inflammatory response as shown by the transient but sharp increase in PMNs in the lungs. The leukocytic reaction mounted against experimentally inoculated meconium closely mimics the response seen in natural cases of MAS (111,112). There is recent laboratory evidence suggesting that the recruitment of PMNs in the lung following aspiration of meconium results from the local release of inflammatory mediators such as TNF- α , IL-1 β and IL-8 (9,10,12). These pro-inflammatory cytokines have been identified as chemotactic for PMNs in many inflammatory diseases of the lung and likely play a significant role in the pathogenesis of MAS (9,10,12,100,101).

The intratracheal inoculation of meconium in neonatal rats significantly increased the activities of ALP, LDH and GGT in the BAL indicating damage to the cells of the respiratory membrane. Based on these findings it is reasonable to suggest that meconium acts as a toxic substance causing transient injury to respiratory cells. Interestingly, the pattern of enzymatic activity which peaked at PID 3 and decreased by PID 7 was similar to that reported in lung injury caused by various pneumotoxins such as paraquat, bromobenzene and oxygen (44), α -naphthylthiourea, ipoamenol (71) and nitrogen dioxide (66,73). However, increased enzymatic activity in BAL fluid as indicator of injury after meconium inoculation has not been described before.

The source of LDH, ALP and GGT in BAL fluid following respiratory injury is not totally understood. As discussed earlier, it is widely accepted that the increased levels of enzymes in BAL following lung injury originate from damaged epithelial cells and not from plasma or phagocytic cells (44,73,113). Results from BAL analyses and electron microscopy indicate that cell injury to the respiratory membrane is moderate, transient and does not lead to severe necrosis or exfoliation of epithelial cells. The sequence and mechanisms in which enzymes are released from the pulmonary cells in neonates after meconium-induced injury requires further investigative work.

The increased total protein obtained from the BAL in the neonatal rats after the inoculation of meconium was a good indicator of protein leakage into the bronchoalveolar space. Based on the results of this investigation, it is evident that homologous meconium alters the vascular permeability in the lungs of neonatal rats. Other reports had already

shown that experimental aspiration of heterologous meconium alters the pulmonary vascular permeability in adult animals (18,77).

It remains unclear whether leakage of protein into the air spaces is caused by the direct effect of meconium on the blood-air barrier or through the indirect effect of locally released cytokines. Results from the BAL analyses in the neonatal rats showed that following inoculation of meconium, the increase in protein coincided with increased numbers of PMNs. Similar findings were observed in adult rats intratracheally inoculated with human meconium (2) and in piglets (4). These findings suggest that protein leakage is likely due to alterations in vascular permeability caused by mediators of pulmonary inflammation and not by the toxic effect of meconium on endothelial cells or type I pneumocytes. This hypothesis is further supported by the fact that electron microscopy failed to reveal significant changes in the cells of the air-blood barrier in the neonatal rats inoculated with meconium (See section 6.3.3.). The role that some cytokines mediators (TNF α) and interleukin 1 (IL1) have on the structural reorganization of the cytoskeleton of endothelial cells inducing "junctional retraction" may also explain the vascular leakage in absence of evidence of direct endothelial damage (114).

It was concluded that unlike amniotic fluid, homologous meconium in neonatal rats causes acute lung injury characterized by damage to the bronchoalveolar lining mucosa, transient influx of PMNs and leakage of protein into the bronchoalveolar space. The consequence of this exudative lung injury in the long term pathophysiology of MAS requires additional work.

3.5. REFERENCES

1. SRINIVASAN HB, VIDYASAGAR D. Meconium aspiration syndrome: current concepts and management. *Compr Ther* 1999; 25: 82-89.
2. CLEARY GM, ANTUNES MJ, CIESIELKA DA, HIGGINS ST, SPITZER AR, CHANDER A. Exudative lung injury is associated with decreased levels of surfactant proteins in a rat model of meconium aspiration. *Pediatrics* 1997; 100: 998-1003.
3. CLEARY GM, WISWELL TE. Meconium-stained amniotic fluid and the meconium aspiration syndrome. An update. *Pediatr Clin North Am* 1998; 45: 511-529.
4. DAVEY AM, BECKER JD, DAVIS JM. Meconium aspiration syndrome: physiological and inflammatory changes in a newborn piglet model. *Pediatr Pulmonol* 1993; 16: 101-108.
5. WISWELL TE, PEABODY SS, DAVIS JM, SLAYTER MV, BENT RC, MERRITT TA. Surfactant therapy and high-frequency jet ventilation in the management of a piglet model of the meconium aspiration syndrome. *Pediatr Res* 1994; 36: 494-500.
6. TYLER DC, MURPHY J, CHENEY FW. Mechanical and chemical damage to lung tissue caused by meconium aspiration. *Pediatrics* 1978; 62: 454-459.
7. WISWELL TE, FOSTER NH, SLAYTER MV, HACHEY WE. Management of a piglet model of the meconium aspiration syndrome with high-frequency or conventional ventilation. *Am J Dis Child* 1992; 146: 1287-1293.
8. SOUKKA H, RAUTANEN M, HALKOLA L, KERO P, KÄÄPÄ P. Meconium aspiration induces ARDS-like pulmonary response in lungs of ten-week-old pigs. *Pediatr Pulmonol* 1997; 23: 205-211.
9. KOJIMA T, HATTORI K, FUJIWARA T, SASAI TM, KOBAYASHI Y. Meconium-induced lung injury mediated by activation of alveolar macrophages. *Life Sci* 1994; 54: 1559-1562.
10. JONES CA, CAYABYAB RG, HAMDAN H. Early production of proinflammatory cytokines in the pathogenesis of neonatal adult respiratory distress syndrome (ARDS) associated with meconium aspiration. *Pediatr Res* 1994; 35: 339A-
11. SHABAREK FM, XUE H, LALLY KP. Human meconium stimulates murine alveolar macrophage procoagulant activity. *Pediatr Res* 1997; 41: 267A-
12. DE BEAUFORT AJ, PELIKAN DM, ELFERINK JG, BERGER HM. Effect of interleukin 8 in meconium on in-vitro neutrophil chemotaxis. *Lancet* 1998; 352: 102-105.

13. CRUICKSHANK AH. The effects of the introduction of amniotic fluid into the rabbits' lungs. *J Pathol Bact* 1949; 61: 527-531.
14. JOVANOVIC R, NGUYEN HT. Experimental meconium aspiration in guinea pigs. *Obstet Gynecol* 1989; 73: 652-656.
15. LOPEZ A, BILDFELL R. Pulmonary inflammation associated with aspirated meconium and epithelial cells in calves. *Vet Pathol* 1992; 29: 104-111.
16. CARVAJAL-DE LA FUENTE V, LOPEZ-MAYAGOITIA A, MARTINEZ-BURNES J, BARRON-VARGAS C, LOREDO-OSTI JC. Efecto antiinflamatorio del líquido amniótico en el pulmón de ratas inoculadas intratraquealmente con sílice. *Vet Mex* 1998; 29: 147-153.
17. OGAWA Y, SHIMIZU H, ITAKURA Y, OHAMA Y, ARAKAWA H, AMIZUKA T, OBATA M, KAKINUMA R. Functional pulmonary surfactant deficiency and neonatal respiratory disorders. *Pediatr Pulmonol Suppl* 1999; 18: 175-177.
18. SUN B, CURSTEDT T, ROBERTSON B. Exogenous surfactant improves ventilation efficiency and alveolar expansion in rats with meconium aspiration. *Am J Respir Crit Care Med* 1996; 154: 764-770.
19. SUN B, HERTING E, CURSTEDT T, ROBERTSON B. Exogenous surfactant improves lung compliance and oxygenation in adult rats with meconium aspiration. *J Appl Physiol* 1994; 77: 1961-1971.
20. GOLDSTEIN RA, ROHATGI PK, BERGOFSKY EH, BLOCK ER, DANIELE RP, DANTZKER DR, DAVIS GS, HUNNINGHAKE GW, KING TEJ, METZGER WJ. Clinical role of bronchoalveolar lavage in adults with pulmonary disease [see comments]. *Am Rev Respir Dis* 1990; 142: 481-486.
21. HUNNINGHAKE GW, GADEK JE, KAWANAMI O, FERRANS VJ, CRYSTAL RG. Inflammatory and immune processes in the human lung in health and disease: evaluation by bronchoalveolar lavage. *Am J Pathol* 1979; 97: 149-206.
22. ROSSIER Y, SWEENEY CR, ZIEMER EL. Bronchoalveolar lavage fluid cytologic findings in horses with pneumonia or pleuropneumonia. *J Am Vet Med Assoc* 1991; 198: 1001-1004.
23. DAVIS GS, GIANCOLA MS, COSTANZA MC, LOW RB. Analyses of sequential bronchoalveolar lavage samples from healthy human volunteers. *Am Rev Respir Dis* 1982; 126: 611-616.
24. REYNOLDS HY. Bronchoalveolar lavage. *Am Rev Respir Dis* 1987; 135: 250-263.

25. WILKIE BN, MARKHAM RJ. Sequential titration of bovine lung and serum antibodies after parenteral or pulmonary inoculation with *Pasteurella haemolytica*. Am J Vet Res 1979; 40: 1690-1693.
26. WILKIE BN, MARKHAM RJ. Bronchoalveolar washing cells and immunoglobulins of clinically normal calves. Am J Vet Res 1981; 42: 241-243.
27. PRINGLE JK, VIEL L, SHEWEN PE, WILLOUGHBY RA, MARTIN SW, VALLI VE. Bronchoalveolar lavage of cranial and caudal lung regions in selected normal calves: cellular, microbiological, immunoglobulin, serological and histological variables. Can J Vet Res 1988; 52: 239-248.
28. TRIGO E, LIGGITT HD, BREEZE RG, LEID RW, SILFLOW RM. Bovine pulmonary alveolar macrophages: antemortem recovery and in vitro evaluation of bacterial phagocytosis and killing. Am J Vet Res 1984; 45: 1842-1847.
29. SWEENEY CR, ROSSIER Y, ZIEMER EL, LINDBORG SR. Effect of prior lavage on bronchoalveolar lavage fluid cell population of lavaged and unlavaged lung segments in horses. Am J Vet Res 1994; 55: 1501-1504.
30. SWEENEY CR, ROSSIER Y, ZIEMER EL, LINDBORG S. Effects of lung site and fluid volume on results of bronchoalveolar lavage fluid analysis in horses. Am J Vet Res 1992; 53: 1376-1379.
31. BEGIN R, MASSE S, ROLA-PLESZCZYNKI M, DRAPEAU G, DALLE D. Selective exposure and analysis of the sheep tracheal lobe as a model for toxicological studies of respirable particles. Environ Res 1985; 36: 389-404.
32. CHEN W, ALLEY MR, MANKTELOW BW, HOPCROFT D, BENNETT R. Pneumonia in lambs inoculated with *Bordetella parapertussis*: bronchoalveolar lavage and ultrastructural studies. Vet Pathol 1988; 25: 297-303.
33. COHEN AB, BATRA GK. Bronchoscopy and lung lavage induced bilateral pulmonary neutrophil influx and blood leukocytosis in dogs and monkeys. Am Rev Respir Dis 1980; 122: 239-247.
34. MUGGENBURG BA, MAUDERLY JL, PICKRELL JA, CHIFFELLE TL, JONES RK, LUFT UC, MCCLELLAN RO, PFLEGER RC. Pathophysiologic sequelae of bronchopulmonary lavage in the dog. Am Rev Respir Dis 1972; 106: 219-232.
35. REYNOLDS HY, KAZMIEROWSKI JA, DALE DC, WOLFF SM. Changes in the composition of canine respiratory cells obtained by bronchial lavage following irradiation or drug immunosuppression. Proc Soc Exp Biol Med 1976; 151: 756-761.

36. KAZMIEROWSKI JA, FAUCI AS, REYNOLDS HY. Characterization of lymphocytes in bronchial lavage fluid from monkeys. *J Immunol* 1976; 116: 615-618.
37. HARMSEN AG, BIRMINGHAM JR, ENGEN RL, JESKA EL. A method for obtaining swine alveolar macrophages by segmental pulmonary lavage. *J Immunol Methods* 1979; 27: 199-202.
38. PADRID PA, FELDMAN BF, FUNK K, SAMITZ EM, REIL D, CROSS CE. Cytologic, microbiologic, and biochemical analysis of bronchoalveolar lavage fluid obtained from 24 healthy cats. *Am J Vet Res* 1991; 52: 1300-1307.
39. PADRID P. Bronchoalveolar lavage in the evaluation of pulmonary disease in the dog and cat [letter; comment]. *J Vet Intern Med* 1991; 5: 52-55.
40. ZINKL JG. The Lower Respiratory Tract. In: Cowell RL, Tyler RD, eds. *Cytology and Hematology*. California: American Veterinary Publications, Inc., 1992: 77-87.
41. COWELL RL, TYLER RD, BALDWIN CJ, MEINKOTH JH. Transtracheal/Bronchoalveolar Washes. In: Cowell RL, Tyler RD, Meinkoth JH, eds. *Diagnostic Cytology and Hematology of the Dog and Cat*. St. Louis, MO: Mosby, 1999: 159-173.
42. SWEENEY CR, BEECH J. Bronchoalveolar Lavage. *Equine Respiratory Disorders*. Pennsylvania: Lea & Febiger, 1991: 55-61.
43. HENDERSON RF, BENSON JM, HAHN FF, HOBBS CH, JONES RK, MAUDERLY JL, MCCLELLAN RO, PICKRELL JA. New approaches for the evaluation of pulmonary toxicity: bronchoalveolar lavage fluid analysis. *Fundam Appl Toxicol* 1985; 5: 451-458.
44. ROTH RA. Effect of pneumotoxins on lactate dehydrogenase activity in airways of rats. *Toxicol Appl Pharmacol* 1981; 57: 69-78.
45. MORGAN A, MOORES SR, HOLMES A, EVANS JC, EVANS NH, BLACK A. The effect of quartz, administered by intratracheal instillation, on the rat lung. I. The cellular response. *Environ Res* 1980; 22: 1-12.
46. VAN SOOLINGEN D, MOOLENBEEK C, VAN LOVEREN H. An improved method of bronchoalveolar lavage of lungs of small laboratory animals: short report. *Lab Anim* 1990; 24: 197-199.
47. HENDERSON RF. Use of bronchoalveolar lavage to detect lung damage. *Environ Health Perspect* 1984; 56: 115-129.

48. HENDERSON RF, MAUDERLY JL, PICKRELL JA, HAHN FF, MUHLE H, REBAR AH. Comparative study of bronchoalveolar lavage fluid: effect of species, age, and method of lavage. *Exp Lung Res* 1987; 13: 329-342.
49. GICLAS PC, KING TE, BAKER SL, RUSSO J, HENSON PM. Complement activity in normal rabbit bronchoalveolar fluid. Description of an inhibitor of C3 activation. *Am Rev Respir Dis* 1987; 135: 403-411.
50. LEFFINGWELL CM, LOW RB. Protein biosynthesis by the pulmonary alveolar macrophage. Comparison of synthetic activity of suspended cells and cells on surfaces. *Am Rev Respir Dis* 1975; 112: 349-359.
51. HOLIAN A, DAUBER JH, DIAMOND MS, DANIELE RP. Separation of bronchoalveolar cells from the guinea pig on continuous gradients of Percoll: functional properties of fractionated lung macrophages. *J Reticuloendothel Soc* 1983; 33: 157-164.
52. DAUBER JH, HOLIAN A, ROSEMILLER ME, DANIELE RP. Separation of bronchoalveolar cells from the guinea pig on continuous density gradients of Percoll: morphology and cytochemical properties of fractionated lung macrophages. *J Reticuloendothel Soc* 1983; 33: 119-126.
53. KAVET RI, BRAIN JD, LEVENS DJ. Characteristics of pulmonary macrophages lavaged from hamsters exposed to iron oxide aerosols. *Lab Invest* 1978; 38: 312-319.
54. KAVET RI, BRAIN JD. Phagocytosis: quantification of rates and intercellular heterogeneity. *J Appl Physiol* 1977; 42: 432-437.
55. HENDERSON RF, LOWREY JS. Effect of anesthetic agents on lavage fluid parameters used as indicators of pulmonary injury. *Lab Anim Sci* 1983; 33: 60-62.
56. LOPEZ A, YONG S, SHARMA A, MORWOOD CM, LILLIE LE, ALBASSAM M. Effect of sex and age on the activities of lactate dehydrogenase and alkaline phosphatase in the lungs of rats. *Can J Vet Res* 1986; 50: 397-401.
57. LOPEZ A, YONG S, SHARMA A, BAILEY D. Effect of sex, age, number of bronchoalveolar lavages and quantitation methods on the bronchoalveolar cell counts in rats. *Can J Vet Res* 1986; 50: 101-105.
58. LOPEZ A, PRIOR M, YONG S, ALBASSAM M, LILLIE LE. Biochemical and cytologic alterations in the respiratory tract of rats exposed for 4 hours to hydrogen sulfide. *Fundam Appl Toxicol* 1987; 9: 753-762.

59. LOPEZ A, YONG S, SHARMA A, PRIOR M. Effect of vehicular volume on the early pulmonary injury and inflammatory response in rats inoculated intratracheally with silica. *Am J Vet Res* 1987; 48: 1282-1285.
60. CHRISTMAN JW, PETRAS SF, VACEK PM, DAVIS GS. Rat alveolar macrophage production of chemoattractants for neutrophils: response to *Escherichia coli* endotoxin. *Infect Immun* 1989; 57: 810-816.
61. MARTINEZ-BURNES J, LOPEZ A, MERINO-MONCADA M, OCHOA-GALVAN P, MONDRAGON I. Pulmonary recruitment of neutrophils and bacterial clearance in mice inoculated with aerosols of *Pasteurella haemolytica* or *Staphylococcus aureus*. *Can J Comp Med* 1985; 49: 327-332.
62. ONOFRIO JM, TOEWS GB, LIPSCOMB MF, PIERCE AK. Granulocyte-alveolar-macrophage interaction in the pulmonary clearance of *Staphylococcus aureus*. *Am Rev Respir Dis* 1983; 127: 335-341.
63. WARNER BB, STUART LA, PAPES RA, WISPE JR. Functional and pathological effects of prolonged hyperoxia in neonatal mice. *Am J Physiol* 1998; 275: L110-L117.
64. LOPEZ A, YONG S. Injury versus inflammatory response in the lungs of rats intratracheally inoculated with bacterial lipopolysaccharide. *Am J Vet Res* 1986; 47: 1287-1292.
65. BRAIN JD, FRANK NR. The relation of age to the numbers of lung free cells, lung weight, and body weight in rats. *J Gerontol* 1968; 23: 58-62.
66. HENDERSON RF, REBAR AH, DENICOLA DB. Early damage indicators in the lungs. IV. Biochemical and cytologic response of the lung to lavage with metal salts. *Toxicol Appl Pharmacol* 1979; 51: 129-135.
67. CHENG PW, BOAT TF, SHAIKH S, WANG OL, HU PC, COSTA DL. Differential effects of ozone on lung epithelial lining fluid volume and protein content. *Exp Lung Res* 1995; 21: 351-365.
68. RABINOVICI R, VERNICK J, HILLEGAS L, NEVILLE LF. Hypertonic saline treatment of acid aspiration-induced lung injury. *J Surg Res* 1996; 60: 176-180.
69. COBBEN NA, DRENT M, JACOBS JA, SCHMITZ MP, MULDER PG, HENDERSON RF, WOUTERS EF, VAN D, V. Relationship between enzymatic markers of pulmonary cell damage and cellular profile: a study in bronchoalveolar lavage fluid. *Exp Lung Res* 1999; 25: 99-111.

70. DRENT M, COBBEN NA, HENDERSON RF, WOUTERS EF, VAN D, V. Usefulness of lactate dehydrogenase and its isoenzymes as indicators of lung damage or inflammation. *Eur Respir J* 1996; 9: 1736-1742.
71. DAY BJ, CARLSON GP, DENICOLA DB. Gamma-glutamyltranspeptidase in rat bronchoalveolar lavage fluid as a probe of 4-ipomeanol and alpha-naphthylthiourea-induced pneumotoxicity. *J Pharmacol Methods* 1990; 24: 1-8.
72. DAY BJ, DENICOLA DB, CARLSON GP. Potentiation of bromobenzene-induced pneumotoxicity by phenobarbital as determined by bronchoalveolar lavage fluid analysis. *Drug Chem Toxicol* 1992; 15: 33-51.
73. TAKAHASHI Y, OAKES SM, WILLIAMS MC, TAKAHASHI S, MIURA T, JOYCE BM. Nitrogen dioxide exposure activates gamma-glutamyl transferase gene expression in rat lung. *Toxicol Appl Pharmacol* 1997; 143: 388-396.
74. INAYAMA Y, TOMIYAMA I, KITAMURA H, NAKATANI Y, ITO T, NOZAWA A, USUDA Y, KANISAWA M. Alkaline phosphatase reactivity in rabbit airway epithelium: a potentially useful marker for airway basal cells. *Histochem Cell Biol* 1995; 104: 191-198.
75. HENDERSON RF, SCOTT GG, WAIDE JJ. Source of alkaline phosphatase activity in epithelial lining fluid of normal and injured F344 rat lungs. *Toxicol Appl Pharmacol* 1995; 134: 170-174.
76. KUHN SH, DE KOCK MA, GEVERS W. Bronchial aspirate alkaline phosphatase: a sensitive marker enzyme to evaluate bronchial cell damage. *Respiration* 1979; 37: 36-41.
77. CALKOVSKA A, SUN B, CURSTEDT T, RENHEIM G, ROBERTSON B. Combined effects of high-frequency ventilation and surfactant treatment in experimental meconium aspiration syndrome. *Acta Anaesthesiol Scand* 1999; 43: 135-145.
78. WAYNFORTH HB. *Experimental and Surgical Technique in the Rat*. New York: Academic Press, 1980.
79. BAKER DEJ. Reproduction and Breeding. In: Baker H J, Lindsey JR, Weisbroth SH, eds. *The Laboratory Rat*. Orlando: Academic Press, 1979: 154-166.
80. PARK CM, CLEGG KE, HARVEY CC, HOLLENBERG MJ. Improved techniques for successful neonatal rat surgery. *Lab Anim Sci* 1992; 42: 508-513.
81. WAYNFORTH HB. *Experimental and Surgical Technique in the Rat*. N.Y.: Academic Press, Inc., 1980.

82. FLECKNELL P. *Laboratory Animal Anaesthesia*. San Diego, CA: Academic Press, 1996.
83. HARKNESS JE, WAGNER JE. *The Biology and Medicine of Rabbits and Rodents*. Philadelphia: Williams & Wilkins, 1995.
84. CANADIAN COUNCIL ON ANIMAL CARE. *Guide to the Care and Use of Experimental Animals*. Ottawa, Ont.: CCAC, 1993.
85. BERGMEYER HU. *Methods of Enzymatic Analysis*. Weinheim, Verlag Chemie, 1983.
86. MATHIEU M, BRETAUDIERE JP, GALTEAU MM, GUIDOLLET J, LALEGERIE P, BAILLY M, BURET P, DORCHE C, LOUISOT P, SCHIELE F. "Enzymology" commission. Current enzymology in clinical chemistry and recommendations for the measurement of catalytic activities in the serum at 30 degrees C. *Ann Biol Clin (Paris)* 1977; 35: 271-273.
87. PERSIJN JP, VAN DER SLIK W. A new method for the determination of gamma-glutamyltransferase in serum. *J Clin Chem Clin Biochem* 1976; 14: 421-427.
88. WATANABE N, KAMEI S, OHKUBO A, YAMANAKA M, OHSAWA S, MAKINO K, TOKUDA K. Urinary protein as measured with a pyrogallol red-molybdate complex, manually and in a Hitachi 726 automated analyzer. *Clin Chem* 1986; 32: 1551-1554.
89. FISHER LD, VAN BELLE G. *Biostatistics: A Methodology for The Health Sciences*. New York: Wiley Intersciences, 1993.
90. SIEGER L. Pulmonary alveolar macrophages in pre- and post-natal rabbits. *J Reticuloendothel Soc* 1978; 23: 389-395.
91. SIEGER L, ATTAR H, OKADA D, THIBEAULT DW. Alveolar macrophages (A.M.) in rabbit and human fetuses and neonates. *J Reticuloendothel Soc* 1975; 18: 47b-
92. ZELIGS BJ, NERURKAR LS, BELLANTI JA, ZELIGS JD. Maturation of the rabbit alveolar macrophage during animal development. I. Perinatal influx into alveoli and ultrastructural differentiation. *Pediatr Res* 1977; 11: 197-208.
93. SUGIMOTO M, ANDO M, SENBA H, TOKUOMI H. Lung defenses in neonates: effects of bronchial lavage fluids from adult and neonatal rabbits on superoxide production by their alveolar macrophages. *J Reticuloendothel Soc* 1980; 27: 595-606.

94. ZINK MC, JOHNSON JA. Cellular constituents of clinically normal foal bronchoalveolar lavage fluid during postnatal maturation. *Am J Vet Res* 1984; 45: 893-897.
95. SCHORN H, EURATOM CW. Some hormonal effects on alveolar phagocytosis in the rat. *J Reticuloendothel Soc* 1975; 18: 35a-
96. FISHER DA, DUSSAULT JH, HOBEL CJ, LAM R. Serum and thyroid gland triiodothyronine in the human fetus. *J Clin Endocrinol Metab* 1973; 36: 397-400.
97. TAINER JA, TURNER SR, LYNN WS. New aspects of chemotaxis. Specific target-cell attraction by lipid and lipoprotein fractions of *Escherichia coli* chemotactic factor. *Am J Pathol* 1975; 81: 401-410.
98. BOWDEN DH, ADAMSON IY. Response of pulmonary macrophages to unilateral instillation of carbon. *Am J Pathol* 1984; 115: 151-155.
99. MERRITT TA. Oxygen exposure in the newborn guinea pig lung lavage cell populations, chemotactic and elastase response: a possible relationship to neonatal bronchopulmonary dysplasia. *Pediatr Res* 1982; 16: 798-805.
100. LUSTER AD. Chemokines--chemotactic cytokines that mediate inflammation. *N Engl J Med* 1998; 338: 436-445.
101. KELLEY J. Cytokines of the lung. *Am Rev Respir Dis* 1990; 141: 765-788.
102. LOPEZ A, ALBASSAM M, YONG S, SHARMA A, LILLIE LE, PRIOR MG. Profiles of type-II pneumocytes in rats inoculated intratracheally with bacterial lipopolysaccharide. *Am J Vet Res* 1987; 48: 1534-1539.
103. NERURKAR LS, ZELIGS BJ, BELLANTI JA. Maturation of the rabbit alveolar macrophage during animal development. II. Biochemical and enzymatic studies. *Pediatr Res* 1977; 11: 1202-1207.
104. DANNENBERG AM, BURSTONE MS, WALTER PC, KINSLEY JW. A histochemical study of phagocytic and enzymatic functions of rabbit mononuclear and polymorphonuclear exudate cells and alveolar macrophages. *J Cell Biol* 1963; 17: 465-486.
105. JIANG X, KOBAYASHI T, NAHIRNEY PC, GARCIA DS, SEGUCHI H. Ultracytochemical localization of alkaline phosphatase (ALPase) activity in neutrophils of the rat lung following injection of lipopolysaccharide. *Kaibogaku Zasshi* 1996; 71: 183-194.

106. COBBEN NA, JACOBS JA, VAN DIEIJEN-VISSEER MP, MULDER PG, WOUTERS EF, DRENT M. Diagnostic value of BAL fluid cellular profile and enzymes in infectious pulmonary disorders. *Eur Respir J* 1999; 14: 496-502.
107. BERENDT RF. Relationship of method of administration to respiratory virulence of *Klebsiella pneumoniae* for mice and squirrel monkeys. *Infect Immun* 1978; 20: 581-583.
108. MILLER RB. A summary of some of the pathogenetic mechanisms involved in bovine abortion. *Can Vet J* 1977; 18: 87-95.
109. LOPEZ A, LÖFSTEDT J, BILDFELL R, HORNEY B, BURTON S. Pulmonary histopathologic findings, acid-base status, and absorption of colostral immunoglobulins in newborn calves. *Am J Vet Res* 1994; 55: 1303-1307.
110. PIERCE AK, REYNOLDS RC, HARRIS GD. Leukocytic response to inhaled bacteria. *Am Rev Respir Dis* 1977; 116: 679-684.
111. BROWN BL, GLEICHER N. Intrauterine meconium aspiration. *Obstet Gynecol* 1981; 57: 26-29.
112. DAVIS RO, PHILIPS JB, HARRIS BAJ, WILSON ER, HUDDLESTON JF. Fatal meconium aspiration syndrome occurring despite airway management considered appropriate. *Am J Obstet Gynecol* 1985; 151: 731-736.
113. HENDERSON RF, DAMON EG, HENDERSON TR. Early damage indicators in the lung I. Lactate dehydrogenase activity in the airways. *Toxicol Appl Pharmacol* 1978; 44: 291-297.
114. MITCHELL RN, COTRAN RS. Acute and chronic inflammation. In: Cotran R S, Kumar V, Collins T, eds. Kumar, Cotran, Robbins Basic Pathology. Philadelphia: W.B. Saunders Company, 1997: 25-46.

4. MICROSCOPIC CHANGES INDUCED BY THE INTRATRACHEAL INOCULATION OF AMNIOTIC FLUID AND MECONIUM IN THE LUNG OF NEONATAL RATS

4.1. Introduction

Meconium aspiration syndrome (MAS) is an important perinatal condition that has complex etiology and causes severe respiratory distress, lung inflammation and occasional death in newborn babies (1,2). In the last three decades, a considerable amount of work has been published regarding the prevention, clinical implications and medical management of MAS (3,4) but little has been done to characterize the lung pathology of this syndrome (5).

The body of knowledge about pulmonary pathology originates from autopsy reports of babies succumbing to acidosis and hypoxia, the main culprits for fatality in MAS. As a result, there is a paucity of information regarding the chronologic changes that occur in the lungs of babies surviving MAS. This fact is particularly intriguing since pulmonary sequelae may persist after the acute pulmonary lesions of MAS have been resolved (5-9).

According to autopsy reports of babies dying acutely of MAS, multifocal atelectasis and consolidation of the lungs are the most relevant gross findings which are in agreement with the classical patchy infiltrates observed in antemortem roentgenographic images (10-12). These patchy infiltrates were subsequently confirmed by microscopy as focal atelectasis, inflammation, hyperinflation and alveolar edema (4,13-15).

Although multifocal (patchy) atelectasis is a cardinal change in the lungs of babies with MAS, the pathogenesis of this lesion has been cause for debate for some years. Most researchers simply explain atelectasis as an obstructive process in which lack of alveolar aeration is the direct result of airflow obstruction caused by meconium plugs in bronchioles

and alveoli. Proponents of this theory believe that meconium plugs act as one-way valves preventing the aeration of some, but not all areas of the baby's lung, hence the patchy appearance of pulmonary parenchyma (4,16). On the other hand, it has been demonstrated that aspirated meconium produces physical displacement of alveolar surfactant which is a critical element in preventing alveolar collapse due to surface tension in the lung (14,15,17). Laboratory investigations have also shown that some chemical components of the meconium, presumably bile salts, free fatty acids and bilirubin, modify the biological properties of the pulmonary surfactant predisposing the alveoli to collapse (15,18-20).

Many authors consider pulmonary inflammation in MAS as a simple chemical pneumonitis caused by the aspiration of meconium into the bronchoalveolar spaces (21,22). Lung specimens collected from cadavers of babies typically show meconium, components of amniotic fluid (keratin and epidermal cells), edema, pulmonary alveolar macrophages (PAM) and neutrophils infiltrating the airspaces (12,23). According to some investigations, recruitment of inflammatory cells and edema are primarily mediated by pro-inflammatory cytokines released by macrophages in response to the pulmonary injury caused by meconium (24-26).

In recent years, evidence has arisen suggesting that the pathogenesis of meconium-induced pneumonitis has some important similarities with adult respiratory distress syndrome (ARDS)(27,28). This fact may explain why recruitment of leukocytes and leakage of fluid into the alveoli is commonly seen in fatal cases of MAS (13). What still remains obscure is the clinical significance of pulmonary inflammation in babies surviving the acute stages of MAS (3).

Although pulmonary inflammation and atelectasis are the obvious microscopic changes in babies with MAS, there are other pulmonary lesions sporadically reported in this syndrome. These include vasoconstriction, hemorrhage, microthrombi and muscularization with increased medial thickness of the distal pulmonary arterioles (29-31). The pathogenesis of these vascular changes remains elusive and some investigators have proposed the release of pro-inflammatory mediators as the main mechanism (29,32), while others have suggested hypoxia or pulmonary hypertension as the main culprits of vascular abnormalities (3,5,6).

Whereas the prevalence and significance of MAS in veterinary medicine remain unknown, microscopic changes typical of this syndrome are usually encountered in diagnostic laboratories. According to one report, 42.5% of calves dying in the first two weeks of life from infectious and noninfectious diseases had microscopic evidence of meconium, keratin or squamous cells in the lungs (33). Atelectasis was common in lobules containing meconium or amniotic fluid and an inflammatory response characterized by neutrophils, macrophages and the occasional multinucleated giant cells was evidently the lung's response to inhaled meconium and keratin (33,34).

Meconium aspiration syndrome has also been recognized in equine medicine as one of the main factors involved with perinatal asphyxia and respiratory distress in newborn foals (35,36). These foals showed multifocal atelectasis associated with aspiration of meconium and squamous epithelial cells. It is also important to mention that a condition morphologically indistinguishable from hyaline membrane disease of human infants has also been recently reported in neonatal foals (37). Lungs of these foals had a distinctive patchy atelectasis characterized by atelectatic areas alternating with airway distension in

neighbouring lobules. There were also cellular debris, presence of hyaline membrane-like lesions and abundant vernix and squames associated with atelectatic areas (37). Hyaline membrane disease and MAS share some similarities, likely because in both conditions the biological properties of surfactant are changed.

Spontaneous MAS has been sporadically reported but not well documented in small animal medicine. According to a case report, a puppy from a litter of healthy dogs died 48 hours after birth and the lungs had microscopic evidence of meconium and epidermal cells associated with moderate alveolar inflammation (38). The microscopic lesions in the lungs of this puppy were consistent with MAS.

Like in many other human diseases, attempts have been made to reproduce MAS experimentally in laboratory animals and under controlled conditions to study the nature and progression of lung lesions. Different animal species have been used as animal models of MAS including, rabbits (14,21,22,39-41), guinea pigs (5), rats (13,42-44), dogs (45), cats (46), pigs (16,28,29,47,48), lambs (49,50) and baboons (51). These animal models have been utilized to investigate, under experimental conditions, the effect of meconium and its natural vehicle in MAS, the amniotic fluid.

One important limiting factor in animal models for lung diseases is to ensure that the inoculum to be tested reaches the intended target areas of the lung. The pulmonary dispersion of meconium following intratracheal experimental inoculation is widely but not uniformly distributed in bronchi, bronchioles and alveoli presumably mimicking the natural cases of MAS (13,43). Overall, the pulmonary findings in laboratory animals given sublethal doses of meconium or amniotic fluid are morphologically similar to the changes

reported in human infants succumbing in the acute stage of MAS (2,16). For instance, intratracheal inoculation of meconium into rabbit lungs induced atelectasis and inflammation characterized by an influx of polymorphonuclear leukocytes at 24 and 48 hours post inoculation (21). The lung water/dry ratios were increased, indicating that meconium also caused pulmonary edema (21).

Atelectasis and microscopic inflammation, identified by infiltrates of polymorphonuclear leukocytes and formation of hyaline membranes in alveoli, developed in the lungs of rabbits when filtered human meconium was introduced into the trachea (22). These inflammatory changes were attributed to the presence of meconium and squamous epithelial cells in the alveolar and bronchial airspaces (22). In a separate study with newborn rabbits, atelectasis was reported as a significant finding following intratracheal inoculation of human meconium (41).

Another study was designed to evaluate, in adult rabbits, the magnitude of atelectasis and chemical pneumonitis induced by human meconium (21). Based on the results of this study it was concluded that meconium, as previously proposed, induces a mechanical obstruction of airways, causing reduced airflow and resulting in atelectasis. But also a chemical pneumonitis characterized by a gradual influx of inflammatory cells and necrosis, contributing to surfactant dysfunction and atelectasis (21). Microscopic findings similar to those found in rabbits have been also reported in the lungs of adult rats endotracheally inoculated with sublethal doses of human meconium. Results of these works confirmed that meconium in the lungs induces acute neutrophilic inflammation, formation of hyaline membranes in the alveoli and atelectasis (42,43).

Larger species such as dogs, cats and pigs have also been used as experimental animal models to study the effect of meconium in the lungs. One study conducted in newborn puppies revealed that large volumes of human meconium administered through an intratracheal cannula into the lungs resulted in cardiopulmonary collapse and sudden death (45). No visible changes were seen in the lungs of these puppies dying peracutely from aspiration of meconium. In contrast, smaller doses of meconium administered to puppies in the same way produced roentgenographic pictures typical of human MAS characterized by "patchy" consolidation which became more evident when the parenchyma became partially aerated (45). Unfortunately, the microscopic lesions in this canine model of MAS were vaguely described as the presence of mononuclear infiltrates without indicating the nature of the infiltrates or the histological location of the lesions (45).

The microscopic pulmonary changes in response to inhaled meconium have also been reported in pigs. In a study designed to test the effect of ventilation in pigs with experimental MAS, piglets aged 1 to 4 days inoculated with meconium developed clinical signs of this syndrome and showed atelectasis and exudative alveolitis associated with visible meconium in airways and alveoli (16). Another study with older pigs (10-weeks-old) showed severe inflammatory response microscopically characterized by pulmonary sequestration of neutrophils, neutrophilic alveolitis, edema and formation of hyaline membranes in response to aspirated meconium (28). According to the authors, these meconium-induced changes, in particular capillary sequestration of neutrophils and formation of hyaline membranes, were typical of adult respiratory distress syndrome (ARDS). The swine model of MAS has also been used to study the effect of meconium aspiration on blood gases and pulmonary

vasculature in addition to inflammation and atelectasis (29,52,53).

The cellular components of the amniotic fluid, namely keratin and squamous epithelial cells, are additional factors that must be considered in the pathogenesis of pulmonary inflammation in MAS. Although not clearly visible in routine histologic stains, amniotic fluid is recognized as a pale basophilic substance generally admixed with keratin, epidermal cells or squames in the lung (12,54,55). Being a highly pro-inflammatory substance, keratin is partly responsible for local recruitment of macrophages and neutrophils in alveolar spaces as demonstrated in other tissues (56,57).

There have been few studies designed to specifically test the effect of amniotic fluid alone on the lungs of laboratory animals. In 1949, a major investigation was conducted to study the effect of rabbit and human amniotic fluids intratracheally inoculated into the lungs of rabbits (39). Results of this investigation showed that large volumes (5 ml) of sterile rabbit amniotic fluid caused atelectasis and recruitment of polymorphonuclear leukocytes and macrophages in the bronchoalveolar spaces. On the other hand, lower volumes (2 ml) of amniotic fluid did not induce detectable lung lesions. Inoculation of squamous keratinized cells along with sterile amniotic fluid had an additional irritant effect in the lungs and induced the formation of multinucleated giant cells typical of a foreign body reaction (39). When cells were completely removed from the human amniotic fluid, inoculation of this cell-free fluid into the rabbit lung only induced a mild pulmonary inflammation (39).

In another study, pulmonary inflammation without atelectasis was seen in guinea pigs inoculated transtracheally with human amniotic fluid (5). A recent study in rats showed that the magnitude of cellular exudation into the alveolar spaces appears to be related to the

volume of amniotic fluid inoculated into the lungs (58). The cause-effect relationship between amniotic fluid and inflammation is presumably caused by the number of cells and keratin suspended in the fluid .

It is important to recognize that the endpoints of these experimental models of MAS were to reproduce the acute pulmonary changes in response to meconium or amniotic fluid. The long term effects of these fetal intestinal contents and placental fluid in the lung have been largely neglected. Also, it is important to note that most experimental studies have been conducted in adult animals in spite of the fact that MAS is a disease of the newborn and the inflammatory response is known to be different from adults in fetuses and neonates. Another issue that cannot be ignored is that human rather than animal meconium has generally been used as the inoculum in many animal models of MAS.

The objective of this study is to evaluate the acute and chronic microscopic changes in lungs under controlled conditions using a novel rat model of MAS with neonates and homologous murine meconium. The effects of meconium and amniotic fluid are evaluated and compared to the effect of sterile saline solution experimentally inoculated into the lung.

4.2 Materials and Methods

4.2.1. Animals

Neonatal pups were obtained from female *Fischer-344* rats bred at AVC. All female rats were bred using vaginal cytology for timing (59,60). Adult rats were housed individually and provided with commercial rat food and water *ad libitum*. Rat pups were kept with the dam and maintained on a 12/12-hour light/dark cycle at 22°C and 50% relative humidity. To reduce infant rejection, dams were preconditioned 7-10 days before parturition by

exposing them in their cages to the smell of the materials to be used afterwards in neonatal rats, i.e., anaesthetic, surgical gloves, tattoo ink, etc.. Preconditioning of pregnant rats was done following the protocol outlined by Park *et al.* (61).

4.2.2. Anesthesia

Adult and neonatal rats were anesthetized with halothane (3% in 100% oxygen; 100-200 ml/min) via a gas anaesthetic machine. The method of anesthesia had been previously standardized from modified procedures described by others (62,63). For a detailed description of anesthesia see section 2.2.1.3.

4.2.3. Inoculum

Meconium was aseptically collected from the intestines of rat pups killed at the time of birth and before the intake of colostrum with an anaesthetic overdose of halothane. Once removed from the intestine, the meconium was maintained frozen at -80°C until preparation of the inoculum. The thawed meconium was suspended in saline solution and homogenized using a Vortex mixer (Fisher Scientific, N.Y.). Based on the results of the dose-range finding study (Section 2.2.1.6.), the final concentration of unfiltered meconium was adjusted to 200 mg of meconium (wet weight) in 1 ml of saline for the acute study. For the chronic study, the concentration of meconium was lowered to 150 mg/ml because of the increased viscosity when meconium was homogenized using sterile glass beads.

Amniotic fluid (AF) was aseptically collected following the same procedure described in section 2.2.1.5. In short, the uterus from full-term pregnant rats was exposed through cesarean section under deep halothane anesthesia. Under sterile conditions, the uterus and placenta were punctured and the AF collected using sterile capillary tubes.

Amniotic fluid was placed in sterile plastic vials and stored at 4-6°C. To ensure sterility of the inocula, samples of the AF and meconium were submitted for routine bacteriological cultures. The AF was not diluted so the final concentration of the inoculum was 100%.

4.2.4. Intratracheal inoculation (ITI)

The method of intratracheal instillation for 7-day-old rat neonates was standardized by adapting techniques described by others (62,63) taking into consideration the small size of neonatal rats. For detailed description of this method see section 2.2.1.7. Briefly, neonates were anaesthetized with halothane and the larynx was visualized using an otoscope with a small sterile speculum (Welch Allyn, Skaneateles Falls, NY). A sterile spinal needle 25-gauge, 8.89 cm length (Becton Dickinson, Franklin Lakes, NJ) with the edge rounded was passed through the laryngeal opening into the proximal trachea. A 1.0 ml disposable syringe (Becton Dickinson and Co., Rutherford, NJ) was connected to the needle and the inoculum injected into the lungs. The total volume of amniotic fluid and of the meconium suspension inoculated into the lungs was 0.05 ml per rat. Neonates from the control group were inoculated with 0.05 ml of sterile saline solution. To prevent hypothermia, pups were maintained in direct observation on a heating pad (37°C) until respiratory movements became stable and they regained consciousness from the anaesthesia. At the time of inoculation, the 7-day-old pups had an average weight of 14.4 ± 0.5 g, (n = 146).

4.2.5. Euthanasia

At the end of the experiment, rats were euthanised with an overdose of halothane and exsanguination by excising the renal arteries as described in section 2.2.1.8. Experiments were conducted following the guidelines of the Canadian Council on Animal Care (64).

4.2.6. Lung fixation

After euthanasia, rat neonates were placed head up in a supine position on a board held at 45° and fastened by means of a rubber band set under the upper incisors and adhesive tape placed laterally across the forelimbs and hindlimbs. The abdomen was opened, and bilateral pneumothorax was induced by diaphragmatic puncture (65,66). The thorax was opened through a bilateral costotomy and the trachea was exposed by removing the cervical muscles. A plastic catheter (Cathlon IV, Critikon Canada Inc, Markham, Ontario) was inserted into the trachea through a transverse section between the first and second tracheal rings. The caliper and length of these catheters were selected according to the age of the rat at the time of euthanasia: 20-gauge and 32 mm length for neonates killed at postinoculation day (PID) 1, 3 and 7 ; 18-gauge and 32mm length for rats killed at PID14; 16-gauge and 57 mm for PID 28; and 14-gauge and 57mm for PID 56 to 112. Under a fume hood, the lungs were fixed *in situ* by intratracheal perfusion of 10% neutral buffered formalin at a uniform pressure of 20 cm. This pressure was generated by gravity and was measured from the liquid level in the reservoir which was maintained at a constant height of 20 cm above the hilus of the lung. A modified “Marriott” bottle system was used to provide a constant volume flow and pressure of the fixative as reported by others (67). The system was made from 60 ml syringes, connected to plastic tubing and to a plastic catheter. The syringes were maintained open (without plunger) to refill and maintain constant levels of fixative in the cylinders. Tubing and adaptors were rebored to a consistent internal diameter as large as possible. The flow rate of fixative was approximately 190 ml/min when not attached to the catheter.

After a minimum of 30 minutes of fixation *in situ*, and before the catheter was

removed, the intrapulmonary pressure of the fixative was preserved by placing a tight ligature around the trachea. The lungs were then dissected free from the thorax and stored in the same fixative for at least 24 h before further manipulation (67).

4.2.7. Light microscopy

A longitudinal slice (2 mm in thickness) of the entire left lung and transverse (2 mm in thickness) sections along the major axes of the right cranial (anterior or apical), middle (cardiac), median (azygous or accessory) and caudal (posterior) lobes were sampled from each rat. The lung samples were processed, embedded in paraffin, sectioned at 3 μ m-thick and stained with hematoxylin and eosin (HE) following routine procedures. Periodic acid-Schiff (PAS) counterstained with light green SF yellowish, PAS counterstained with hematoxylin, Alcian Blue-PAS and Hall's stain (68,69) were used for the detection of meconium in the lung. The von Kossa stain was also used to confirm pulmonary deposits of calcified material (68,69).

Lung sections were evaluated using an Olympus BH-2 light microscope (Olympus Optical Co. Ltd, Japan) and the following parameters were studied: 1- presence and distribution of meconium in the lungs; 2- types of lesions and 3- distribution of lesions (lobes, areas of lobes, bronchioles, alveoli, interstitium).

A scoring system was used to evaluate the frequency and severity of histologic changes. In this scoring system, consideration was given to changes that could be directly associated with the presence of meconium. The scoring system was defined as absent (-) when meconium or changes were not found, minimal (\pm) for sporadic evidence of meconium or of changes, mild (+) when meconium and changes were present but with low frequency,

moderate (++) when meconium and changes were pronounced but in not all lung lobes and severe (+++) when meconium and associated changes were pronounced and commonly observed in all lobes. The variables selected for evaluation of histologic changes using light microscopy included: 1. presence of meconium in bronchi and bronchioles; 2. presence of meconium in alveoli; 3. presence of polymorphonuclear neutrophils (PMN) in bronchioles; 4. presence of PMN in alveoli; 5. presence of macrophages (PAM) in bronchioles; 6. presence of PAM in alveoli; 7. alveolar edema; 8. atelectasis; 9. hyperinflation; 10. thickening of alveolar septa; 11. histiocytic-granulomatous inflammation; 12. presence of multinucleated giant cells; 13. mineralization.

4.2.8. Experimental design

One hundred and forty six male 7-day-old *Fischer 344* pups (average body weight of 14.4 ± 0.5 g) were inoculated and assigned randomly to three experimental groups of twenty rats (70). According to treatment, the experimental groups were named: 1- saline solution, 2- amniotic fluid, and 3- meconium and the study was conducted in two independent experiments according to the following experimental design:

- I. Acute microscopic changes: 1,3,7 and 14 PID (Table XII).
- II. Chronic microscopic changes 14, 28, 56, 112 PID (Table XIII).

Body weights were recorded at the time of inoculation and throughout the experiment. Seven neonates in each study died of respiratory collapse or were euthanised due to inoculation complications and their lungs were not included in the microscopic study. Therefore, 132 neonates were used (Table XII, XIII).

**Table XII. Acute microscopic changes in the lung of 7-day-old neonatal rats intratracheally inoculated with amniotic fluid and meconium.
(Experimental design: number of subjects in each group)**

| Groups | Post- inoculation Day | | | | | Total |
|---------------------------|-----------------------|----|----|----|----|-------|
| | 1 | 3 | 7 | 14 | | |
| Control (Saline solution) | 4 | 5 | 5 | 5 | 19 | |
| AF (100%, 0.05 ml) | 4 | 4 | 5 | 5 | 18 | |
| Meconium (20%, 0.05 ml) | 4 | 5 | 5 | 5 | 19 | |
| Total | 12 | 14 | 15 | 15 | 56 | |

AF:Amniotic fluid

Note: Only one dose per treatment was used.

**Table XIII. Chronic microscopic changes in the lung of 7-day-old neonatal rats intratracheally inoculated with amniotic fluid and meconium.
(Experimental Design: number of subjects in each group)**

| Groups | Post- inoculation Day | | | | Total |
|---------------------------|-----------------------|----|----|-----|-------|
| | 14 | 28 | 56 | 112 | |
| Control (Saline solution) | 6 | 6 | 8 | 8 | 28 |
| AF (100%, 0.05 ml) | 6 | 6 | 6 | 7 | 24 |
| Meconium (15%, 0.05 ml) | 5 | 6 | 6 | 6 | 23 |
| Total | 17 | 18 | 20 | 21 | 76 |

AF:Amniotic fluid

Note: Only one dose per treatment was used.

4.2.9. Statistical analysis

The body weights of the animals are expressed as means and standard deviations (SD). The effect of treatment and interactions on body weight were statistically evaluated by using Analysis of Variance (GLM-ANOVA) according to the following model:

$$Y_{ij} = \mu + T_i + D_j + TD_{ij} + E_{ij}$$

where:

Y_{ij} = individual observation on the j day of the i -th treatment.

μ = general population mean.

T_i = Effect of the i -th treatment; ($i = 1, 2, 3$)

D_j = Effect of the j -th day ($j = 1, 2, 3, 4, 5, 6, 7, 8, 9$)

TD_{ij} = interaction

E_{ij} = Random error associated with each observation $\sim NI(0, \sigma^2 e)$ with 103 and 600 degree of freedom for the acute and chronic studies respectively.

Differences in body weights between groups of treatment and postinoculation days were examined with One-Way Analysis of Variance (ANOVA) followed by the non-parametric Kruskal-Wallis test (70). A p-value below 0.05 was considered statistically significant.

4.3. Results

4.3.1. Body weight

When the body weight of all groups of rats and all PID of the acute study were analyzed together in the overall analysis, no significant changes were observed ($p = 0.260$). Rats inoculated with amniotic fluid gained weight the same as the control rats treated with

saline solution and no significant weight differences ($p=0.898$) were observed between these two groups at PID 1, 3, 7 and 14 (Fig. 20). However, the average weight gained of rats inoculated with 200 mg/ml of meconium decreased at PID 1, which was verified by a significant treatment effect detected with ANOVA ($p=0.00$) and nonparametric testing ($p=0.025$). There was no significant difference in weight gained in the rats inoculated with meconium compared to control groups at PID 3, 7 and 14 (Fig. 20).

In the rats of the chronic study, inoculation of 150 mg/ml of meconium induced a significant overall reduction ($p=0.000$) in body weight when compared with rats of the saline control group. These statistical differences found by GLM-ANOVA were also detected when animal weights were analysed with nonparametric tests ($p=0.001$). Rats of the control and amniotic groups had the same tendency to gain weight and showed no significant average weight differences between groups ($p>0.05$). At the time of inoculation, the average body weights of rats inoculated with meconium were the same as those inoculated with saline ($p=0.396$). However at PID 1, a significant reduction in weight gained was detected in rats treated with meconium. Weight differences from PID 1 to 12 between the meconium and control groups were substantiated in parametric and nonparametric testing ($p=0.000$) as shown in Fig. 21 A. No differences in body weight and large standard deviations were found at PID 14. Fig. 21A shows the body weights for the first twelve days of the chronic study for comparison with the acute study (Fig. 20).

At PID 28, the rats of the meconium group had higher average (parametric: $p=0.042$; nonparametric: $p=0.004$) body weights than the rats of the saline control group (Fig. 21B). However, differences were not detected ($p>0.05$) using Tukey's comparison test. At PID 56

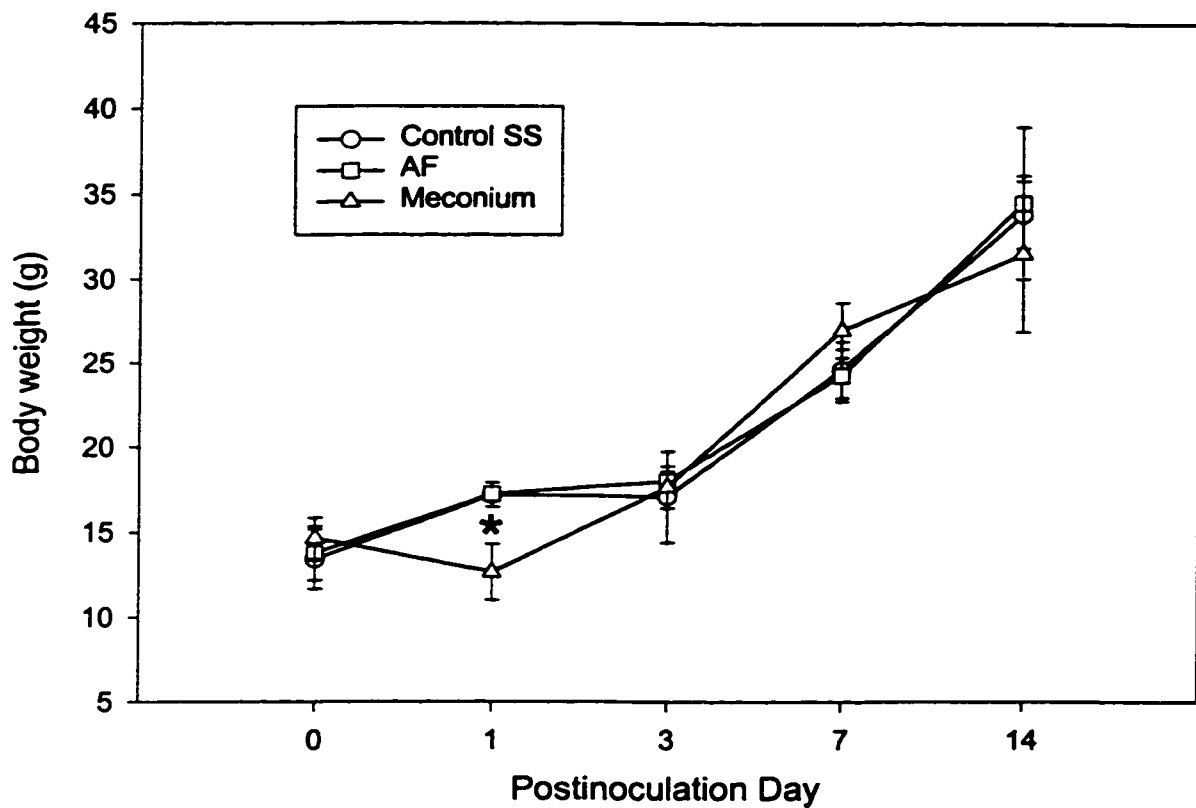


Fig. 20. Body weight of the neonates in the acute study. Mean (\pm SD) of body weight obtained from four or five neonates per group at different postinoculation times. *Significantly ($p < 0.01$) different from control determined at the same time.

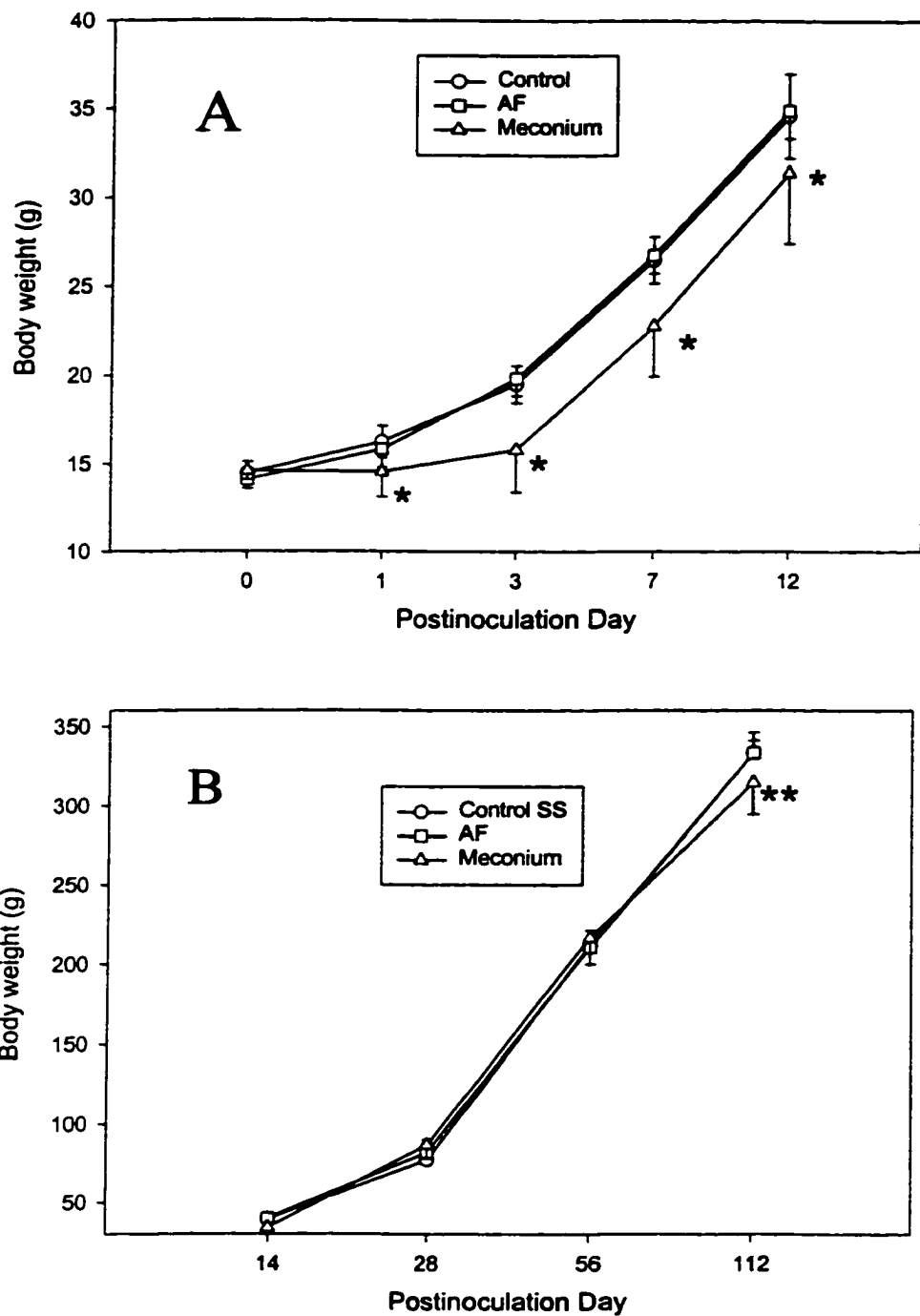


Fig. 21. Body weight of the neonates in the chronic study. Mean (\pm SD) of body weight obtained from five to six neonates per group at different postinoculation times. Fig. 21A. Body weight of the first 14 postinoculation days. Fig. 21B. Body weight from PID 14 to 112. Significantly *($p < 0.01$) **($p < 0.05$) different from control.

no significant differences ($p=0.931$) in body weight were found between the meconium and saline control groups. However, at PID 112, the averages of body weight of rats in the meconium group were again significantly lower ($p=0.012$ and $p=0.022$) than the rats inoculated with saline solution (Fig. 21B).

4.3.2. Acute study

4.3.2.1. Gross lesions

The lungs of rat neonates inoculated with saline or amniotic fluid and killed at 1, 3, 7 and 14 PID did not show noticeable gross changes. In contrast, the lungs of rats inoculated with meconium had multifocal areas of consolidation and a green discolouration. During fixation, the lungs inoculated with meconium did not apparently distend as well as those inoculated with saline or amniotic fluid. Also, in rats inoculated with meconium the perfusion with fixative emphasized the multifocal discolouration and gave the lungs a characteristic "meaty appearance" (54). These changes were not observed in the lungs of rats inoculated with amniotic fluid or saline solution.

4.3.2.2. Microscopic lesions

The lungs of rat neonates inoculated with saline solution and killed at PID 1, 3, 7 and 14 were well aerated, had a normal alveolar expansion pattern and did not reveal any relevant microscopic changes (Fig. 22). Inflammation was not microscopically evident in the lungs of animals inoculated with saline except for the presence of occasional minimal pyogranulomas.

The lungs of rats inoculated with amniotic fluid were uniformly distended and contained occasional squamous epithelial cells and keratin at PID 1 and 3. This cell debris

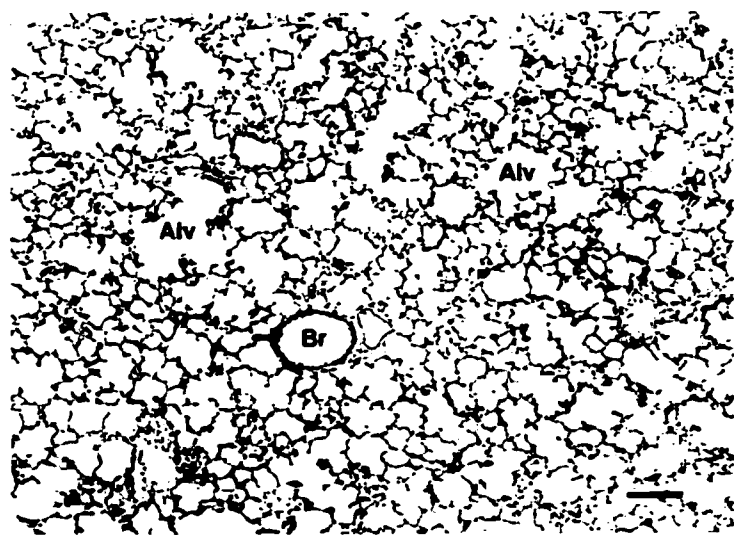


Fig. 22. Neonatal rat lung; saline control PID 1. Alveoli are well distended with no evidence of inflammation. Alveoli (Alv), bronchiole (Br). HE stain. Bar = 100 μ m.



Fig. 23. Neonatal rat lung; amniotic fluid PID 1. Foreign body response in proximal alveolar region (PAR). Influx of macrophages (arrows) and neutrophils (arrowheads). HE stain. Bar = 50 μ m.

was widely but unevenly distributed in all pulmonary lobes. At PID 1 and 3, the proximal alveolar region and alveoli of rats inoculated with amniotic fluid contained neutrophils and mainly macrophages (Fig. 23). This predominantly histiocytic response associated with keratin or squames progressively decreased at PID 7 and was no longer observed at PID 14. The presence of squamous epithelial cells and keratin in alveoli also decreased with time and was less evident at PID 7 and no longer seen at PID 14.

Meconium was identified microscopically on HE stain as amorphous, gold-yellow granular material present in the airways and alveoli (Figs. 24A, 25, 26). Epithelial cellular debris, squamous epithelial cells, squames and keratin were commonly seen admixed with the golden material in the meconium plugs. From all special stains tested for their usefulness in detecting meconium microscopically, Periodic acid-Schiff stain counterstained with light green gave the best results (Fig. 24C) since meconium appeared deep red, contrasted with keratin green and the lung tissue green and purple. Meconium and keratin stained red in lungs stained with periodic acid schiff and counterstained with hematoxylin (Fig. 24B). Keratin also appeared birefringent. Meconium and its mucins in the lung stained with different intensities of blue, red and purple when Alcian blue-PAS stains were used (Fig. 24D). In sections stained with the Hall's method, meconium appeared pale green but was difficult to detect since lung tissue had a similar color (Fig. 24E).

The success rate of meconium delivery into the lungs was 100% as all rats of the meconium group had evidence of this material at PID 1. The lobar distribution of meconium was widespread as shown by the percentage of lung lobes containing this material in conducting airways or alveoli at PID 1. Meconium was observed in 100% of right cranial

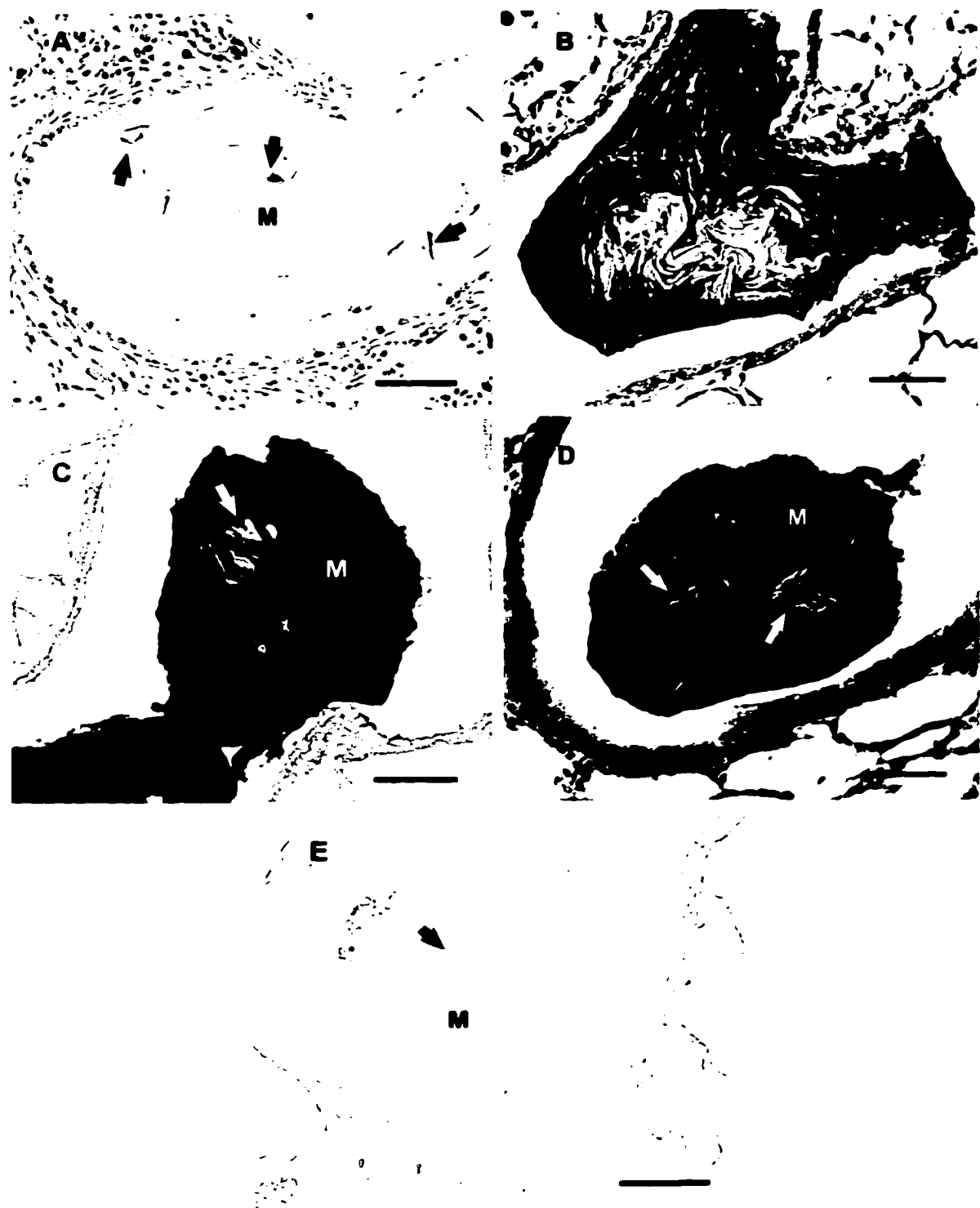


Fig. 24. Lungs from neonatal rats inoculated with meconium. Meconium (M) is present in bronchioles and exhibits different stainabilities. Fig. 24A. HE stain. Fig. 24B. Periodic acid schiff (PAS) counterstained with hematoxylin. Fig. 24C. PAS stain counterstained with light green. Fig. 24D. Alcian blue-PAS stain. Fig. 24E. Hall's stain for bilirubin. Keratin (arrows). Bars = 50 μ m.

lobes, 100% of right middle lobes, 75-100% of right caudal lobes and 100% of left pulmonary lobe (See section 2.3.7.).

The bronchi and bronchioles of all rats (100%) inoculated with meconium had microscopic evidence of this material at PID 1 and 3 (Fig. 25)(See also table XIV). The percentage of rats with meconium in conducting airways decreased from 100% at PID 3 to 60% at PID 14. Within the lung, meconium was evident in the conducting airways from 90 to 95% of the different lobes at PID 1 and 3, and the percentage of airways with meconium was down to 25% and 32% by PID 7 and 14 respectively.

Regarding lobar distribution, meconium was found in conducting airways of 100% of left, cranial, middle, and median lobes except the caudal lobe with 3 out of 4. The presence of meconium in conducting airways decreased in all lobes progressively from PID 1 to 14, reaching only 40% of different lobes at PID 14. The only exception was the right median lobes in which there was no evidence of meconium at PID 14 (See Section 2.3) .

The alveolus was the pulmonary structure with highest prevalence of meconium compared to bronchioles in the acute study (See section 2.3.7.), that is, meconium was microscopically evident in alveoli of all rats at PID 1,3,7 and 14 (Fig. 26)(Table XIV). The proportion of lung lobes that exhibited microscopic evidence of meconium in alveoli ranged between 100%, 75%, 60% and 84% at PID 1, 3,7, and 14 respectively. In individual rats, meconium was evident in alveoli in 100% of lung lobes at PID 1 and 3, remaining in 60 to 100% of lobes at PID 14 (See section 2.3.7.).

Meconium, when present in bronchioles and alveolar spaces, was commonly but not always surrounded by a rim of macrophages and polymorphonuclear leukocytes (Fig. 27).

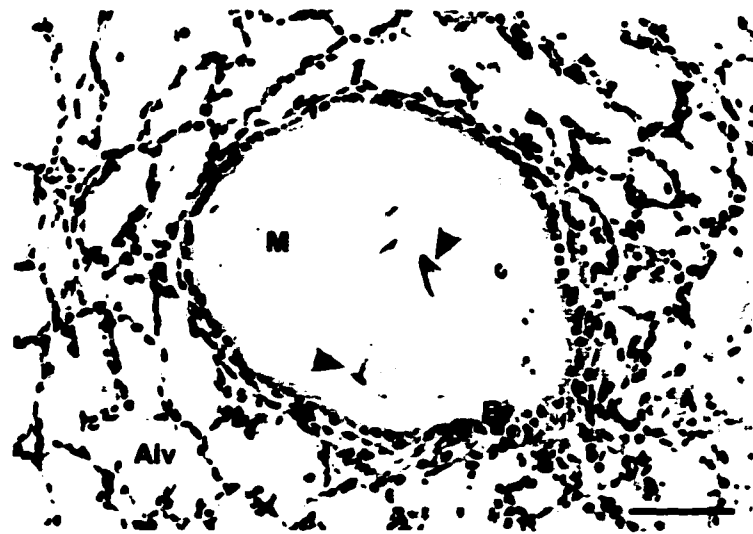


Fig. 25. Neonatal rat lung; meconium PID 3. Meconium (M) fills the bronchiole (Br), but is not present in alveoli (Alv). Keratin (arrowheads) is present in the meconium plug. HE stain. Bar = 50 μ m.



Fig. 26. Neonatal rat lung; meconium PID 1. Meconium (M) fills an alveolus. Alveoli (Alv), bronchiole (Br), blood vessel (Bv). HE stain. Bar = 50 μ m.

Table XIV. Histologic scoring for the evaluation of the frequency and severity of changes induced after the intratracheal inoculation of meconium in the lungs of neonatal rats.

| Microscopic Variable | Postinoculation Day | | | | | | |
|----------------------|---------------------|-----|----|----|----|----|-----|
| | 1 | 3 | 7 | 14 | 28 | 56 | 112 |
| Meconium-bronchioles | +++ | +++ | ++ | + | + | + | + |
| Meconium-alveoli | +++ | +++ | ++ | ++ | ++ | ++ | ++ |
| PMN-bronchioles | +++ | + | - | - | - | - | - |
| PMN-alveoli | +++ | ++ | + | - | - | - | - |
| PAM-bronchioles | + | + | + | + | + | + | + |
| PAM-alveoli | ++ | ++ | + | + | + | + | + |
| Edema | ± | - | - | - | - | - | - |
| Atelectasis | +++ | ++ | - | ± | - | - | - |
| Hyperinflation | +++ | +++ | ++ | + | ± | ± | ± |
| Thickening-alveoli | +++ | ++ | - | - | - | - | - |
| Granuloma formation | - | + | + | ++ | ++ | ++ | ++ |
| Giant Cells | - | ± | + | ++ | ++ | ++ | ++ |
| Mineralization | - | - | - | + | + | ++ | ++ |

(- = absent; ± = minimal; + = mild; ++ = moderate; +++ = severe)

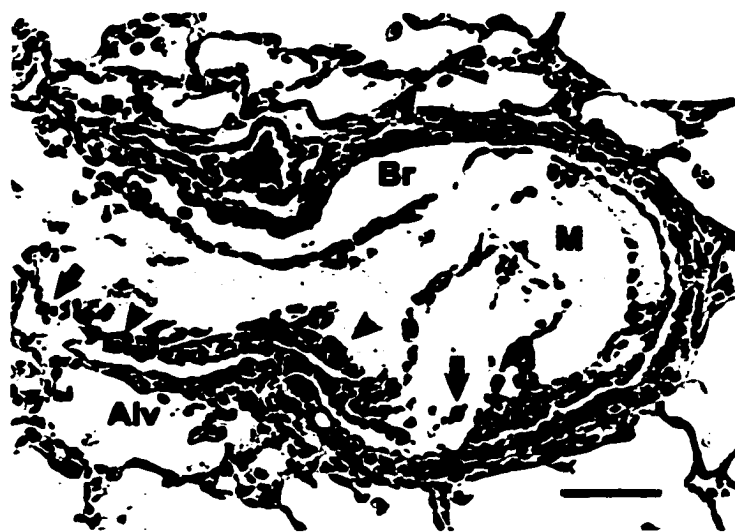


Fig. 27. Neonatal rat lung; meconium PID 1. Meconium (M), present in bronchiole (Br) is surrounded by neutrophils (arrows) and macrophages (arrowheads). HE stain. Bar = 50 μ m.

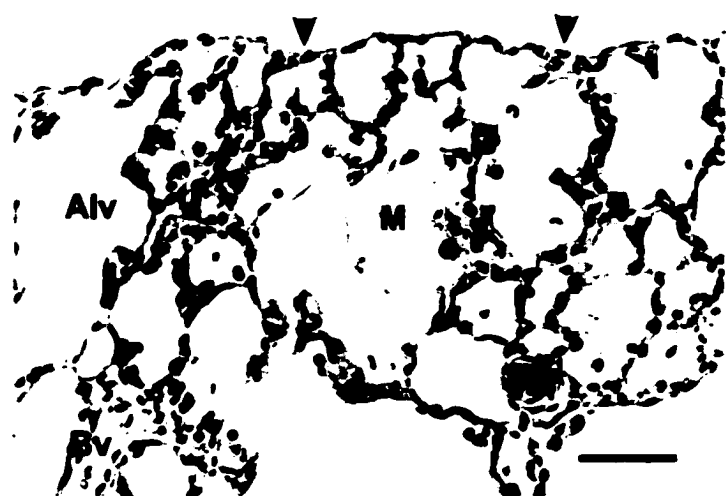


Fig. 28. Neonatal rat lung; meconium PID 1. Meconium (M) within alveoli (Alv), blood vessels (Bv), pleura (arrowheads). HE stain. Bar = 30 μ m.

This change was particularly evident at PID 1 and 3.

The distribution of lesions within the lungs following intratracheal inoculation of meconium was not entirely uniform. Focal areas of atelectasis associated with intraalveolar accumulation of meconium often alternated with well-aerated areas containing no visible meconium. Moreover, atelectasis and inflammation were also seen in some areas of the lung that contained no visible meconium. Complete obstruction of bronchi with meconium was not observed in any rat. Meconium in subpleural regions of the lung was evident as early as PID 1 (Fig. 28).

Atelectasis or alveolar collapse with parallelism of alveolar walls was present at PID 1 and 3 in all rats (100%) inoculated with meconium (Fig. 29A). This alteration in lung aeration appeared as a diffuse or locally extensive lesion and was present in 50% and 35% of the lung lobes at PID 1 and 3 respectively. Non-atelectatic lung from a control rat is shown in Fig. 29B for comparison. Atelectasis was no longer observed in the lungs of rats inoculated with meconium and killed at PID 7 and 14 (Table XV). Air trapping and hyperinflation, sometimes juxtaposed to areas of atelectasis, were also observed in the lungs of rats inoculated with meconium (Fig. 30). Hyperinflation with over distension of alveoli was observed in all rats (100%) inoculated with meconium and killed at PID 1, 3, 7 and 14, but its severity decreased progressively over time (Table XIV).

Inflammatory and structural changes in response to intratracheal inoculation of meconium were noticeable in the first few days postinoculation. At PID 1 and PID 3,

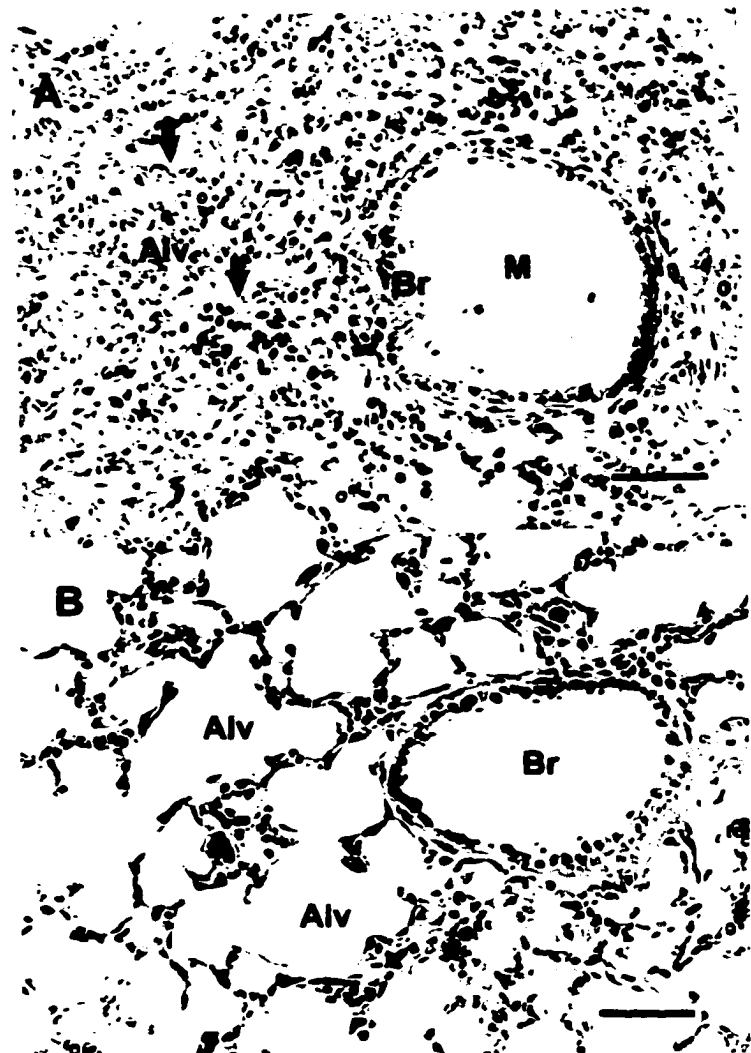


Fig. 29A. Neonatal lung; meconium PID 1. Collapsed alveoli (Alv)(arrows) are evident close to a bronchiole (Br) filled with meconium (M). HE stain. Bars = 50 μ m.

Fig. 29B. Neonatal rat lung; control PID 1. Bronchiole (Br) and alveoli (Alv) are clean and normally distended. HE stain. Bar = 50 μ m.

Table XV. Acute study. Neonatal lungs with evidence of atelectasis after the intratracheal inoculation of meconium and its interlobar distribution.

| PID | N | Atelectasis | | | | | | |
|-----|---|-------------|-------|------|------------|-----------|-----------|-----------|
| | | Animals | Lobes | Left | R. Cranial | R. Middle | R. Median | R. Caudal |
| 1 | 4 | 4/4 | 10/20 | 4/4 | 2/4 | 1/4 | 3/4 | 0/4 |
| 3 | 4 | 4/4 | 7/20 | 2/4 | 1/4 | 1/4 | 3/4 | 0/4 |
| 7 | 4 | 0/4 | 0/20 | 0/4 | 0/4 | 0/4 | 0/4 | 0/4 |
| 14 | 5 | 1/5 | 1/25 | 0/5 | 1/5 | 0/5 | 0/5 | 0/5 |

Table XVI. Acute study. Neonatal lungs with exudative inflammation after the intratracheal inoculation of meconium and its interlobar distribution.

| PID | N | Exudative inflammation | | | | | | |
|-----|---|------------------------|-------|------|------------|-----------|-----------|-----------|
| | | Animals | Lobes | Left | R. Cranial | R. Middle | R. Median | R. Caudal |
| 1 | 4 | 4/4 | 18/20 | 4/4 | 4/4 | 4/4 | 3/4 | 3/4 |
| 3 | 4 | 4/4 | 13/20 | 2/4 | 3/4 | 1/4 | 4/4 | 3/4 |
| 7 | 4 | 1/4 | 2/20 | 0/4 | 0/4 | 1/4 | 1/4 | 0/4 |
| 14 | 5 | 0/5 | 0/25 | 0/5 | 0/5 | 0/5 | 0/5 | 0/5 |



Fig. 30. Rat lung; meconium PID1. Atelectatic alveoli (arrowheads) alternating with hyperinflation (*) close to meconium (M) in bronchiole (Br). HE stain. Bar = 100 μ m.

bronchioles and alveoli contained many polymorphonuclear leukocytes and macrophages, and the pulmonary interstitium appeared mildly edematous (Fig. 31A)(See also Table XIV). This exudative inflammatory reaction was present in 100% of the rat neonates at PID 1 and 3 and in 25% at PID 7 and was not observed at PID 14. Neither exudative inflammation nor interstitial alveolar distension was observed in the control animals (Fig. 31B). The percentage of lung lobes with exudative neutrophilic inflammation decreased progressively from 90% at PID 1 to 65% at PID 3 and only 10% by PID 7. Regarding lobar distribution at PID 1, meconium-induced inflammation was observed in 100% of the left, right cranial and right middle lobes, and in 75% of the median and caudal lung lobes. The frequency with which the neutrophilic exudative changes were seen in the pulmonary lobes notably decreased with time. By PID 7, only 10% of all lung lobes had evidence of exudative neutrophilic inflammation and by PID 14 this type of exudation was no longer visible in the lungs (Table XVI).

An important lesion found at PID 1 and 3 in all rats (100%) inoculated with meconium was a remarkable thickening of the alveolar septa (Fig. 31A). This change was closely associated with areas of exudative inflammation, affecting almost all pulmonary lobes (95-100%) and was not observed in any of the rats of the control or amniotic fluid groups (Fig. 31B). Alveolar thickening was no longer observed in the rats of the meconium group at PID 7 or 14 (Table XIV). All lobes showed alveolar thickening (100%) at PID 1, thickening decreased to 25% only in middle lobes at PID 3 and it was not present at PID 7 and 14 (Table XVII).

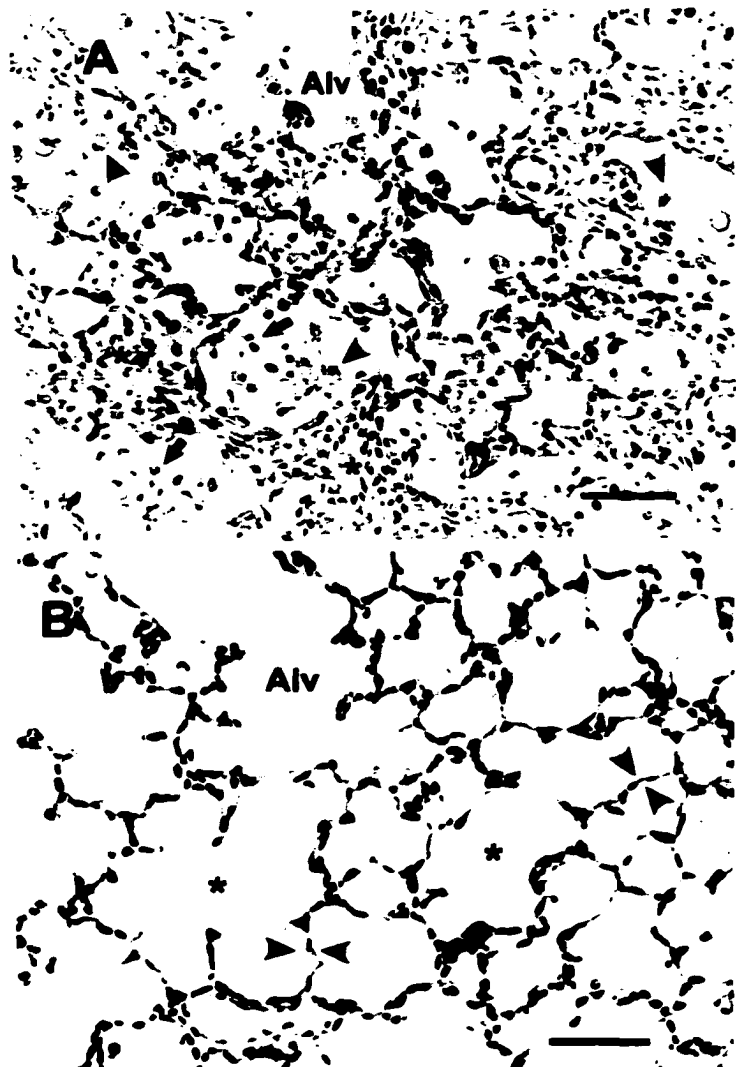


Fig. 31A. Neonatal rat lung; meconium PID 1. Exudative inflammation with neutrophils (arrows) and macrophages (arrowheads) within alveoli (Alv). Note the thickened alveolar septa (*) compared to control 31B. HE stain. Bar = 50 μ m.

Fig. 31B. Neonatal rat lung; saline control PID 1. Alveoli (Alv) with clean air spaces (*) and non distended alveolar septa (arrowheads). HE stain. Bar = 50 μ m.

Intratracheal inoculation of meconium also caused a mild thickening of the pleura at PID 1,3, and 7. This pleural change was characterized by focal accumulation of neutrophils and macrophages, mainly confined to subpleural locations. Meconium was also observed, surrounded by neutrophils and macrophages, on the pleural surface. Histopathologic changes of the pleura were observed only in rats of the meconium group.

The lungs of rats inoculated with meconium also contained a moderate number of enlarged pulmonary alveolar macrophages with cytoplasmic vacuoles containing golden pigment (Fig. 32). These meconium-laden macrophages were particularly conspicuous at PID 1, 3 and 7 and their number decreased at PID 14.

Intraalveolar hemorrhage and alveolar macrophages containing red blood cells (erythrophagocytosis) were occasionally seen in areas of the lung with meconium-induced alveolitis. Loss of cilia (deciliation) and vacuolation of bronchiolar epithelial cells were other changes often associated with meconium in the airways. Affected bronchioles also showed migration of neutrophils through the interstitium and epithelial wall.

The neutrophilic exudation started to resolve at PID 3 and by PID 14 the inflammatory reaction became predominantly histiocytic and granulomatous (Table XIV). The histiocytic response was moderate and multifocal, and was composed of macrophages which were in close association with meconium lodged in the alveoli and proximal alveolar regions of the lungs (Fig. 33). Granulomatous response was characterized by the presence of multinucleated giant cells (Fig. 34) after PID 7 (Table XIV). With time, meconium

Table XVII. Acute study. Neonatal rat lungs with presence of thickening of the alveolar septa after intratracheal inoculation of meconium and their interlobar distribution.

| PID | N | Thickening of the alveolar septa | | | | | | |
|-----|---|----------------------------------|-------|------|------------|-----------|-----------|-----------|
| | | Animals | Lobes | Left | R. Cranial | R. Middle | R. Median | R. Caudal |
| 1 | 4 | 4/4 | 20/20 | 4/4 | 4/4 | 4/4 | 4/4 | 4/4 |
| 3 | 4 | 4/4 | 19/20 | 4/4 | 4/4 | 3/4 | 4/4 | 4/4 |
| 7 | 4 | 0/4 | 0/20 | 0/4 | 0/4 | 0/4 | 0/4 | 0/4 |
| 14 | 5 | 0/5 | 0/25 | 0/5 | 0/5 | 0/5 | 0/5 | 0/5 |



Fig. 32. Neonatal rat lung; meconium PID 1. Meconium (M) is present in a terminal bronchiole (Br) along with meconium-laden macrophages (arrows). Alveolus (Alv), blood vessel (Bv). HE stain. Bar = 30 μ m.

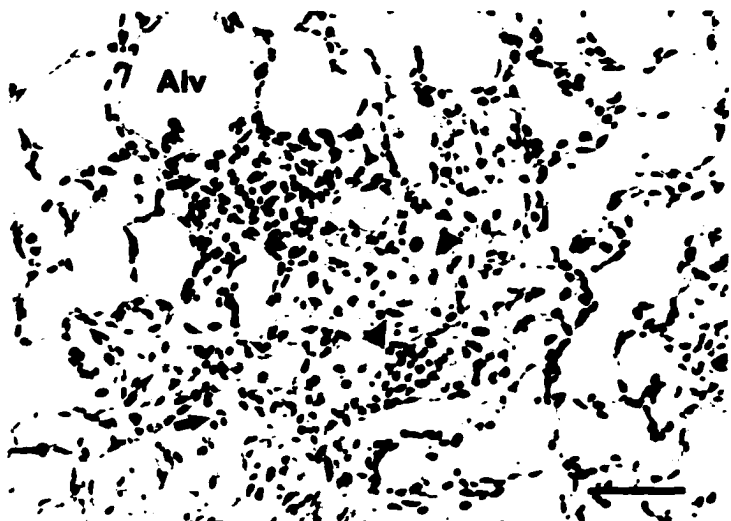


Fig. 33. Neonatal lung; meconium PID 7. Transition from neutrophilic (arrows) to histiocytic inflammation composed of macrophages (arrowheads) in alveoli (Alv). HE stain. Bar = 50 μ m.

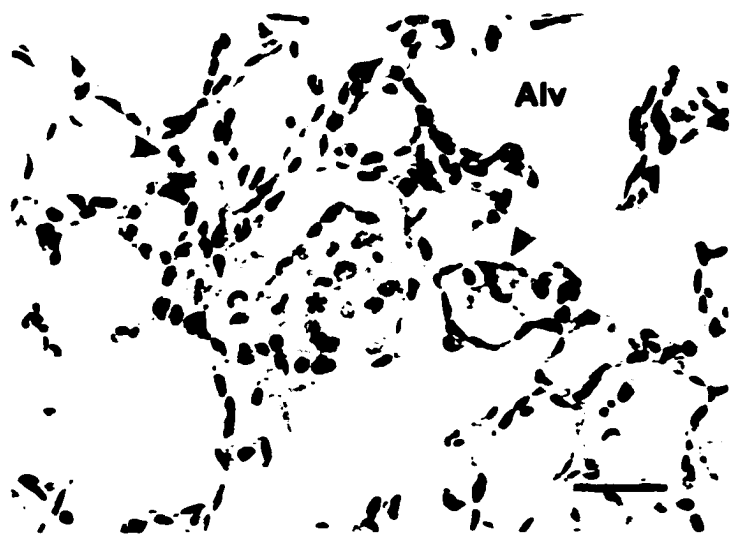


Fig. 34. Neonatal lung; meconium PID 14. Granulomatous response characterised by macrophages (arrowheads) and multinucleated giant cells (*) in an alveolus (Alv). HE stain. Bar = 30 μ m.

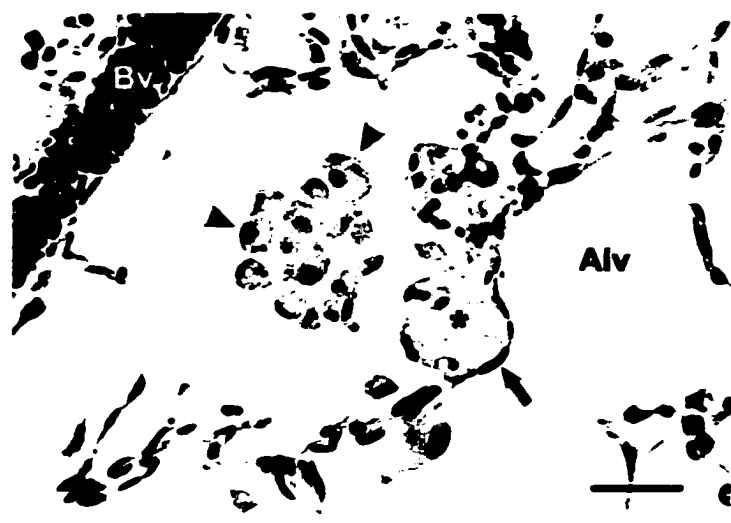


Fig. 35. Neonatal lung; meconium PID 28. Granuloma formation in alveoli (Alv) by macrophages (arrowheads) and giant cells (*). Presence of fibroblastic cells (arrows) surrounding granuloma. Blood vessel (Bv). HE stain. Bar = 30 μ m.

aspirated into the lung became well delimited and completely surrounded, and “sequestered” by macrophages and multinucleated giant cells. At PID 14, meconium showed early calcification visible with HE stain and subsequently corroborated by von Kossa stain.

4.3.3. Chronic study

Microscopically, all rats of the meconium group had meconium in the lungs either in the conducting airways or more commonly in the alveoli (Table XIV). Meconium was present in conducting airways in 80% of animals at PID 14 and 28, and only in 50% of rats by PID 112. The proportion of lung lobes with microscopic evidence of meconium in conducting airways diminished from 56% at PID 14 to 13.3% at PID 112. In contrast, meconium always remained visible in the alveoli in all rats (100%) killed at PID 14, 28, 56 and 112. The presence of meconium in alveoli for the different lung lobes ranged from 60 to 83%.

At PID 14, the histiocytic and granulomatous reaction was the predominant microscopic finding in 80% of the rats inoculated with meconium (Table XIV). Atelectasis was only occasionally seen in the lungs of rats killed at PID 14 and in none of the animals killed at PID 28, 56 or 112. Thickening of the alveolar septa was not detected in any rat killed after PID 14 (Table XIV).

At PID 28, multifocal granulomatous inflammation remained visible in 100% of the rats and was characterized by alveolar macrophages and multinucleated giant cells (Fig. 35)(Table XIV). This inflammatory reaction was commonly associated with the presence of meconium in alveoli and bronchioles. The microscopic appearance of meconium and

keratin in the lungs notably changed with time. The keratin and cellular debris (squames) were no longer evident in the lungs by PID 28. In addition, the core of the meconium plug was composed of a poorly stained, pale basophilic matrix surrounded by a rim of PAM. Some of these phagocytic cells still contained gold-yellow pigment in the cytoplasm. Meconium remained surrounded and covered by a discontinuous coating of columnar epithelial cells, and by PID 28 fibroblastic cells began to appear (Fig. 36). Calcification confirmed by von Kossa stain was also found at PID 28 (Table XIV).

At PID 56, the multifocal granulomatous inflammation was still present in all rats (100%) inoculated with meconium and this material remained evident in bronchioles, proximal alveolar regions and alveoli (Table XIV). However, the tinctorial characteristics of meconium on HE stained sections began to change by PID 56, and the original gold matrix turned into a pink and grey color. At this time, meconium appeared intensely red in PAS stain, indicating the presence of neutral mucins, and stained purple by the Alcian blue-PAS method, indicating a combination of neutral and acid mucins. The meconium sequestered in alveoli became completely surrounded by a single and discontinuous layer of columnar epithelial cells and fibroblastic cells (Fig. 37). Sporadic foci of osseous metaplasia appeared in some alveoli. Focal calcification of meconium matrix was still evident (Fig. 38).

At PID 112, a sparse multifocal granulomatous inflammation persisted, as well as, the presence of giant cells in all animals. At this postinoculation time, meconium remained visible mainly in bronchioles, proximal alveolar regions and alveolar areas (Fig. 39).



Fig. 36. Rat lung; meconium group PID 28. Meconium (M) in an alveolus (Alv) surrounded by fibroblastic cells (arrows) and a region of columnar epithelial cells (arrowheads). HE stain. Bar = 30 μ m.



Fig. 37. Rat lung; meconium group PID 56. Meconium (M) sequestered in the wall of an alveolus and encapsulated by fibroblastic cells (arrows) and multinucleated cells (*). Evidence of bronchiolization (arrowheads). Alveolus (Alv). HE stain. Bar = 30 μ m.



Fig 38. Rat lung; meconium group PID 56. Meconium remained trapped in alveoli (Alv) and encapsulated by fibroblastic cells (arrow heads). Meconium pigment is still present at the periphery (arrow). Focal calcification (*) is evident . HE stain. Bar = 30 μ m.

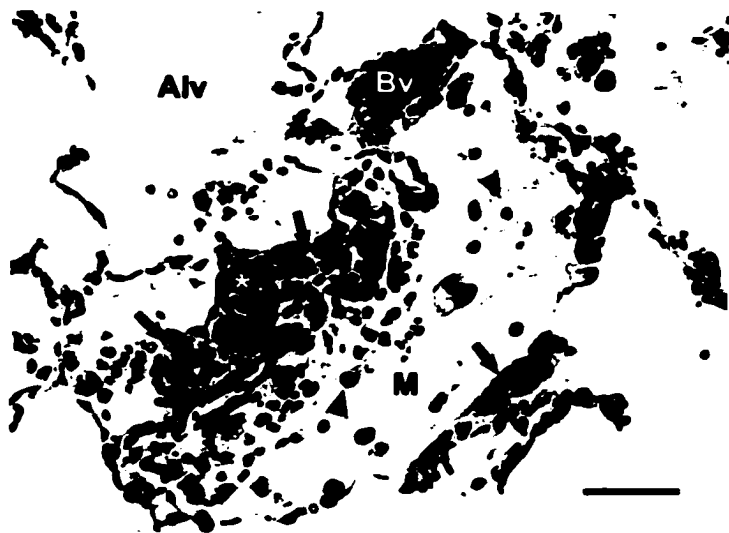


Fig. 39. Rat lung; meconium group PID 112. Persistent multifocal granulomatous inflammation in alveoli (Alv). Meconium (M) basophilic matrix, with macrophages (arrowheads), multinucleated cells (arrows) and gold pigment (*). Blood vessel (Bv). HE stain. Bar = 30 μ m.

The dense arrangement of meconium changed into loose pale matrix in HE and the color was purple in Alcian blue-PAS stain. Calcification of sequestered meconium in areas of granulomatous response was present in most animals (Table XIV).

4.4. Discussion:

The reduced weight gain in rats inoculated with meconium and killed at PID 1 to PID 3 revealed that meconium has an early systemic effect beyond the respiratory tract, an effect that could be explained in several ways. It is plausible that the chemical pneumonitis induced by meconium had a generalized side effect like the one described in the systemic inflammatory response syndrome (SIRS) and which occurs in any inflammatory reaction regardless of etiology(71-73). It is known that in SIRS there is an increased catabolic state promoted by mediators of inflammation, particularly cytokines (71). Interestingly, the cytokines responsible for the generalized malaise in many illnesses and SIRS (TNF α , IL-1, IL-6 and IL-8), are also involved in the pathogenesis of pulmonary lesions in experimental MAS (24,25,74-76).

Changes in blood gases resulting from airway obstruction and pulmonary inflammation could also be a contributing factor in the reduced weight gain in rats of the meconium group. Hypoxemia, acidosis and hypercapnia, the most common physiological derangements in babies with MAS, have been associated with neonatal stress and weight loss (1,77). In veterinary medicine, fetal stress, hypoxia, acidosis which is common in prolonged labour and dystocia, have also been proposed as causes of “weak calf syndrome” and perinatal death (78-80). During perinatal hypoxia and acidosis, tissue changes are not restricted to the respiratory tract and can involve distant organs (33,81,82). There are few

studies with experimental MAS in which rodents were weighed to allow comparisons with the result obtained in the neonatal rats of this study (13,41-43). According to these reports, no significant changes in body weight were detected in rats inoculated with meconium, however these were short term studies ranging from only 60 min to 6 hours postinoculation (13,42,43).

Reduction in weight gain in rats dosed with meconium had an unexpected bimodal distribution in the chronic study. The initial reduction (PID 1-12) was followed by a moderate weight gain (after PID 28 and until PID 55) and stable growth period (PID 56), followed finally by another reduction in body weights (PID 112). It is common for human beings and animals recovering from disease-associated weight loss to recover a few days later with an accelerated weight gain (83). As a compensatory mechanism, this phenomenon has been referred to as “catch-up growth” and it is similar to hyperanabolic states also seen in animals recovering from disease (84). The catch-up phenomenon has been recently reported in premature neonatal babies after injury (83). The reason for a second wave of weight loss in rats inoculated with meconium after the catch-up growth remained an enigma. Although babies with MAS could have lower birth weights (85,86), it is not yet clear if these low weights persist weeks later.

In contrast to meconium, inoculation of sterile amniotic fluid caused only mild pulmonary changes which did not translate into significant reduction in body weights. This finding indicates that aspiration of small volumes of amniotic fluid has little significance on the overall state of the neonatal rat.

Early work of Cruickshank in 1949 with adult rabbits showed that intratracheal

inoculation of 10 ml of saline solution induced subpleural collapse in addition to attraction of polymorphonuclear leukocytes into the lungs (39). This observation was later supported by another study in which investigators attributed small areas of atelectasis to inoculation of saline solution in rabbits (41). In contrast to these findings, rats of the saline control group did not have evidence of atelectasis and this discrepancy could be explained in at least two ways. First, it is possible that the degree of alveolar collapse in rats inoculated with saline solution was mild allowing for re-distention of the lung at the time of fixation, thus masking the presence of atelectasis. The second, and most likely, explanation is that the small volume of 0.05 ml of saline introduced into the lung was insufficient to cause changes in surfactant and alveolar collapse.

The inflammatory response in the lungs of rats inoculated with amniotic fluid was characterized microscopically by mild and transient alveolar collapse and influx of leukocytes into the airspaces. Elicited by keratin, keratinized cells and squames in the lung, the histiocytic response is a typical foreign body reaction and mimics the reaction occurring in spontaneous aspiration of amniotic fluid (39,58). Under normal conditions, "foreign" materials reach the amniotic fluid when components of fetal skin like squamous cells, keratin, squames and lanugo exfoliate into the contents of the amniotic sac (87). The histiocytic reaction to amniotic fluid is primarily attributed to the suspended cellular elements and not to the fluid itself, a view that was substantiated in a study in which the typical foreign body reaction in rabbits was abrogated when the suspended cells and keratin were removed from amniotic fluid prior to inoculation (39). A study recently conducted in rats inoculated with bovine amniotic fluid revealed, as it may be expected, that the magnitude

of pulmonary inflammation paralleled the volume of the inoculum introduced into the lung (58).

Amniotic fluid, like saline solution, did not induce relevant atelectasis, suggesting that the viscosity of this feto-placental fluid was insufficient to cause airway obstruction (88). It should be noted again, that the fixation method may have been in part responsible for redistention of mildly atelectatic lungs.

Compared to saline solution and amniotic fluid, inoculation of rats with meconium caused the most significant histopathologic changes in the lungs. Severe atelectasis, one of the two most conspicuous changes in these rats, was consistent with findings in other studies and further supports the view that mechanical obstruction is one of the mechanisms involved in alveolar collapse in MAS (5).

The multifocal to locally extensive atelectasis in neonatal rats at PID 1 and 3 did not coincide with the widespread atelectasis described in adult rats inoculated with human meconium (43). This discrepancy is most likely due to the particle size of meconium. Large particles of unfiltered meconium are trapped in large airways and cause physical obstruction while small particles ($<3\mu\text{m}$) in filtered meconium readily reach the alveolar region, displace pulmonary surfactant and cause severe atelectasis and respiratory failure (14,42,43). Based on these observations, it is clear that results obtained in experiments with filtered meconium cannot be safely extrapolated to clinical practice, largely because filtered meconium does not obstruct larger airways such as occurs in natural MAS (41). Atelectasis in the rats inoculated with meconium developed not only because of airway obstruction and surfactant displacement, but also due to the added effect of alveolar inflammation (14,15). A recent

study showed that free radicals released by leukocytes at the site of inflammation cause lipid peroxidation of the surfactant (89). In summary, homologous meconium intratracheally inoculated to neonatal rats causes obstruction of airways, reaches the alveoli and causes the same type of lesions reported in natural cases of MAS in humans as well as in animals.

One interesting finding observed in rats of the meconium group was the coexistence of atelectatic and hyperinflated areas in the same sections of the lung. In human MAS, this has been attributed to pulmonary interdependence (collateral ventilation) and aberrant movement of air in obstructed lungs (1,46,90-93). Complete obstruction of a terminal bronchiole leads to atelectasis while partial obstruction may result in a "ball-valve" effect in which gas flows into the airway on inspiration, however it then becomes trapped and causes hyperinflation (1,4,22). Pneumothorax, pneumomediastinum, or pulmonary interstitial emphysema, are sequelae sporadically reported in MAS, and were not observed in the rats inoculated with meconium.

The distribution of atelectasis in all but one of the pulmonary lobes was an unexpected finding in the rats inoculated with meconium. Although the numbers studied were small, it is difficult to explain why the right caudal lobe of rats in the meconium group did not develop atelectasis in spite of the fact that both meconium and inflammation were present in this lobe. Hypothetical possibilities are: an unexplained difference in the pressure of fixative entering this particular lobe, reduced susceptibility of the right caudal lobe to airway obstruction, increased collateral ventilation or increased resistance of this lobe to surfactant displacement. Differences in susceptibility of specific lung lobes to disease have been documented in human and veterinary pathology. For instance, the middle lung lobe of

children is particularly susceptible to atelectasis in the so-called "middle lobe" or "atelectactic syndrome in children" while the cranial right lobe in animals appear to be more susceptible to infection (54,94,95). Future studies should investigate why the right caudal lobe of rats appears to be refractory to atelectasis.

Inoculated meconium in the rats dispersed from the terminal bronchioles into the contiguous alveolar acini and was also observed reaching the pleural tissue. This peripheral "migration" of meconium has been documented in rabbits (40,96) and dogs within the first two hours after inoculation (13), and piglets within the first few hours after aspiration (17). The mechanisms responsible for movement and redistribution of meconium within the lung are suggested to be due to gasping (inspiration effort) and the ball-valve effect forcing meconium to the periphery of the lung (96-98). *In situ* perfusion with formalin at 20 cm of water pressure yielded dependable results in the neonatal rats similar to what has been reported with older rats (67,99). The modified "Marriot Bottle" could be recommended for intratracheal lung fixation in neonatal rats since it produces a consistent and uniform distention of alveoli in the immature lung (67).

It is not always easy to detect meconium in the lungs microscopically, particularly when present in small quantities or when the characteristic bright gold-yellow color begins to fade away (1,100). Consistent with previous reports (23,33,101), meconium was easily detected by its bright gold-yellow color in rats killed during the first few weeks postinoculation. However, as time passed, the characteristic color faded away and by PID 28 the gold tinge had practically vanished due to chemical degradation within the lung. Since meconium contains the bile pigment bilirubin, hence its yellow color, it has been

recommended that Hall's stain method be used to confirm the presence of bilirubin in tissues. Contrary to what the literature suggests (33), the Hall's method did not show any real advantage over routine stains. Special stains such as Alcian blue-PAS and PAS counterstained with either light green or hematoxylin proved superior to Hall's stain for the identification of meconium in the rat lung. The advantage resided in the mucopolysaccharides and mucins in meconium which stain well with PAS and Alcian blue-PAS (100,102,103). These three staining methods should prove of value in evaluating the presence and distribution of inoculated meconium in experimental models of MAS as previously suggested by others (12,41,51).

There were notable microscopic differences in pulmonary inflammation amongst rats inoculated with saline solution, amniotic fluid and meconium. Lack of relevant lesions in rats inoculated with sterile saline solution supports the general assumption that saline is a reliable and almost innocuous vehicle for intratracheal instillation (14,17,28). It should be kept in mind however, that even a sterile saline solution attracts neutrophils into the alveolar spaces as shown by more sensitive tests such as BAL (104-106).

The mild and transient histiocytic response in lungs inoculated with amniotic fluid (PID 1 and 3) coincided with the low frequency in which squamous epithelial cells and keratin were observed microscopically in alveoli and airways. It has been recognized that rabbit amniotic fluid is less turbid and has fewer squamous cells than does human amniotic fluid, so it is not surprising that the inflammatory response is more intense when human amniotic fluid is used as inoculum(39). The amniotic fluid in term pregnancy rats was not grossly turbid and contained relatively low numbers of cells, explaining, in part, why the

inflammatory reaction was less severe than in experimental models with human amniotic fluid (39). In reviewing the literature, there is a lack of data about the particle and cellular composition of amniotic fluid in different species of animals. It would be useful in the future to compare the cellularity and density of keratin in amniotic fluid of human beings and animals as well as the relationship between this cellularity and severity of inflammation.

The transient nature of the inflammatory response in rats of the amniotic group was consistent with the rapid disappearance of squamous epithelial cells from the lungs of the rats. According to one study, squamous epithelial cells intratracheally inoculated into rabbits are no longer recognisable in the lungs five days after inoculation (39). It is presumed that squamous epithelial cells, like any other particle, are eliminated through the mucociliary escalator (107).

A pivotal consideration regarding the inflammatory response to aspirated amniotic fluid is the presence of anti-inflammatory factors in this fluid. Recent investigations have shown that human amniotic fluid contains high levels of interleukin-1 receptor antagonist (IL-1-ra) which blocks interleukin-1 (IL-1), one of the most important biochemical mediators of acute inflammation (108). Human amniotic fluid also contains IL-10, an important inflammatory cytokine that down-regulates the local inflammatory response (109). This novel information may help to elucidate why the inflammatory response to keratin and amniotic fluid in the lung appears less intense than in other organs such as the skin where free keratin induces a dramatic granulomatous reaction (33,56,57,110).

Meconium induced a rapid influx of polymorphonuclear leukocytes and alveolar macrophages into the bronchoalveolar spaces and this finding is consistent with reports

describing natural MAS in humans and experimental animals (2,16). Recruitment of inflammatory cells was most dramatic between 12 and 24 hours after meconium administration in rabbits and piglets (17,21). What was not clear in this study of rats inoculated with meconium was the confirmation of necrosis as it was difficult to discriminate microscopically fragmented neutrophils in alveolar walls from epithelial karyorrhexis. In cases like this, ultrastructural evaluation could be much more revealing than routine histopathology (See Chapter 6).

The mechanisms responsible for attracting leukocytes into the lung following aspiration of meconium are presumably the same as for other forms of pneumonia in which cytokines are involved (111,112). Tumor necrosis factor- α (TNF α), interleukin 1 β (IL-1 β), and interleukin-8 (IL-8) have been identified as important pro-inflammatory cytokines accountable for the recruitment of leukocytes in the lung following meconium aspiration (24,26,113). *In vitro* studies confirmed that IL-8, a powerful chemoattractant for neutrophils, is present in human meconium and suggest that this chemokine could be a major mediator of inflammation in acute MAS (114).

The multifocal granulomatous response in the lungs of rats inoculated with meconium was similar to that described in adults rabbits inoculated with human amniotic fluid with meconium and killed 8,11,15 and 32 days later (39). In this study, although keratinised epithelial cells were no longer found in rabbits after PID 15, at PID 32 there were scattered granulomas. Similar granulomas were microscopically observed in the lungs of rats in the present study inoculated with meconium and killed 7 days later. It is not totally known if such granulomas develop in the lungs of babies surviving the acute episode of

MAS. Granulomas associated with meconium have been described in humans in the peritoneal cavity, serosa of genital organs, and just recently in the lung (115-120).

Some rats of the meconium group developed characteristic nodules covered by epithelium. According to the literature, these nodules start forming when inhaled materials produce focal epithelial injury, either by the direct toxic effect of the material, or through phagocytic enzymes released by alveolar macrophages (7). Once damaged, the erosive lesions are followed by compensatory hyperplasia of alveolar or bronchiolar epithelia (7,121). This type of response has been also described as a response to inhaled foreign materials, creating an epithelium-covered inflammatory nodule (121). Extrapolating from these studies, it is assumed that the unusual epithelium-covered nodules in rats of the meconium groups could be the result of focal epithelial erosion at the sites of meconium entrapment followed by repair or the additional foreign body response.

Mineralization was also a conspicuous change in the lungs of some rats inoculated with meconium. This change appeared at PID 14, remained visible up to the end of the study and was interpreted as dystrophic mineralization of inflammatory foci (122). Although pulmonary mineralization has not been described in MAS, this change has been reported in abdominal tissues of fetuses or newborn babies with meconium peritonitis and in umbilical cords of babies with MAS (123-126).

The unexpected finding of meconium on pleural surface is enigmatic. One possible explanation could be the leakage of meconium induced by air trapping, emphysema and pneumothorax which are characteristic in this syndrome. A recent study also documented the rupture of the lung with meconium-thorax in human neonates (98). However, the

contribution of mechanical rupture of the lung during inoculation could also be responsible for the presence of meconium in pleura.

The prototypical pulmonary lesion in aspiration of meconium has been referred to as "chemical pneumonitis" based on the assumption that necrosis and inflammation are primarily attributed to the chemical effect of bile and enzymatic components of meconium (21). However, it is well recognized that the pathogenesis of pulmonary lesions in MAS is more complex than simple chemical damage to respiratory epithelia. Free radicals, lipid metabolites and phagocytic enzymes locally released by neutrophils and macrophages during inflammation are known to contribute to the overall injury caused by meconium as occurs for other inhaled toxins and pneumotoxins (24,26,113,114,127). Also, there is solid evidence that in addition to the chemical and inflammatory damage, hypoxia is also involved in the epithelial necrosis reported in natural or experimental models of MAS (5). It was not possible to ascertain how much the inflammatory process and hypoxia contributed to the lung injury in the rats of the meconium group. The apparent thickening of alveolar septa was associated to areas of exudative inflammation, however, it is difficult to distinguish microatelectasis from alveolar septal thickening when exudate is present, even in perfused lungs. The significance of alveolar septal thickening that developed following intratracheal administration of meconium is discussed in detail in Chapters 5 and 6.

There are still many unanswered questions regarding the role of meconium in pulmonary necrosis: 1.- Could meconium cause necrosis in non-hypoxic lung? 2- Could it be possible that the paucity in reported necrosis is because this lesion has not been part of the objectives of most studies with experimental MAS? 3.- Could the necrotic change be too

subtle to be detected easily in light microscopy? 4.- Could necrosis be dependent on the concentration of meconium in the inoculum? A recent study showed that necrosis in the lungs are highly dependent on the concentration of instilled meconium and to a much lesser extent on reduced lung oxygenation and hypoxia (Dr. Pekka Kääpä, personal communication).

Pulmonary edema is described in some experimental models of MAS but its pathogenesis remains unclear. Vascular leakage of fluid into the alveoli, and development of hyaline membranes occurs within a few hours after inoculation of human meconium in adult rabbits (21) and rats (13,42,43). These lesions, which are indicative of early microvascular damage, were only seen at PID 1 in some localized areas of the lungs in rats inoculated with meconium in the present study. The discrepancy between results from this study and those reported in the literature may be related to the volume and concentration of the meconium inoculum or because low protein edema fluid is difficult to detect in lungs fixed by intratracheal formalin infusion. The alveolar walls of adult rats are predominantly lined by type I pneumocytes, a cell exquisitely sensitive to injury. The ratio of type II to type I pneumocytes is higher in the neonatal alveoli (65,128) and type II pneumocytes are more resistant to injury (65). It is also possible that alveolar injury is dose-dependent and the concentration of meconium given to the neonatal rats was insufficient to induce leakage.

Recently, MAS was added to the long list of diseases that have a characteristic pathway of acute lung injury best exemplified in adult respiratory distress syndrome or simply ARDS (27,28). The hallmark lesions of ARDS, namely protein-rich alveolar edema, alveolitis and hyaline membranes, were not seen in any of the rats of the meconium groups in this study. The discrepancy could be explained by reviewing the pathogenesis currently

proposed for ARDS: alveolar injury and subsequent edema and hyaline membranes occur when neutrophils sequestered in the alveolar capillaries release powerful enzymes and free radicals (129,130). These alveolar changes appear to have a threshold type of response that is reached when a cascade of events leads to uncontrollable levels of circulating cytokines and “explosive” degranulation of neutrophils inside the alveolar capillaries (131-133). It is presumed that the inflammatory response in rats inoculated with meconium did not reach the threshold required for ARDS to develop. In other words, the sublethal concentration of meconium used in the neonatal rats caused an exudative alveolitis that did not progress into ARDS, a scenario consistent with the nonfatal outcome in some babies with MAS (1,134). In contrast, the ARDS-like syndrome reproduced experimentally with higher doses of meconium mimics the rare fatal cases of MAS in which babies die in spite of medical intervention (28). Future studies should investigate the dose-response relationship between meconium and ARDS-like syndrome in neonatal rats.

In conclusion, results of this study showed that intratracheal inoculation of homologous meconium in seven-day-old rats causes a bimodal reduction in body weight which remains detectable up to 112 PID. In contrast, inoculation of amniotic fluid does not cause any weight changes in rats. Epithelial cells, keratin and pigments are progressively removed from the inoculated meconium, leaving behind a loose, poorly pigmented matrix which remains visible in the alveoli up to 112 days postinoculation. The Hall's method for detection of bilirubin does not work as well as PAS and Alcian blue stains for detecting degraded meconium in the lungs. Meconium induces a rapid influx of neutrophils and macrophages in the lungs followed by a persistent multifocal histiocytic and granulomatous

reaction. The granulomatous foci eventually calcify and become partially covered by cuboidal epithelium. Sublethal doses of meconium cause atelectasis and hyperinflation with thickening of the alveolar walls but do not induce alveolar edema or formation of hyaline membranes. Intratracheal inoculation of amniotic fluid only induces a mild and transient histiocytic inflammation with no persistent foci of chronic inflammation in the lungs while saline solution does not cause detectable microscopic changes.

4.5. REFERENCES

1. SRINIVASAN HB, VIDYASAGAR D. Meconium aspiration syndrome: current concepts and management. *Compr Ther* 1999; 25: 82-89.
2. CLEARY GM, WISWELL TE. Meconium-stained amniotic fluid and the meconium aspiration syndrome. An update. *Pediatr Clin North Am* 1998; 45: 511-529.
3. KATZ VL, BOWES WAJ. Meconium aspiration syndrome: reflections on a murky subject. *Am J Obstet Gynecol* 1992; 166: 171-183.
4. WISWELL TE, BENT RC. Meconium staining and the meconium aspiration syndrome. Unresolved issues. *Pediatr Clin North Am* 1993; 40: 955-981.
5. JOVANOVIC R, NGUYEN HT. Experimental meconium aspiration in guinea pigs. *Obstet Gynecol* 1989; 73: 652-656.
6. THIBEAULT DW, HALL FK, SHEEHAN MB, HALL RT. Postasphyxial lung disease in newborn infants with severe perinatal acidosis. *Am J Obstet Gynecol* 1984; 150: 393-399.
7. MACFARLANE PI, HEAF DP. Pulmonary function in children after neonatal meconium aspiration syndrome. *Arch Dis Child* 1988; 63: 368-372.
8. SWAMINATHAN S, QUINN J, STABILE MW, BADER D, PLATZKER AC, KEENS TG. Long-term pulmonary sequelae of meconium aspiration syndrome. *J Pediatr* 1989; 114: 356-361.
9. GUPTA AK, ANAND NK. Wheezy baby syndrome: a possible sequelae of neonatal meconium aspiration syndrome. *Indian J Pediatr* 1991; 58: 525-527.
10. BRADY JP, GOLDMAN SL. Management of Meconium Aspiration Syndrome. In: Thibeault D W, Gregory GA, eds. *Neonatal Pulmonary Care*. Connecticut: Appleton-Century-Crofts, 1986: 483-498.
11. BACSIK RD. Meconium aspiration syndrome. *Pediatr Clin North Am* 1977; 24: 463-479.
12. BROWN BL, GLEICHER N. Intrauterine meconium aspiration. *Obstet Gynecol* 1981; 57: 26-29.
13. CLEARY GM, ANTUNES MJ, CIESIELKA DA, HIGGINS ST, SPITZER AR, CHANDER A. Exudative lung injury is associated with decreased levels of surfactant proteins in a rat model of meconium aspiration. *Pediatrics* 1997; 100: 998-1003.

14. SUN B, CURSTEDT T, ROBERTSON B. Surfactant inhibition in experimental meconium aspiration. *Acta Paediatr* 1993; 82: 182-189.
15. MOSES D, HOLM BA, SPITALE P, LIU MY, ENHORNING G. Inhibition of pulmonary surfactant function by meconium. *Am J Obstet Gynecol* 1991; 164: 477-481.
16. WISWELL TE, FOSTER NH, SLAYTER MV, HACHEY WE. Management of a piglet model of the meconium aspiration syndrome with high-frequency or conventional ventilation. *Am J Dis Child* 1992; 146: 1287-1293.
17. DAVEY AM, BECKER JD, DAVIS JM. Meconium aspiration syndrome: physiological and inflammatory changes in a newborn piglet model. *Pediatr Pulmonol* 1993; 16: 101-108.
18. CLARK DA, NIEMAN GF, THOMPSON JE, PASKANIK AM, ROKHAR JE, BREDENBERG CE. Surfactant displacement by meconium free fatty acids: an alternative explanation for atelectasis in meconium aspiration syndrome. *J Pediatr* 1987; 110: 765-770.
19. SUN B, CURSTEDT T, ROBERTSON B. Long-term cycling of surfactant films in Wilhelmy balance. *Reprod Fertil Dev* 1996; 8: 173-181.
20. BAE CW, TAKAHASHI A, CHIDA S, SASAKI M. Morphology and function of pulmonary surfactant inhibited by meconium. *Pediatr Res* 1998; 44: 187-191.
21. TYLER DC, MURPHY J, CHENEY FW. Mechanical and chemical damage to lung tissue caused by meconium aspiration. *Pediatrics* 1978; 62: 454-459.
22. AL MATEEN KB, DAILEY K, GRIMES MM, GUTCHER GR. Improved oxygenation with exogenous surfactant administration in experimental meconium aspiration syndrome. *Pediatr Pulmonol* 1994; 17: 75-80.
23. DAVIS RO, PHILIPS JB, HARRIS BAJ, WILSON ER, HUDDLESTON JF. Fatal meconium aspiration syndrome occurring despite airway management considered appropriate. *Am J Obstet Gynecol* 1985; 151: 731-736.
24. JONES CA, CAYABYAB RG, HAMDAN H. Early production of proinflammatory cytokines in the pathogenesis of neonatal adult respiratory distress syndrome (ARDS) associated with meconium aspiration. *Pediatr Res* 1994; 35: 339A-
25. JONES CA, CAYABYAB RG, KWONG KY, STOTTS C, WONG B, HAMDAN H, MINOO P, DELEMOS RA. Undetectable interleukin (IL)-10 and persistent IL-8 expression early in hyaline membrane disease: a possible developmental basis for the

predisposition to chronic lung inflammation in preterm newborns. *Pediatr Res* 1996; 39: 966-975.

26. SHABAREK FM, XUE H, LALLY KP. Human meconium stimulates murine alveolar macrophage procoagulant activity. *Pediatr Res* 1997; 41: 267A-
27. OGAWA Y, SHIMIZU H, ITAKURA Y, OHAMA Y, ARAKAWA H, AMIZUKA T, OBATA M, KAKINUMA R. Functional pulmonary surfactant deficiency and neonatal respiratory disorders. *Pediatr Pulmonol Suppl* 1999; 18: 175-177.
28. SOUKKA H, RAUTANEN M, HALKOLA L, KERO P, KÄÄPÄ P. Meconium aspiration induces ARDS-like pulmonary response in lungs of ten-week-old pigs. *Pediatr Pulmonol* 1997; 23: 205-211.
29. SOUKKA H, VIINIKKA L, KÄÄPÄ P. Involvement of thromboxane A2 and prostacyclin in the early pulmonary hypertension after porcine meconium aspiration. *Pediatr Res* 1998; 44: 838-842.
30. PERLMAN EJ, MOORE GW, HUTCHINS GM. The pulmonary vasculature in meconium aspiration. *Hum Pathol* 1989; 20: 701-706.
31. LEVIN DL, WEINBERG AG, PERKIN RM. Pulmonary microthrombi syndrome in newborn infants with unresponsive persistent pulmonary hypertension. *J Pediatr* 1983; 102: 299-303.
32. SOUKKA H, JALONEN J, KERO P, KÄÄPÄ P. Endothelin-1, atrial natriuretic peptide and pathophysiology of pulmonary hypertension in porcine meconium aspiration. *Acta Paediatr* 1998; 87: 424-428.
33. LOPEZ A, BILDFELL R. Pulmonary inflammation associated with aspirated meconium and epithelial cells in calves. *Vet Pathol* 1992; 29: 104-111.
34. LOPEZ A, LÖFSTEDT J, BILDFELL R, HORNEY B, BURTON S. Pulmonary histopathologic findings, acid-base status, and absorption of colostral immunoglobulins in newborn calves. *Am J Vet Res* 1994; 55: 1303-1307.
35. FURR M. Perinatal asphyxia in foals. *Compend Contin Educ Pract Vet* 1996; 18: 1342-1351.
36. KOTERBA A, HAIBEL G. Respiratory distress in a premature foal secondary to hydrops allantois and placentitis. *Compend Contin Educ Pract Vet* 1983; 5: 121-125.
37. DUBIELZIG RR. Pulmonary lesions of neonatal foals. *Equine Med Surg* 1977; 1: 419-425.

38. FUENTEALBA C, LOPEZ A. Intrauterine aspiration pneumonia. Diseases of the respiratory system. Western Conference of Veterinary Diagnostic Pathologists; Saskatoon, Saskatchewan: 1998;
39. CRUICKSHANK AH. The effects of the introduction of amniotic fluid into the rabbits' lungs. *J Pathol Bact* 1949; 61: 527-531.
40. FRANTZ ID, WANG NS, THACH BT. Experimental meconium aspiration: Effects of glucocorticoid treatment. *J Pediatr* 1975; 86: 438-441.
41. SUN B, CURSTEDT T, SONG GW, ROBERTSON B. Surfactant improves lung function and morphology in newborn rabbits with meconium aspiration. *Biol Neonate* 1993; 63: 96-104.
42. SUN B, HERTING E, CURSTEDT T, ROBERTSON B. Exogenous surfactant improves lung compliance and oxygenation in adult rats with meconium aspiration. *J Appl Physiol* 1994; 77: 1961-1971.
43. SUN B, CURSTEDT T, ROBERTSON B. Exogenous surfactant improves ventilation efficiency and alveolar expansion in rats with meconium aspiration. *Am J Respir Crit Care Med* 1996; 154: 764-770.
44. CALKOVSKA A, SUN B, CURSTEDT T, RENHEIM G, ROBERTSON B. Combined effects of high-frequency ventilation and surfactant treatment in experimental meconium aspiration syndrome. *Acta Anaesthesiol Scand* 1999; 43: 135-145.
45. GOODING CA, GREGORY GA, TABER P, WRIGHT RR. An experimental model for the study of meconium aspiration of the newborn. *Radiology* 1971; 100: 137-140.
46. MAMMEL MC, GORDON MJ, CONNETT JE, BOROS SJ. Comparison of high-frequency jet ventilation and conventional mechanical ventilation in a meconium aspiration model. *J Pediatr* 1983; 103: 630-634.
47. WISWELL TE, PEABODY SS, DAVIS JM, SLAYTER MV, BENT RC, MERRITT TA. Surfactant therapy and high-frequency jet ventilation in the management of a piglet model of the meconium aspiration syndrome. *Pediatr Res* 1994; 36: 494-500.
48. SOUKKA H, HALKOLA L, AHO H, RAUTANEN M, KERO P, KÄÄPÄ P. Methylprednisolone attenuates the pulmonary hypertensive response in porcine meconium aspiration. *Pediatr Res* 1997; 42: 145-150.
49. FOUST R, TRAN NN, COX C, MILLER TFJ, GREENSPAN JS, WOLFSON MR, SHAFFER TH. Liquid assisted ventilation: an alternative ventilatory strategy for acute

meconium aspiration injury. *Pediatr Pulmonol* 1996; 21: 316-322.

50. SHELDON G, BRAZY J, TUGGLE B, CRENSHAW CJ, BRUMLEY G. Fetal lamb lung lavage and its effect on lung phosphatidylcholine. *Pediatr Res* 1979; 13: 599-602.
51. BLOCK MF, KALLENBERGER DA, KERN JD, NEPVEUX RD. In utero meconium aspiration by the baboon fetus. *Obstet Gynecol* 1981; 57: 37-40.
52. HANDMAN H, RAIS BK, RIVERA O, SEALE WR, SHORT BL. Use of intratracheal pulmonary ventilation versus conventional ventilation in meconium aspiration syndrome in a newborn pig model [see comments]. *Crit Care Med* 1997; 25: 2025-2030.
53. KÄÄPÄ P, JAHNUKAINEN T, GRÖNLUND J, RAUTANEN M, HALKOLA L, VÄLIMÄKI I. Adenosine triphosphate treatment for meconium aspiration- induced pulmonary hypertension in pigs. *Acta Physiol Scand* 1997; 160: 283-289.
54. LOPEZ A. Respiratory System. In: Carlton W W Meds. Thomson's Special Veterinary Pathology. St. Louis, Missouri: Mosby, 1995: 116-174.
55. DUNGWORTH DL. The Respiratory System. In: Jubb K V F, Kennedy PC, Palmer N, eds. Pathology of Domestic Animals. San Diego, California: Academic Press, 1993: 539-699.
56. GROSS TL, IHRKE PJ, WALDER EJ. Veterinary Dermatopathology: A macroscopic and microscopic evaluation of canine and feline skin disease. Missouri: Mosby-Year Book, Inc., 1992.
57. YAGER JA, WILCOCK BP. Color Atlas and Text of Surgical Pathology of the Dog and Cat: Dermatopathology and Skin Tumors. London: Mosby-Year Book Europe Limited, 1994.
58. CARVAJAL-DE LA FUENTE V, LOPEZ-MAYAGOITIA A, MARTINEZ-BURNES J, BARRON-VARGAS C, LOREDO-OSTI JC. Efecto antiinflamatorio del líquido amniótico en el pulmón de ratas inoculadas intratraquealmente con sílice. *Vet Mex* 1998; 29: 147-153.
59. WAYNFORTH HB. Experimental and Surgical Technique in the Rat. New York: Academic Press, 1980.
60. BAKER DEJ. Reproduction and Breeding. In: Baker H J, Lindsey JR, Weisbroth SH, eds. The Laboratory Rat. Orlando: Academic Press, 1979: 154-166.
61. PARK CM, CLEGG KE, HARVEY CC, HOLLENBERG MJ. Improved techniques

for successful neonatal rat surgery. *Lab Anim Sci* 1992; 42: 508-513.

62. FLECKNELL P. *Laboratory Animal Anaesthesia*. San Diego, CA: Academic Press, 1996.
63. HARKNESS JE, WAGNER JE. *The Biology and Medicine of Rabbits and Rodents*. Philadelphia: Williams & Wilkins, 1995.
64. CANADIAN COUNCIL ON ANIMAL CARE. *Guide to the Care and Use of Experimental Animals*. Ottawa, Ont.: CCAC, 1993.
65. PINKERTON KE, BARRY BE, ONEIL JJ, RAUB JA, PRATT PC, CRAPO JD. Morphologic changes in the lung during the lifespan of Fischer 344 rats. *Am J Anat* 1982; 164: 155-174.
66. BARRY BE, MILLER FJ, CRAPO JD. Effects of inhalation of 0.12 and 0.25 parts per million ozone on the proximal alveolar region of juvenile and adult rats. *Lab Invest* 1985; 53: 692-704.
67. TYLER WS, DUNGWORTH DL, PLOPPER CG, HYDE DM, TYLER NK. Structural evaluation of the respiratory system. *Fundam Appl Toxicol* 1985; 5: 405-422.
68. LUNA L. *Manual of Histologic Staining Methods of the Armed Forces Institute of Pathology*. Toronto, Canada: McGraw-Hill, 1968.
69. BANCROFT JD, COOK HC, STIRLING RW, TURNER DR. *Manual of Histological Techniques and their Diagnostic Application*. Edinburgh: Churchill Livingstone, 1994.
70. FISHER LD, VAN BELLE G. *Biostatistics: A Methodology for The Health Sciences*. New York: Wiley Intersciences, 1993.
71. RANGEL FM, PITTEL D, COSTIGAN M, HWANG T, DAVIS CS, WENZEL RP. The natural history of the systemic inflammatory response syndrome (SIRS). A prospective study. *JAMA* 1995; 273: 117-123.
72. DEMLING RH, LALONDE C, IKEGAMI K. Physiologic support of the septic patient. *Surg Clin North Am* 1994; 74: 637-658.
73. NELSON KM, LONG CL. Physiological basis for nutrition in sepsis. *Nutr Clin Pract* 1989; 4: 6-15.
74. SUNDARESAN R, SHEAGREN JN. Current Understanding and Treatment of Sepsis. *Infect Med* 1995; 12: 261-268.
75. WU JM, YEH TF, WANG JY, WANG JN, LIN YJ, HSIEH WS, LIN CH. The role of

pulmonary inflammation in the development of pulmonary hypertension in newborn with meconium aspiration syndrome (MAS). *Pediatr Pulmonol Suppl* 1999; 18: 205-208.

76. HSIEH TT, HSIEH CC, HUNG TH, CHIANG CH, YANG FP, PAO CC. Differential expression of interleukin-1 beta and interleukin-6 in human fetal serum and meconium-stained amniotic fluid. *J Reprod Immunol* 1998; 37: 155-161.
77. WENDERLEIN JM. [Evolution promotes a minimal effect of fetal labor stress during birth]. *Z Geburtshilfe Neonatol* 1997; 201: 82-85.
78. BESSER TE, SZENCI O, GAY CC. Decreased colostral immunoglobulin absorption in calves with postnatal respiratory acidosis. *J Am Vet Med Assoc* 1990; 196: 1239-1243.
79. BOYD JW. Relationships between acid-base balance, serum composition and colostrum absorption in newborn calves. *Br Vet J* 1989; 145: 249-256.
80. LOGAN EF, SMYTH JA, KENNEDY DG, RICE DA, ELLIS WA. Stillbirth and perinatal weak calf syndrome [see comments]. *Vet Rec* 1991; 129: 99-
81. MELLOR DJ. Integration of perinatal events, pathophysiological changes and consequences for the newborn lamb. *Br Vet J* 1988; 144: 552-569.
82. KAUP FJ. The normal structure of the intestinal barrier of the new born calf and its alterations under the influence of hypoxia 1991; Aus Dem Institut für Pathologie Der Tierärztlichen Hochschule Hannover; 12 p.
83. TUETING JL, BYERLEY LO, CHWALS WJ. Anabolic recovery relative to degree of prematurity after acute injury in neonates. *J Pediatr Surg* 1999; 34: 13-16.
84. SAMUELS SE, BARACOS VE. Tissue protein turnover is altered during catch-up growth following *Escherichia coli* infection in weanling rats. *J Nutr* 1995; 125: 520-530.
85. USTA IM, MERCER BM, SIBAI BM. Risk factors for meconium aspiration syndrome. *Obstet Gynecol* 1995; 86: 230-234.
86. HERNÁNDEZ C, LITTLE BB, DAX JS, GILSTRAP LC, ROSENFIELD CR. Prediction of the severity of meconium aspiration syndrome. *Am J Obstet Gynecol* 1993; 169: 61-70.
87. MILLER RB. A summary of some of the pathogenetic mechanisms involved in bovine abortion. *Can Vet J* 1977; 18: 87-95.

88. DASARI G, PRINCE I, HEARN MT. Investigations into the rheological characteristics of bovine amniotic fluid. *J Biochem Biophys Methods* 1995; 30: 217-225.
89. BOUHAFS RK, JARSTRAND C. Phagocyte-induced lipid peroxidation of lung surfactant. *Pediatr Pulmonol* 1999; 27: 322-327.
90. ROBINSON NE. Overview of Respiratory Function: Ventilation of The lung. In: Cunningham J Geds. *Textbook of Veterinary Physiology*. Philadelphia: W.B. Saunders Company, 1992: 533-546.
91. POLGAR G, WENG TR. The functional development of the respiratory system from the period of gestation to adulthood. *Am Rev Respir Dis* 1979; 120: 625-695.
92. VEIT HP, FARRELL RL. The anatomy and physiology of the bovine respiratory system relating to pulmonary disease. *Cornell Vet* 1978; 68: 555-581.
93. VIDYASAGAR D, HARRIS V, PILDES RS. Assisted ventilation in infants with meconium aspiration syndrome. *Pediatrics* 1975; 56: 208-213.
94. YOUSSEF FW, ESQUINAS RG. The middle lobe syndrome in pediatrics. A study of 27 cases. *An Esp Pediatr* 1998; 49: 582-586.
95. VEIT HP, FARRELL RL, TROUTT HF. Pulmonary clearance of *Serratia marcescens* in calves. *Am J Vet Res* 1978; 39: 1646-1650.
96. TRAN N, LOWE C, SIVIERI EM, SHAFFER TH. Sequential effects of acute meconium obstruction on pulmonary function. *Pediatr Res* 1980; 14: 34-38.
97. GOODING CA, GREGORY GA. Roentgenographic analysis of meconium aspiration of the newborn. *Radiology* 1971; 100: 131-140.
98. KEARNEY MS. Chronic intrauterine meconium aspiration causes fetal lung infarcts, lung rupture, and meconium embolism. *Pediatr Dev Pathol* 1999; 2: 544-551.
99. PINKERTON KE, CRAPO JD. Morphometry of the Alveolar Region of the Lung. In: Witschi M D, Brain JD, eds. *Toxicology of Inhaled Materials*. New York: Springer-Verlag, 1985: 259-285.
100. RAPOPORT S, BUCHANAN DJ. The composition of meconium: Isolation of blood-group-specific polysaccharides. Abnormal composition of meconium in meconium ileus. *Science* 1950; 112: 150-153.
101. SERGI C, STEIN KM, BEEDGEN B, ZILOW E, LINDERKAMP O, OTTO HF. Meconium aspiration syndrome complicated by massive intravascular thrombosis. *Am*

102. RUBIN BK, TOMKIEWICZ RP, PATRINOS ME, EASAD. The surface and transport properties of meconium and reconstituted meconium solutions. *Pediatr Res* 1996; 40: 834-838.
103. HOUNSELL EF, LAWSON AM, STOLL MS, KANE DP, CASHMORE GC, CARRUTHERS RA, FEENEY J, FEIZI T. Characterisation by mass spectrometry and 500-MHz proton nuclear magnetic resonance spectroscopy of penta- and hexasaccharide chains of human foetal gastrointestinal mucins (meconium glycoproteins). *Eur J Biochem* 1989; 186: 597-610.
104. COHEN AB, BATRA GK. Bronchoscopy and lung lavage induced bilateral pulmonary neutrophil influx and blood leukocytosis in dogs and monkeys. *Am Rev Respir Dis* 1980; 122: 239-247.
105. DAMIANO VV, COHEN A, TSANG AL, BATRA G, PETERSEN R. A morphologic study of the influx of neutrophils into dog lung alveoli after lavage with sterile saline. *Am J Pathol* 1980; 100: 349-364.
106. MUGGENBURG BA, MAUDERLY JL, PICKRELL JA, CHIFFELLE TL, JONES RK, LUFT UC, MCCLELLAN RO, PFLEGER RC. Pathophysiologic sequelae of bronchopulmonary lavage in the dog. *Am Rev Respir Dis* 1972; 106: 219-232.
107. TOEWS GB. Pulmonary defense mechanisms. *Semin Respir Infect* 1993; 8: 160-167.
108. BRY K, TERAMO K, LAPPALAINEN U, WAFFARN F, HALLMAN M. Interleukin-1 receptor antagonist in the fetomaternal compartment. *Acta Paediatr* 1995; 84: 233-236.
109. GREIG PC, HERBERT WN, ROBINETTE BL, TEOT LA. Amniotic fluid interleukin-10 concentrations increase through pregnancy and are elevated in patients with preterm labor associated with intrauterine infection. *Am J Obstet Gynecol* 1995; 173: 1223-1227.
110. DAVIS JR, MILLER HS, FENG JD. Vernix caseosa peritonitis: report of two cases with antenatal onset. *Am J Clin Pathol* 1998; 109: 320-323.
111. MAUS U, ROSSEAU S, KNIES U, SEEGER W, LOHMEYER J. Expression of pro-inflammatory cytokines by flow-sorted alveolar macrophages in severe pneumonia. *Eur Respir J* 1998; 11: 534-541.
112. SIMEONOVA PP, LEONARD S, FLOOD L, SHI X, LUSTER MI. Redox-dependent regulation of interleukin-8 by tumor necrosis factor-alpha in lung epithelial cells. *Lab*

Invest 1999; 79: 1027-1037.

113. KOJIMA T, HATTORI K, FUJIWARA T, SASAI TM, KOBAYASHI Y. Meconium-induced lung injury mediated by activation of alveolar macrophages. *Life Sci* 1994; 54: 1559-1562.
114. DE BEAUFORT AJ, PELIKAN DM, ELFERINK JG, BERGER HM. Effect of interleukin 8 in meconium on in-vitro neutrophil chemotaxis. *Lancet* 1998; 352: 102-105.
115. HEYDENRYCH JJ, MARCUS PB. Meconium granulomas of the tunica vaginalis. *J Urol* 1976; 115: 596-598.
116. HERZ MG, STANLEY WD, TOOT PJ, FREEDMAN SI, ANG EP. Symptomatic maternal intraperitoneal meconium granulomata: report of two cases. *Diagn Gynecol Obstet* 1982; 4: 147-149.
117. FREEDMAN SI, ANG EP, HERZ MG, STANLEY WD, TOOT PJ. Meconium granulomas in post Cesarean section patients. *Obstet Gynecol* 1982; 59: 383-385.
118. FREEDMAN SI, ANG EP, TOOT PJ. Meconium granulomas or vernix-induced peritonitis [letter]. *JAMA* 1986; 255: 906-
119. OOI K, RILEY C, BILLSON V, OSTÖR AG. Ceroid granulomas in the female genital system. *J Clin Pathol* 1995; 48: 1057-1059.
120. KHAN AM, SHABAREK FM, KUTCHBACK JW, LALLY KP. Effects of dexamethasone on meconium aspiration syndrome in newborn piglets. *Pediatr Res* 1999; 46: 179-183.
121. BOORMAN GA, EUSTIS SL. Lung. In: Boorman G A, Eustis SL, Elwell MR, Montgomery CA, MacKenzie WF, eds. *Pathology of the Fischer Rat: Reference and Atlas*. California: Academic Press, 1990: 339-367.
122. MITCHELL RN, COTRAN RS. Cellular Pathology II: Adaptations, Intracellular Accumulations, and Cell Aging. In: Cotran R S, Kumar V, Collins T, eds. *Robbins Pathologic Basis of Disease*. Philadelphia: W.B. Saunders Company, 1999: 31-49.
123. FOROUHAR F. Origin of calcification in healed meconium peritonitis. *Med Hypotheses* 1984; 14: 51-56.
124. RUMLOVA E, KWASNY R. Scrotal enlargement following healed meconium peritonitis. *Z Kinderchir* 1988; 43: 216-217.
125. BENIRSCHKE K, PEKARSKE SL. *Placental pathology casebook*. Extensive

calcification of the umbilical cord and placenta. *J Perinatol* 1995; 15: 81-83.

126. DIRKES K, CROMBLEHOLME TM, CRAIGO SD, LATCHAW LA, JACIR NN, HARRIS BH, DALTON ME. The natural history of meconium peritonitis diagnosed in utero. *J Pediatr Surg* 1995; 30: 979-982.
127. SHENKAR R, ABRAHAM E. Mechanisms of lung neutrophil activation after hemorrhage or endotoxemia: roles of reactive oxygen intermediates, NF-kappa B, and cyclic AMP response element binding protein. *J Immunol* 1999; 163: 954-962.
128. BURRI PH. Morphology and respiratory function of the alveolar unit. *Int Arch Allergy Appl Immunol* 1985; 76 Suppl 1: 2-12.
129. PUGIN J, VERGHESE G, WIDMER MC, MATTHAY MA. The alveolar space is the site of intense inflammatory and profibrotic reactions in the early phase of acute respiratory distress syndrome [see comments]. *Crit Care Med* 1999; 27: 304-312.
130. MATTHAY MA, FOLKESSON HG, CAMPAGNA A, KHERADMAND F. Alveolar epithelial barrier and acute lung injury. *New Horiz* 1993; 1: 613-622.
131. DOWNEY GP, GRANTON JT. Mechanisms of acute lung injury. *Curr Opin Pulm Med* 1997; 3: 234-241.
132. SIBILLE Y, REYNOLDS HY. Macrophages and polymorphonuclear neutrophils in lung defense and injury. *Am Rev Respir Dis* 1990; 141: 471-501.
133. FULKERSON WJ, MACINTYRE N, STAMLER J, CRAPO JD. Pathogenesis and treatment of the adult respiratory distress syndrome. *Arch Intern Med* 1996; 156: 29-38.
134. COLTART TM, BYRNE DL, BATES SA. Meconium aspiration syndrome: a 6-year retrospective study. *Br J Obstet Gynaecol* 1989; 96: 411-414.

5. MORPHOMETRIC CHANGES INDUCED BY THE INTRATRACHEAL INOCULATION OF MECONIUM IN THE LUNG OF NEONATAL RATS

5.1. Introduction

It is essential in experimental pathology to quantify accurately the magnitude of morphologic changes in order to do meaningful statistical comparisons between treated and untreated groups. For this purpose, morphometry and stereology have been widely used in the last few decades to quantify the effect of toxic substances in laboratory animals and human beings (1-3).

Before addressing the relevance of morphometry in lung pathology, it is important to review briefly the origin and applications of these methods in biomedical sciences. Stereology is defined as a body of mathematical methods relating three-dimensional parameters defining the structure to two-dimensional measurements obtainable on sections of the structure (4). Morphometry applies the principles of a group of geometric and stereological formulas and statistical methods to solve problems in microscopic anatomy. In stereology and its applied branch, morphometry, measurements obtained from two-dimensional sections like microscopic slides are used to generate valuable information about those same objects in three dimensions (2). The rudiments of stereology and hence morphometry were developed by the French geologist Delesse in 1848, when he proved that the volume of elements contained in rock deposits was directly related to the profile areas of these elements on rock shears (4). This principle had been in use as a tool of geologists since 1916. Later, Chalkey in 1943 demonstrated that point-counting methods could be

applied to biological systems on histological sections (5). The basic principle of morphometry in biomedical sciences is to apply mathematical and statistical formulas to quantify or measure “objects” such as cells or organelles (4,6).

The application of morphometric methods has many advantages in experimental research. First, morphometry allows for an objective evaluation without bias that may be introduced by the observer. It has great sensitivity in identifying subtle changes which otherwise could be missed by routine gross or microscopic examination. Morphometric studies also eliminate the subjective bias of some grading techniques that are routinely used in diagnostic pathology (6). For instance, the subjectiveness of descriptive qualifiers such as “mild”, “moderate” and “severe” have limited value in experimental research due to inter- and intra-observer variations. In other words, what appears to be “mild” for one observer could be “moderate” or “severe” to another. It has also been demonstrated that subjective grading has poor repeatability (7,8). In contrast, morphometry yields numerical values that, expressed as continuous variables, can be analysed with rigorous statistical methods (9). In summary, morphometry and point count stereology are powerful tools that allow for unbiased and methodical quantification of structural changes in spontaneous and experimental diseases. Morphometric methods can be applied to any organ, tissue, cellular structure or organelle in the body (4,9).

Concerning the lung, morphometry has been indispensable in evaluating the noxious effects caused by inhalation of gases, particles, vapours and other toxic substances (2,3,10). Although there are several methods described in the literature for lung morphometry, those proposed by the group of Dr. Weibel in Switzerland in 1963 and the group of Dr. Crapo in

North Carolina have become the “golden standards” or “preferred choices” (2,4). These methods have been adapted or modified by other researchers to address specific questions in experimental lung research. For instances, Bo Sun *et al.* adapted the traditional morphometric methods to quantify the degree of atelectasis in animals treated with pulmonary surfactant (11,12).

Since sampling bias is one of the most common sources of error in experimental pathology, it is crucial to recognise the complexity of the lung structure. Composed of many branching compartments or strata, namely bronchi, bronchioles, alveoli, interstitium, blood and lymphatic vessels, the lung is a difficult organ to sample for morphometric determinations (6). To overcome this problem, a systematic tiered or multiple stage lung sampling method was established by some investigators. The first step in this tiered sampling approach, is to stabilize the pulmonary tissue by intratracheal perfusion of fixative before samples are taken. To ensure lung integrity and homogeneity, fixation is done *in situ*, under constant pressure and regulated flow rate, and the volume of fixative entering the bronchoalveolar spaces is carefully controlled. Once the pulmonary tissue has been stabilized by fixation, the volume of the lung is calculated by gravimetric or volumetric methods to be used later as reference value in most morphometric formulas (6,13).

For the purposes of morphometry and light microscopy, the pulmonary tissue is divided into two distinct compartments referred to as parenchymal and nonparenchymal. The parenchymal compartment includes the alveolar septa, and alveolar air spaces, while the nonparenchymal fractions are comprised of the bronchiolar and bronchial tissues and their airspaces, pulmonary interstitium, blood and lymphatic vessels. Once these two main

fractions or their subdivisions have been calculated, the specific cells comprising each of the pulmonary compartments are further identified and quantified by electron microscopy (2,6). Numerical data obtained by this tiered-based approach is subsequently analysed with standard mathematical formulas for each fraction of the lung (Table XVIII). For instance, changes in the numerical values applied to the alveolar compartments accurately reflect changes in alveoli as in cases of alveolar thickening, alveolar hyperplasia, fibrosis, emphysema, atelectasis, etc. (2,6).

The most common morphometric values in a tiered-sampling system in the lung are volume fractions, absolute volumes, surface density and arithmetic mean thickness of alveolar walls (Table XVIII). Volume fractions of the compartments of the lung define the fractional volume of the region of interest with respect to the volume of reference space (ie., fraction of parenchyma per total lung or parenchymal fractional volume of alveoli). The product of the total lung volume times the fraction that makes up the region of interest yields the absolute volume of that specific “region” per whole lung. The volume densities of a particular tissue (epithelium, endothelium) are obtained using point counting methods, and are the number of points falling upon each individual tissue compartment divided by the total number of test points using high magnification at light microscopic level or electron microscopy. Absolute volumes per both lungs also can be obtained by multiplying the volume density of a particular compartment (ie., cells) times the parenchymal fraction and the total fixed lung volume. The surface density of the alveolar epithelium and capillary endothelium can be determined by counting the number of times test lines intercept the

Table XVIII. Formulas used in the morphometric study. (Modified from Pinkerton, KE and Crapo, JD. Morphometry of the alveolar region of the lung. In Toxicology of Inhaled Materials. Handbook of Experimental Pharmacology, edited by Witshi, HP and Brain, JD, Springer-Verlag, NY,260-261,1985).

| | | |
|----------------------------------|--|-----|
| Volume fraction of compartments | $V_v = P_i/P_t$ | (1) |
| Absolute Volumes | $Abs_v = (V_v) * (\text{Fixed lung Vol})$ | (2) |
| Volume density of alveolar septa | $V_{vap} = P_i/P_t$ | (3) |
| Specific Surface Density | $S_{vs} = (2I/Lo)^*(Vo/Vref)$ | (4) |
| Arithmetic mean thickness: | | |
| Alveolar septa "Classical" | $\tau_t = \frac{Z \times P_i}{2 \times (I_a)}$ | (5) |
| Modified | $\tau_t = (Vo/Vref)/(1/(2S_{vs}))$ | (6) |

V_v = Volume fraction of compartments

P_i = number of points on tissue being studied, P_t = total points

I_a = number of intersections per test line length

Z = length of test line

P_i = number of points falling on tissue

I_a = number of line intersections with the alveolar surface

Lo = Total length of the lines falling on alveolar septa

Vo = Volume of object (alveolar septa)

$Vref$ = Volume of reference space (Lung)

S_{vs} = "Specific Surface Density"

Abs_v = Absolute volume

V_{vap} = Volume density of alveolar septa regarding parenchyma

airspace-epithelial surface and the plasma-endothelial cell surface. The arithmetic mean thickness of the alveolar septa or of the air-blood barrier corresponds to the ratio of the volume density to surface density (2,4,14).

It is axiomatic that morphometric values vary considerably as a result of anatomic differences that exist between animal species (15,16). These anatomic differences and other variables such as age are important biological variations that need to be carefully considered in inhalation studies.

According to information available in the literature, rats are the preferred animal species for morphometric studies and experimental lung research (6,17,18). The reason for this is not only reasonable price, availability from commercial sources, genetic homogeneity, and easy husbandry, but because the rat lungs are particularly suitable for morphometric techniques (6). Records also show that the Fischer 344 rat has important advantages over other strains for inhalation studies and particularly lung morphometry because of a stable lung structure. Fischer 344 rats have a slow and a predictable growth rate, and never reach large body size as is the case with other laboratory strains like Wistar, Long Evans and Sprague-Dawley. In addition, there are reports suggesting that the Fischer 344 rat has a comparatively lower prevalence of spontaneous pulmonary diseases (17). Because of this strain's suitability for inhalation studies, the morphometric lung values of the Fischer 344 have been established for its entire life span. Results from these investigations showed that the biological variations in lung morphometry are relatively small in Fischer 344 rats and 4 to 8 rats per treatment group are usually adequate to detect meaningful differences between experimental treatments (17,19).

Aspiration of meconium in the neonate induces airway obstruction, pulmonary inflammation, chemical pneumonitis, atelectasis and hyperinflation (12,20,21). Although these pulmonary changes are typically observed in natural and experimental cases of Meconium aspiration syndrome (MAS), there is a paucity of information regarding the magnitude of pulmonary lesions induced by the aspiration of meconium (22-24). In one study of experimental MAS in adult rabbits, the composite histologic score was calculated to assess the presence of leukocytes, alveolar macrophages and focal atelectasis in the lungs to determine the efficacy of glucocorticoid in the treatment of MAS. Results from this investigation showed a significant difference between animals inoculated with meconium and controls receiving saline. The meconium group had higher average leukocyte numbers and atelectasis than control. However, treatment with cortisol failed to decrease the average of inflammatory response and atelectasis (25). Another study in piglets inoculated with meconium described a histologic scoring system to characterize the severity of lesions associated with meconium. The presence of atelectasis, exudative debris, meconium, and alveolar inflammation was evaluated and associated with the usefulness of three methods of high-frequency ventilation (26). However, none of these studies determined the effect of meconium on the alveolar wall.

Using experimental models of MAS in newborn rabbits, Bo Sun (12,27) evaluated the volume fractions of alveolar spaces, edema and inflammatory changes by means of point count stereology. Results of these investigations revealed that experimental MAS caused a reduction of volume fraction of alveolar space due to atelectasis and also increased field-to-field variability of alveolar expansion. Aspiration of meconium also caused a statistically

significant reduction in lung-thorax compliance. The effect of surfactant replacement in improving pulmonary gas exchange, compliance, alveolar expansion and lung morphology was evaluated in these studies (12,27). In other studies, the same group (11,28) found that the lungs of rats with experimental MAS had diffuse and prominent atelectasis, intra-alveolar edema, and hyaline membranes. Significant reduction in volume fraction of airspaces due to atelectasis was found using point counting methods. These morphological abnormalities were reversed by treatment with exogenous surfactant (11,28).

Several studies of spontaneous and experimental MAS have suggested that the alveolar wall may thicken due to the chemical effects of meconium in the lungs. A retrospective study in neonatal calves revealed a constant alveolitis associated with aspiration of meconium (29). Although the inflammatory response in these calves was mild, it was unclear whether aspiration of meconium was causing thickening of the alveolar walls as this change is difficult to judge in routine histopathology (30,31). Similarly, other investigators suggested but were unable to substantiate the thickening of the alveolar walls in rabbits experimentally inoculated with meconium (21).

Since there is little information regarding lung morphometry in neonatal MAS under laboratory conditions, the general objective of this study was to determine the magnitude and distribution of lung changes in rat pups intratracheally inoculated with meconium. The specific objectives were to study the distribution of the lesions within the different compartments of the lungs and quantify the average thickness of the alveolar septa by morphometric methods.

5.2. Material and Methods

5.2.1. Animals:

Fischer-344 pregnant rats were obtained from commercial sources (Charles River, Québec) 14 -16 days before parturition as original breeding stock at AVC. Once rat pups were born, female and some male neonates were selected to be part of a time-pregnancy program following the reproductive protocols published by others (32,33) and described in detail in section 2.2.1. Rats were housed individually, provided with commercial rat food and water *ad libitum*, and maintained on a 12/12-hour light/dark cycle at 22° C and 50% relative humidity. To reduce infant rejection and cannibalism, dams were preconditioned following the protocol described in section 2.2.2. (34). Pups used in this morphometric study were 7-day-old males weighing an average of 15.6 \pm 1.1 g.

5.2.2. Anesthesia.

Neonates were anesthetized with halothane (3% in 100% oxygen; 100-200 ml/min) via a gas anesthetic machine as described in Section 2.2.4. Pups were randomly selected and removed from the dam one at a time.

5.2.3. Inoculum

The method for the collection and preservation of meconium is described in detail in Section 2.2.6. In short, newborn rat pups were humanely euthanised immediately after birth and before the intake of colostrum. Meconium aseptically collected from the intestine was placed in sterile plastic vials and frozen at -80° C. The stock inoculum was prepared by mixing unfiltered frozen meconium with 0.9% NaCl solution to a final concentration of 15% wet weight.

5.2.4. Intratracheal inoculation of meconium (ITI).

The detailed method for the intratracheal inoculation of meconium is provided in Section 2.2.8. In summary, the laryngeal opening in neonatal rats was visualized with an otoscope (Welch Allyn, Skaneateles Falls, NY) under deep halothane anesthesia (33,35). A sterile spinal needle (25 gauge, 0.51 mm x 8.89 cm length, Becton Dickinson and Company, Franklin Lakes, NJ) was inserted into the larynx and 0.05 ml of the inoculum was slowly instilled into the lungs. Pups were kept under direct observation after inoculation on a heating pad (38 °C) and fully recovered pups were put back in their cage with the dam.

5.2.5. Euthanasia.

Rats were weighted and euthanised by severing the renal arteries under deep halothane anesthesia (36). The experiments followed the guidelines of the Canadian Council on Animal Care (37).

5.2.6. Experimental design

Twenty-four male, 7-day-old neonates were randomly assigned to two experimental groups (Control and Meconium). Four rats of each group were killed at 1, 3, and 7 days postinoculation (PID 1,3 and 7) (Table XIX).

Table XIX. Experimental design. Number of neonatal rats per treatment and days postinoculation.

| Treatment | Post-inoculation (Days) | | | Total |
|---------------------------|-------------------------|---|---|-------|
| | 1 | 3 | 7 | |
| Control (Saline solution) | 4 | 4 | 4 | 12 |
| Meconium (15%) | 4 | 4 | 4 | 12 |
| Total | 8 | 8 | 8 | 24 |

5.2.7. Lung sampling

Samples of the lung were obtained using the tiered random sampling method proposed by others (6) with some modifications (Fig. 40). The fixed lungs were dissected and the different lobes were separated before samples of each lobe were taken. The model was modified because identification of parenchyma and nonparenchyma in neonatal lungs is only possible using a dissecting microscope or low magnification light microscopy. Low magnification light microscopy was used to characterize parenchyma and nonparenchyma. The tiered or stratified sampling method permits light and/or electron microscopy to be focussed on specific strata of interest.

5.2.8. Lung processing

5.2.8.1. In situ perfusion of lung for light microscopy

After euthanasia, the lungs of the neonatal rats were perfused *in situ* with fixative using the procedure described in detail in Section 4.2.6. Briefly, the trachea was exposed and a catheter (20gauge, 32mm length, Cathlon IV, Critikon Canada Inc., Ontario) was inserted through a transverse tracheal incision. Glutaraldehyde (2%; buffered to pH 7.4 using 0.1 Molar sodium cacodylate, at a total osmolality of 350mosmol) was instilled intratracheally at a constant pressure of 20 cm of fixative for a minimum of 30 minutes (13).

5.2.8.2. Lung volume

Following fixation *in situ*, the lungs were removed from the thoracic cavity and stored in fixative for at least 2 hours before further manipulation. The heart, major blood vessels, esophagus, thymus and lymph nodes were carefully dissected from the lungs. The proximal (cranial) portion of the trachea was separated leaving only a small portion of the

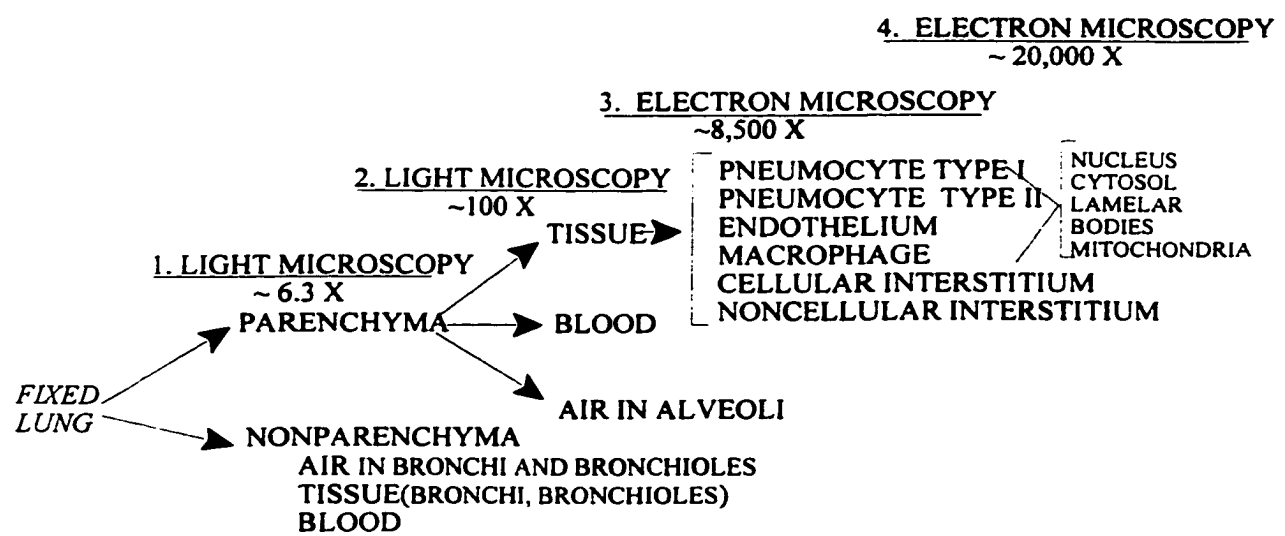


Fig. 40. Flow diagram of the tiered or multiple stage sampling procedure for morphometric analysis of lung tissue. The approximate degree of magnification for sampling is given for each level . Modified from Pinkerton, KE and Crapo, JD. Morphometry of the alveolar region of the lung. In Toxicology of Inhaled Materials. Handbook of Experimental Pharmacology, edited by Witshi, HP and Brain, JD, Springer-Verlag, NY,260-261, 1985.

lower trachea attached to the lung.

Total lung volume was determined by the gravimetric method based on volume of fluid displaced by the immersed lung (4,6). The rationale of this method is as follows: Since specific gravity of isotonic saline solution is approximately 1.0, the volume of the fixed lungs equals the volume of saline displaced by the immersed lungs. This displacement of saline is reflected as a change in the weight of the total system. The lung volumes were calculated as follows: 1- Using a digital balance (XE-510, Denver Instruments, USA), tare weight was determined with a clamp immersed in the saline solution to the same level to be used in immersing the lung. 2- The lungs were clamped at the lower trachea and then completely suspended in the saline solution without touching the sides or bottom of the container (Fig. 41). 3- The difference in the tare weight and final weight was considered equal to the volume of the lungs assuming that the specific gravity of the fluid is 1.0. The volume of the lung was expressed in cm^3 .

5.2.8.3. *Light microscopy*

A representative longitudinal slice of each animal's entire left lung (2 mm thickness) and four transverse sections (2 mm thickness) along the major axes of the lobes of the right lung were trimmed and embedded in paraffin (38). Sections 3 μm -thick were stained with hematoxylin and eosin and periodic acid Schiff (PAS). The longitudinal section of the left lung allows one to evaluate, in a first step, qualitative changes occurring in bronchi, bronchioles, alveolar ducts and alveolar walls. This first step in the tiered sample method was helpful to evaluate the effect of meconium at different strata of the lung.

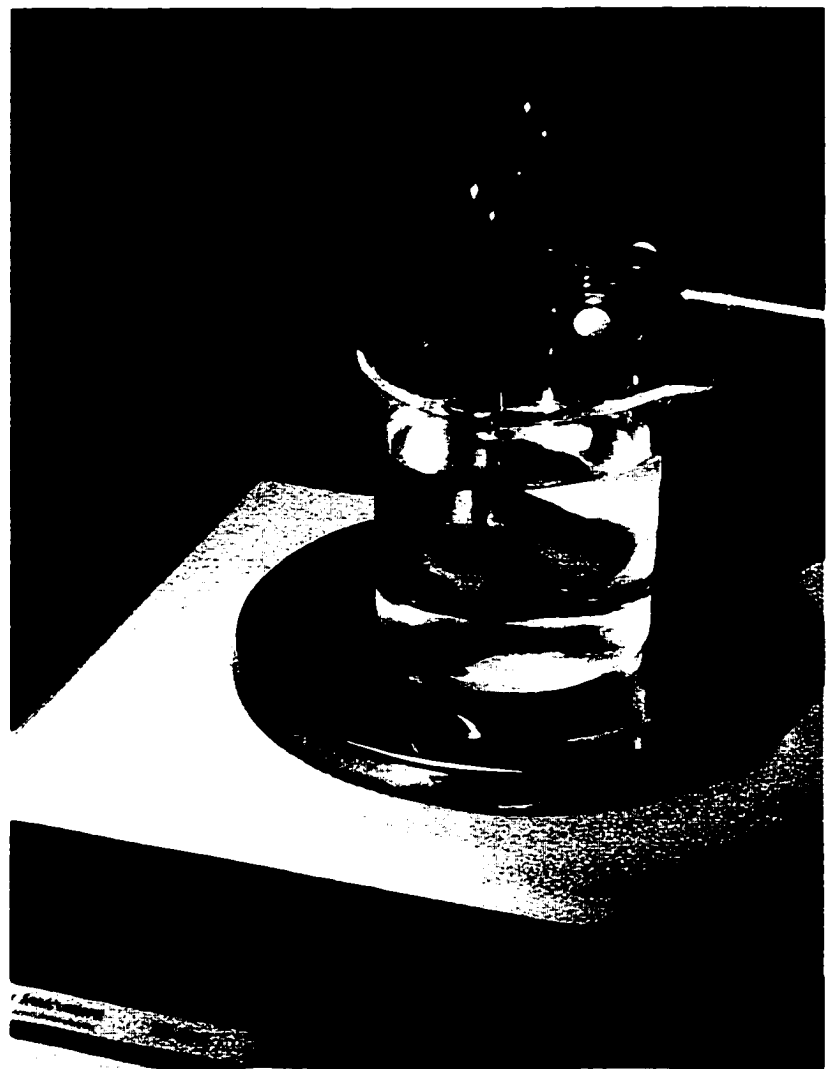


Fig. 41. Gravimetric method used for determination of the fixed lung volume by the weight of displaced fluid. The fixed lungs were clamped at the lower trachea and were completely suspended in the saline solution without touching the sides or bottom of the container.

5.2.9. Morphometry

5.2.9.1. Pilot Study

5.2.9.1.1. *Morphometric procedures*

5.2.9.1.1.1. *Alveolar fraction of the lung (Volume fraction of the alveolar region).*

The apical and middle lobes of the right lung and the left lung of rats inoculated with meconium and euthanised at PID 1 were used to determine the alveolar fraction by the point counting method (6). The objective of this first pilot study was to evaluate the different compartments of the lung in three lobes at PID 1 and select, based on homogeneity and distribution of changes, one lobe for subsequent morphometric studies.

5.2.9.1.1.2. *Random selection of lung fields.*

Lung fields were selected using a systematic sampling method with a random starting point (9,39). Using light microscopy at a magnification of 6.3 X, the total length of the major axis of each lung lobe section was measured in millimetres using a scale on the microscope stage. To obtain the distance between fields, the total length of the lung lobe was divided by the number of fields to be used for morphometric determinations. A random number was chosen between 0 and 1 and this number was multiplied by the distance between fields. The resulting value was located in the section using the scale on the stage and it represented the first field to be counted. The second field was chosen adding the distance between fields and so on. A total of five different fields was selected from each lobe by this sampling procedure. Images for every field were captured using a Pixera Camera that was attached to a Zeiss light photo microscope (Carl Zeiss, Canada Ltd., Don Mills, Ontario). The images were finally digitized into a 1690 X 890 pixel RGB digital image using Photo

Studio from Pixera and saved as Tagged Image Format Files (TIFF) (Pixera Visual Communication, Suite Model PVC100C, Pixera Corporation, Los Gatos, CA).

5.2.9.1.1.3. Volume fractions of the compartments of the lung (V_v)

The digitized lung images were exported to Scion Image (Beta 3 Release, Scion Corporation, NIH-Image software), analysed at a final magnification of 6,200 times, and projected in the computer screen containing a multipurpose test grid with 84 lines and 168 test points (4). The ends of each line constituted a point (Fig. 42). Volume fractions of the structures of interest were analysed using point counting performed with the computer program of public domain <<http://rsb.info.nih.gov/nih-image/>> developed by the National Institute of Health (NIH) and modified for Windows by Scion Corporation (Maryland).

The fraction of the lung comprised by the region of interest (alveolar walls, alveolar airspaces, bronchi and bronchioles, air from bronchi and bronchioles and blood vessels) was the number of points falling on the region of interest divided by the total number of points falling on the lung section (6) (Equation 1, Table XVIII).

For the purpose of this study, the determination of alveolar (parenchymal) and nonalveolar (nonparenchymal) tissue fractions was based on the criterion that nonalveolar structures consist of interlobular connective tissue, bronchi and bronchioles, and blood vessels with a diameter greater than 25 μm . Alveolar (parenchymal) fraction included the alveolar septa and the alveolar airspaces. Structures to be counted were divided into five different categories: 1- alveolar walls; 2- alveolar air spaces; 3- blood vessels larger than 25 μm in diameter; 4- bronchi and bronchioles; and 5- bronchiolar air spaces. The volume fractions of the following compartments were determined: lung parenchyma consisting of

alveolar walls plus alveolar air spaces, and nonparenchyma comprising the airways down to the respiratory bronchioles, the blood vessels greater than 25 μm and the interlobular connective tissue.

5.2.9.1.1.4. Absolute volume of the compartments (Absv)

The absolute volumes of the different compartments of both lungs were obtained by multiplying each individual tissue compartment fraction by the total fixed lung volume (Equation 2, Table XVIII).

5.2.9.1.1.5. Volume density, surface density and arithmetic mean thickness.

Ten different fields per lobe were selected as the second level of the cascade using the same systematic sampling with a random starting point described in the previous section (9,39). Using a Zeiss microscope at high magnification (100X), images were captured and digitized with the Pixera system as previously described. Images were then exported and projected in a PC high resolution monitor at a final magnification of 10,000 times (Fig. 43). A multipurpose test lattice overlay with 84 lines each measuring 1.7 cm in length was placed over the monitor screen (4). When the morphometry was performed, the identity of the lung sample was unknown to the observer.

5.2.9.1.1.5.1. Volume density (Vvap)

The *volume density* of the alveolar septal portion of the parenchyma was determined by using the ends of each lattice line as points in the systematically sampled fields. The *volume density* of the alveolar septa was calculated by dividing the number of points falling on the alveolar septa by the total number of test points in the grid (168 points). In this study the reference volume of the structure of interest was considered as the total alveolar septa

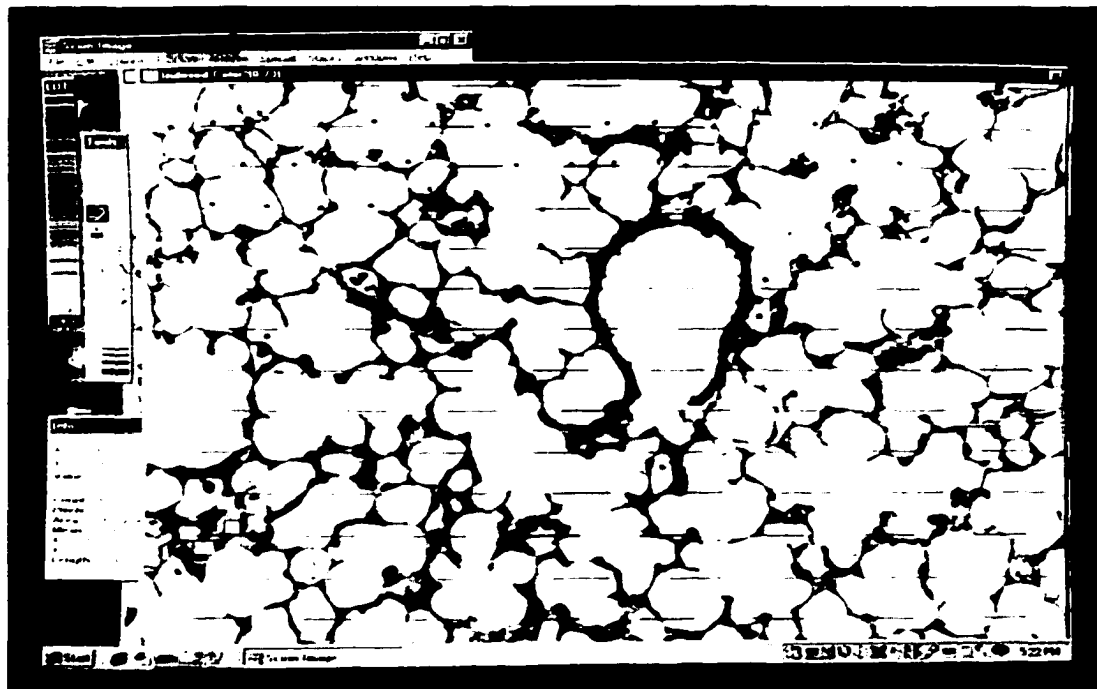


Fig. 42. Computer screen containing a test grid with 84 lines and 168 test points used to determine the volume fractions of the compartments of the lung by point counting.

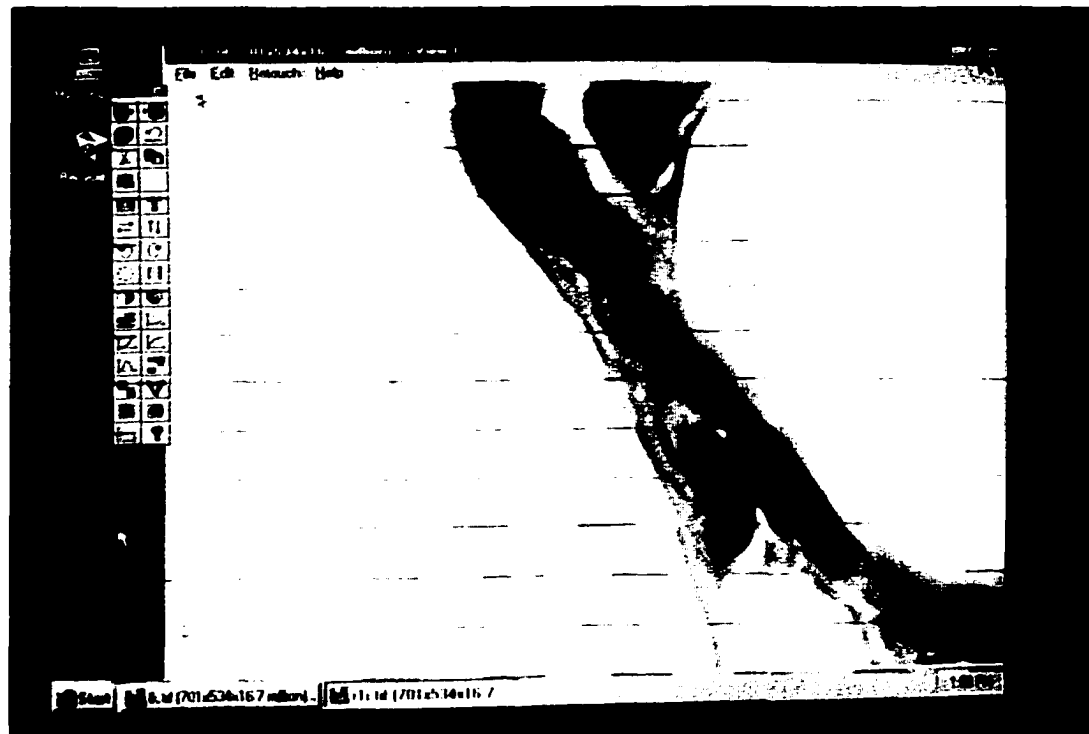


Fig. 43. Computer monitor containing a test grid to determine the volume density and surface density of the alveolar septum using point counting and line intersections.

without subdividing it into the different cellular compartments (Equation 3, Table XVIII).

5.2.9.1.1.5.2. *Surface density (S_{vs})*

The *surface density* of the alveolar septa was determined by counting the number of times the test line intercepted the airspace-epithelial surface. Since the test line is of known length (1.7 cm), the equation 4 in Table XVIII was used to determine the surface density of the alveolar septa. A modification of the classical formula was also applied to calculate the surface density of the alveolar septa. In this classical formula ($S_v = 2I_L$), the surface density is equal to twice the number of intercepts with the surface of interest divided by the total length of all the test line segments. This formula, used mainly in EM, assumes a random and systematic sampling of fields including the fields in which empty airspaces are found. In the present study, in spite of the systematic sampling of fields used, only fields containing alveolar septa were used for the counting. The specific surface density of the object (alveolar septa) in relation to the volume of the same object (alveolar septa) was obtained with the following modified formula, which can be derived from the classical formula (Equation 4, Table XVIII):

$$S_{vs} = (2I_o/L_o) * (V_o/V_{ref})$$

in which

I_o = Number of line intersections with the alveolar surface

L_o = Total length of the lines falling on alveolar septa

(V_o/V_{ref}) = Volume fraction of the alveolar septa on reference space (total lung), from point counting reported previously.

5.2.9.1.1.5.3. Arithmetic mean tissue thickness measurements (τ_t)

The arithmetic mean thickness of tissue (AMT) in the alveolar septa τ_t was calculated as the volume to surface ratio of alveolar tissue. The arithmetic mean tissue thickness may be determined separately for the epithelium, interstitium, and endothelium. In this study, the arithmetic mean thickness of the entire alveolar septa regardless of the different cellular compartments, was obtained. Table XVIII shows the classical formula (Equation 5) and the formula used to determine arithmetic mean thickness of the alveolar septa in this study (Equation 6). The AMT was obtained according to the following formula (Table XVIII; Equation 6):

$$\tau_t = (V_o/V_{ref})/(1/(2S_{vs}))$$

In which:

V_o/V_{ref} = Volume fraction of the alveolar septa on reference space (total lung).

S_{vs} = Specific surface density of the alveolar septa.

Measurements were exported to a worksheet in Quattro Pro® (Corel WordPerfect Suite - Version 8, Copyright © 1997 Corel Corporation Limited, Ontario, CA).

5.2.9.1.2. Statistical analysis

The following hypotheses were tested:

| Main effect | Null Hypotheses | Alternative Hypotheses |
|-------------|-----------------------|---------------------------|
| Treatment | Meconium = Control | At least one is different |
| Time | PID 1 = PID 3 = PID 7 | At least one is different |

Values are expressed as means and standard deviations (SD). The effects of treatment and interactions were statistically evaluated by Analysis of Variance (GLM-ANOVA)

according to the following model:

$$Y_{ij} = \mu + T_i + D_j + TD_{ij} + E_{ij}$$

where:

Y_{ij} = individual observation on the j day of the i -th treatment.

μ = general population mean.

T_i = Effect of the i -th treatment; ($i = 1, 2$)

D_j = Effect of the j -th day ($j = 1, 2, 3$)

TD_{ij} = interaction

E_{ij} = Random error associated with each observation $\sim NI(0, \sigma^2 e)$ with 122 and 253

degrees of freedom for volume fractions and arithmetic mean thickness respectively.

Differences between groups of treatment, days postinoculation, and lobes were examined with One-Way Analysis of Variance (ANOVA) followed by the non-parametric Kruskal-Wallis test (40). A p-value below 0.05 was considered statistically significant.

5.3. Results

5.3.1. General condition of the animals

Body weights and survival rates in the rat neonates used for morphometric studies are shown in Table III. Of the 25 pups inoculated with meconium or saline, only one neonate (1/25) did not survive the inoculation procedure. The remaining 24 pups survived the 7 days of the experiment without major evidence of discomfort. Complications following inoculation were only observed in the meconium group in which two neonatal rats developed respiratory failure. One of these rats recovered after a few minutes while the other one died without ever recovering from anesthesia. There were no complications following the intratracheal inoculation of saline solution in the neonatal rats of control group. The survival

rate was 100% for the control group and 92.3% for the meconium group. The lungs of the pup that died following inoculation were not included in morphometric analyses.

5.3.2. *Body weights*

Prior to inoculation, there were no significant differences in body weights between saline control and meconium groups (Table XX). Inoculation of meconium induced a slight but non significant reduction ($p>0.05$) in weight throughout the 7 experimental days (Fig. 44). However, when the average per group of daily body weight gain as a percentage after inoculation was calculated, a remarkable difference was observed in the meconium group compared with the control. The percentage daily weights gained in rats of the meconium group were 7%, 5% and 0.5% lower than in the control group at day PID 1, 2 and 3 respectively. By PID 4 differences in daily weight gain were no longer detected (Fig. 45).

Table XX. Number of rats, body weight at the inoculation time, and survival rate (body weights are given as means \pm SD).

| Group | n | Body weight (g) | Survival rate | |
|--------------------------|----|-----------------|---------------|------|
| | | | n | % |
| Saline solution(Control) | 12 | 15.8 \pm 1.15 | 12 | 100 |
| Meconium (15%) | 13 | 15.4 \pm 1.18 | 12 | 92.3 |
| Total | 25 | 15.6 \pm 1.17 | 24 | 96.0 |

5.3.3. Pilot Study.

5.3.3.1. *Volume fractions (V_v)*

The volume fractions of the different compartments of the lung for the right apical and middle lobes and the left lung pooled at PID 1 are summarized in Table XXI. Also

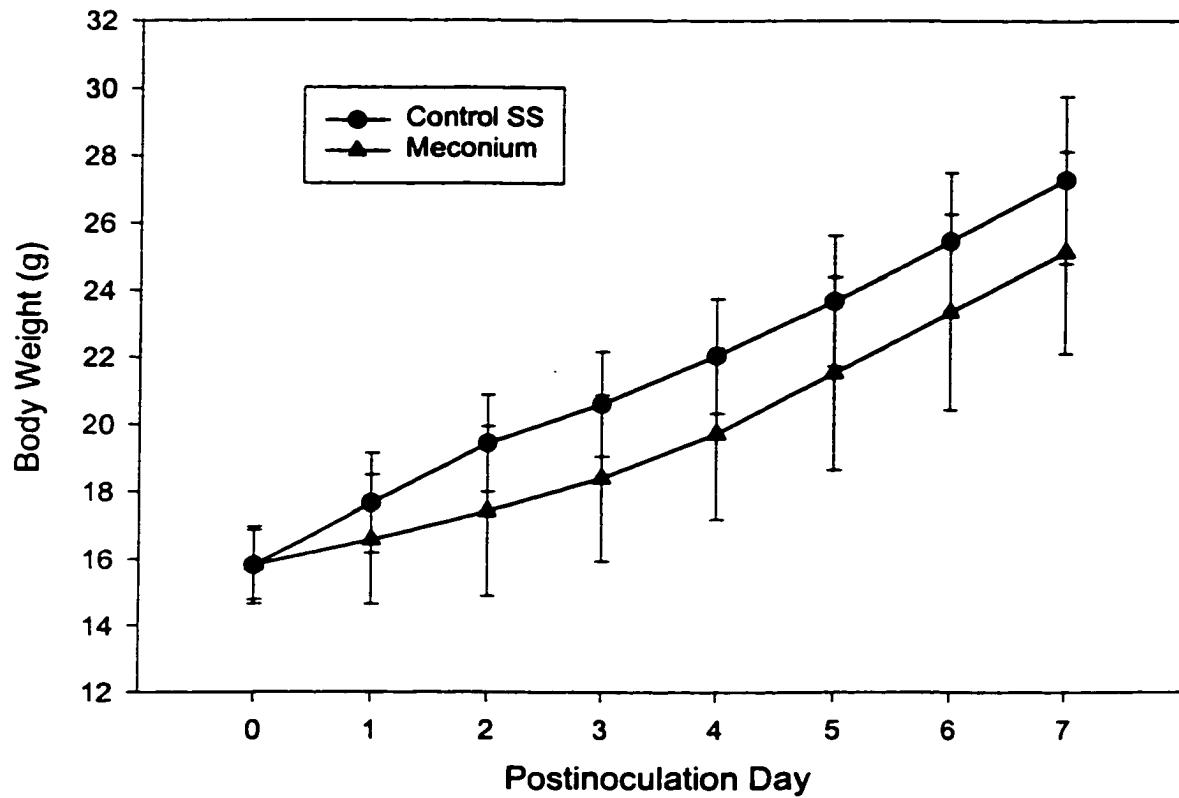


Fig. 44. Body weight of the neonatal rats at different postinoculation times. Symbols and bars represent means and SD (n = 4 animals in each group).

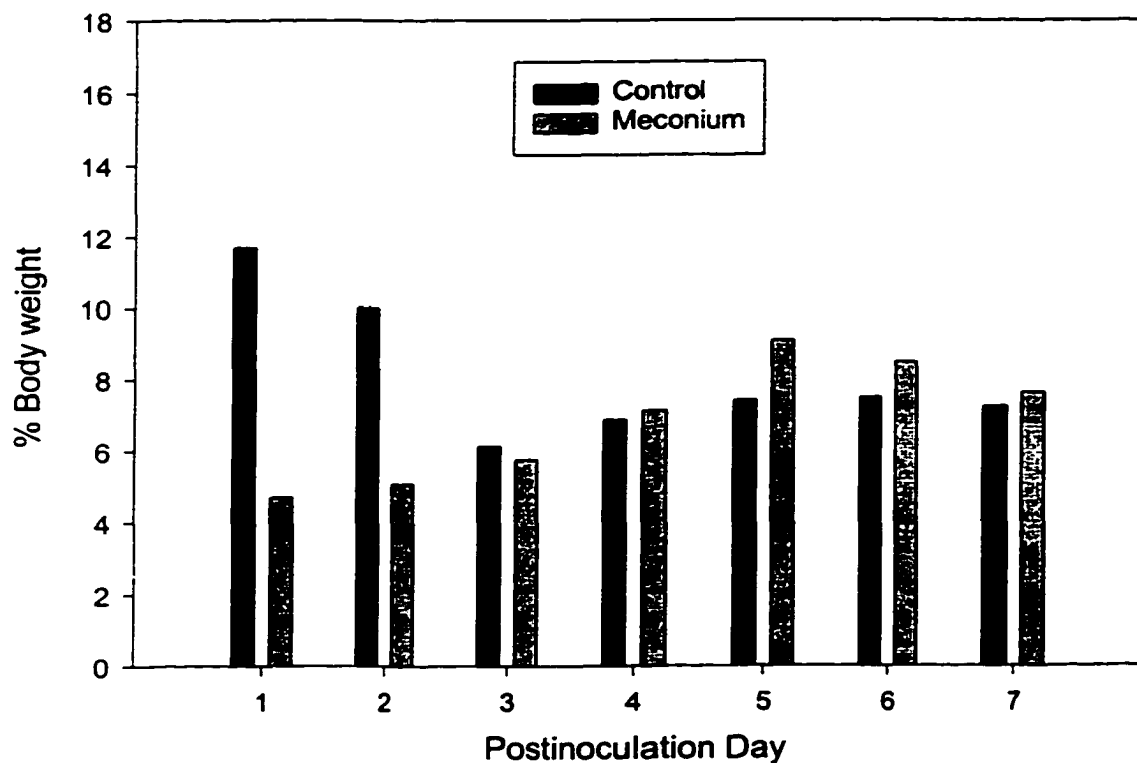


Fig. 45. Percentage of daily body weight gained per group at different postinoculation times. Bars represent means of 4 animals each group.

included are the number of fields and points counted per group.

No significant differences in the volume fractions of the different compartments of the lungs were found between meconium and control groups ($p>0.05$). There were no significant differences detected within treatment groups ($p>0.05$) and no significant differences were found between animals ($p>0.05$). When the volume fractions of the different compartments of the lung were compared by lobes, no overall significant differences were found, except that alveoli from the apical lobe had higher average volume fraction (ANOVA $p= 0.012$), and nonparametric ($p= 0.003$) and less variation. Differences in the alveolar compartment between lobes were found within the meconium group, but not within the control group.

The total alveolar fractions (parenchymal fractions) determined by point counting sections on the left lung, and right apical and middle lobes were 0.82 ± 0.01 for the control group and 0.81 ± 0.04 for the meconium group (Table XXI).

No significant differences ($p>0.05$) were found when the volume fractions of the parenchyma and nonparenchyma were analysed by treatment or by lobe (Table XXI) .

5.3.3.2. Absolute volumes or fixed lung volumes (Absv)

Overall analysis of the right apical lobe, right middle lobe and left lung showed no significant differences between lobes when the volume fraction was multiplied by the fixed lung volume, with exception of alveoli (ANOVA $p=0.012$, nonparametric= 0.003). The apical lobe had higher average in absolute volume of alveoli. Differences in alveolar volume were not found within the groups. Inoculation of meconium did not induce significant changes ($p>0.05$) in the absolute volume of the compartments of the lung at PID 1. No

differences were observed on volumes between animals, with the exception of alveolar air adjusted to volume ($p=0.019$).

The absolute volumes of the parenchyma and nonparenchyma did not change ($P>0.05$) in the meconium group at PID 1. No significant differences ($p>0.05$) in parenchyma and nonparenchyma were found between right apical lobe, right middle lobe and left lung. The absolute volume of the different compartments of the lungs for the right lobe, middle lobe and left lung at PID 1 are summarized in Table XXII.

In summary, inoculation of meconium did not induce significant changes in the lung volume or volume fractions of the compartments at PID 1 excepting differences by lobes in alveoli within the meconium group.

5.3.3.3. Volume density of alveolar septa (V_{valv})

When the volume density of the alveolar septa (V_{valv}) was calculated at high magnification using parenchyma as the reference space, it was revealed that inoculation of meconium induced higher average volume density of alveolar septa ($p=0.01$) (Table XXIII). However, there were no significant differences observed between lobes ($p>0.05$) in any of the treatment groups (Table XXIV). The coefficient of variability in the control group was lower in the right apical lobe (0.13) compared with the left lung and right middle lobe (0.18 and 0.17) respectively (Table XXIV). After inoculation of meconium the coefficient of variability was essentially the same in the different pulmonary lobes. There were no significant interaction between treatment and pulmonary lobes ($p>0.05$).

5.3.3.4. Surface density (S_{vs})

Intratracheal inoculation with meconium induced a significant ($p=0.01$) decrease in

the specific surface density of the alveolar septa (Table XXIII). The “specific surface density” of the alveolar septa did not show significant ($p>0.05$) differences between lobes in the control group (Table XXIV). The coefficient of variability in the control group was lower in the right apical lobe (0.12) than in the left lung (0.24) and the right middle lobes (0.36). However, a significant difference between lobes was detected when meconium and control groups were analysed together ($p=0.007$ in parametric, and 0.012 in nonparametric testing) as shown in Table XXIV.

5.3.3.5. Arithmetic mean thickness of alveolar septa (τ_v)

The thickness of the alveolar septa in rats inoculated with saline solution (control group) did not vary significantly ($p>0.05$) and the smallest coefficient of variability occurred in the right apical lobe (Table XXIV). When the thickness of the alveolar septa was compared between lobes of meconium and control groups, there was a significant difference ($p=0.033$) with higher average in the meconium group (Table XXIV).

In the meconium group there was a smaller variation in arithmetic mean thickness from the middle lobe, but with higher average values (Table XXIV). There were no significant interaction ($p>0.05$) between treatment and pulmonary lobes.

Based on the results of the pilot study in which no significant differences were found in the different lobes in the control animals and the lower coefficient of variability in the apical lobe of the control group, it was decided that using only the right apical lobe was appropriate for morphometric evaluations in neonatal rats inoculated with meconium at PID 1, 3 and 7.

Table XXI. Pilot Study. Number of rats, lobes, fields, points counted and volume fractions of the different compartments of the lung at day 1 Postinoculation. Values are means \pm standard deviation.

| Group | Rats | Lobes | Fields | Points | Volume Fraction | | | | | | |
|---------------------|----------|-----------|------------|---------------|-----------------|---|---|---|--------------------|--------------------|--------------------|
| | | | | | n | n | n | n | Vvp | Vvn | Vvalv |
| Control (Saline) | 4 | 12 | 60 | 10,080 | | | | | 0.82 ± 0.01 | 0.18 ± 0.01 | 0.29 ± 0.01 |
| Meconium (15%) | 4 | 12 | 60 | 10,080 | | | | | 0.81 ± 0.04 | 0.18 ± 0.04 | 0.28 ± 0.00 |
| Total | 8 | 24 | 120 | 20,160 | | | | | | | |

p = parenchyma

n = non-parenchyma

alv = alveolar septa

alair = air from alveoli

bv = blood vessels $>25\mu\text{m}$

br = bronchi and bronchioles

airbr = air from bronchi and bronchioles.

Vvp + Vvn = 1

Vvalv + Vvalair + Vvbv + Vvbr + Vvairbr = 1.

Vvp = Vvalv + Vvalair.

Table XXII. Pilot Study. Number of rats, body weight, fixed lung volume and volumes of the different compartments of the lung at day 1 Postinoculation. Values are means \pm standard deviation.

| Group | Rats | Body | Fixed | Absolute Volumes (cm ³) | | | | | | | |
|---------------------|------|---------------------|--------------------|-------------------------------------|--------------------|--------------------|--------------------|--------------------|--------------------|--------------------|-----------------|
| | | | | n | Weight (g) | Volume (g) | Vvp | Vvn | Vvalv | Vvalair | Vvbv |
| Control (Saline) | 4 | 17.6 ± 1.47 | 1.22 ± 0.05 | 0.99 ± 0.19 | 0.23 ± 0.19 | 0.36 ± 0.02 | 0.64 ± 0.02 | 0.10 ± 0.02 | 0.03 ± 0.01 | 0.07 ± 0.03 | Vvbr Vvairbr |
| Meconium (15%) | 4 | 16.56 ± 1.92 | 1.30 ± 0.07 | 1.05 ± 0.24 | 0.24 ± 0.22 | 0.36 ± 0.02 | 0.70 ± 0.11 | 0.11 ± 0.01 | 0.04 ± 0.01 | 0.07 ± 0.04 | |
| Total | 8 | | | | | | | | | | |

p = parenchyma

n = non-parenchyma

alv = alveolar septa

alair = air from alveoli;

bv = blood vessels >25 μ m

br = bronchi and bronchioles

airbr = air from bronchi and bronchioles.

Vvp = Vvalv + Vvalair.

Table XXIII. Pilot Study. Number of rats, lobes, fields, points counted, Volume Density, Surface Density and Arithmetic Mean Thickness (AMT) of the alveolar septa at day 1 Postinoculation. Values are means \pm SD.

| Group | Rats n | Lobes n | Fields n | Points n | Volume Density | Surface Density | AMT (μ m) |
|---------------------|-----------|------------|-------------|-------------|-----------------------|-----------------------|--------------------|
| Control (saline) | 4 | 12 | 120 | 21,160 | 0.256 \pm 0.040 | 0.119 \pm 0.02 | 5.47 \pm 0.83 |
| Meconium (15%) | 4 | 12 | 120 | 21,160 | 0.376* \pm 0.043 | 0.084* \pm 0.012 | 8.17 \pm 1.17 |
| Total | 8 | 24 | 240 | 40,320 | | | |

* treatment effect ($p < 0.01$)

Table XXIV. Pilot Study. Volume Density, Surface Density and Arithmetic Mean Thickness of the alveolar septa in different lobes at day 1 Postinoculation. Values are means \pm SD. AMT= Arithmetic Mean Thickness; R.=Right.

| Group | Lobe | Volume Density | Surface Density* | AMT** (μ m) |
|---------------------|-----------|-------------------------------|-------------------------------|-----------------------------|
| Control (Saline) | Left | 0.267 \pm 0.049 CV= 0.18 | 0.116 \pm 0.028 CV= 0.24 | 5.52 \pm 1.26 CV= 0.22 |
| | R. Apical | 0.254 \pm 0.034 CV= 0.13 | 0.132 \pm 0.017 CV= 0.12 | 5.21 \pm 1.04 CV= 0.20 |
| | R. Middle | 0.248 \pm 0.042 CV= 0.17 | 0.108 \pm 0.039 CV= 0.36 | 5.67 \pm 1.25 CV= 0.22 |
| Meconium (15%) | Left | 0.367 \pm 0.052 CV= 0.14 | 0.082 \pm 0.017 CV= 0.20 | 7.50 \pm 1.74 CV= 0.23 |
| | R. Apical | 0.364 \pm 0.051 CV= 0.14 | 0.099 \pm 0.024 CV= 0.25 | 7.22 \pm 1.77 CV= 0.24 |
| | R. Middle | 0.398 \pm 0.052 CV= 0.13 | 0.072 \pm 0.012 CV= 0.17 | 9.79 \pm 2.21 CV= 0.22 |

* Significant difference between lobes ($p < 0.01$) but not within control group

** Significant difference between lobes ($p < 0.05$) but not within control group

CV= Coefficient of Variation

5.3.4. Main Study: Results of morphometric study in the apical lobe day 1, 3 and 7 postinoculation.

5.3.4.1. Fixed lung volume

Following intratracheal fixation, the lungs of rats inoculated with meconium appeared grossly different compared with the controls. However, statistical analyses did not reveal any significant changes ($p>0.05$) in pulmonary weights that were attributable to treatment (Table XXV). Parametric and nonparametric testing showed no significant differences ($p>0.05$) within days (Table XXV). As expected, there was a significant increase ($p<0.01$) in lung weights associated to the normal growth of rats (age) and no significant ($P>0.05$) interaction between treatment and day was detected in these animals.

5.3.4.2. Volume fraction of the compartments (Vv)

Morphometric analyses did not reveal any significant ($p>0.05$) overall changes in the volume fractions that could be attributed to inoculation of meconium in any of the pulmonary compartments. The volume fractions of the different compartments of the lung and the number of lobes, fields and points counted are summarized in Table XXVI.

The *volume fraction* of the alveolar septal compartment ($Vvalv$) increased from PID 1 to PID 3 but significantly decreased at PID7. This tendency was also substantiated by the significant ($p<0.01$) overall day effect in this pulmonary compartment. No significant treatment and day interactions were found in the alveolar compartment ($p>0.05$).

Air fractions from alveoli ($Vvalair$) remained the same at PID 1 and 3, but increased at PID 7. These differences were corroborated by a significant overall day effect ($p<0.05$). Although the averages for alveolar air were higher in the meconium group, no significant

Table XXV. Main Study. Number of rats, body weight, fixed lung volume and absolute volumes of the different compartments of the apical lobe at day 1, 3 and 7 Postinoculation. Values are means \pm standard deviation.

| Group | Day | N | Body Weight | Fixed Volume | Absolute Volumes (cm ³) | | | | | | |
|------------------|-----|---|--------------------|--------------------------------|-------------------------------------|--------------------------------|---------------------------------|----------------------------------|--------------------------------|--------------------------------|---------------------------------|
| | | | | | PI | (g) | (g) | Vvp | Vvn | Vvalv* | Vvalair †* |
| Control (Saline) | 1 | 4 | 17.6 ± 1.47 | 1.222 ± 0.048 C=0.03 | 0.989 ± 0.059 C=0.06 | 0.233 ± 0.094 C=0.40 | 0.382 ± 0.023 C=0.06 | 0.606 ± 0.066 C=0.109 | 0.126 ± 0.049 C=0.39 | 0.033 ± 0.029 C=0.89 | 0.073 ± 0.071 C=0.96 |
| | 3 | 4 | 20.6 ± 1.55 | 1.395 ± 0.073 C=0.05 | 1.163 ± 0.094 C=0.08 | 0.228 ± 0.102 C=0.44 | 0.474 ± 0.044 C=0.09 | 0.689 ± 0.065 C=0.09 | 0.131 ± 0.073 C=0.56 | 0.040 ± 0.029 C=0.72 | 0.056 ± 0.030 C=0.53 |
| | 7 | 4 | 27.2 ± 2.49 | 1.568 ± 0.078 C=0.05 | 1.279 ± 0.171 C=0.134 | 0.285 ± 0.124 C=0.43 | 0.443 ± 0.088 C=0.19 | 0.836** ± 0.192 C=0.23 | 0.125 ± 0.028 C=0.22 | 0.069 ± 0.043 C=0.62 | 0.090 ± 0.069 C=0.76 |
| Meconium (15%) | 1 | 4 | 16.5 ± 1.92 | 1.299 ± 0.079 C=0.06 | 1.061 ± 0.141 C=0.133 | 0.240 ± 0.031 C=0.13 | 0.399 ± 0.022 C=0.05 | 0.661 ± 0.133 C=0.20 | 0.139 ± 0.023 C=0.16 | 0.032 ± 0.034 C=1.06 | 0.069 ± 0.075 C=1.09 |
| | 3 | 4 | 18.4 ± 2.46 | 1.440 ± 0.201 C=0.13 | 1.229 ± 0.249 C=0.202 | 0.217 ± 0.094 C=0.43 | 0.510 ± 0.131 C=0.257 | 0.719 ± 0.119 C=0.16 | 0.100 ± 0.025 C=0.25 | 0.038 ± 0.029 C=0.76 | 0.078 ± 0.056 C=0.72 |
| | 7 | 4 | 25.1 ± 3.04 | 1.655 ± 0.062 C=0.03 | 1.421 ± 0.081 C=0.05 | 0.233 ± 0.047 C=0.20 | 0.440 ± 0.052 C=0.118 | 0.980** ± 0.067 C=0.06 | 0.128 ± 0.065 C=0.50 | 0.049 ± 0.022 C=0.45 | 0.055 ± 0.021 C=0.383 |

† Overall significant treatment effect (p<0.05)

* Overall significant day effect (p<0.01)

p = parenchyma

n = non-parenchyma

** Significant difference (p=0.05)

C=Coeficient of variation

bv = blood vessels >25 μ m

br = bronchi and bronchioles

Vvp = Vvalv + Vvalair.

alv = alveolar septa

alair = air from alveoli

airbr = air from bronchi and bronchioles.

Table XXVI. Main Study. Number of rats, lobes, fields, points counted and volume fractions of the compartments of the apical lobe at different postinoculation times. Values are means \pm standard deviation.

| Group | Day | Rat | Lobes | Fields | Points | Volume Fraction | | | | | | |
|---------------------|-----|-----|-------|--------|--------|--------------------------------|--------------------------------|--------------------------------|--------------------------------|--------------------------------|--------------------------------|--------------------------------|
| | | | | | | n | n | n | n | Vvp | Vvn | Vvalv* |
| Control (Saline) | 1 | 4 | 4 | 20 | 3,360 | 0.810 ± 0.070 C=0.08 | 0.189 ± 0.070 C=0.37 | 0.313 ± 0.026 C=0.08 | 0.497 ± 0.063 C=0.12 | 0.102 ± 0.037 C=0.36 | 0.026 ± 0.024 C=0.89 | 0.059 ± 0.057 C=0.97 |
| | 3 | 4 | 4 | 20 | 3,360 | 0.836 ± 0.070 C=0.08 | 0.163 ± 0.080 C=0.46 | 0.340 ± 0.021 C=0.06 | 0.496 ± 0.056 C=0.11 | 0.094 ± 0.055 C=0.58 | 0.028 ± 0.018 C=0.65 | 0.039 ± 0.018 C=0.46 |
| | 7 | 4 | 4 | 20 | 3,360 | 0.816 ± 0.079 C=0.09 | 0.184 ± 0.079 C=0.43 | 0.285 ± 0.068 C=0.23 | 0.530 ± 0.092 C=0.17 | 0.080 ± 0.018 C=0.22 | 0.044 ± 0.028 C=0.63 | 0.058 ± 0.043 C=0.74 |
| Total | | 12 | 12 | 60 | 10,080 | | | | | | | |
| Meconium (15%) | 1 | 4 | 4 | 20 | 3,360 | 0.814 ± 0.079 C=0.09 | 0.185 ± 0.028 C=0.15 | 0.307 ± 0.015 C=0.05 | 0.506 ± 0.083 C=0.16 | 0.108 ± 0.024 C=0.22 | 0.024 ± 0.026 C=1.07 | 0.059 ± 0.057 C=1.11 |
| | 3 | 4 | 4 | 20 | 3,360 | 0.846 ± 0.075 | 0.153 ± 0.075 | 0.349 ± 0.047 | 0.497 ± 0.035 | 0.071 ± 0.023 | 0.026 ± 0.023 | 0.054 ± 0.044 |
| | 7 | 4 | 4 | 20 | 3,360 | 0.858 ± 0.029 C=0.03 | 0.141 ± 0.029 C=0.20 | 0.265 ± 0.020 C=0.07 | 0.597 ± 0.041 C=0.07 | 0.077 ± 0.037 C=0.48 | 0.030 ± 0.01 C=0.46 | 0.033 ± 0.013 C=0.39 |
| Total | | 12 | 12 | 60 | 10,080 | | | | | | | |

*Significant day effect ($p<0.01$)

p = parenchyma

n = non-parenchyma

C=Coeficient of variation

bv = blood vessels $>25\mu\text{m}$

br = bronchi and bronchioles

alair = air from alveoli

Vvp + Vvn = 1

Vvalv + Vvalair + Vvbv + Vvbr + Vvairbr = 1.

Vvp = Vvalv + Vvalair

airbr=air from bronchioles.

alv = alveolar septae

treatment effect was detected when values were compared to the saline control group ($p>0.05$). No significant treatment by day interactions were found ($p>0.05$) following inoculation of meconium. No significant day effect was found in volume fractions of blood vessels ($Vv bv$), bronchi and bronchioles ($Vv br$) and air from bronchioles ($Vv air br$) ($p>0.05$).

The volume fractions of parenchyma and nonparenchyma for the apical lobe for the different times postinoculation are summarized in Table XXVI. None of these fractions showed significant differences when analysed by treatment, day or animal ($p>0.05$).

5.3.4.3. Absolute volume of the compartments (Absv)

The absolute volumes of the pulmonary compartments obtained when the volume fractions were adjusted to the fixed lung volume are summarized in Table XXV. Intratracheal inoculation of meconium did not induce significant ($p>0.05$) changes in the absolute volumes of the compartments with the exception of air from alveoli. Rats of the meconium group had higher volumes of alveolar air ($p < 0.05$) compared with the control animals. Although a significant day effect ($p<0.01$) was found in alveolar air, the interaction between treatment and days was not significant ($p>0.05$). Rats inoculated with meconium had higher ($p=0.05$) volumes of alveolar air ($Absvalair$) at PID 7.

The absolute alveolar volume in both meconium and saline groups changed significantly through time ($p<0.01$) with a tendency to increase from PID 1 to PID 3 and then decrease at PID 7. This tendency was similar to that found in the volume fraction of this compartment. However, neither treatment effects nor interactions were found in any group ($p>0.05$). No significant day effect was found in any of the other volumes (blood vessels, bronchi, bronchioles and air from bronchi and bronchioles) of the compartments ($p>0.05$).

The absolute volumes of parenchymal and nonparenchymal values for rats inoculated with saline solution and meconium at different days postinoculation are summarized in Table XXV. An overall significant treatment effect ($p=0.034$) on parenchyma was found in the results of GLM-ANOVA. Comparison between the control and meconium groups showed significant increase ($p=0.021$) in parenchymal absolute volume of the meconium group only at PID 7.

Absolute volumes of parenchyma increased from day 1 to day 7 in both groups. This finding was further substantiated by a significant overall day effect ($p=0.000$). The volumes of non parenchyma (blood vessels, bronchi, bronchioles and air from these airways) did not change ($p>0.05$) with the inoculation of meconium nor were changes found between the different postinoculation times.

5.3.4.4. Volume density (V_{vap}) of the alveolar septa

The volume densities of the alveolar septa in the apical lobe at different postinoculation times are summarized in Table XXVII. Inoculation of meconium caused a significant ($p<0.01$) increase in the volume density of the alveolar septa using parenchyma as the reference space. These differences remained significant ($p<0.01$) throughout the postinoculation times (Fig. 46). A significant overall day effect ($p<0.01$) was found in the volume density of the alveolar septa in which values remained unchanged at PID 1 and 3, but decreased significantly at PID 7.

Table XXVII. Main Study. Volume Density, Surface Density and Arithmetic Mean Thickness of the alveolar septa in the apical lobe at different postinoculation times. Values are means \pm Standard deviations. AMT= Arithmetic Mean Thickness.

| Group | Day PI | Volume Density † * | Surface Density † * | AMT (μ m) † * |
|---------------------|-----------|------------------------------|------------------------------|------------------------------|
| Control (Saline) | 1 | 0.25 \pm 0.03 C= 0.13 | 0.13 \pm 0.01 C= 0.12 | 5.21 \pm 1.04 C= 0.20 |
| | 3 | 0.25 \pm 0.03 C= 0.12 | 0.13 \pm 0.02 C= 0.16 | 4.89 \pm 0.43 C= 0.89 |
| | 7 | 0.20 \pm 0.01 C= 0.08 | 0.17 \pm 0.05 C= 0.29 | 3.83 \pm 0.34 C= 0.09 |
| Meconium (15%) | 1 | 0.36 \pm 0.05 † C= 0.14 | 0.09 \pm 0.02 † C= 0.25 | 7.22 \pm 1.77** C= 0.24 |
| | 3 | 0.37 \pm 0.05 † C= 0.15 | 0.09 \pm 0.01 † C= 0.17 | 7.65 \pm 1.56** C= 0.20 |
| | 7 | 0.33 \pm 0.02 † C= 0.08 | 0.09 \pm 0.01 † C= 0.12 | 7.25 \pm 0.92** C= 0.12 |

† Significant treatment effect ($p<0.01$)

* Overall day effect ($p<0.01$)

** Significant difference ($p<0.05$)

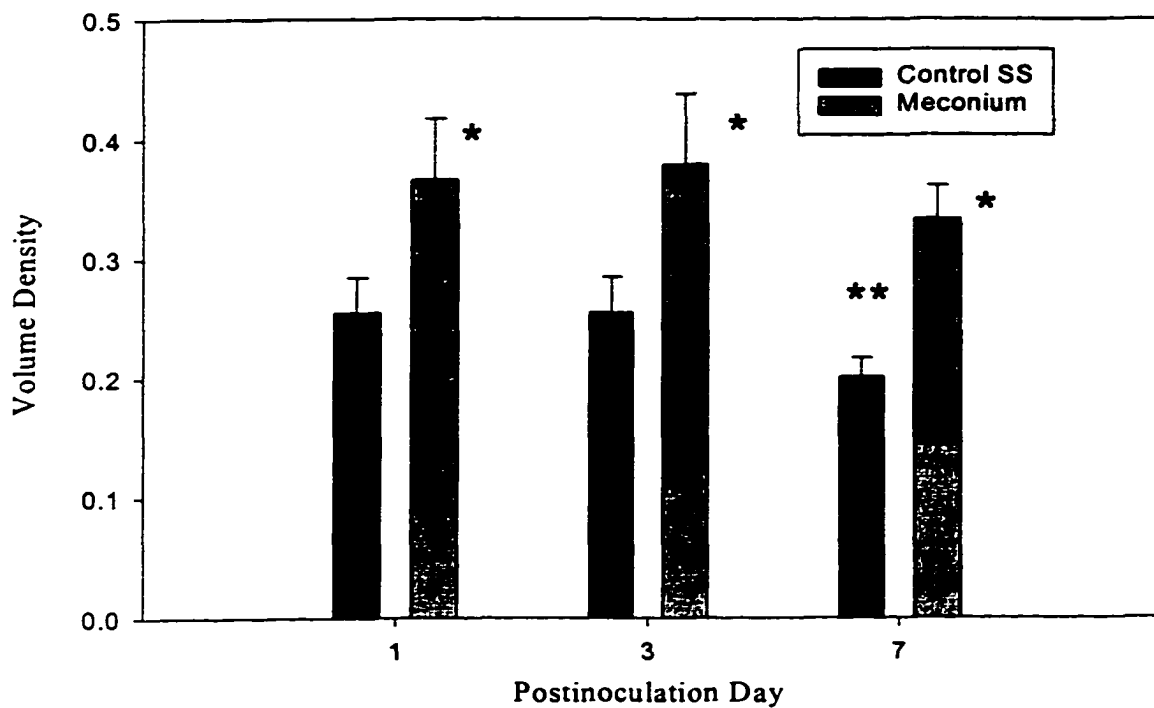


Fig. 46. Main Study. Volume density of the alveolar septa in the apical lobe at different postinoculation times. Symbols and bars represent mean and SD ($n=4$ animals each group).
 * Significant treatment effect ($P<0.01$), ** Significant day effect ($p<0.01$).

5.3.4.5. Surface density (S_v)

Intratracheal inoculation with meconium induced a significant ($p<0.01$) reduction in surface density at PID 1, 3 and 7. Also, a significant day effect ($p<0.01$) was observed characterized by an overall increase from PID 1 to 7 in the rats inoculated with saline solution but not in the meconium group (Table XXVII).

5.3.4.6. Arithmetic mean thickness of the alveolar septa (τ_v)

The thickness of the alveolar septa increased significantly ($p<0.01$) as result of meconium inoculation (Table XXVII). These differences between rats inoculated with saline and those inoculated with meconium remained significant ($p=0.05$) during the entire length of the experiment (Fig. 47). In rats inoculated with saline, the thickness of the alveolar septa decreased ($p=0.002$) from PID 1 to PID 7 (Fig. 47). An overall day effect was not detected when arithmetic mean thickness of both groups was analysed together ($p=0.174$).

Based on the non-constant variation in the residuals of volume density, surface density and arithmetic mean thickness, the response was transformed to logarithms and ANOVA analysis performed again. The same significant treatment effects and differences were found each day.

The overall significance of the treatment effect ($p<0.01$) detected by Generalized Linear Models of ANOVA, was also corroborated for each PID using one-way ANOVA ($p<0.01$), the non-parametric Kruskal-Wallis test ($P=0.001$) and contrast testing for days of interest ($p<0.05$).

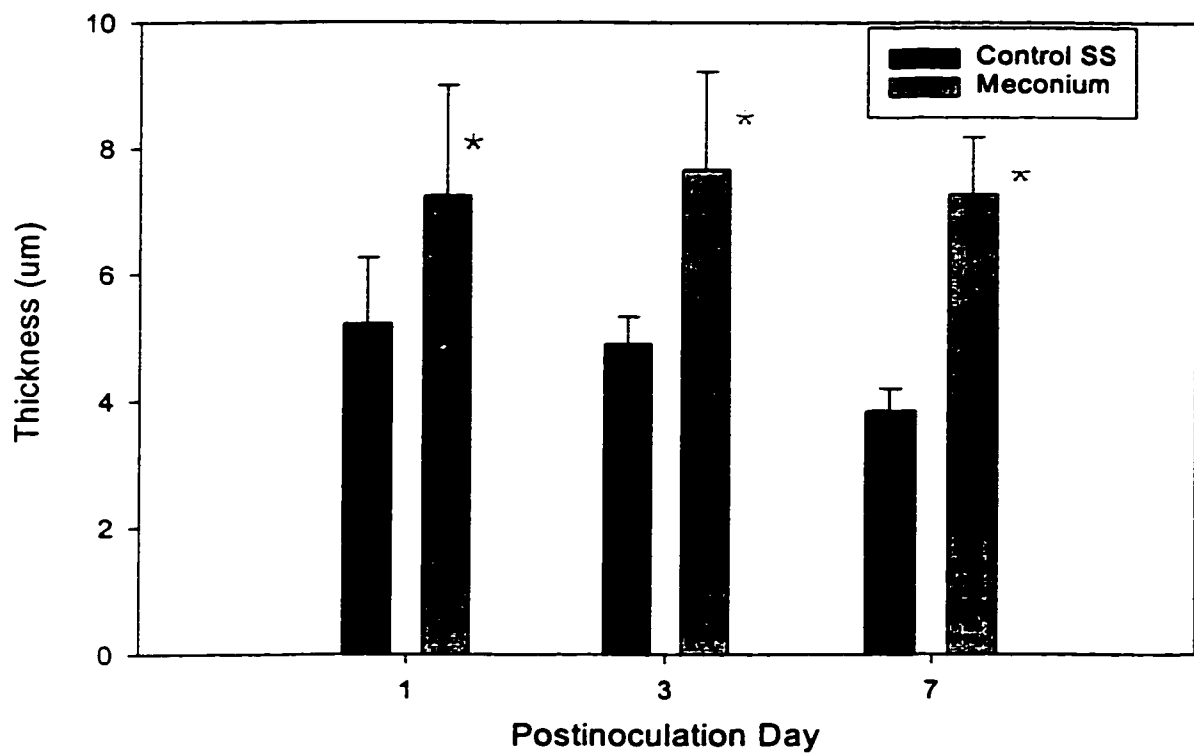


Fig. 47. Main Study. Arithmetic Mean Thickness of alveolar septa at different postinoculation times. Symbols and bars represent means and SD (n = 4 animals each group). * Significant treatment effect ($p < 0.01$).

5.4. Discussion

5.4.1. Clinical observations and mortality

The frequency of complications associated with intratracheal inoculation was slightly higher in rats treated with meconium. This was not an unexpected finding since the viscosity of meconium has a tendency to cause airway obstruction while saline fluid moves freely in the airways and is rapidly cleared by the lymphatic system (41,42). Considering the small size of the neonates, the 7.7% mortality associated with the inoculation of meconium was lower than in other models of experimental MAS in rats (11,28) and in rabbits (12,21,25,27).

5.4.2. Body weight

The negative effect of meconium on the daily body weight gained at PID 1, 2 and 3 was similar to that found in the rats of the acute morphological study reported in section 4.3.1. This negative effect is likely the result of the multiple pathophysiology in this syndrome. Possible causes include not only the mechanical and physiological changes and the respiratory distress, but also hypoxemia, acidosis and hypercapnia (22,29,43).

Results obtained from the microscopic study showed that the pulmonary changes caused by inoculation of meconium are distributed in all pulmonary lobes. The tendency for intratracheal inoculates to reach all lobes of the neonatal and mature murine lung has been reported by others (41,44) and justifies the use of a single lobe as a valid morphometric sample. Using only the right apical lobe for the final study was also justified by the results of the pilot study in which statistical analyses failed to reveal significant lobe differences in morphometrical values for the left lung and right apical and middle lobes of control rats.

5.4.3. Lung volume and weight

Fixed lung volume increased slightly after inoculation of meconium but the magnitude of these changes was not large or severe enough to achieve statistical significance. This fact may have been due to the small number of animals per group, or more likely, because the magnitude of inflammation induced by meconium was not sufficiently severe as to cause detectable changes in lung volume. Unfortunately, it is not possible to compare this finding with results from other morphometric studies of experimental MAS in rats since in those, lung volume determination were not done (11,28,45). The increase in fixed lung volume by day and the lack of interaction between treatment and day suggest that the volume change was due to the normal growth of the lungs (17). Fixed lung volumes for 7-day-old rats were consistent with the volumes reported in normal CFN-COBS-strain of rats (46). However, the volumes reported by other investigators are lower in spite of the close similarities in body weight and comparable ages (46).

It was not possible to compare the lung volumes with other reports since information available in the literature includes values for Fischer 344 rats older than 6 weeks (17). An unpublished study indicates that the fixed lung volume for a 7-day-old male Fischer 344 is around 1.45 ml, a value slightly higher than the 1.22 ml obtained in the 8-day-old rats of the control group inoculated with saline solution alone in the present study (Dr. Kent Pinkerton, personal communication).

Reports of experimental MAS indicating that intratracheal inoculation of meconium increases the wet/dry ratio in the lungs of rabbits suggest an early microvascular endothelial damage caused by meconium in the lungs (21).

Lung weight-body weight ratios were evaluated in a rabbit model of MAS using intratracheal inoculation of human meconium into fetal rabbits with the aim of assessing edema and its possible decrease with glucocorticoid treatment. However, the ratios obtained for all groups were similar to those described by other authors to be normal after the first 6 hours of life (25).

5.4.4. Volume fractions of compartments (Vv)

The higher values in the alveolar septal fraction at PID 1 and 3 followed by a decrease at PID 7 could have several explanations. It is possible that morphometric values of alveolar walls in atelectatic lungs might increase parallel with the decrease in alveolar air, then the initial increase might be interpreted as the effect of collapse of the lung. The decrease of alveolar fractions at PID 7 could also be due to lung reinflation and recovery from atelectasis (27). A second explanation could be that the increase in thickness at PID 1 and 3, followed by a slight decrease at PID 7 could be due to resolution of the inflammatory response and decrease of alveolar thickness. Nevertheless, this reasoning does not totally explain why the same tendency was found in rats inoculated with saline solution alone. Moreover, the overall and per day correlation between alveolar fraction and alveolar thickness is too low ($r = 0.11$). The last and most likely explanation could be the normal growth of the parenchyma. The same tendency found in this study has also been reported in CFN rats, using total tissue and not only alveoli (46). It has been demonstrated that the volume fractions of tissue in the lung increased from 7 to 10 days of age and decreased at day 13 of age in normal CFN rats (46). Also, an increase in alveolar density from days 4 to 7 after birth has been described in normal neonatal CFN rats. This temporary increase

followed by reduction in alveolar density when the rat is 13-days-old suggest that those changes in volume fractions seen in the saline and meconium rats are in part due to normal lung growth (46).

Considering the lack of treatment effect in alveolar fractions, the non-interaction between treatment and PID as well as the low correlation between alveolar fraction and thickness, we conclude that the decrease in the alveolar fraction from day 3 to 7 PI is related to the normal lung growth and not to inoculation of meconium.

The overall change in volume fractions of alveolar air from 0.50 to 0.53 in the control and meconium groups respectively, using the total lung as reference space, is similar to the value of ~0.5 described in rats and rabbits inoculated with saline using the parenchyma as a reference space (11,12,27). These authors also described a decrease of 25 to 30 % after meconium inoculation in contrast to the lack of change in volume fractions of air in the neonatal rats of the present investigation.

The higher alveolar-air fraction at PID 7 concurred with the decrease in alveolar fractions at PID 7, suggesting that inoculation of meconium may also induce hyperinflation of the lungs.

The general average of alveolar air in the meconium group was higher than in the control, but the magnitude of this change was not large enough to achieve statistical significance. Since the values of alveolar air increased in both meconium and saline groups, it is likely that changes simply reflect the normal growth of the lungs as previously reported by other investigators (17).

Morphometric analyses did not detect any significant decrease in alveolar air

fractions, implying that atelectasis was not present in rats intratracheally inoculated with meconium. However, lack of atelectasis is explained by the distention of collapsed alveoli caused by the intratracheal perfusion of glutaraldehyde. The confounding effect of fixation has been demonstrated by others who postulate that besides pressure and flow rate, the types of fixative (formalin vs. glutaraldehyde) influence the degree of pulmonary distention (6,47). If so, the perfusion of fixative likely distended atelectatic lungs in rats inoculated with meconium and the structural rigidity conferred by the glutaraldehyde did not allow the alveolar recoil to revert to the atelectatic state. This assumption, is supported by the fact that atelectasis was clearly present in lungs inoculated with meconium and fixed by immersion rather than by intratracheal perfusion with fixative. Similarly, the lungs of rats inoculated with meconium but fixed with formalin for the acute morphologic study (section 4.3.2) had a notable degree of atelectasis. The problem with lungs fixed by formalin is that the lack of tissue hardening makes them much more prone to slow deflation when there is no longer fixative pressure and to compression during handling and sectioning.

The volume fractions of parenchyma and nonparenchyma of the apical lobe at different postinoculation times did not change with inoculation of meconium, day or animal. Volume fractions of the parenchyma (alveolar fractions) in rats inoculated with saline and meconium were similar to the value reported in normal CFN-COBS rats of the same age. (46). As reported by other investigators in Fischer 344 rats, age does not have any effect on the values of the parenchymal fraction (alveolar fraction and air from alveoli) of the normal lung (17).

The fact that inoculation of meconium caused no change in volume fractions of

parenchyma was not an unexpected finding. It has been reported that exposure to pneumotoxins (oxygen and asbestos) does not induce detectable morphometric changes in the parenchymal fraction of the lungs (19,48). From these morphometric studies reported by other investigators and from the results obtained from rats inoculated with meconium, it appears that the parenchymal fraction changes very little after acute injury as long as the degree of inflation of the fixed lung is held constant (6).

A total of 168 points per micrograph and 5 photographs per lung lobe was considered sufficient to evaluate the volume fraction of the parenchyma (V_{vp}) (0.8) or alveoli (V_{valv}) (0.5) with 2.5% of error in the present study. These values (0.8) obtained in the control rats were consistent with those reported by others (46). It has been suggested that the accuracy of point count stereology can be improved by evaluating more micrographs (more samples) rather than increasing the number of points (> 168 points) per micrograph (6).

5.4.5. Absolute volumes of compartments ($Absv$)

The significant day effect that was detected when the alveolar values were adjusted to fixed lung volume (higher values at PID 1 and 3 and lower at day 7) also can be attributed to the normal growth of the lungs rather than to the effect of meconium in the lungs.

Although morphometric values for absolute volume of alveolar air ($Absvalair$) had the same tendency to increase in both treatment groups, rats inoculated with meconium displayed higher $Absvalair$ values. Normal growth and increase in alveolar air due to the expansion versus reduction of interstitium are normally found in neonates (6,46). Hence, in addition to the normal growth, a significant hyperinflation effect induced by meconium could be considered as an explanation of the increase in the volume of alveolar air.

The increase by age in total airspace volume (fixed lungs) has been described in normal Fischer 344 rats which correlates well with changes in body weight (17,47). It has been demonstrated that intratracheal fixation of lungs with glutaraldehyde at a constant pressure of 20 cm is equivalent to 70-90% of the physiological total lung capacity of living anaesthetised rats (17). Hence, the same assumptions of lung capacity can be applied in this study. Unfortunately, it was not possible to compare the body weights and lung volumes from this study with those described in Fischer 344 rats, because the specific body weight and fixed lung volumes at different ages were not reported in that study (17).

Considering that the volume fraction of the parenchyma and nonparenchyma remained unchanged with time, the increase in absolute volume of parenchyma adjusted to lung weight is likely the result of an increase in air due to age.

5.4.6. *Volume density (V_{vap})*

Volume density of alveolar septa (*V_{vap}*) regarding parenchyma as a reference space under high magnification (100X) increased significantly in the meconium group suggesting an increase in density of the alveolar wall. The increase in density of alveolar septa could be due initially to the apparent distension by edema and the recruitment of neutrophils in alveolar capillaries. In some studies, the increase in density of cellular compartments (epithelial, endothelial, interstitial) following acute exposure to pneumotoxicants (ozone) has been reported in rats (2). However, the volume density of the whole alveolar septa regardless of cellular compartments was evaluated in the present study.

There was also a decrease in volume density of *V_{vap}* at PID 7 in both control and meconium groups with an overall significant day effect. This remarkable day effect in

volume density of alveolar septa in the meconium group at PID 1 and 3 and the subsequent return to baseline levels at PID 7 suggest a resolution of the inflammatory response in the lungs. This change in *Vvap* following acute lung injury has also been reported in animals exposed to pneumotoxins (2,3). In addition to the effect of meconium on *Vvap*, statistical analyses also showed that in part, the decrease at PID 7 was also due to the effect of normal growth of the neonatal lung as reported by others (17).

5.4.7. *Surface density (Sv)*

The surface density of the alveolar septa in the control group remained unchanged at PID 1 and 3 but increased significantly at PID 7. A similar pattern has also been reported in rats 7-13 days old in which increase in the alveolar surface was presumed to be the result of age (46). The surface density of the alveolar septa changed inversely to the volume density of the septa. According to the literature, age and lung growth result in an increase in alveolar surface area and concomitant decrease in arithmetic mean thickness of the air-blood barrier (17,46). This same pattern was found in rats inoculated with saline solution indicating that the outgrowth of secondary alveolar septa from primary septa occurred during the first week of age as previously reported by others (17,46).

5.4.8. *Arithmetic mean thickness (AMT) of alveolar septa (τ_s)*

The reduction of AMT of the alveolar septa in the control group from PID 1 to 7 is consistent with reports describing attenuating thickness of the air-blood barrier of normal CFN and Fischer 344 rats during the first week of age (17,46). This lower AMT in young rats was the reflection of a reduced thickness of the alveolar interstitial compartment, and to a lesser extent of a reduction in the thickness of epithelial and endothelial cells (17,46).

There are difficulties in interpreting the meaning of "arithmetic mean thickness" and comparing values reported by different investigators. First, since it is really a volume to surface ratio, it represents the average thickness and not necessarily the thickness at every point in the alveolar septa. However, in actual practice the magnitude of this systematic standard error for normal lung tissues is 5%-10% and its importance depends largely on the type and objectives of the study. To verify this value in preliminary studies, random lines were set from one alveolar surface to the opposite one in order to obtain an average thickness and match the results with those obtained with the standard formula for arithmetic mean thickness, resulting in substantial agreement (4,6).

The second problem in interpreting or comparing "AMT," is that this value notably depends on the magnification used for measurements. A higher magnification tends to decrease the calculated septal thickness as the apparent (recognizable) surface area increases (6). In this study high resolution light microscopy was used to calculate the thickness of the alveolar septa instead of the thickness of the air-blood barrier which requires electron microscopy. Although AMT is only an average value for septal thickness, it has good sensitivity for detecting changes in mean septal thickness induced by fibrosis or edema (6).

Inoculation of meconium induced a significant increase in thickness of the alveolar septa at different postinoculation times with a peak at day 3 PI. Different causes have been described as inducing an increase in alveolar septal thickness, and they could be the result of changes in one or more of the cellular compartments of the alveoli such as an increase in: 1- Mean cell volume or in numbers of type I and type II pneumocytes, mean cell surface area and surface of basement membrane covered. 2- Volume of cellular interstitium

and endothelium due to edema or deposition of a collagen matrix in the interstitium. 3- Aggregation of leukocytes in alveolar capillaries. 4- Volume and number of macrophages in proximal alveolar regions since an increase in cytoplasmic size and vacuolization are common findings in macrophages activated by phagocytosis of foreign material (6).

The increase in thickness of the alveolar septa resulting from the inoculation of meconium is primarily related to the acute edematous distension of the alveolar interstitium. This fact was later corroborated by ultrastructural studies in which a noticeable edematous separation of the alveolar interstitium was seen in the alveolar walls (detailed description in section 6.3). This is a nonspecific change since similar lesions are described in the early phases of alveolar inflammation caused by other substances (50,51).

Physical aggregation or sequestration of polymorphonuclear leukocytes in the capillaries or alveolar interstitium probably play a lesser role in alveolar thickening during the acute reaction to meconium. A study in rabbits inoculated with meconium revealed influx of neutrophils into the lungs but no apparent microscopic changes in the thickness of alveolar walls (21). In that study, 6 hours after meconium inoculation, water assessment showed increased fluid content in lungs. This supporting our findings that increased thickness of the alveolar walls is primarily the result of edema rather than cellular exudation.

Although aggregation of leukocytes was not thought to be primarily responsible for the increase in alveolar thickness in rats inoculated with meconium, it is possible that release of edematogenic factors by the inflammatory cells, as is advocated in the theory of adult respiratory distress syndrome (ARDS), may have indirectly been responsible for alveolar edema (52-54). It is recognized that changes in the alveolar walls seen in ARDS are not

necessarily the immediate result of direct injury caused by toxin, gases or pneumotoxicants, but instead are often the result of endothelial and alveolar injury resulting from the release of proinflammatory mediators by sequestered leukocytes in the alveolar capillaries (51). Interestingly, a recent report proposes that an ARDS-like reaction is involved in the pathogenesis of pulmonary injury in experimental and natural cases of MAS (55).

Intratracheal inoculation induced microscopic changes in the alveolar wall that were clearly detected by morphometric analyses. For instance, increases in alveolar septa thickness were detected in the PID 1, 3 and 7 indicating that the acute alveolar injury and host response caused by meconium could be transient and may return to baseline levels. This pattern of injury and host response is common to a number of mild pneumotoxicants (2,49). Although morphometric methods are sensitive enough to detect alveolar thickening, electron microscopy is required to determine the precise site and nature of the lesion responsible for this abnormal alveolar thickness (14).

In summary, morphometric studies showed that meconium induces an acute alveolitis characterized by exudation of leukocytes into the alveolar space and thickening of the alveolar walls. This last change seems related to accumulation of fluid rather than interstitial infiltration of leukocytes. Thickening of the alveolar walls should be added to the list of pulmonary lesions associated with acute MAS such as atelectasis, hyperinflation and inflammation. This study also supports the view that changes in some volume fractions in the neonatal rat are primarily due to the normal growth and maturation of the lung and need to be carefully considered in experimental lung research.

5.5. REFERENCES

1. LIPPMANN M, SCHLESINGER RB. Interspecies comparisons of particle deposition and mucociliary clearance in tracheobronchial airways. *J Toxicol Environ Health* 1984; 13: 441-469.
2. BARRY BE, CRAPO JD. Application of morphometric methods to study diffuse and focal injury in the lung caused by toxic agents. *Crit Rev Toxicol* 1985; 14: 1-32.
3. BARRY BE, MILLER FJ, CRAPO JD. Effects of inhalation of 0.12 and 0.25 parts per million ozone on the proximal alveolar region of juvenile and adult rats. *Lab Invest* 1985; 53: 692-704.
4. WEIBEL ER. *Stereological Methods*. New York: Academic Press, 1979.
5. DUNNILL MS. Quantitative Methods in the Study of Pulmonary Pathology. *Thorax* 1962; 17: 320-328.
6. PINKERTON KE, CRAPO JD. Morphometry of the Alveolar Region of the Lung. In: Witschi M D, Brain JD, eds. *Toxicology of Inhaled Materials*. New York: Springer-Verlag, 1985: 259-285.
7. COLLAN Y. Morphometry in pathology: another look at diagnostic histopathology. *Pathol Res Pract* 1984; 179: 189-192.
8. COLLAN Y, TORKKELI T, KOSMA VM, PESONEN E, KOSUNEN O, JANTUNEN E, MARIUZZI GM, MONTIRONI R, MARINELLI F, COLLINA G. Sampling in diagnostic morphometry: the influence of variation sources. *Pathol Res Pract* 1987; 182: 401-406.
9. HOWARD CV, REED MG. *Unbiased Stereology. Three-Dimensional Measurement in Microscopy*. New York: Springer-Verlag, 1998.
10. LAST JA, GERRIETS JE, HYDE DM. Synergistic effects on rat lungs of mixtures of oxidant air pollutants (ozone or nitrogen dioxide) and respirable aerosols. *Am Rev Respir Dis* 1983; 128: 539-544.
11. SUN B, HERTING E, CURSTEDT T, ROBERTSON B. Exogenous surfactant improves lung compliance and oxygenation in adult rats with meconium aspiration. *J Appl Physiol* 1994; 77: 1961-1971.
12. SUN B, CURSTEDT T, ROBERTSON B. Surfactant inhibition in experimental meconium aspiration. *Acta Paediatr* 1993; 82: 182-189.
13. TYLER WS, DUNGWORTH DL, PLOPPER CG, HYDE DM, TYLER NK. Structural

evaluation of the respiratory system. *Fundam Appl Toxicol* 1985; 5: 405-422.

14. WEIBEL ER, KNIGHT BW. A morphometric study on the thickness of the pulmonary air-blood barrier. *J Cell Biol* 1964; 21: 367-384.
15. MCLAUGHLIN RFJ, TYLER WS, CANADA RO. Subgross pulmonary anatomy of the rabbit, rat, and guinea pig, with additional notes on the human lung. *Am Rev Respir Dis* 1966; 94: 380-387.
16. PLOPPER CG, JONES, TC, DUNGWORTH, DL, MOHR, U. *Structure and Function of the Lung*. 2nd. New York: Springer Verlag. 1996; p.135 *Monographs on Pathology of Laboratory Animals*.
17. PINKERTON KE, BARRY BE, ONEIL JJ, RAUB JA, PRATT PC, CRAPO JD. Morphologic changes in the lung during the lifespan of Fischer 344 rats. *Am J Anat* 1982; 164: 155-174.
18. CUMMINGS EC Salem, H *Physiological Measurements Following Inhalation Exposures*. New York: Marcel Dekker. 1987; p.153 12. *Inhalation Toxicology: Research Methods, Applications, and Evaluation*.
19. CRAPO JD, PETERS GM, MARSH SJ, SHELBURNE JS. Pathologic changes in the lungs of oxygen-adapted rats: a morphometric analysis. *Lab Invest* 1978; 39: 640-653.
20. CLEARY GM, WISWELL TE. Meconium-stained amniotic fluid and the meconium aspiration syndrome. An update. *Pediatr Clin North Am* 1998; 45: 511-529.
21. TYLER DC, MURPHY J, CHENEY FW. Mechanical and chemical damage to lung tissue caused by meconium aspiration. *Pediatrics* 1978; 62: 454-459.
22. SRINIVASAN HB, VIDYASAGAR D. Meconium aspiration syndrome: current concepts and management. *Compr Ther* 1999; 25: 82-89.
23. DAVEY AM, BECKER JD, DAVIS JM. Meconium aspiration syndrome: physiological and inflammatory changes in a newborn piglet model. *Pediatr Pulmonol* 1993; 16: 101-108.
24. JOVANOVIC R, NGUYEN HT. Experimental meconium aspiration in guinea pigs. *Obstet Gynecol* 1989; 73: 652-656.
25. FRANTZ ID, WANG NS, THACH BT. Experimental meconium aspiration: Effects of glucocorticoid treatment. *J Pediatr* 1975; 86: 438-441.
26. WISWELL TE, FOSTER NH, SLAYTER MV, HACHEY WE. Management of a piglet model of the meconium aspiration syndrome with high-frequency or

conventional ventilation. *Am J Dis Child* 1992; 146: 1287-1293.

27. SUN B, CURSTEDT T, SONG GW, ROBERTSON B. Surfactant improves lung function and morphology in newborn rabbits with meconium aspiration. *Biol Neonate* 1993; 63: 96-104.
28. SUN B, CURSTEDT T, ROBERTSON B. Exogenous surfactant improves ventilation efficiency and alveolar expansion in rats with meconium aspiration. *Am J Respir Crit Care Med* 1996; 154: 764-770.
29. LOPEZ A, BILDFELL R. Pulmonary inflammation associated with aspirated meconium and epithelial cells in calves. *Vet Pathol* 1992; 29: 104-111.
30. LOPEZ A. Respiratory System. In: Carlton W W, McGavin MD eds.. *Thomson's Special Veterinary Pathology*. St. Louis, Missouri: Mosby, 1995: 116-174.
31. DUNGWORTH DL. The Respiratory System. In: Jubb KVF, Kennedy PC, Palmer N, eds. *Pathology of Domestic Animals*. San Diego, California: Academic Press, 1993: 539-699.
32. BAKER DEJ. Reproduction and Breeding. In: Baker H J, Lindsey JR, Weisbroth SH, eds. *The Laboratory Rat*. Orlando: Academic Press, 1979: 154-166.
33. WAYNFORTH HB. Experimental and surgical technique in the rat. New York: Academic Press, 1980.
34. PARK CM, CLEGG KE, HARVEY CC, HOILLENBERG MJ. Improved techniques for successful neonatal rat surgery. *Lab Anim Sci* 1992; 42: 508-513.
35. HENRY CJ, KOURI E Salem, H. Specialized Test Article Administration: Nose-Only Exposure and Intratracheal Inoculation. New York: Marcel Dekker. 1987; p.121 12. *Inhalation Toxicology: Research Methods, Applications, and Evaluation*.
36. WEIHE WH. The Laboratory Rat. In: Poole T Beds. *The UFAW Handbook on the Care and Management of Laboratory Animals*. England: Longman Scientific & Technical, 1987: 309-330.
37. CANADIAN COUNCIL ON ANIMAL CARE. *Guide to the Care and Use of Experimental Animals*. Ottawa, Ont.: CCAC, 1993.
38. LUNA L. *Manual of histologic staining methods of the Armed Forces Institute of Pathology*. Toronto, Canada: McGraw-Hill, 1968.
39. CRUZ OL, WEIBEL ER. Sampling designs for stereology. *J Microsc* 1981; 122: 235-257.

40. FISHER LD, VAN BELLE G. *Biostatistics: A Methodology for The Health Sciences*. New York: Wiley Intersciences, 1993.
41. PRITCHARD JN, HOLMES A, EVANS JC, EVANS N, EVANS RJ, MORGAN A. The distribution of dust in the rat lung following administration by inhalation and by single intratracheal instillation. *Environ Res* 1985; 36: 268-297.
42. WISWELL TE, BENT RC. Meconium staining and the meconium aspiration syndrome. Unresolved issues. *Pediatr Clin North Am* 1993; 40: 955-981.
43. BESSER TE, SZENCI O, GAY CC. Decreased colostral immunoglobulin absorption in calves with postnatal respiratory acidosis. *J Am Vet Med Assoc* 1990; 196: 1239-1243.
44. RUZINSKI JT, SKERRETT SJ, CHI EY, MARTIN TR. Deposition of particles in the lungs of infant and adult rats after direct intratracheal administration. *Lab Anim Sci* 1995; 45: 205-210.
45. CLEARY GM, ANTUNES MJ, CIESIELKA DA, HIGGINS ST, SPITZER AR, CHANDER A. Exudative lung injury is associated with decreased levels of surfactant proteins in a rat model of meconium aspiration. *Pediatrics* 1997; 100: 998-1003.
46. BURRI PH, DBALY J, WEIBEL ER. The postnatal growth of the rat lung. I. Morphometry. *Anat Rec* 1974; 178: 711-730.
47. HAYATDAVOUDI G, CRAPO JD, MILLER FJ, ONEIL JJ. Factors determining degree of inflation in intratracheally fixed rat lungs. *J Appl Physiol* 1980; 48: 389-393.
48. PINKERTON KE, PRATT PC, BRODY AR, CRAPO JD. Fiber localization and its relationship to lung reaction in rats after chronic inhalation of chrysotile asbestos. *Am J Pathol* 1984; 117: 484-498.
49. SCHWARTZ LW Salem, H Pulmonary Responses to Inhaled Irritants and the Morphological Evaluation of Those Responses. New York: Marcel Dekker. 1987; p.293 12. *Inhalation Toxicology: Research Methods, Applications, and Evaluation*.
50. MATTHAY MA, FOLKESSON HG, CAMPAGNA A, KHERADMAND F. Alveolar epithelial barrier and acute lung injury. *New Horiz* 1993; 1: 613-622.
51. PUGIN J, VERGHESE G, WIDMER MC, MATTHAY MA. The alveolar space is the site of intense inflammatory and profibrotic reactions in the early phase of acute respiratory distress syndrome. *Crit Care Med* 1999; 27: 304-312.
52. MATTHAY MA. Conference summary: acute lung injury. *Chest* 1999; 116: 119S-126S.

53. CONNER ER, WARE LB, MODIN G, MATTHAY MA. Elevated pulmonary edema fluid concentrations of soluble intercellular adhesion molecule-1 in patients with acute lung injury: biological and clinical significance. *Chest* 1999; 116: 83S-84S.
54. SIBILLE Y, REYNOLDS HY. Macrophages and polymorphonuclear neutrophils in lung defense and injury. *Am Rev Respir Dis* 1990; 141: 471-501.
55. SOUKKA H, RAUTANEN M, HALKOLA L, KERO P, KÄÄPÄ P. Meconium aspiration induces ARDS-like pulmonary response in lungs of ten-week-old pigs. *Pediatr Pulmonol* 1997; 23: 205-211.

6. ULTRASTRUCTURAL EVALUATION OF THE BRONCHIOLAR AND ALVEOLAR REGION IN NEONATAL RATS INTRATRACHEALLY INOCULATED WITH MECONIUM

6.1. Introduction

Meconium aspiration syndrome (MAS) has been recognized for many years as an important cause of neonatal respiratory distress in newborn babies (1,2). Histologically, pulmonary lesions are described as being mild to moderate and death is generally attributable to severe metabolic and respiratory acidosis, airway obstruction, atelectasis and impaired gas exchange. Neonates that survive the acute episode of this syndrome have a higher predisposition to a variety of perinatal and postnatal conditions such as pulmonary hypertension, persistent fetal circulation, airway obstruction and airway hyperreactivity (1,3-6). Whereas the mechanisms responsible for intrauterine defecation and aspiration of meconium are well understood, the pathogenesis of pulmonary lesions in MAS remains largely enigmatic.

Meconium is a complex material normally present in the fetal intestine and constitutes the first fecal material to be expelled soon after birth (6,7). It contains large quantities of squamous epithelial cells and keratin that originate when dermal and oropharyngeal epithelia exfoliate and mix with the amniotic fluid, which under normal conditions, is subsequently swallowed into the gastrointestinal tract (1,8). During fetal stress and hypoxia, increased intestinal peristalsis and abnormal relaxation of the anal sphincter cause abnormal meconium defecation into the amniotic sac. When amniotic fluid contaminated with meconium is aspirated, the airways and alveolar mucosa are irritated by

the keratin, epidermal cells and intestinal secretory products like bile, resulting in a local foreign body inflammatory response in the lung (6).

Most of what is known about the morphologic changes that take place in the lungs following meconium aspiration comes largely from autopsy reports of babies with MAS and, to a lesser extent, from experimental studies in animals inoculated with meconium. According to autopsy reports, the lungs of babies succumbing to MAS have multifocal atelectasis often referred to as “patchy atelectasis” (7,9,10). Microscopically, bronchi, bronchioles and alveoli contain variable amounts of meconium which appears as a bile-pigmented yellow material containing vernix caseosa (originated from fetal skin), squamous cells, keratin and cellular debris (11). In addition to atelectasis, air trapping and hyperinflation, aspiration of meconium induces a local inflammatory reaction commonly referred to as chemical pneumonitis (6,12). Microscopically, the inflammatory changes in MAS are primarily centered around the terminal bronchiolar and alveolar regions of the lungs where aspirated meconium typically induces edema and exudation of inflammatory cells. (12,13). Intraalveolar hyaline membranes, one of the morphologic hallmarks of another pediatric conditions known as “hyaline membrane disease” (neonatal respiratory distress syndrome), have also been reported in the lungs of some babies dying of severe MAS (14). The origin of these membranes is still uncertain but they are presumed to arise when pulmonary surfactant and exuded plasma proteins which combine and condense along the surface of alveolar walls (14-16).

In animals, meconium-induced bronchiolitis and alveolitis have been sporadically reported in calves, foals and puppies dying in the first two weeks of life (17-19). The

bronchi and bronchioles of these cases had microscopic evidence of meconium, keratin, mild alveolar exudation of neutrophils, macrophages and a few giant cells. The microscopic changes in the lungs of these animals were consistent with the pulmonary lesions of babies succumbing to MAS(2,17-20). Experimentally, pulmonary lesions similar to those reported in spontaneous MAS have been reproduced under laboratory conditions with intratracheal inoculation of meconium (12,21). One criticism of the majority of experimental models of MAS, since this syndrome occurs in the newborn, has been the use of adult rather than neonatal animals (13,22-25). Also interesting is the fact that there is a lack of studies in which homologous meconium is inoculated into the animal lungs; This raises the question of whether inoculation of human meconium in another animal species is a valid experimental approach.

Although animal models have been widely utilized to study the physiological changes in neonates with MAS, little has been done to study in detail the microscopic lesions induced by meconium in the lungs (12,20,26,27). As in spontaneous cases of MAS, experimental models in laboratory animals have shown that the inflammatory response concentrates in the terminal bronchioles and alveoli where neutrophils and macrophages are typically found (12,21). This is not unusual since many inhalation toxicology studies have proven that bronchioles and alveoli are the most susceptible sites for particle deposition and injury in the lungs (28-30). Many reports indicate that enzymes and free radicals released by phagocytic cells at the site of inflammation may injure bronchiolar and alveolar cells (31-34). Although it is well known that MAS induces bronchiolitis and alveolitis, it is still unknown whether injury to bronchiolar and alveolar cells, particularly type I pneumocytes (pneumonocytes),

may result from direct exposure to or the inflammatory response induced by meconium. This question could be best answered by ultrastructural study of bronchiolar and alveolar cell in neonatal animals inoculated with meconium.

There is controversial evidence suggesting that epithelial and endothelial necrosis in the lungs may occur as a direct result of meconium aspiration (12). This assumption is largely based on some chemical components of meconium such as bile and biliary salts that are presumed toxic for cell membranes (35-37). Other investigators believe that pulmonary necrosis, when present, is attributable to hypoxic lung injury and not to the direct toxic effects of the meconium (11,27). This ambiguity in experimental results could be explained in several ways: First, necrosis may be a subtle or infrequent lesion and therefore overlooked in some MAS studies. Second, necrosis of type II pneumocytes is not detectable by light microscopy. Finally, necrosis may not have been an end-point in many experimental studies (16,24,38,39). Recent reports suggest that necrosis is dependent on the concentration of meconium, therefore, this cellular change could only occur when animals are inoculated with higher concentrations of meconium which are probably seldom used in models of experimental MAS (Dr. Pekka Kääpä, personal communication). Finally, it has also been suggested that fragments of degenerated neutrophils trapped in alveolar walls may be confused with pyknosis and karyorrhexis, two of the most noticeable cell changes in necrosis (Section 4.3.2.1).

Thickening of the alveolar walls, a distinct morphologic change described frequently in the lungs of animals exposed to a variety of pneumotoxins (40-42) has not been properly evaluated in MAS. Although experimental studies have reported leukocyte

sequestration in alveolar capillaries and alveolar interstitium, it is uncertain if increase in alveolar thickness is a substantial microscopic lesion of animals experimentally inoculated with meconium. In an experimental study conducted in rabbits, the authors described a mild alveolar thickening as one the microscopic changes induced by meconium inoculation (12). Results of this Thesis (Section 4.3.2.2) showed microscopic evidence of alveolar thickening in the rats inoculated with meconium and killed at PID 1, 3 and 7, a fact that was corroborated by morphometric analyses described in Section 5.3.4.6.. According to the result of the morphometric study, rats of the meconium group had a 38% increase in alveolar wall thickness after one day of the inoculation compared to the rats of the saline control group. The structural changes in the alveolar walls that translate into an increase in septal thickness in rats inoculated with meconium could not be resolved at the light microscopic level and require analysis at the ultrastructural level.

In the last two decades, laboratory methods have been developed to assess accurately cellular integrity of the terminal bronchiolar and proximal alveolar regions of the lungs, the two most common sites for injury caused by inhalation of toxic substances (28,30,43-45). Proper ultrastructural evaluation of bronchiolar and alveolar cells has been achieved under controlled exposure to pneumotoxic substances followed by systematic sampling and processing of pulmonary tissue (29,30). In inhalation toxicology, these techniques are often conducted in the Fischer-344 rats since this strain is comparatively resistant to spontaneous pulmonary diseases, has uniform lung growth and has a lung size suitable for systematic sampling of bronchioles and alveoli (46). Adequate fixation is also critical to ensure optimal preservation of cell structures, homogenous distention of airways and alveoli and elimination

of postmortem artifacts frequently encountered in routine necropsy specimens submitted for transmission electron microscopy.

Since there is a lack of TEM studies in natural or experimental MAS, this study was designed to investigate the effect of meconium on the ultrastructure of terminal bronchiolar and proximal alveolar regions of neonatal Fischer 344 rats.

6.2. Material and methods

6.2.1. Animals

Neonates were obtained from pregnant *Fischer-344* rats originally purchased from commercial sources (Charles River, Québec) and bred at AVC. Selected male and female rats were subsequently used in a timed-pregnancy program based on vaginal cytology and following the reproductive protocols (47,48) described in detail in Section 2.2.1.. Neonates were housed with their dams, provided with commercial rat food, and water *ad libitum*, and maintained on a 12/12-hour light/dark cycle at 22° C and 50% relative humidity. To avoid infant rejection and cannibalism, pregnant dams were preconditioned 7-10 days before parturition following the protocol outlined by Park *et al.* (49) and described in Section 2.2.2.

6.2.2. Anesthesia

Rat neonates were anaesthetized with halothane (3% in 100% oxygen; 100-200 ml/min)(Fluothane®, MTC Pharmaceutical, Mississauga, Ontario, Canada) via a gas anesthetic machine using a modified protocol (50,51) at AVC. A detailed anesthesia protocol is described in section 2.2.4.

6.2.3. Inoculum

Meconium was aseptically collected from the intestine of newborn female rats

euthanised immediately after birth and prior to the intake of colostrum as described in Section 2.2.6. Briefly, collected meconium was pooled in sterile plastic vials and frozen at -80° C. After thawing, unfiltered meconium was mixed and suspended with 0.9% NaCl solution using sterile glass beads. The final concentration of unfiltered meconium was 15% wet weight in a volume of 0.05 ml.

6.2.4. Intratracheal inoculation of meconium

Neonates were intratracheally inoculated using the modified method (48,52) previously standardized and described in Section 2.2.8. In short, under deep halothane anesthesia, the larynx was visualized through the mouth using an otoscope and a small speculum (Welch Allyn, Skaneateles Falls, NY). A sterile spinal needle (25-gauge, 0.51 mm x 8.89 cm length, Becton Dickinson and Company, Franklin Lakes, NJ) with the edge rounded connected to a 1.0 ml syringe was used to instill the inoculum into the trachea. After inoculation, pups were observed on a heat pad (38°C) until they recovered from anesthesia and were reunited with the dam.

6.2.5. Euthanasia

All neonates were euthanised by exsanguination (severing the renal arteries) under deep halothane anesthesia as described in Section 2.2.9. Experiments followed the guidelines of the Canadian Council on Animal Care (53).

6.2.6. Experimental design

Twenty-four, male, 7-day-old neonates with an average weight of 15.6 ± 1.1 g were randomly assigned to two experimental groups (Control and 15% Meconium). Four neonates per group were killed at 1, 3, and 7 days postinoculation (PID 1,3 and 7) for lung

perfusion (Table XXVIII).

Table XXVIII. Ultrastructural study. Number of neonatal rats per treatment and days postinoculation.

| Treatment | Post-inoculation (Days) | | | Total |
|---------------------------|-------------------------|---|---|-------|
| | 1 | 3 | 7 | |
| Control (Saline solution) | 4 | 4 | 4 | 12 |
| Meconium (15%) | 4 | 4 | 4 | 12 |
| Total | 8 | 8 | 8 | 24 |

6.2.7. *Intratracheal lung perfusion of fixative*

Following euthanasia, the lungs of neonates were perfused *in situ* with fixative using the procedure described in Section 4.2.6. Briefly, the thorax was opened, the trachea was exposed and a 32mm length 20-gauge plastic catheter, (Cathlon IV™ Critikon Canada Inc, Ontario) was inserted through a transverse slit made in the wall of the trachea. The abdomen was opened, both hemidiaphragms were punctured to collapse the lungs and fixative was perfused intratracheally via the catheter at a constant pressure of 20 cm of fixative. The pressure was generated by gravity and was measured from the liquid level in the reservoir which was maintained at constant height (20 cm) above the hilus of the lung fixed *in situ*. To provide constant flow and pressure a modified "Marriott bottles system" was used (43) The system was made from 60 ml syringes connected to plastic tubing and the cathether. A stopper was used to control air flow. Syringes without plunger were maintained open after detachment of the stopper allowing refilling of fixative to the cylinder. Tubing, adaptors and valves were rebored to as large and consistent an internal diameter as possible. The rate of

flow of fixative was approximately 190 ml/min when not attached to the catheter.

The composition of the fixative used was 2% glutaraldehyde (JBS-Chem. Dorval, Quebec, Canada) buffered to pH 7.38 at room temperature using 0.1 Molar sodium cacodylate buffer and having a total osmolarity of 350 mosmol (Advanced wide-range osmometer 3WII, Advanced Instrument, Inc., MA). After a minimum of 30 minutes of fixation *in situ*, a tight ligature was placed around the trachea before removing the catheter to maintain the intrapulmonary pressure of the fixative, and the lungs were dissected free. Lungs were then immersed in 50 ml of fixative for two hours. Perfusion *in situ* was carried out under a fume hood.

6.2.8. Sampling

Samples of lung were obtained using a modified tiered random sampling model proposed by Pinkerton and Crapo (29) and illustrated in fig. 40, section 5.2.7. After fixation, the lungs were dissected and the different lobes separated before samples were taken. Using the tiered stage sampling method (29) and low magnification light microscopy, the lung was divided into a series of different morphological compartments or strata, from which samples representative of the strata of interest were randomly selected and used for electron microscopy.

6.2.9. Isolation of the alveolar region

The method described by Pinkerton *et al.* was modified and used to isolate the terminal bronchiole and alveolar region in neonatal rats (29). For small animals, such as the rat, the alveolar region of the lung can be reasonably assumed to be homogeneous and tissue samples randomly selected anywhere in the alveolar region are representative of this stratum.

As a first step, two representative longitudinal slices (approx. 2mm in thickness) of each animal's entire left lung and two transverse sections across the long axis of the right cranial lobes were sampled. Trimming was done while the pulmonary tissue was partially immersed in fixative. The first slice was used for morphometry in light microscopy and the parallel second facing slice was used to obtain the blocks for TEM.

6.2.10. Tissue processing

Processing of lung tissues for TEM followed the routine protocol adopted in the Electron Microscopy Laboratory at the Atlantic Veterinary College. Two samples were collected per lung and they were minced into more than 10 small pieces of approx. 1.0 mm³. Tissue pieces were immersed in 4 ml of fixative in glass vials for 90 minutes at room temperature, then washed in 0.1 M cacodylate buffer, 3 x 10 minutes on a rotator. Samples were postfixed in 1% osmium tetroxide (Marivac Ltd, Halifax, NS) in 0.1M cacodylate buffer pH 7.38 for 1 hour at room temperature, and washed with distilled water 1 x 10 minutes. Tissues were dehydrated through a graded series of alcohol solutions (50% ethanol 1 x 10 minutes; 70% ethanol, 2 x 10 minutes; 95% ethanol, 2 x 10 minutes and 100% ethanol, 2 x 15 minutes) to propylene oxide (PO) 2 x 10 minutes, and infiltrated with increasing proportions of Epon/Araldite (JBS-Chem. Dorval, Quebec, /Marivac LTD) in propylene oxide until they were in 100% Epon/Araldite (50:50 Epon/Araldite: PO, 30 minutes; 75:25 Epon/Araldite: PO, 30 minutes and 100% Epon/Araldite, 60 minutes in a vacuum desiccator). Ten pieces were randomly selected from each sample. Tissue pieces were embedded individually within Epon/Araldite in labelled micromoulds (Marivac Ltd) and polymerized in a vacuum oven (Model 1410, Johns Scientific Inc., ON) overnight at

65°- 70°C thereby generating ten blocks of tissue per area of lung sampled.

6.2.11. Thick sections and light microscopy

Blocks of tissue were randomly selected from the ten original embedded blocks of each of the two areas of the lung sampled. The only criterion used to select the tissues was proper orientation at the face of the block to minimize trimming of resin. Thick sections (0.5- μ m-thick) were cut using glass knives and an Ultracut E Microtome (Reichert Jung, Austria), mounted on glass slides and stained with 1% toluidine blue in a 1% sodium borate solution (54). Thick sections were examined using a light microscope (Nikon Labophot 104, Nikon Canada Inc., ON), sections with larger blood vessels or bronchi were discarded and new blocks were selected in no particular order. Tissue blocks containing mainly alveolar regions and terminal bronchioles were selected from control animals inoculated with saline solution and from animals with microscopic changes associated with the effect of meconium inoculation. Criteria for selection of blocks from animals inoculated with meconium included: 1. presence of meconium, 2. presence of neutrophils, 3. presence of alveolar macrophages, 4. thickening of alveolar septa, 5. granuloma formation, 6. multinucleated giant cells. These alterations were not present in control animal tissue, therefore, representative regions were only selected. Light micrographs were taken using 35mm Kodak TMX 100 Film in a Photo- Microscope III, Zeiss (Carl Zeiss, West Germany).

6.2.12. Thin sections and transmission electron microscopy

Sections of terminal bronchioles and adjacent alveolar sacs were identified and selected for further thin sections. Sections were cut at 70-80 nm using a diamond knife (Diatome, 45° angle, Marivac, Ltd.) and an Ultracut E Microtome and collected on uncoated

200-mesh copper grids. Sections were stained at room temperature with 5% uranyl acetate in 50% ethanol for 30 minutes, rinsed with distilled water and then stained with lead citrate (Sato) for 2 minutes and rinsed in distilled water (55). Thin sections were examined with a Hitachi H7000 transmission electron microscope (Hitachi, Tokyo, Japan) operating at an accelerating voltage of 75 kV. Images were recorded on 8.3 cm x 10.2 cm Kodak Estar Thick Base 4489 Electron Microscope film. Negatives were developed with Kodak Developer D-19, fixed in Kodak Rapid Fixer, immersed in Kodak Photoflo 200 solution, rinsed in distilled water and air dried. Prints were generated using a Durst Laborator S-45 Special Enlarger (Bolzano, Italy); work and final prints were made using Kodak Polycontrast III RC Paper and developed in a Kodak Ektamatic Processor (Eastman Kodak, Rochester, NY). Several micrographs were taken from selected sites of each sample with the aim of evaluating the ultrastructural changes induced by meconium.

6.3. Results

6.3.1. Intratracheal lung perfusion

The lung perfusion *in situ* with the modified system was able to maintain constant pressure of the fixative during fixation time without significant leak of fixative. The lungs underwent a rapid expansion during the first minute of fixation due to the initial flow of fixative. Once fixed, the lungs became firmer and pale yellow.

6.3.2. Gross lesions

Lungs from rats inoculated with meconium exhibited a multifocal green discoloration which became more evident after perfusion. No differences were noted grossly in the distension pattern between meconium-treated lungs and controls. Following fixation, the

lungs of neonates inoculated with meconium appeared heavier than controls, but not enough to achieve statistical significance as has been discussed in section 5.3.4.1.

6.3.3. Morphological changes

6.3.3.1. Meconium

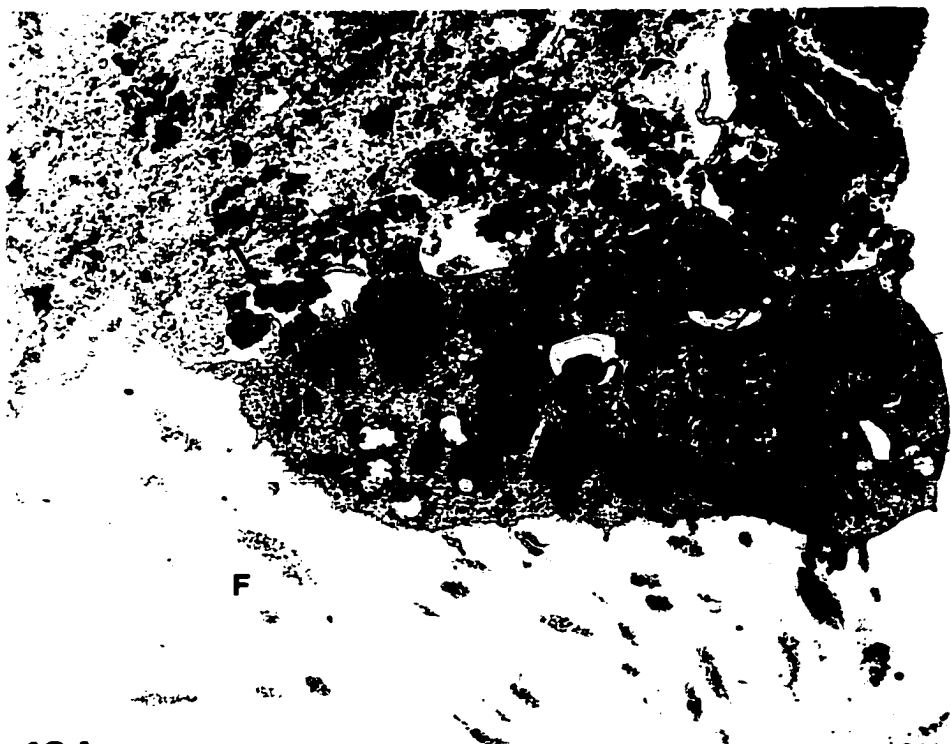
In thick sections stained with toluidine blue, meconium was visible in the bronchiolar and alveolar spaces as an amorphous pale material. Alveolar macrophages (PAM) and polymorphonuclear leukocytes (PMN) were commonly observed around the meconium. Ultrastructurally, meconium appeared as a mixture of different regions admixed with phagocytic cells (Fig. 48A). One of the regions was composed of an electron-lucent matrix of a loose fine fibrillar network interspersed with elongated aggregates of electron-dense material (Figs. 48A,B). Another region of the meconium plug was composed of electron-dense aggregates of cellular debris (Figs. 48A,C). Apparently activated PAM and PMN were also observed in this matrix (Figs. 49A,C). Some PAM at the interface between regions contained internalized electron-dense aggregates in phagolysosomes and presented large pseudopods at the surface towards the region of cellular debris (Figs. 48A,C). Enlarged PAMs exhibiting abundant debri-laden phagolysosomes were also present on the surface of the meconium (Fig. 49A). Degenerated neutrophils, and undetermined cell types were observed associated with this region of cellular debris (Fig. 49B). Degenerating cells exhibited highly vacuolated cytoplasm, a pyknotic nucleus with condensed chromatin, with no apparent nuclear envelope, and remnants of cytoplasmic material (Fig. 49B). Viable PMN were identified by their lobulated nucleus with dense heterochromatin and by the characteristic granules in the cytoplasm (Fig. 49C).

Fig. 48. Meconium in bronchiole of a neonatal rat, meconium group, PID3.

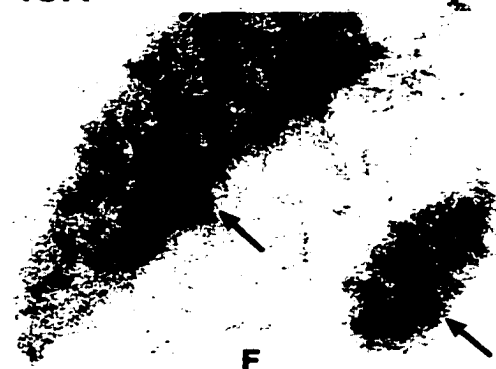
Fig. 48A. Alveolar macrophage (PAM) at the interface of the electron-lucent matrix of fibrillar network (F) of meconium and the electron-dense aggregates (D). The PAM has internaled cellular debris (arrows), with large pseudopods (arrowheads) and numerous phagolysosomes. Bar = 2 μ m.

Fig. 48B. High magnification of the electron-lucent matrix showing a loose fine fibrillar network (F) of meconium and multiple elongated aggregates of electron-dense material (arrows). Bar = 300nm.

Fig. 48C. High magnification of PAM cytoplasmic extensions (arrows) appearing ready to engulf electron-dense aggregates of meconium. Remnants of membranous materials (arrowheads) in electron-dense phase. Bar = 300 nm.



48A



F

48B



48C

Fig. 49. Meconium plug in bronchiole at PID 3.

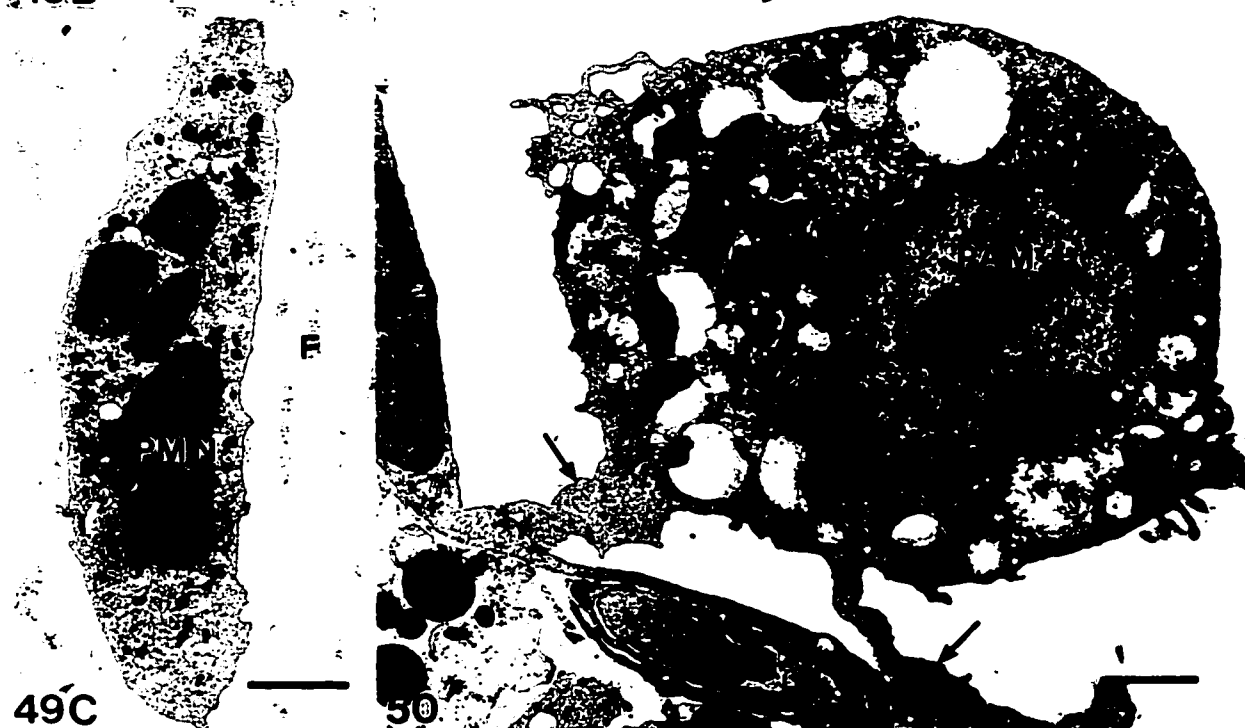
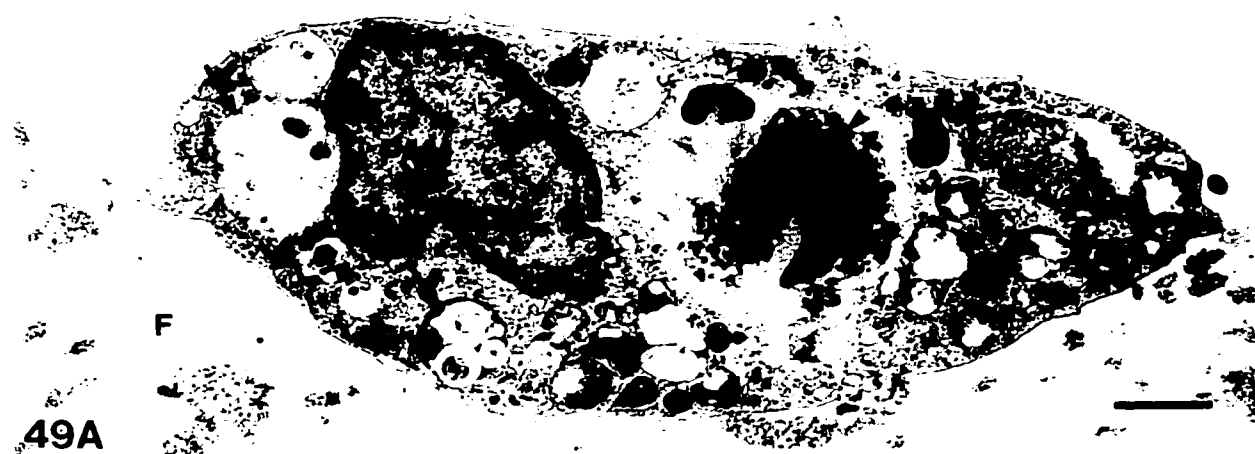
Fig 49A. Enlarged PAM at the periphery of the fibrillar region of the meconium plug (F) with abundant debris-laden-phagolysosomes (arrows). Large nuclear remnants are also present (arrowhead).

Bar = 2 μ m.

Fig. 49B. Degenerating PMN with pyknotic nucleus (arrow) and other necrotic cells at the periphery of meconium (F) exhibiting loss of nuclear and cytoplasmic integrity (arrowheads). Bar = 3 μ m.

Fig. 49C. Polymorphonuclear leukocyte (PMN) within the electron-lucent matrix of meconium (F). Bar = 3 μ m.

Fig. 50. Alveolar region from a rat inoculated with meconium, PID 1, showing an enlarged macrophage (PAM) containing numerous phagolysosomes (PL), vacuoles and pseudopods (arrows) closely apposed to a type I pneumocyte (EP I). Bar = 3 μ m.



Compared to control rats, the number of macrophages appeared to increase in alveolar spaces in the lungs of neonates inoculated with meconium at PID 1, 3 and 7. In these lungs, examination of alveoli in areas not associated with a meconium plug showed macrophages containing debris-laden-phagolysosomes and vacuoles and with pseudopods extending along the alveolar surface (Fig. 50).

6.3.3.2. Bronchiolar response to meconium

At PID 1 and 3, ciliated epithelial cells in bronchioles showed evidence of deciliation, particularly in areas of the lungs that contained or were close to meconium or to degenerated macrophages and neutrophils (Fig. 51A). The presence of basal bodies at the apex of some ciliated cells and the absence of the normal length of cilia at the surface confirmed that deciliation was a genuine morphologic change and not an artifact produced by the plane of section (Fig. 51B). Detached cilia showing their characteristic arrangement of microtubules were commonly observed in the meconium plug (Figs. 51A,C). Deciliation was not observed at PID 7 nor was it detected in any of the control rats inoculated with saline. No ultrastructural changes were evident in dome-like projections of the nonciliated epithelial cells associated with the presence of meconium (Fig. 51D). No other remarkable ultrastructural changes were observed in ciliated and nonciliated epithelial cells in bronchioles of the meconium group compared with the control animals.

6.3.3.3. Alveolar response to meconium

At the alveolar level, type I pneumocytes did not show notable ultrastructural alterations at PID 1 and 3 in the rats inoculated with meconium. However, at PID 1 and 3, inoculation of meconium induced an apparent increase in type II pneumocytes, many of

Fig. 51. Bronchiole from a rat inoculated with meconium, PID 3.

Fig 51 A. Ciliated epithelial cells (C) showing evidence of deciliation. Basal bodies (large arrows) and short cilia (arrowhead) are in close association with the meconium plug (M) containing degenerating macrophage (PAM) and fragments of detached cilia (small arrows). Bar = 1 μ m.

Fig. 51 B. High magnification of the apical surface of a ciliated cell showing evidence of an abbreviated cilium (arrowhead) and basal bodies (arrows). A degenerating PAM is present in close proximity to the ciliated cell. Bar = 300 nm.

Fig. 51 C. High magnification of the remnant of a detached cilium within the meconium matrix. Note the characteristic microtubule arrangement (arrowhead). Bar = 300 nm.

Fig. 51 D. A non ciliated epithelial cell (NC) showing that the integrity of the characteristic dome-like structure at the apex (*) is maintained. A ciliated epithelial cell (C) with normal cilia (arrows) is also present. A degenerating cell (arrowhead) is observed in the meconium plug (M). Bar = 1 μ m.



which exhibited microvilli and numerous secretory granules with the characteristic lamellar arrangement of surfactant (Fig. 52). Surfactant in the form of unfolded lamellae and myelin structures were present free in alveolar spaces close to the surface of type II pneumocytes (Figs. 52,53).

At PID 1 and 3, a remarkable inflammatory response in the alveolar regions was clearly associated with the presence of meconium in the lungs. Areas of inflammation were characterized by the presence of enlarged and activated macrophages demonstrating numerous and remarkably long cytoplasmic extensions (pseudopods) which protruding into the alveolar air spaces and were in close contact with meconium (Fig. 54A). The interstitium beneath this region had distended interstitial spaces (edema) with increased cellularity. A layer of elongated macrophages which contained phagolysosomes and some with lamellar structures covered the meconium matrix (Fig. 54A). Cellular debris mixed with fibrin and characteristic lattice work arrangements of surfactant were also present in the alveolar spaces (Fig. 54A). Fibrin was recognized by its characteristic electron-dense aggregates of aligned fibrils (*Inset*). Fibrin was also found in close association with the surface of PAMs and sometimes partially enclosed by cell processes (Fig. 54 B). In spite of all these alveolar changes, the type I pneumocytes adjacent to areas of meconium-induced inflammation did not exhibited any ultrastructural changes.

Platelet aggregations in blood vessels and in alveolar capillaries were observed in the lungs of some neonates inoculated with meconium mainly at PID 1 and less frequently at PID 3 and 7 (Fig. 55). This aggregation of platelets in capillaries occurred concomitantly with intracapillary sequestration of PMN (Fig. 56). Small aggregations of platelets were

Fig. 52,53. Alveoli; rat inoculated with meconium, PID 1.

Fig. 52. A typical type II pneumocyte (EPII) showing lamellar bodies (LB) and microvilli (arrowheads). Note the characteristic intraalveolar surfactant arrangements (arrows). Capillary (C). Bar = 2 μ m.

Fig 53. Characteristic attenuated cytoplasmic extension of an intact type I pneumocyte (arrow). Pneumocyte type II (EPII) with microvilli. Lamellar myelin structures of surfactant in alveolar airspace (arrowheads). Bar = 2 μ m.

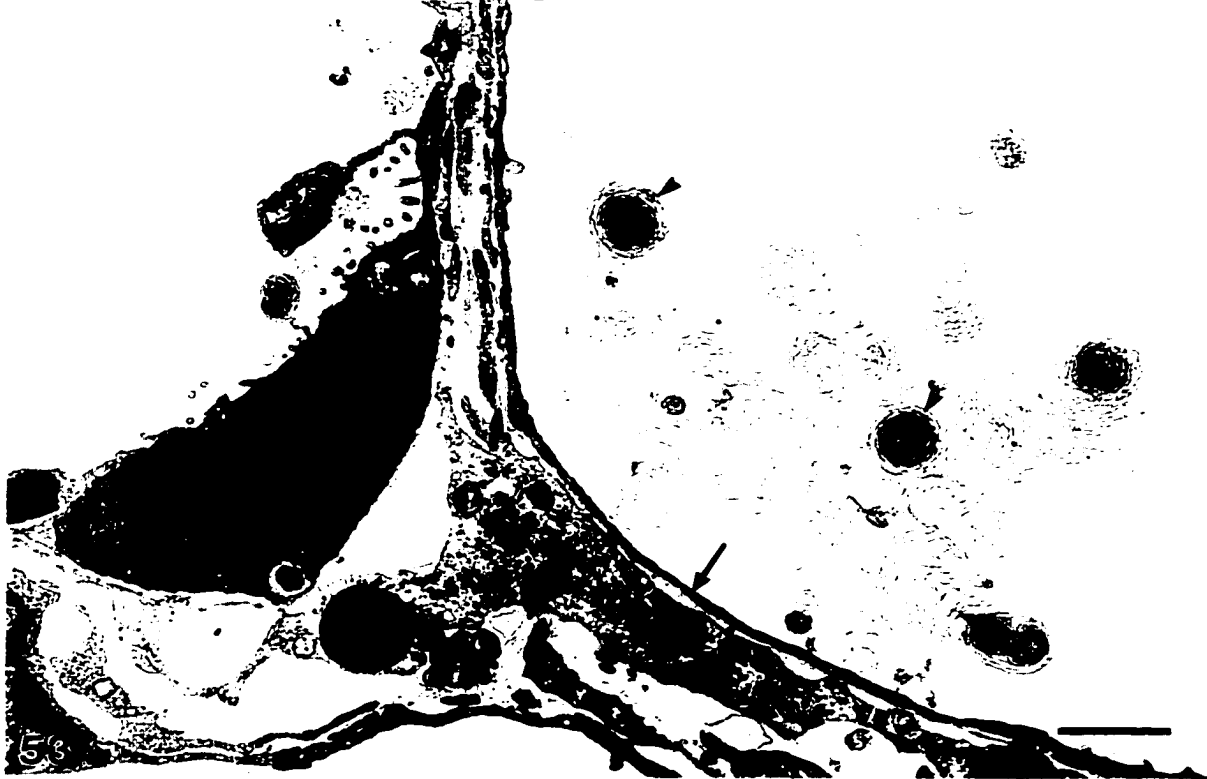
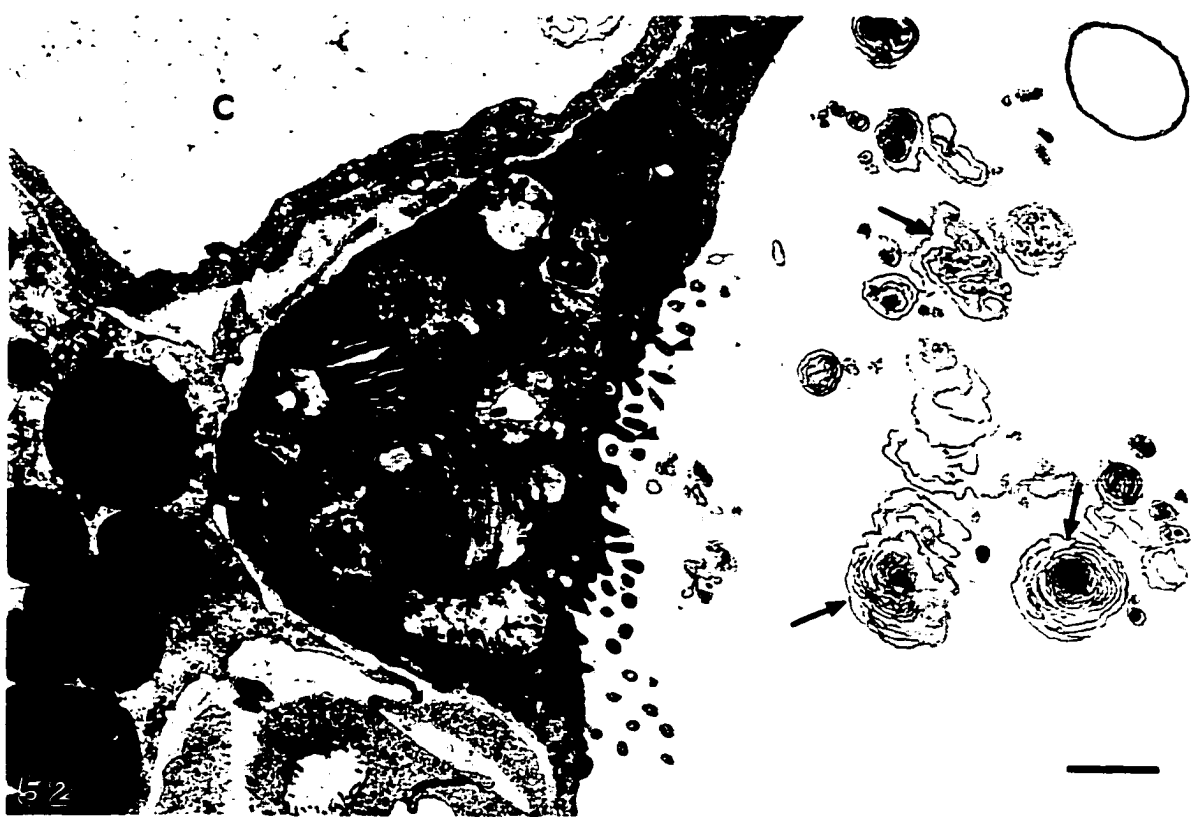


Fig. 54. Alveoli, rat inoculated with meconium, PID 1.

Fig. 54 A. Enlarged macrophages with multiple large pseudopods (large arrows) in contact with meconium (M). A layer of elongated PAMs (PAM) covers the meconium. Fibrin (small arrow) and surfactant (arrowhead) are present in the alveolar space (Alv). Bar = 2 μ m.

Inset: High magnification of fibrin (arrow) and lattice arrangements of surfactant (arrowhead) in alveolar space. Bar = 200 nm.

Fig. 54 B. Alveolar macrophage (PAM) with large pseudopods (arrow) covering the meconium-macrophage complex (M). Fibrin (arrowhead) partially enclosed by PAM. Bar = 2 μ m.

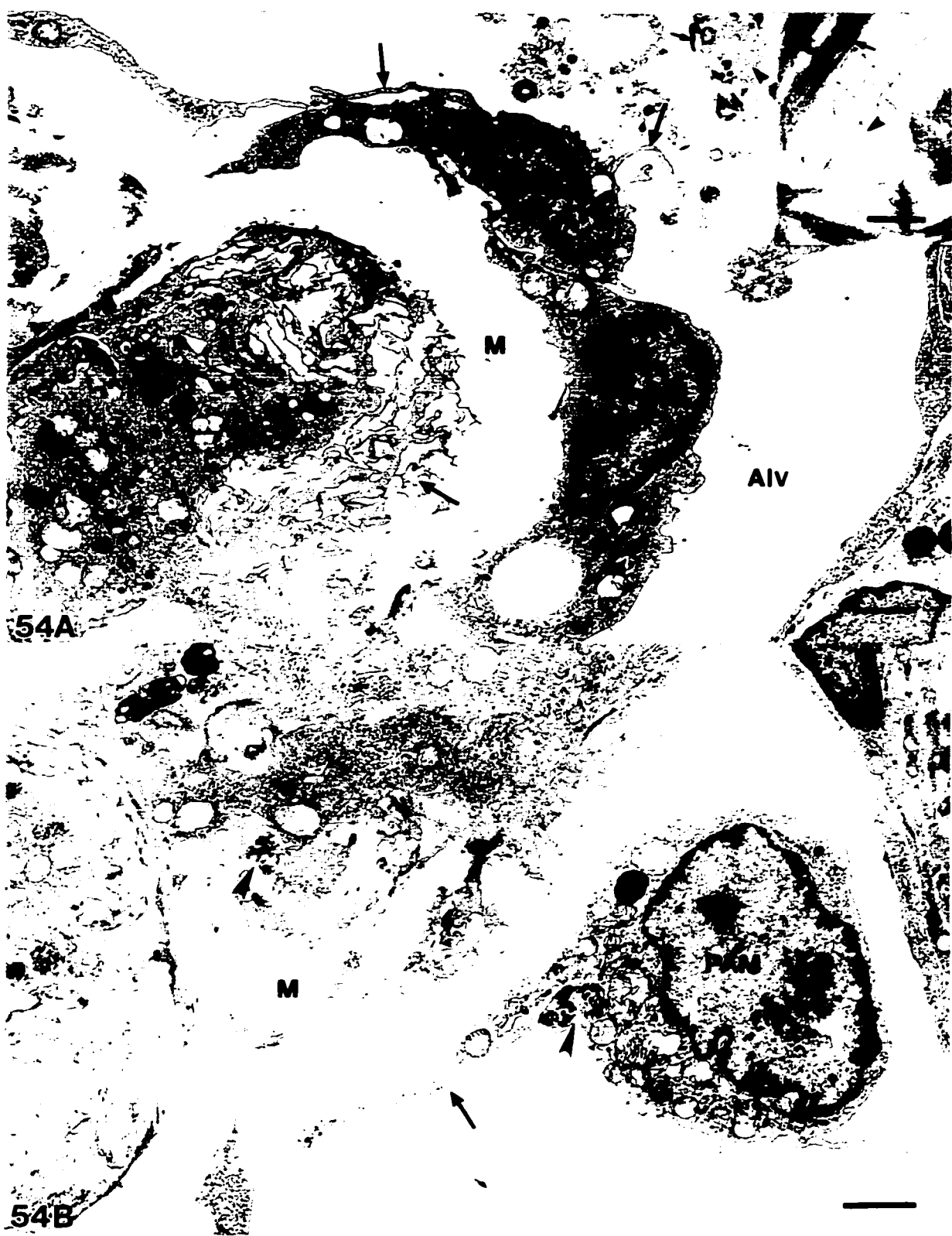
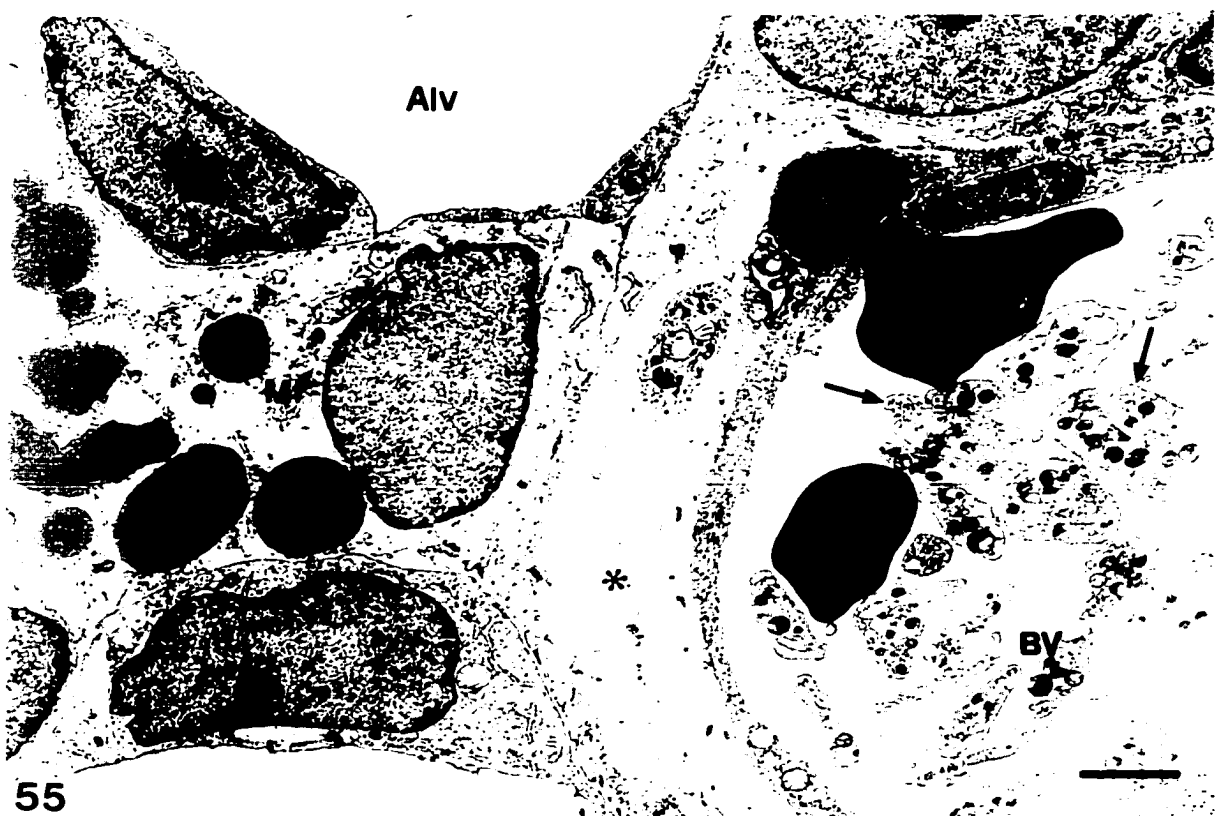


Fig. 55,56. Alveolar septum from meconium group, PID 1.

Fig. 55. A blood vessel (BV) shows aggregation of platelets (arrows). Note the edema with distension of interstitial space (*). Myofibroblast (M) with lipid droplets (L). Alveolar space (Alv). Bar = 2 μ m.

Fig. 56. Sequestration of neutrophils (PMN) in capillary (C) associated with interstitial edema (*). Distended interstitial area contains portions of myofibroblasts (M). Type II pneumocyte (EP II), Alveolar space (Alv). Bar = 2 μ m.



55



56

only occasionally observed in the lungs of control animals at PID 1 and 3 but not at PID 7.

Edematous distension of the interstitial spaces was commonly observed in the meconium inoculated animals, mainly at PID 1 and 3 (Fig. 57B) compared to controls (Fig. 57A). Sequestration of platelets and PMN in capillaries of alveolar walls was sometimes observed in association with areas of interstitial edema (Figs. 55,56).

In thick sections, a severe and multifocal neutrophilic and histiocytic response was observed in the lungs of PID 7 neonates inoculated with meconium. This remarkable inflammatory response was characterized by recruitment of PMN, PAM, and some apparent multinucleated cells mixed with cellular debris in the alveolar spaces (Fig. 58). At the TEM level, PMN (Fig. 59A) and PAM, were often enlarged with numerous internalized lamellar bodies. While some lamellar bodies (myelinosomes) were closely packed electron-dense structures, others were loosely packed with irregular lamellae (Fig. 59B). Apparent multinucleated cells observed in the thick sections represented clusters of macrophages aggregated in alveolar spaces at the TEM resolution.

Distension of alveolar interstitium with less edema but with conspicuously increased cellularity was associated with areas of inflammation in the PID 7 meconium group in thick sections. Thickening of the epithelial surface was primarily due to hypertrophy and hyperplasia of type II pneumocytes mainly in the proximal alveolar region and alveolar areas with inflammation (Fig. 60). At TEM level, type II pneumocyte profiles were found in close proximity, reflecting the increased number (hyperplasia) of these cells (Fig. 61). An apparent increase in size and change in morphology of lamellar bodies in the cytoplasm of type II pneumocytes was observed in the lungs of the meconium group (Figs. 62,64) at PID 7

Fig. 57. Alveolar septum, PID 1

Fig. 57 A. Control rat. Note the non distended (*) interstitial space. Membranous extensions from type I pneumocytes (arrows). Myofibroblast (M) with lipid droplets (L). Alveolar space (Alv). Bar = 2 μ m.

Fig. 57B. Rat meconium group. Distension of interstitial space with edema (*). Membranous extensions from type I pneumocytes (arrows). Myofibroblasts (M) with lipid droplets (L). Alveolar space (Alv). Bar = 2 μ m.

Alv



57A

Alv



57B

Fig. 58. Light micrograph of thick resin section; alveolar space, PID 7. Conspicuous recruitment of neutrophils (arrows) and alveolar macrophages (arrowhead) after meconium inoculation. Bar = 20 μ m.

Fig. 59. Alveolar space, Meconium group, PID 7.

Fig 59A. Enlarged neutrophils (PMN) with multiple internalized lamellar bodies (arrowheads). Alveolar space (Alv). Bar = 2 μ m.

Fig. 59 B. High magnification; Neutrophil (PMN) with internalized lamellar bodies, some of which are electron-dense and closely packed structure (arrow), while others show irregular and loose arrangements (arrowhead). Bar = 300 nm.

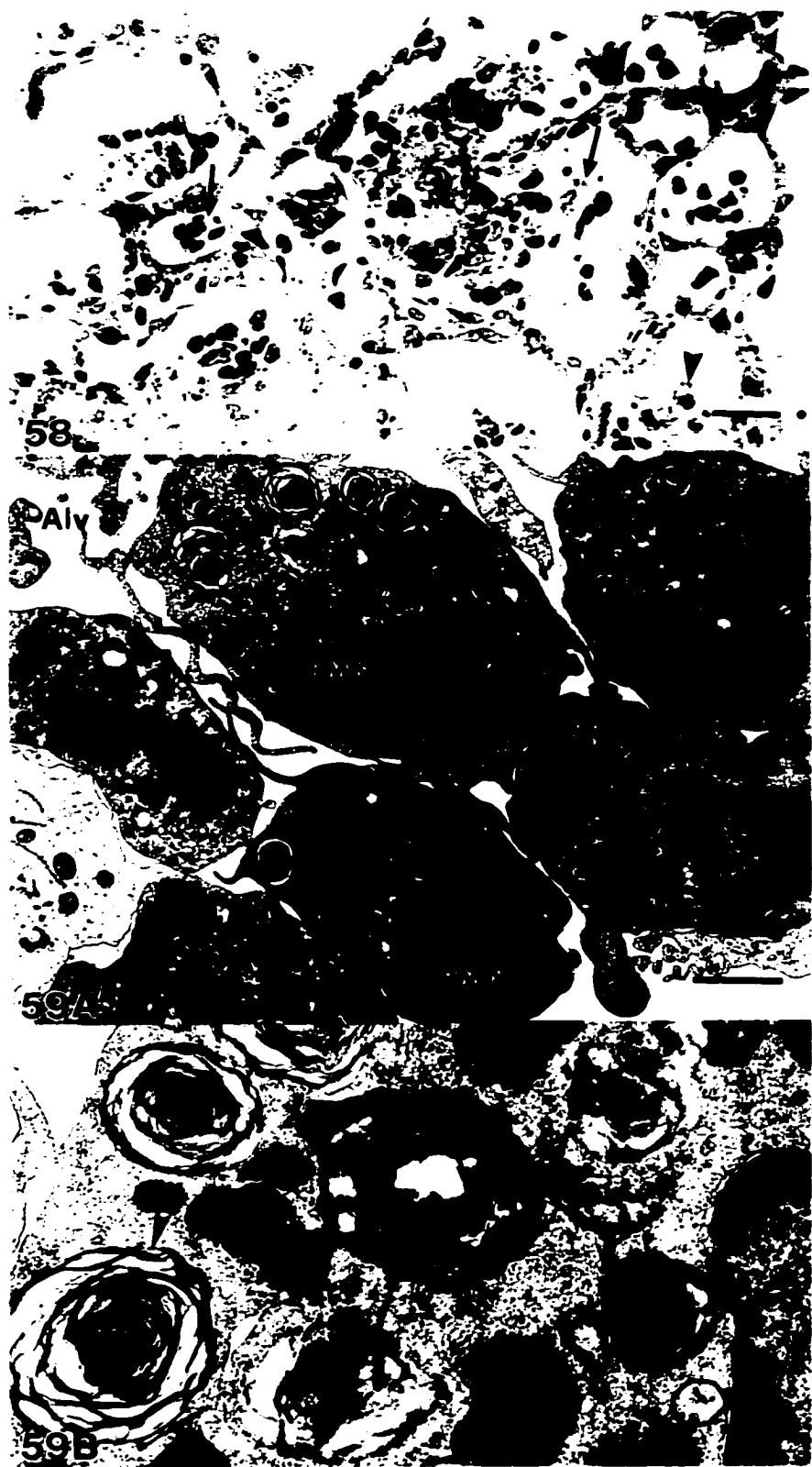


Fig. 60. Light micrograph of a thick resin section; alveolar septa, meconium group, PID 7. Hypertrophy and hyperplasia of type II pneumocytes (arrows) resulting in increase thickness of alveolar septum. Alveolar space (Alv). Bar = 10 μ m.

Fig. 61. Alveolus; meconium group, PID 7. Close proximity of type II pneumocytes profiles (EP II) indicating hyperplasia. Irregular arrangement of lamellar structures and fusion of lamellar bodies (arrows). Alveolar airspace (Alv). Bar = 2 μ m.

Fig. 62. Type II pneumocyte; meconium group, PID 7. Increased size of lamellar bodies (LB) with irregular and loose arrangement of lamellar structures (arrow). Note the fusion of lamellar bodies (arrowheads). Bar = 2 μ m.



compared with the controls (Fig. 63). Type II pneumocytes exhibited abundant and irregular arrangement of lamellar bodies and fusion of two or more lamellar bodies (Figs. 62,64). Release of lamellar structures to the alveolar space associated with fused lamellar bodies was also observed (Fig. 65). Hypertrophy and hyperplasia of type II pneumocytes or increased release of lamellar bodies into the alveolar space was not a feature in the lungs of control animals.

Although perivascular spaces were markedly distended and alveolar epithelium and interstitium of rats inoculated with meconium were hyperplastic at PID 7, endothelial cells did not exhibit changes. Platelet aggregation and sequestration of PMN in capillaries of alveolar walls were present in the meconium groups but not in controls. An increased thickness of alveolar septa in areas of proliferative response (Fig. 66) was correlated with densely packed interstitial cells, including fibroblasts, myofibroblasts, extravascular PMN, and red blood cells (Figs. 67,68). Isolated necrotic cells, some with lamellar bodies (Fig. 69) and others cells with unrecognizable characteristics other than pyknotic nuclear material were observed in the interstitial space or in alveolar pockets (Fig. 70).

Focal, proliferative responses in proximal alveolar regions were observed in lungs from neonates inoculated with meconium and killed at PID 7. Also, there was a notable increase in cellularity at the region of transition between the terminal bronchioles and alveoli extending from the interstitium through to the alveolar space (Fig. 71). The interstitium of these proliferative areas contained numerous myofibroblasts and fibroblasts, along with PAM, PMN, red blood cells and fibrin, both within the interstitium and in the alveolar space.

Fig. 63. Type II pneumocyte (EPII); control group, PID 7. Normal size of lamellar bodies showing regular arrangement of lamellar structures (arrows). Bar = 500 nm.

Fig. 64. Type II pneumocyte (EPII); meconium group, PID 7. Numerous lamellar bodies with irregular arrangement of lamellae (arrows). Bar = 500 nm.

Fig. 65. Type II pneumocyte; meconium group, PID 7. Fusion of lamellar bodies (arrows) and release of lamellar structures (arrowheads) to the alveolar airspace (Alv). Bar = 500 nm.



63



64

Alv



65

Fig. 66. Light micrograph of a thick resin section; alveolar septa, meconium group at PID 7. Increased thickness of interstitium with high cellularity (arrows). Alveolar space (Alv). Bar = 20 μ m.

Fig. 67. Alveolar septum; meconium group, PID 7. Proliferative response with densely packed fibroblastic cells (F), myofibroblasts (M), extravascular neutrophils (PMN), and red blood cell (*). Bar = 2 μ m.

Fig. 68. Alveolar septum; meconium group, PID 7. Proliferation of fibroblastic cells (F), myofibroblasts (M), presence of neutrophils (PMN), and red blood cell (*) in interstitial matrix. Bar = 2 μ m.



Fig. 69. Alveolar interstitium; meconium group, PID 7. Necrotic cell with pyknosis (arrow) and lamellar bodies (arrowhead) adjacent to interstitium or in an alveolar pocket, associated with proliferation of fibroblastic cells (F) and myofibroblasts (M) in interstitial matrix. Red blood cell (*) Bar = 2 μ m.

Fig. 70. Alveolar interstitium; meconium group, PID 7. Necrotic cell with pyknosis (arrow) and fragmentation of chromatin (arrowhead), fibroblastic cells (F) undifferentiated cells (U), myofibroblasts (M), and presence of neutrophils (PMN) in interstitial matrix. PAM in alveolar space (Alv). Bar = 2 μ m.

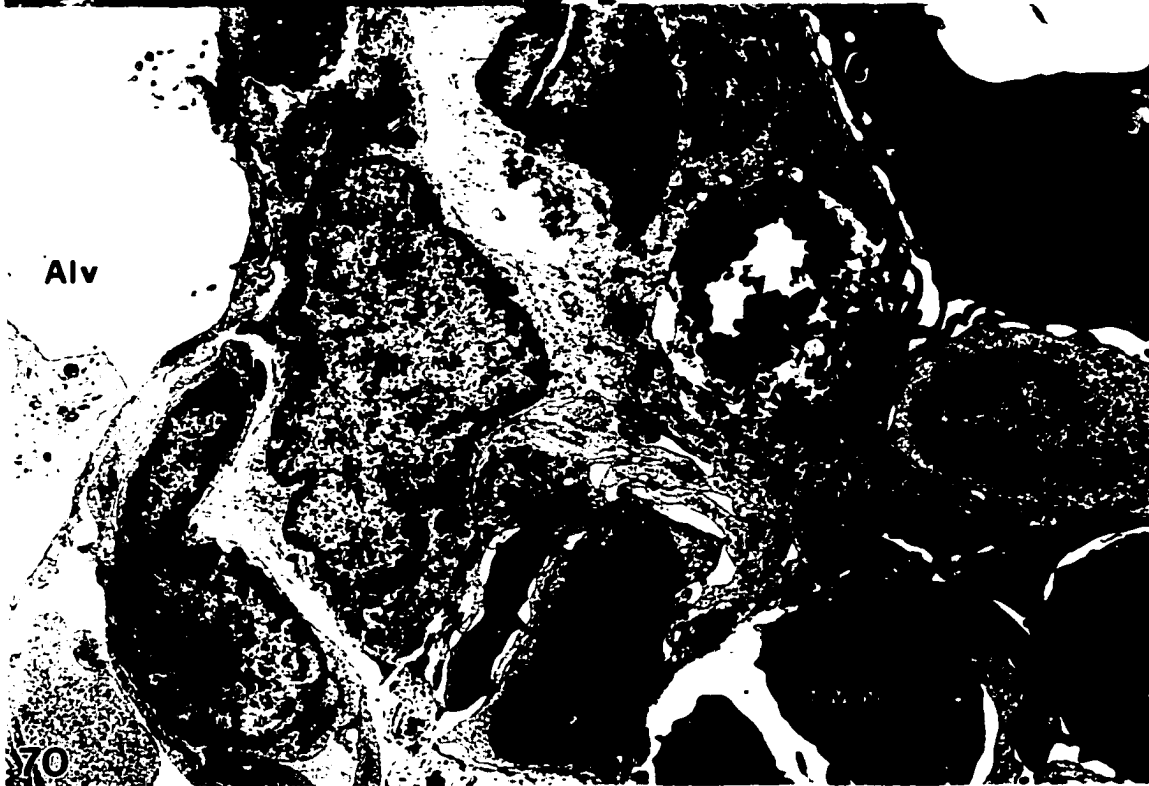


Fig. 71. Light micrograph of thick resin section from meconium group showing a large proliferative mass (P) at the region of transition between terminal bronchiole (arrow) and alveoli (arrowhead) and protruding from the interstitium (I) to the alveolar space (Alv). Boxed area enlarged in Fig. 73. Bar = 20 μ m.

Fig. 72. Transition of bronchiolar nonciliated cell (NC) to alveolus, meconium group, PID 7. Proliferation of myofibroblasts (M) and macrophage (PAM) migrating from interstitium through discontinuities in alveolar surface (arrow) to the alveolar air space (Alv). Bar = 2 μ m.

Fig. 73. Light micrograph of boxed area in fig. 71; meconium group, PID 7. A proliferative mass consists primarily of myofibroblasts (M) rich in lipid droplets (arrows), and fibroblastic cells (arrowheads) migrating from alveolar interstitium (I) to the alveolar airspace (Alv). Bar = 10 μ m.

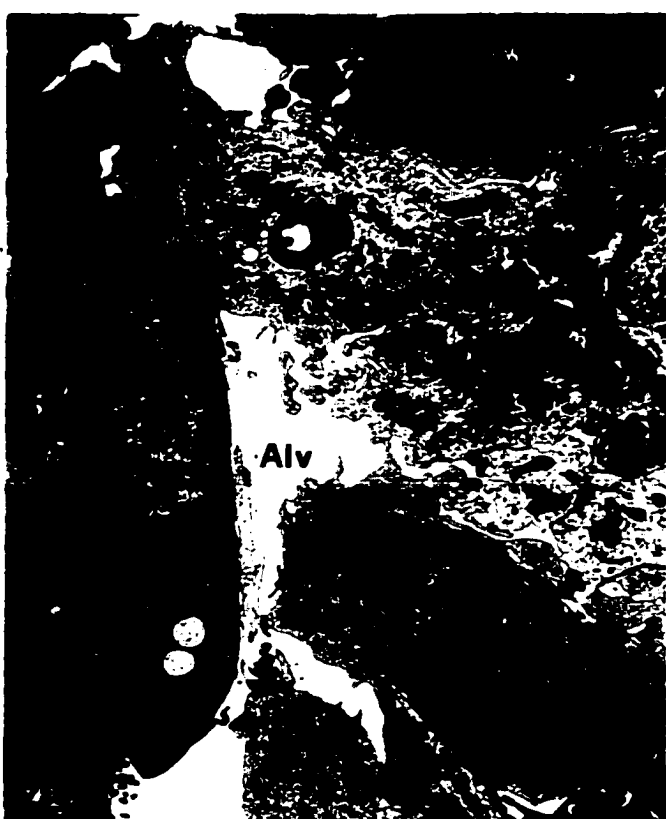
Fig. 74. Proliferative mass; meconium group, PID 7, showing myofibroblasts (M) rich in lipid droplets (arrows). Alveolar airspace (Alv). Bar = 2 μ m.



71



73



Fibroblasts, myofibroblasts and macrophages also protruded through alveolar gaps or defects suggesting a cell migration into the alveolar air spaces (Figs. 72,73). The external surface of this proliferative process in contact with the airspace was not covered by recognizable bronchiolar or alveolar epithelial cells (Fig. 74), and the cells forming the intraalveolar nodules were fibroblast-like cells and lipid-laden myofibroblasts. However, some other cells involved in this highly proliferative response were undetermined because of the lack of characteristic features or undifferentiated appearance.

All type I pneumocytes, whether or not they were associated with areas of proliferative inflammation, remained without significant changes as were those in controls at PID 7.

6.4. Discussion

Using the random sampling procedure suggested by others (29) it was possible to identify, in thick sections, the transition between terminal bronchioles and the alveolar region in rat neonates. It was easy to identify and select the dichotomous branching from the terminal bronchiole and alveolar sacs as it occurs in adult rats from which ultrathin sections could be made for TEM.

Transitions from ciliated to nonciliated cells in the terminal bronchiole and to pneumocytes type I in the proximal alveolar region were preserved and readily recognized. Preservation of epithelial cells in terminal bronchioles and alveoli was confirmed by evaluation of the integrity of membranes, cilia, microvilli and mitochondria. In all cell types some mitochondria were swollen with portions of the matrix appearing vacuolated and without detail at PID 1 and 3 but not at PID7. This swelling of mitochondria could be an

effect of inadequate osmolarity for all different cell types and ages of animals used in this study. There are different fixation protocols described in the literature with a wide range of osmolarities from 200 to 550mosmol (30,43,46,56). Since no fixation procedure is available that satisfies all demands, the choice and standardization of a particular fixation procedure is always a compromise (56).

As reported in other studies, the pulmonary interstitium of the neonatal rats showed many myofibroblasts rich in lipid droplets. These lipid-containing cells are normally found in the interstitium of neonatal rats (46), mice (57) and hamsters (58). The myofibroblast is the predominant cell in the interstitial space and it contains highly branched cytoplasmic processes. Myofibroblasts are located in the interalveolar septa and around capillaries and form a link between the basement membranes of adjacent alveoli. In contrast to the fibroblast, the myofibroblast contains bundles of actin and myosin (myofilaments). Contractile properties, such as regulating the blood flow under hypoxic conditions, are attributed to these cells. Myofibroblasts can also synthesize collagen and therefore it has been suggested that they may play a role in the modulation of the flexibility of the alveolar wall (59).

6.4.1. Meconium

Unlike in routine histology of paraffin sections, meconium was difficult to recognize in thick resin sections stained with toluidine blue because of its pale appearance. Although there are very few reports about the ultrastructural appearance of meconium, it is known that it has an amorphous and spherical appearance but, unlike surfactant, it lacks multilamellar arrangements (60). Structurally, the morphologic appearance of the meconium in the rat lung

had similar conformational phases as those shown in electron micrographs of human meconium (60) and consisted of a mixture of a loose fibrillar matrix and an electron-dense matrix of cellular debris. Based on the known composition of meconium, the loose fine fibrillar network could be formed by the abundant mucopolysaccharides contained in meconium (8,61). The different cells contained in meconium originate from amniotic fluid, gastrointestinal tract, and fetal skin, and, along with the degenerated PAM and PMN account for the electron-dense matrix of cellular debris (8,62,63).

The fact that meconium was surrounded by PAMs and PMNs was not surprising since this material is known to act as a foreign body in the lungs (9,26). Ultrastructurally, the presence of meconium in the cytoplasm of activated PAM corroborates the role of these phagocytic cells as the main scavengers in the alveolar milieu, not only in adult animals but also in neonates (59,64). Interestingly, activated PMNs, were also associated with the removal of meconium and cellular debris, suggesting that these leukocytes also participate in the clearance of aspirated meconium. The recruitment of PMN in airways and alveoli with meconium could be explained by the release of chemokines from activated PAM that may act as chemoattractant for PMN (65,66). On the other hand, it has been demonstrated that meconium *per se* contains the cytokine interleukin 8 (IL-8) which is a potent chemoattractant for PMN (67).

6.4.2. Bronchiolar response to meconium

Ultrastructural changes in the bronchiolar epithelium were only observed in the ciliated cells of the neonatal rats inoculated with homologous meconium at PID 1 and 3. This change was characterized by the loss of cilia, a process commonly referred to in the

literature as deciliation (30,68). Deciliation was primarily associated with the presence of meconium in the airways and fragments of cilia were frequently observed within the meconium plugs. Damage to bronchiolar epithelium with deciliation and necrosis has been described in rabbits after inoculation of human meconium (12) and following inhalation of numerous pneumotoxins (30,69). According to previous investigations, meconium causes epithelial damage as a result of chemical irritation caused by bile and various enzymes present in this material (12,39). Since there was ultrastructural evidence of degeneration of leukocytes with release of their granules, it is also possible that released lysosomal enzymes could have played a role in the deciliation of ciliated cells in the rat neonates as suggested by others (31-33).

6.4.3. Alveolar response to meconium

Inoculation of meconium into the neonatal rat lung induced a rapid influx of PMN and PAM into alveolar spaces that persisted from PID 1 to 7. Rapid recruitment of inflammatory cells has been also documented after inoculation of meconium in rabbits and pigs (12,20,21,70). It has been suggested that mediators of inflammation are responsible for the attraction of leukocytes after inoculation of meconium. Some of these mediators include tumor necrosis factor- α (TNF- α), interleukin 1 β (IL-1 β), and IL-8, which have been identified as important pro-inflammatory cytokines in meconium aspiration syndrome (31-33).

Intracapillary sequestration of PMN and platelet aggregation in neonates inoculated with meconium was closely associated with interstitial edema. Interestingly, local aggregation of platelets with increased production of thromboxane A₂ has been proposed as

the possible cause of pulmonary hypertension in infants with MAS and may play a role in the hypertensive response characteristic of this syndrome (71). Secretory components released by activated platelets may also be important mediators for the subsequent neutrophil recruitment and lung injury as suggested for other pneumotoxins (30).

Edema, vascular sequestration of leukocytes and aggregation of platelets in the lungs of neonatal rats inoculated with meconium in the present study were features suggestive of adult respiratory distress syndrome (ARDS). Similar observations have been also reported in piglets experimentally inoculated with meconium (70). These authors indicated that the pathogenesis of MAS shares many similarities with ARDS and suggested that degranulation of polymorphonuclear leukocytes in alveolar capillaries may be an event following aspiration of meconium (70).

The chronology of ultrastructural changes seen in the lungs of neonatal rats inoculated with meconium parallels that of ARDS. For instance, the structural alterations in the acute stage of ARDS (72-74) comprise an early and predominant interstitial and alveolar edema, consistent with the interstitial edema found in the present study. Presumably, this change resulted from damage to the air-blood barrier. Since there was no convincing evidence that type I pneumocytes were injured by meconium, it is possible, as reported by others, that changes in permeability were primarily centered on the endothelial side of the air-blood barrier (72-74). Nonetheless, some studies have shown that edema, intraalveolar hemorrhage and formation of exudates can occur in ARDS without significant ultrastructural changes in the endothelium (72). Generally, in ARDS, endothelial layers seem unaffected, even in close vicinity to a total epithelial destruction, and the endothelial

cell layer, separated merely by the fused basement membrane, is usually continuous, with intact cell junctions (72). Based on this information, it is likely that the movement of plasma fluid and blood cells in rats inoculated with meconium was due to an enlargement of the endothelial cell junctions rather than necrosis of the endothelium.

Some researchers have reported the formation of intraalveolar hyaline membranes in pig neonates inoculated with meconium (70). Although there was an interstitial edema, leakage of protein (BAL analyses; see section 3.3.4.2.) and intraalveolar fibrin, formation of hyaline membranes was not a feature in the neonatal rats inoculated with meconium. This discrepancy between rats and pigs could be due to species difference, artifacts of fixation or dose of meconium (12,38,56,75). Future studies should investigate if hyaline membranes develop with higher doses of meconium or could be better visualized by using other methods of fixation.

There is firm evidence in previous reports that, following acute lung injury, necrosis of type I pneumocytes is rapidly followed by hyperplasia of type II pneumocytes (41,72,76,77). It is then generally assumed that proliferation of type II cells is indicative of a previous rapid loss of type I pneumocytes. However, experimental studies in rat lungs dosed with bacterial lipopolysaccharide (LPS) have demonstrated that hyperplasia of type II cells can be observed even when there is minimal ultrastructural change in type I cells (77). These observations may explain why, in this study, rat neonates inoculated with meconium developed hyperplasia of type II pneumocytes at PID 7 and yet type I cells did not show ultrastructural evidence of necrosis.

The thickening of the alveolar septa in rats inoculated with meconium which was

corroborated by morphometry (section 5.3.4.6.) was also detected by TEM. The thickening of alveolar septa at PID 1 and 3 was primarily due to interstitial edema, while at PID 7, there were also proliferative changes contributing to the alveolar thickening.

At the alveolar surface, the hypertrophy and hyperplasia of pneumocytes type II in the lungs after inoculation of meconium at PID 7 resembles the effect of LPS on these cells described in adult rats (78). Increase in size of type II pneumocytes, swollen mitochondria and localized cisternal dilation of endoplasmic reticulum were found after LPS inoculation in rats (78)(78). Volume density and number of lamellar bodies remained unaltered in LPS-injured P-II. Distension, necrosis and desquamation of type II pneumocytes were also described (78).

An interesting ultrastructural finding in these rat neonates inoculated with meconium was the presence of numerous lamellar bodies in PMN and PAM. Similar changes have been described in rats inoculated with other pneumotoxins (78) where phagocytosed lamellar bodies originated from necrotic and desquamated type II pneumocytes. The lamellar structures are called myelinosomes and originate from the secretory granules, composed mainly of phospholipids, which are released by type II pneumocytes (79).

Intratracheal inoculation of meconium caused an apparent increase in the number and size of lamellar bodies in pneumocytes type II and hypertrophy and hyperplasia of these cells. These findings suggest that meconium caused activation of type II pneumocytes and a subsequent overexpression of surfactant. It has been suggested recently that meconium has a direct effect on the type II pneumocyte of adult rats (80). This possible overexpression is also supported in the present study by the fact that PMN and PAM contained many

internalized lamellar bodies.

The interstitial proliferative response that occurred in the lungs of neonatal rats at PID 7 following the inoculation of meconium was considered consistent with lung repair. Many studies have shown that proliferation of mesenchymal cells in the pulmonary interstitium is part of the repair process of the lung after acute injury regardless of its cause (72,81,82).

Morphometric and morphological studies have shown that intraalveolar fibrosis is a pattern of pulmonary structural remodeling in human patients with diffuse alveolar damage. In the early proliferative phase, activated myofibroblasts proliferated and migrated into alveolar spaces through gaps in the epithelial basement membrane and produced intraalveolar fibrosis (81). The same type of epithelial regeneration with hyperplasia of type II pneumocytes and cuboidal cells, and proliferation and migration of fibroblasts and myofibroblasts in alveoli was observed in human babies with respiratory distress syndrome (82).

6.4.4. Site of injury

The tendency for ultrastructural changes to be located at the proximal alveolar region and neighboring alveoli in the neonatal rats suggests that these areas are likely the main sites of injury and inflammatory response after inoculation of meconium. This was not an unexpected finding since the bronchoalveolar junctions are the most common sites targeted by many types of pneumotoxins (28-30). Interestingly, this site has the highest population of type II pneumocytes and alveolar macrophages (83). The proximal alveolar region has significant functional importance because it is a critical intersection between the conducting and respiratory portions of the lung(29).

6.4.5. Conclusions

In conclusion, results of this ultrastructural study shows that intratracheal inoculation of homologous meconium in seven-day-old rats induces acute inflammation formed by recruitment of PMN and PAM to the alveolar space, and sequestration of PMN and aggregation of platelets in capillaries. These changes parallel the leakage in the air-blood barrier with interstitial edema and escape of red cells and fibrin strands into the alveolar interstitium and alveolar space. Interstitial edema and sequestration of PMN are largely responsible for the early increase in thickness of the interstitial space at PID 1 and 3, followed by proliferation of mesenchymal cells and type II pneumocytes at PID 7. Meconium also induced notable deciliation of bronchiolar cells at PID 1 and 3. As part of the effect of meconium and repair mechanism, there is hypertrophy and hyperplasia of type II pneumocytes, and proliferation of mesenchymal cells in the interstitium. This fibroblastic response also spills through gaps from interstitium into the alveoli causing focal intraalveolar fibrosis. Inoculation of 150 mg/ml of unfiltered meconium in this study did not induce detectable ultrastructural changes in type I pneumocytes or endothelial cells.

6.5. REFERENCES

1. SRINIVASAN HB, VIDYASAGAR D. Meconium aspiration syndrome: current concepts and management. *Compr Ther* 1999; 25: 82-89.
2. CLEARY GM, WISWELL TE. Meconium-stained amniotic fluid and the meconium aspiration syndrome. An update. *Pediatr Clin North Am* 1998; 45: 511-529.
3. SWAMINATHAN S, QUINN J, STABILE MW, BADER D, PLATZKER AC, KEENS TG. Long-term pulmonary sequelae of meconium aspiration syndrome. *J Pediatr* 1989; 114: 356-361.
4. MACFARLANE PI, HEAF DP. Pulmonary function in children after neonatal meconium aspiration syndrome. *Arch Dis Child* 1988; 63: 368-372.
5. GUPTA AK, ANAND NK. Wheezy baby syndrome: a possible sequelae of neonatal meconium aspiration syndrome. *Indian J Pediatr* 1991; 58: 525-527.
6. WISWELL TE, BENT RC. Meconium staining and the meconium aspiration syndrome. Unresolved issues. *Pediatr Clin North Am* 1993; 40: 955-981.
7. BRADY JP, GOLDMAN SL. Management of Meconium Aspiration Syndrome. In: Thibeault D W, Gregory GA, eds. *Neonatal Pulmonary Care*. Connecticut: Appleton-Century-Crofts, 1986: 483-498.
8. RAPOPORT S, BUCHANAN DJ. The composition of meconium: Isolation of blood-group-specific polysaccharides. Abnormal composition of meconium in meconium ileus. *Science* 1950; 112: 150-153.
9. BACSIK RD. Meconium aspiration syndrome. *Pediatr Clin North Am* 1977; 24: 463-479.
10. BROWN BL, GLEICHER N. Intrauterine meconium aspiration. *Obstet Gynecol* 1981; 57: 26-29.
11. KATZ VL, BOWES WAJ. Meconium aspiration syndrome: reflections on a murky subject. *Am J Obstet Gynecol* 1992; 166: 171-183.
12. TYLER DC, MURPHY J, CHENEY FW. Mechanical and chemical damage to lung tissue caused by meconium aspiration. *Pediatrics* 1978; 62: 454-459.
13. SUN B, CURSTEDT T, ROBERTSON B. Surfactant inhibition in experimental meconium aspiration. *Acta Paediatr* 1993; 82: 182-189.
14. SEO IS, GILLIM SE, MIRKIN LD. Hyaline membranes in postmature infants. *Pediatr*

Pathol 1990; 10: 539-548.

15. SEEGER W, GRUBE C, GÜNTHER A. Proteolytic cleavage of fibrinogen: amplification of its surfactant inhibitory capacity. Am J Respir Cell Mol Biol 1993; 9: 239-247.
16. SUN B, HERTING E, CURSTEDT T, ROBERTSON B. Exogenous surfactant improves lung compliance and oxygenation in adult rats with meconium aspiration. J Appl Physiol 1994; 77: 1961-1971.
17. LOPEZ A, BILDFELL R. Pulmonary inflammation associated with aspirated meconium and epithelial cells in calves. Vet Pathol 1992; 29: 104-111.
18. FURR M. Perinatal asphyxia in foals. Compend Contin Educ Pract Vet 1996; 18: 1342-1351.
19. FUENTEALBA C, LOPEZ A. Intrauterine aspiration pneumonia. Diseases of the respiratory system. Western Conference of Veterinary Diagnostic Pathologists ; Saskatoon, Saskatchewan: 1998;
20. WISWELL TE, FOSTER NH, SLAYTER MV, HACHEY WE. Management of a piglet model of the meconium aspiration syndrome with high-frequency or conventional ventilation. Am J Dis Child 1992; 146: 1287-1293.
21. DAVEY AM, BECKER JD, DAVIS JM. Meconium aspiration syndrome: physiological and inflammatory changes in a newborn piglet model. Pediatr Pulmonol 1993; 16: 101-108.
22. HOLOPAINEN R, SOUKKA H, HALKOLA L, KÄÄPÄ P. Meconium aspiration induces a concentration-dependent pulmonary hypertensive response in newborn piglets. Pediatr Pulmonol 1998; 25: 107-113.
23. GOODING CA, GREGORY GA, TABER P, WRIGHT RR. An experimental model for the study of meconium aspiration of the newborn. Radiology 1971; 100: 137-140.
24. FRANTZ ID, WANG NS, THACH BT. Experimental meconium aspiration: Effects of glucocorticoid treatment. J Pediatr 1975; 86: 438-441.
25. SUN B, CURSTEDT T, SONG GW, ROBERTSON B. Surfactant improves lung function and morphology in newborn rabbits with meconium aspiration. Biol Neonate 1993; 63: 96-104.
26. CRUICKSHANK AH. The effects of the introduction of amniotic fluid into the rabbits' lungs. J Pathol Bact 1949; 61: 527-531.

27. JOVANOVIC R, NGUYEN HT. Experimental meconium aspiration in guinea pigs. *Obstet Gynecol* 1989; 73: 652-656.
28. BOORMAN GA, SCHWARTZ LW, DUNGWORTH DL. Pulmonary effects of prolonged ozone insult in rats. Morphometric evaluation of the central acinus. *Lab Invest* 1980; 43: 108-115.
29. PINKERTON KE, CRAPO JD. Morphometry of the Alveolar Region of the Lung. In: Witschi M D, Brain JD, eds. *Toxicology of Inhaled Materials*. New York: Springer-Verlag, 1985: 259-285.
30. BARRY BE, CRAPO JD. Application of morphometric methods to study diffuse and focal injury in the lung caused by toxic agents. *Crit Rev Toxicol* 1985; 14: 1-32.
31. JONES CA, CAYABYAB RG, HAMDAN H. Early production of proinflammatory cytokines in the pathogenesis of neonatal adult respiratory distress syndrome (ARDS) associated with meconium aspiration. *Pediatr Res* 1994; 35: 339A-
32. SHABAREK FM, XUE H, LALLY KP. Human meconium stimulates murine alveolar macrophage procoagulant activity. *Pediatr Res* 1997; 41: 267A-
33. KOJIMA T, HATTORI K, FUJIWARA T, SASAI TM, KOBAYASHI Y. Meconium-induced lung injury mediated by activation of alveolar macrophages. *Life Sci* 1994; 54: 1559-1562.
34. SHENKAR R, ABRAHAM E. Mechanisms of lung neutrophil activation after hemorrhage or endotoxemia: roles of reactive oxygen intermediates, NF-kappa B, and cyclic AMP response element binding protein. *J Immunol* 1999; 163: 954-962.
35. HENDERSON RD, FUNG K, CULLEN JB, MILNE EN, MARRYATT G. Bile aspiration: an experimental study in rabbits. *Can J Surg* 1975; 18: 64-69.
36. LIBERMAN J. Proteolytic enzyme activity in fetal pancreas and meconium. *Gastroenterology* 1966; 50: 183-190.
37. OELBERG DG, DOWNEY SA, FLYNN MM. Bile salt-induced intracellular Ca⁺⁺ accumulation in type II pneumocytes. *Lung* 1990; 168: 297-308.
38. SUN B, CURSTEDT T, ROBERTSON B. Exogenous surfactant improves ventilation efficiency and alveolar expansion in rats with meconium aspiration. *Am J Respir Crit Care Med* 1996; 154: 764-770.
39. AL MATEEN KB, DAILEY K, GRIMES MM, GUTCHER GR. Improved oxygenation with exogenous surfactant administration in experimental meconium aspiration syndrome. *Pediatr Pulmonol* 1994; 17: 75-80.

40. CRAPO JD, PETERS GM, MARSH SJ, SHELBURNE JS. Pathologic changes in the lungs of oxygen-adapted rats: a morphometric analysis. *Lab Invest* 1978; 39: 640-653.
41. BARRY BE, MILLER FJ, CRAPO JD. Effects of inhalation of 0.12 and 0.25 parts per million ozone on the proximal alveolar region of juvenile and adult rats. *Lab Invest* 1985; 53: 692-704.
42. MERCER RR, COSTA DL, CRAPO JD. Effects of prolonged exposure to low doses of nitric oxide or nitrogen dioxide on the alveolar septa of the adult rat lung [see comments]. *Lab Invest* 1995; 73: 20-28.
43. TYLER WS, DUNGWORTH DL, PLOPPER CG, HYDE DM, TYLER NK. Structural evaluation of the respiratory system. *Fundam Appl Toxicol* 1985; 5: 405-422.
44. BREEZE RG, WHEELDON EB. The cells of the pulmonary airways. *Am Rev Respir Dis* 1977; 116: 705-777.
45. BURRI PH. Morphology and respiratory function of the alveolar unit. *Int Arch Allergy Appl Immunol* 1985; 76 Suppl 1: 2-12.
46. PINKERTON KE, BARRY BE, ONEIL JJ, RAUB JA, PRATT PC, CRAPO JD. Morphologic changes in the lung during the lifespan of Fischer 344 rats. *Am J Anat* 1982; 164: 155-174.
47. BAKER DEJ. Reproduction and Breeding. In: Baker H J, Lindsey JR, Weisbroth SH, eds. *The Laboratory Rat*. Orlando: Academic Press, 1979: 154-166.
48. WAYNFORTH HB. Experimental and surgical technique in the rat. New York: Academic Press, 1980.
49. PARK CM, CLEGG KE, HARVEY CC, HOLLENBERG MJ. Improved techniques for successful neonatal rat surgery. *Lab Anim Sci* 1992; 42: 508-513.
50. FLECKNELL P. *Laboratory Animal Anaesthesia*. San Diego, CA: Academic Press, 1996.
51. HARKNESS JE, WAGNER JE. *The Biology and Medicine of Rabbits and Rodents*. Philadelphia: Williams & Wilkins, 1995.
52. HENRY CJ, KOURIE E. Specialized Test Article Administration: Nose-Only Exposure and Intratracheal Inoculation. In: *Salem Heds*. New York: Marcel Dekker, 1987: 121-134.
53. CANADIAN COUNCIL ON ANIMAL CARE. *Guide to the Care and Use of Experimental Animals*. Ottawa, Ont.: CCAC, 1993.

54. BOZZOLA JJ, RUSSELL LD. *Electron Microscopy: Principles and Techniques for Biologists*. Sudbury, Massachusetts: Jones and Bartlett Publishers, 1992.
55. SATO T. A modified method for lead staining of thin sections. *J Electron Microsc (Tokyo)* 1968; 17: 158-159.
56. FEHRENBACH H, OCHS M. Studying lung ultrastructure. In: Uhlig S, Taylor AE, eds. *Methods in Pulmonary Research*. Basel: Birkhäuser Verlag, 1998: 429-454.
57. MEYRICK B, REID LM. Ultrastructure of alveolar lining and its development. In: Hodson W Aeds. *Development of the lung*. New York: Marcel Dekker Inc., 1977: 135-202.
58. SPIT BJ. Induction of lipid droplets in fibroblasts of the hamster lung by a diet high in vitamin A. *Exp Lung Res* 1983; 4: 247-257.
59. DORMANS JA. The ultrastructure of various cell types in the lung of the rat: a survey. *Exp Pathol* 1983; 24: 15-33.
60. BAE CW, TAKAHASHI A, CHIDA S, SASAKI M. Morphology and function of pulmonary surfactant inhibited by meconium. *Pediatr Res* 1998; 44: 187-191.
61. HOUNSELL EF, LAWSON AM, STOLL MS, KANE DP, CASHMORE GC, CARRUTHERS RA, FEENEY J, FEIZI T. Characterisation by mass spectrometry and 500-MHz proton nuclear magnetic resonance spectroscopy of penta- and hexasaccharide chains of human foetal gastrointestinal mucins (meconium glycoproteins). *Eur J Biochem* 1989; 186: 597-610.
62. ANTONOWICZ I, SHWACHMAN H. Meconium in health and in disease. *Adv Pediatr* 1979; 26: 275-310.
63. KÄÄPÄ P, KYTÖLÄ J, SOUKKA H, AHOTUPA M. Human meconium has potent antioxidative properties. *Biol Neonate* 1997; 72: 71-75.
64. PENNEY DP. The ultrastructure of epithelial cells of the distal lung. *Int Rev Cytol* 1988; 111:231-69: 231-269.
65. MAUS U, ROSSEAU S, KNIES U, SEEGER W, LOHMEYER J. Expression of pro-inflammatory cytokines by flow-sorted alveolar macrophages in severe pneumonia. *Eur Respir J* 1998; 11: 534-541.
66. SIBILLE Y, REYNOLDS HY. Macrophages and polymorphonuclear neutrophils in lung defense and injury. *Am Rev Respir Dis* 1990; 141: 471-501.
67. DE BEAUFORT AJ, PELIKAN DM, ELFERINK JG, BERGER HM. Effect of

interleukin 8 in meconium on in-vitro neutrophil chemotaxis. *Lancet* 1998; 352: 102-105.

68. GHADILLY FN. Endocytic structures and cell processes. *Ultrastructural Pathology of the Cell and Matrix*. London: Butterworths, 1988: 1131-1214.
69. LOPEZ A, PRIOR M, LILLIE LE, GULAYETS C, ATWAL OS. Histologic and ultrastructural alterations in lungs of rats exposed to sub-lethal concentrations of hydrogen sulfide. *Vet Pathol* 1988; 25: 376-384.
70. SOUKKA H, RAUTANEN M, HALKOLA L, KERO P, KÄÄPÄ P. Meconium aspiration induces ARDS-like pulmonary response in lungs of ten-week-old pigs. *Pediatr Pulmonol* 1997; 23: 205-211.
71. LEVIN DL, WEINBERG AG, PERKIN RM. Pulmonary microthrombi syndrome in newborn infants with unresponsive persistent pulmonary hypertension. *J Pediatr* 1983; 102: 299-303.
72. BACHOFEN M, WEIBEL ER. Structural alterations of lung parenchyma in the adult respiratory distress syndrome. *Clin Chest Med* 1982; 3: 35-56.
73. MATTHAY MA, FOLKESSON HG, CAMPAGNA A, KHERADMAND F. Alveolar epithelial barrier and acute lung injury. *New Horiz* 1993; 1: 613-622.
74. FULKERSON WJ, MACINTYRE N, STAMLER J, CRAPO JD. Pathogenesis and treatment of the adult respiratory distress syndrome. *Arch Intern Med* 1996; 156: 29-38.
75. CLEARY GM, ANTUNES MJ, CIESIELKA DA, HIGGINS ST, SPITZER AR, CHANDER A. Exudative lung injury is associated with decreased levels of surfactant proteins in a rat model of meconium aspiration. *Pediatrics* 1997; 100: 998-1003.
76. HERTZ MI, SNYDER LS, HARMON KR, BITTERMAN PB. Acute Lung Injury. In: Cohen K, Diegelman RF, Lindblad WJ, eds. *Wound healing. Biochemical & Clinical Aspects*. Philadelphia: W.B. Saunders Company, 1992: 396-415.
77. SUGAHARA K, IYAMA K, SANO K, KUROKI Y, AKINO T, MATSUMOTO M. Overexpression of surfactant protein SP-A, SP-B, and SP- C mRNA in rat lungs with lipopolysaccharide-induced injury. *Lab Invest* 1996; 74: 209-220.
78. LOPEZ A, ALBASSAM M, YONG S, SHARMA A, LILLIE LE, PRIOR MG. Profiles of type-II pneumocytes in rats inoculated intratracheally with bacterial lipopolysaccharide. *Am J Vet Res* 1987; 48: 1534-1539.
79. GHADILLY FN. Lysosomes. *Ultrastructural Pathology of the Cell and Matrix*.

London: Butterworths, 1988: 589-740.

80. HIGGINS ST, WU AM, SEN N, SPITZER AR, CHANDER A. Meconium increases surfactant secretion in isolated rat alveolar type II cells. *Pediatr Res* 1996; 39: 443-447.
81. FUKUDA Y, ISHIZAKI M, MASUDA Y, KIMURA G, KAWANAMI O, MASUGI Y. The role of intraalveolar fibrosis in the process of pulmonary structural remodeling in patients with diffuse alveolar damage. *Am J Pathol* 1987; 126: 171-182.
82. TAKEMURA T, AKAMATSU H. Ultrastructural study on the pulmonary parenchyma of the neonates following prolonged mechanical ventilation. *Acta Pathol Jpn* 1987; 37: 1115-1126.
83. CRAPO JD, BARRY BE, CHANG LY, MERCER RR. Alterations in lung structure caused by inhalation of oxidants. *J Toxicol Environ Health* 1984; 13: 301-321.

7. GENERAL DISCUSSION AND CONCLUSIONS

Intratracheal inoculation of homologous meconium in neonatal rats proved to be a reliable model to reproduce the lesions typically reported in the lungs of babies with MAS. These changes are a combination of abnormal aeration such as hyperinflation and atelectasis, as well the classic inflammatory reaction caused by the meconium in the lung. Pulmonary changes were homogeneously consistent in all rat neonates which indicate that MAS can be consistently reproduced under laboratory conditions. Based on the results of an extensive literature search, this was the first time that a murine neonatal model has been successfully used to induce MAS without the need of surgery to perform tracheal cannulation.

Intratracheal inoculation (ITI) using the modified otoscope proved to be a simple, reproducible, noninvasive and rapid method to deliver amniotic fluid and meconium into the lungs of 7-day-old neonatal rats. With adequate experience, an operator can inoculate a large number of neonates per day. This ITI method for neonatal rats also allows the delivery of accurate doses of inoculum which distributes widely in all pulmonary lobes. With minimal complications and mortalities in rat neonates, the desired doses of meconium produced the typical lesions observed in the lungs of human babies with MAS (1). This ITI method should prove useful in testing other pneumotoxicants because it avoids the need for cervical surgery which has been required for intratracheal inoculations of neonatal rats previously (2).

In experimental models of murine MAS, the cesarean section approach in pregnant rats constitutes a simple and humane method for the collection of sterile homologous amniotic fluid. On the other hand, collection of homologous meconium from the intestine of neonatal rats is cumbersome and requires a large number of neonates to ensure sufficient

meconium for the inoculum preparation. Comparative studies should investigate if the use of human, bovine, equine or porcine meconium may be appropriate in the neonatal rat model of MAS.

The time-pregnancy program ensures uniform groups of neonates of the same size, sex and weight. The temperate behavior and maternal instincts of the Fisher-344 rat were evident even with randomization and crossfostering. Since ITI does not involve a surgical procedure, cannibalism and rejection do not occur even in rats not exposed to the preconditioning protocol.

The cytological and biochemical analyses of BAL fluid are valuable tools to test the effect of pneumotoxins in the lungs of experimental animals but require knowledge of the baseline parameters of healthy animals (3). The baseline cell counts in BAL fluid collected from fetal and neonatal rats were unknown before this study. Results of the kinetic studies showed that one day before parturition PAMs are already present in the fetal bronchoalveolar space and the cell numbers increase substantially during the first three days of life. Three days after birth, the bronchoalveolar cell counts stabilize with numbers comparable to those reported in young or adult rats. The bronchoalveolar cell counts for rat neonates are similar to values reported for babies, rabbits and foals during the fetal and neonatal periods (4-7). It has been suggested that the prenatal influx of PAM is an adaptive physiological response to prepare the alveoli for postnatal life (6). Hormones, lipids and lipoproteins present in the pulmonary surfactant may play a role in the leukotaxis and recruitment of leukocytes in the neonatal lung (8). During the immediate postnatal period, a transient influx of PMNs into the bronchoalveolar space was also demonstrated in the neonatal rats and this PMN

migration could be explained by the lung distension at birth, or by the chemokines released by PAMs or by chemotactic agents naturally present in pulmonary surfactant (6). To our knowledge this is the first description of the leukocyte kinetics in the bronchoalveolar space of normal fetal and neonatal Fisher 344 rats.

The biochemical analysis of BAL showed that neonatal rats are born with high activities of alkaline phosphatase and lactate dehydrogenase, and that gamma-glutamyl transferase and protein increase for a short time during the first few days of life. These findings are presumably associated with the increased substrate availability, cellular debris and increased release of surfactant by type II pneumocytes during the perinatal period (9).

It was concluded that a low volume of saline solution is an innocuous and reliable vehicle for ITI in neonatal rats. Intratracheal inoculation of 0.05 ml of sterile saline in 7-day-old Fisher 344 rats did not cause detectable changes in the cellular and biochemical composition of BAL fluid. This fact was further substantiated by microscopic and ultrastructural studies of lungs in neonates inoculated with saline solution alone.

This study also showed that ITI of 0.05ml of sterile amniotic fluid elicits only mild injury and inflammatory response in the lung. Microscopic studies revealed that keratin and squamous debris present in amniotic fluid induce a transient foreign body response without significant alterations to the respiratory membrane or air-blood barrier. Although free keratin is highly pro-inflammatory in other neonatal tissues (10), this material does not appear to cause severe pulmonary injury or inflammation in neonatal rats. Similar observations have been reported in calves (11) and it has been suggested that the pulmonary response may be down-regulated by unknown components of amniotic fluid (12). Future studies *in vivo* and

in vitro should test if amniotic fluid alone or if amniotic fluid as vehicle to suspend meconium protects or modifies the inflammatory response.

In contrast to amniotic fluid, intratracheal inoculation of 0.05 ml of 20% unfiltered meconium induced an acute exudative response as shown by the transient but sharp increase in PMNs in the lungs. This influx of PMNs was substantiated by BAL fluid analyses as well as by microscopic examinations of the lungs. The pulmonary recruitment of PMNs following aspiration of meconium could be explained by the local release of inflammatory mediators such as tumor necrosis factor- α (TNF- α) and interleukin 1 β and 8 (IL-1 β , IL-8). These chemotactic cytokines have been linked to the inflammatory response that occurs in the lungs of patients with MAS (13-15).

The ultrastructural studies confirmed that a sublethal dose of meconium also promotes influx of PAM into the alveolar spaces, PMN sequestration in vascular spaces and platelet aggregation in pulmonary capillaries. These changes occur in parallel with an increased vascular permeability characterized by leakage of protein, interstitial edema and escape of red blood cells and fibrin into the alveoli and alveolar interstitium. Also, meconium causes a transient and mild injury to the cells of the respiratory membrane but these changes generally do not lead to necrosis or exfoliation of epithelial cells. Since meconium causes only minimal injury to the blood-air barrier, it is presumed that the leakage of protein into the bronchoalveolar space results from increased vascular permeability with junctional retraction caused by the local release of inflammatory mediators.

As reported in natural cases of MAS in newborn babies (16), experimental ITI of meconium in neonatal rats typically produces atelectasis, hyperinflation and transient

thickening of the alveolar septa. However, what was not observed in rat neonates was the formation of hyaline membranes occasionally reported in MAS (17). The ultrastructural study confirmed that the acute thickening of the alveolar septa was related initially to accumulation of fluid and sequestration of PMN, followed by a proliferation of mesenchymal cells and type II pneumocytes. Morphometric studies also showed that thickening of the alveolar septa is an important change in experimental MAS.

Chronologically, the neutrophilic pulmonary response caused by meconium is followed by a multifocal, histiocytic and granulomatous reaction. These granulomatous foci eventually calcify or become partially covered by cuboidal epithelial cells. As part of the repair mechanism, there are hypertrophy and hyperplasia of type II pneumocytes, proliferation of interstitial mesenchymal cells and sporadic focal intraalveolar fibrosis. Morphological changes induced by meconium tend to primarily affect the proximal alveolar region and neighboring alveoli in the neonatal rats. Epithelial cells, keratin and pigments are progressively removed from the meconium and eventually this material appears microscopically as a poorly pigmented matrix visible in alveoli for up to 16 weeks after inoculation.

The experimental model of ITI of meconium in 7-day-old Fisher 344 neonates clearly mimics the pulmonary lesions observed in MAS in human babies. To our knowledge, this is the first protocol described for intratracheal (transoral) inoculation in neonatal rats. This neonatal rat model offers a reliable and accessible option to study the pathogenesis of pulmonary lesions and should provide a reliable model to investigate treatment of MAS.

There is strong evidence that aspiration of meconium occurs in domestic neonates including calves (11), foals (18) and dogs (19). The morphologic changes in the lungs in these domestic species are similar to those seen in human babies with MAS and to neonatal rats experimentally inoculated with meconium and amniotic fluid. Although the significance of MAS in veterinary medicine has not yet been established, this syndrome should be considered in the differential diagnosis of neonates with meconium, epidermal squames and inflammatory response in the lungs. Future studies should test if animal neonates born with meconium-stained amniotic fluid are prone to develop respiratory distress as documented in human perinatology.

REFERENCES

1. CLEARY GM, WISWELL TE. Meconium-stained amniotic fluid and the meconium aspiration syndrome. An update. *Pediatr Clin North Am* 1998; 45: 511-529.
2. RUZINSKI JT, SKERRETT SJ, CHI EY, MARTIN TR. Deposition of particles in the lungs of infant and adult rats after direct intratracheal administration. *Lab Anim Sci* 1995; 45: 205-210.
3. HENDERSON RF, BENSON JM, HAHN FF, HOBBS CH, JONES RK, MAUDERLY JL, MCCLELLAN RO, PICKRELL JA. New approaches for the evaluation of pulmonary toxicity: bronchoalveolar lavage fluid analysis. *Fundam Appl Toxicol* 1985; 5: 451-458.
4. SIEGER L. Pulmonary alveolar macrophages in pre- and post-natal rabbits. *J Reticuloendothel Soc* 1978; 23: 389-395.
5. SIEGER L, ATTAR H, OKADA D, THIBEAULT DW. Alveolar macrophages (A.M.) in rabbit and human fetuses and neonates. *J Reticuloendothel Soc* 1975; 18: 47b.
6. ZELIGS BJ, NERURKAR LS, BELLANTI JA, ZELIGS JD. Maturation of the rabbit alveolar macrophage during animal development. I. Perinatal influx into alveoli and ultrastructural differentiation. *Pediatr Res* 1977; 11: 197-208.
7. ZINK MC, JOHNSON JA. Cellular constituents of clinically normal foal bronchoalveolar lavage fluid during postnatal maturation. *Am J Vet Res* 1984; 45: 893-897.

8. SCHORN H, EURATOM CW. Some hormonal effects on alveolar phagocytosis in the rat. *J Reticuloendothel Soc* 1975; 18: 35a.
9. NERURKAR LS, ZELIGS BJ, BELLANTI JA. Maturation of the rabbit alveolar macrophage during animal development. II. Biochemical and enzymatic studies. *Pediatr Res* 1977; 11: 1202-1207.
10. DAVIS JR, MILLER HS, FENG JD. Vernix caseosa peritonitis: report of two cases with antenatal onset. *Am J Clin Pathol* 1998; 109: 320-323.
11. LOPEZ A, BILDFELL R. Pulmonary inflammation associated with aspirated meconium and epithelial cells in calves. *Vet Pathol* 1992; 29: 104-111.
12. LOPEZ A, LÖFSTEDT J, BILDFELL R, HORNEY B, BURTON S. Pulmonary histopathologic findings, acid-base status, and absorption of colostral immunoglobulins in newborn calves. *Am J Vet Res* 1994; 55: 1303-1307.
13. KOJIMA T, HATTORI K, FUJIWARA T, SASAI TM, KOBAYASHI Y. Meconium-induced lung injury mediated by activation of alveolar macrophages. *Life Sci* 1994; 54: 1559-1562.
14. JONES CA, CAYABYAB RG, HAMDAN H. Early production of proinflammatory cytokines in the pathogenesis of neonatal adult respiratory distress syndrome (ARDS) associated with meconium aspiration. *Pediatr Res* 1994; 35: 339A-
15. DE BEAUFORT AJ, PELIKAN DM, ELFERINK JG, BERGER HM. Effect of interleukin 8 in meconium on in-vitro neutrophil chemotaxis. *Lancet* 1998; 352: 102-105.
16. BRADY JP, GOLDMAN SL. Management of Meconium Aspiration Syndrome. In: Thibeault D W, Gregory GA, eds. *Neonatal Pulmonary Care*. Connecticut: Appleton-Century-Crofts, 1986: 483-498.
17. SOUKKA H, RAUTANEN M, HALKOLA L, KERO P, KÄÄPÄ P. Meconium aspiration induces ARDS-like pulmonary response in lungs of ten-week-old pigs. *Pediatr Pulmonol* 1997; 23: 205-211.
18. DUBIELZIG RR. Pulmonary lesions of neonatal foals. *Equine Med Surg* 1977; 1: 419-425.
19. FUENTEALBA C, LOPEZ A. Intrauterine aspiration pneumonia. Diseases of the respiratory system. Western Conference of Veterinary Diagnostic Pathologists; Saskatoon, Saskatchewan: 1998.